The Involvement of Microglial Activation in Schizophrenia

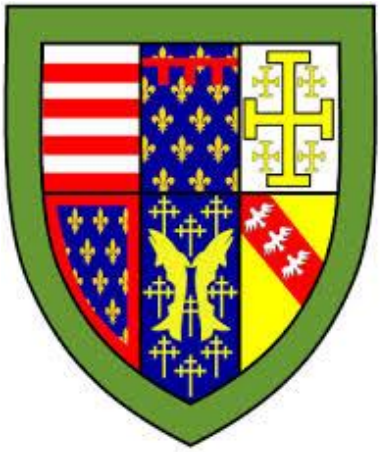

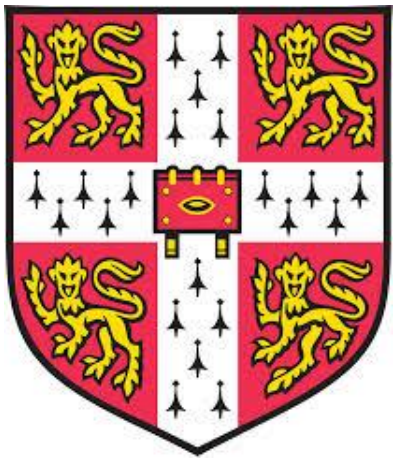

Geertje Frederique van Rees

Department of Chemical Engineering and Biotechnology

University of Cambridge

Queens' College

November 2017

This dissertation is submitted for the degree of Doctor of Philosophy

To my parents

Herman & Tineke

Declaration and Statement of Length

This dissertation is the result of my own work and includes nothing which is the outcome of work done in collaboration except as declared in the **Acknowledgements** or elsewhere in the text. No part of this thesis has been submitted for any other qualification at the University of Cambridge or at any other institution. This text does not exceed the prescribed 65,000-word limit and does not contain more than 150 figures, as set by the Degree Committee of Engineering.

Cambridge, United Kingdom, Nov 2017

Publications arising from this work

- **Van Rees GF***, Lago SG*, Cox DA*, Tomasik J, Rustogi N, Weigelt K, Ozcan S, Cooper JD, Drexhage H, Leweke FM, Bahn S. Evidence of microglial activation following exposure to serum from first-onset drug-naïve schizophrenia patients. *Brain, Behaviour and Immunity*. 2018; 67; 364-373.
- **Van Rees GF***, Lago SG*, Cox DA*, van der Doef T, Tomasik J, de Witte L, Bahn S. In vivo PET imaging of neuroinflammation in treated schizophrenia patients linked to changes in microglia stat3 signalling. (manuscript in preparation)

Other publications

- Lago SG*, Tomasik J*, **van Rees GF**, Steeb H, Cox DA, Rustogi N, Ramsey JM, Bishop JA, Petryshen T, Haggarty SJ, van Beveren NJ, Bahn S. A novel pipeline for drug discovery in neuropsychiatric disorders using high-content single-cell screening of signalling network responses *ex vivo*. (*Submitted)*
- Lago SG*, Tomasik J*, **van Rees GF**, Ramsey JM, Haenisch F, Cooper JD, Broek JA, Suarez-Pinilla P, Ruland T, Mikova O, Kabacs N, Arolt V, Baron-Cohen S, Crespo-Facorro B, Bahn S. Exploring the neuropsychiatric spectrum using high-content functional analysis of single-cell signalling networks *ex vivo. Accepted at Molecular Psychiatry, May 2018*
- Tomasik J*, Lago SG*, **van Rees GF**, Fuetterer M, Steeb H, Ramsey JM, Haenisch F, Broek JA, Ruland T, Suarez-Pinilla P, Kabacs N, Mikova O, van Beveren NJ, Arolt V, Vioque EG, Baron-Cohen S, Crespo-Facorro B, Bahn S. Expression of cell surface metabolic markers in peripheral blood mononuclear cells across four major neuropsychiatric diseases: schizophrenia, bipolar disorder, depression and autism spectrum disorder. (manuscript in preparation)
- Cooper JD*, Ozcan S*, Gardner RM, Rustogi N, Wicks S, **van Rees GF**, Dalman C, Karlsson H, Bahn S. Schizophrenia-risk and urban birth are associated with proteomic changes in neonatal dried blood spots. *Translational Psychiatry.* 2017; 7(1290); 1-14.

*shared first author

Abstract

Abnormal activation of brain microglial cells is widely implicated in the pathogenesis of schizophrenia. The disrupted balance of microglia phenotypes has been hypothesized to influence the clinical course of the disease and affect symptom severity. Previously, the pathophysiology of microglial activation was considered to be intrinsic to the central nervous system. We hypothesised that due to their perivascular localization, microglia can also be activated by factors present in circulating blood.

We applied a high-content functional screening platform, to characterize alterations in microglial intracellular signalling cascades induced by schizophrenia patient serum relative to control serum. Using automated sample preparation, fluorescent cellular barcoding and flow cytometry, the applied platform is capable of detecting multiple parallel cell signalling responses in microglia.

First, we exposed a human microglia cell line to serum isolated from first-onset drug-naïve schizophrenia patients (n=60) and healthy controls (n=79). We were able to show that peripheral blood serum obtained from schizophrenia patients induced differential microglial cell signalling network responses *in vitro*. We subsequently assessed whether antipsychotic drug-treatment can normalise the abnormal microglial signalling responses previously identified by exposing microglia cells to serum from antipsychotic treated schizophrenia patients (n=15) and controls (n=17). In addition, in order to assess microglia activation *in vivo,* we obtained positron emission tomography (PET) imaging data from collaborators, who used a radiotracer to assess potential altered microglia activation in patients suffering from schizophrenia. Finally, as a proof of concept study, we attempted to validate these findings by assessing the effect of serum collected from first-onset drug-naïve schizophrenia patients (n=9), controls (n=12) as well as serum isolated from the same patients subjected to six weeks of clinical treatment with the antipsychotic olanzapine (n=9). This study aimed to identify normalisation of previously detected differences in microglia signalling pathways based on successful *in vivo* treatment.

We demonstrate that peripheral blood serum isolated from schizophrenia patients, independent of their treatment status, is sufficient to trigger microglial cell signalling network responses *in vitro,* which are indicative of altered STAT3 signalling. We further explored the composition of the serum for differential expression of analytes, previously associated with neuropsychiatric disorders, and the utility of the detected microglial cellular phenotype as a target for novel drug discovery.

Contents

Declaration and Statement of Length iii

Publications arising from this work iv

Abstract v

Contents vi

List of Figures xi

List of Tables xiii

Chapter 1 | Introduction 2

1.1 Schizophrenia clinical representation 2

1.2 Aetiology 4

1.2.1 Genetic predisposition 4

1.2.2 Altered neurotransmitter signalling 5

1.2.3 Environmental factors 6

1.2.4 Immune component in Schizophrenia 7

1.3 The difference between peripheral and central nervous system inflammation 10

1.4 The involvement of microglia 12

1.5 Imaging neuroinflammation *in vivo* 16

1.6 The need for new treatments 18

1.6.1 Overview of currently available antipsychotic drugs 18

1.6.2 Towards new drug targets 20

1.6.3 Circumventing the blood brain barrier 21

1.7 Phosphoflow as a discovery platform for microglial polarisation 23

1.8 Thesis aim and outline 25

Chapter 2 | Methods Parameters & Backgrounds 28

2.1 Introduction 28

2.2 Methods: Backgrounds 28

2.2.1 Multiplexed Immunoassay 28

2.2.2. Flow Cytometry 29

2.2.3 Mass Spectrometry based Targeted Proteomics 34

2.3 Methods: Parameters 37

2.3.1 Clinical sample recruitment and collection 37

2.3.2 Microglia cell culture 38

2.3.3 Stimulation of microglia 38

2.3.4 Fluorescent cell barcoding 41

2.3.5 Intracellular staining of cell signalling epitopes 41

2.3.6 Data acquisition using flow cytometry 44

2.3.7 Multiplexed immunoassays 44

2.3.8 Mass spectrometry based targeted proteomics 45

2.3.9 Statistical data analysis 49

Chapter 3 | Platform Robustness, Sensitivity & Efficacy 53

3.1 Introduction 53

3.2 Results 53

3.2.1 Multiplexing different cell populations 53

3.2.2 Proof of Concept Studies 57

3.2.3 Functional characterization of intracellular pro- and anti-inflammatory microglial reactive states 61

3.3 Discussion 64

3.3.1 Comparison of the multi-parameter phospho-specific flow cytometry platform to conventionally used methods to functionally profile microglia 64

3.3.2 Detection of changes in homeostatic equilibrium 67

3.3.3 Detection of early, specific microglia signalling cascades 68

3.3.4 Outlook 70

Chapter 4 | Drug Target Discovery in Microglia 73

4.1 Introduction 73

4.2 Results 74

4.2.1 Serum from first-onset drug-naïve schizophrenia patients induced pro-inflammatory microglia activation *in vitro* 74

4.2.2 Detection of changes in patient serum capable of inducing altered microglia phenotype 77

4.2.3 Exploration of sensitivity towards drug screening on activation epitopes 78

4.3 Discussion 81

4.3.1 Altered STAT3 signalling in microglia cells following patient serum exposure 81

4.3.2 Implication of cytokine signalling pathway in microglia following schizophrenia patient serum exposure 84

4.3.3 Altered 4EBP1 signalling in microglia upon schizophrenia patient serum exposure 85

4.3.4 Implication of increased mTORC1 signalling in microglia following schizophrenia patient serum exposure 87

4.3.5 Potential crosstalk between STAT3 and mTORC1 signalling pathways 88

4.3.6 Changes in schizophrenia serum may be linked to pro-inflammatory polarization in microglia 89

Chapter 5 | *In vivo* Microglia Activation 93

5.1 Introduction 93

5.2 Results 94

5.2.1 PET study design 94

5.2.2 Detection of increased [^{11}C](*R*)-PK11195 in temporal brain region of antipsychotic treated patients 96

5.2.3 Microglial exposure to serum from treated schizophrenia patients does not indicate normalisation of microglial activation phenotype 99

5.2.4 Changes in expression of serum proteins in antipsychotic treated patients relative to controls. 102

5.2.5 Correlations across the identified microglia signalling epitopes, serum MRM peptides and PET brain regions. 104

5.3 Discussion 108

5.3.1 Detection of increased TSPO in the temporal brain region of schizophrenia patients treated with antipsychotic medication 109

5.3.2 Changes in STAT3 (pS727) signalling in microglia following patient serum exposure 110

5.3.3 Identification of decreased CrkL (pY207) activity in microglia associated with serum exposure from drug-treated patients 110
5.3.4 Altered serum proteins in drug-treated schizophrenia patients 111
5.3.5 Limitations 112

Chapter 6 | Longitudinal Study 114

6.1 Introduction 114
6.2 Results 114
6.2.1 Follow-up study design 114
6.2.2 Signature for effects of disease and clinical antipsychotic treatment on microglia signalling 117
6.2.3 Comparison of *in vitro* effects of olanzapine exposure on identified cell signalling epitopes to changes associated with T6 serum exposure 120
6.2.4 Identification of disease-related serum changes potentially involved in inducing altered microglia signalling 122
6.2.5 Symptom subscale correlations to identified microglial reversal epitopes and serum reversal protein Apo C-I 125
6.3 Discussion 127
6.3.1 Partial validation by comparison of current results to those of different schizophrenia patient cohorts and same patient PBMC data 127
6.3.2 Identification of reversal epitopes PDPK1 (pS241) and GSK3β (pS9) indicative of effective *in vivo* treatment 128
6.3.3 Validation of serum proteins in comparison to previous schizophrenia patient sample cohorts 130
6.3.4 Identification of the normalisation of serum protein apolipoprotein C-I 131

Chapter 7 |Conclusion 134

7.1 Overview of main findings 134
7.1.1 Summary 134
7.1.2 Identification of altered STAT3 phosphorylation state in microglia after exposure to serum from schizophrenia patients 135
7.1.3 Changes in apolipoprotein expression in patient serum may indicate altered microglial TREM2 signalling 137
7.2 Identification of common microglial signalling hub as novel drug target 139
7.2.1 Cellular phenotype screening approach for the identification of new drug targets 139

7.2.2 Altered microglial STAT3 signalling overlaps with signalling changes in MDD 140

7.2.3 Altered microglial STAT3 signalling phenotype as new drug target for the treatment of negative symptoms 141

7.2.4 Final thoughts on the utility of the identified microglial phenotype 142

7.3 Limitations and future work 144

7.3.1 Clinical samples 144

7.3.2 Experimental design 145

7.3.3 The need for the investigation of microglial pathways 147

Acknowledgements & Collaborations 149

References 151

List of Figures

Figure 1.1 Neurodevelopmental hypothesis of schizophrenia; from Selemon & Zecevic (2015).....6
Figure 1.2 Triggers, actions and outcomes of neuroinflammation; from Xanthos & Sandkühler (2013) 11
Figure 1.3 Overview of microglial M1 and M2 phenotypical repertoire 13
Figure 1.4 The two-hit, three-hit and microglia hypotheses of schizophrenia 15
Figure 1.5 Overview of pathways across the blood brain barrier; from Abbott *et al*. (2006) 22
Figure 1.6 Overview of dissertation outline.....26
Figure 2.1 Overview of magnetic bead technology used to quantify serum concentration of proteins and small molecules 29
Figure 2.2 A schematic overview of a flow cytometer set up 31
Figure 2.3 Layout of a barcode matrix to encode 27 cell populations.....33
Figure 2.4 Schematic overview of the ESI interface.....35
Figure 2.5 Schematic overview of analyte filtering across the three quadrupoles. 37
Figure 3.1 Gating structure for the functional analysis of 64 fluorescently cell barcoded populations of SV40 microglia cells.....54
Figure 3.2 Median fluorescence intensities across 64 barcoded microglia populations for each functional fluorescence channel.....56
Figure 3.3 Z factor analysis across 64 barcoded SV40 microglial cell populations for each functional fluorescence channel. 57
Figure 3.4 Cell culture supernatant and serum titration. 59
Figure 3.5 Comparison between 75% serum from a person suffering from a common cold and 75% exposure to stimulated PBMC supernatant.....60
Figure 3.6 Functional characterization of SV40 human microglial cells as a sensor for early signalling events induced by pro- and anti-inflammatory microglial stimuli.....62
Figure 3.7 Stain indices of antibody clones against SV40 microglial cell signalling epitopes. 63
Figure 3.8 Overview of signal transduction pathways from the functional characterization.....69
Figure 4.1 Phenotypic alteration of microglial cell signalling in response to serum from drug-naïve schizophrenia patients. 76
Figure 4.2 Model for Stat3 signalling. 83
Figure 4.3 Overview of mTORC1 and mTORC2 signalling pathways.....86
Figure 4.4 Overview of complement signalling cascades; from Stephan *et al.* (2012).....90
Figure 5.1 Overview of BP_{ND} across the different brain regions in combined patient group. 97

Figure 5.2 Overview of BP_{ND} across the different brain regions for separated patient sub-groups and controls. 98
Figure 5.3 Differential responses in microglia signalling pathways upon serum exposure from schizophrenia patients and matched controls. 100
Figure 5.4 Correlation plots for the brain regions of interest between BP_{ND} and STAT3 (pS727). 105
Figure 6.1 Clinical response of schizophrenia patients at the 6 weeks' time point of antipsychotic treatment with olanzapine. 116
Figure 6.2 Differential responses in microglia signalling pathways following exposure to serum from olanzapine-treated schizophrenia patients at treatment time-points T0 and T6 and matched controls. 118
Figure 6.3 Olanzapine responses in microglia relative to vehicle across the identified reversal and T6 epitopes. 121
Figure 6.4 Volcano plots showing differences in serum peptides in patients relative to controls and to patients after 6 weeks of olanzapine treatment. 123
Figure 6.5 Overview of significant correlation between changes in PDPK1 (pS241) and changes in GSK3β (pS9). 126
Figure 7.1 Identified altered STAT3 phosphorylation sites in microglia exposed to schizophrenia patient serum. 136
Figure 7.2 Schematic representation of altered STAT3 signalling pathway in microglia upon exposure to serum from schizophrenia patients. 138

List of Tables

Table 1.1 DSM-5 criteria for diagnosing schizophrenia. 3
Table 1.2 Overview of recent publications reporting PET tracer binding potential in individuals with psychosis. 17
Table 2.1. List of ligands used for incubation with SV40 microglial cells. 40
Table 2.2 List of antibodies used to detect intracellular cell signalling epitopes. 42
Table 2.3 List of analytes measured in clinical serum samples by multiplexed immunoassays. 45
Table 2.4 Complete list of analytes measured in clinical serum samples by MRM mass spectrometry. 46
Table 4.1 Demographic characteristics of clinical samples used in the microglial serum exposure study. 75
Table 4.2 Alterations in microglial cell signalling epitope expression in response to serum from first-onset drug-naive schizophrenia patients relative to healthy controls. 75
Table 4.3 Altered serum analytes in first-onset drug-naive schizophrenia patients) relative to healthy controls.....79
Table 4.4 Common functional pathways of altered serum analytes from Table 4.3 and Figure 4.1C..80
Table 5.2 Demographic characteristics of the schizophrenia patients and controls. 95
Table 5.3 Overview of [^{11}C](*R*)-PK11195 binding potential across different brain regions using the combined patient group.....96
Table 5.4 Overview of [^{11}C](*R*)-PK11195 binding potential across different brain regions with patients separated according to treatment status. 97
Table 5.5 Alterations in microglial cell signalling epitope expression in response to serum exposure of antipsychotic free and treated schizophrenia patients relative to healthy controls. 101
Table 5.6 Altered serum analytes between schizophrenia patients relative to healthy controls. 103
Table 5.7 Correlation matrix from the correlation analysis across PET tracer, microglia signalling epitopes and serum analytes for the healthy control group. 106
Table 5.8 Correlation matrix from the correlation analysis across PET tracer, microglia signalling epitopes and serum analytes for the antipsychotic treated schizophrenia patients. 107
Table 6.1 Demographic characteristics of the drug-naïve schizophrenia patients before and after 6 weeks olanzapine treatment and controls. 115
Table 6.2 Alterations in microglia signalling pathways following exposure to serum from olanzapine-treated schizophrenia patients at treatment time-points T0 and T6 and matched controls. 119
Table 6.3 Altered serum analytes in drug naïve schizophrenia patients relative to healthy controls or patients after 6 weeks of olanzapine treatment.....124

Abbreviations

4EBP1	Eukaryotic translation initiation factor 4E-binding protein 1
AF	Alexa Fluor
Akt	protein kinase B
ANOVA	analysis of variance
AP	antipsychotic
Apo	apolipoprotein
AR	antigen receotor
Arg1	arginase 1
BBB	blood brain barrier
BMI	body mass index
BMP	bone morphogenetic protein
BP_{ND}	binding potential
CCL22	C-C motif chemokine 22
CD206	mannose receptor
CLC	cardiotrophin-like cytokine
CNS	central nervous system
CNTF	ciliary neurotophic factor
COX-2	cyclo-oxygenase 2
CREB	cAMP response element-binding protein
CSF	Cerebrospinal fluid
CST	Cytometer Setup and Tracking
CT-1	cardiotrophin-1
CV	coefficient of variation
DC	discovery cohort
Deptor	DEP domain containing mTOR-interacting protein
DISC1	disrupted in schizophrenia 1
DMSO	dimethyl sulfoxide
DRD2	dopamine receptor 2
DSM	Diagnostic and Statistical Manual of Mental Disorders
EGF	epidermal growth factor
EGFP	enhanced greep fluorescent protein
eIF4E	Eukaryotic translation initiation factor 4E
ELISA	enzyme linked immuno sorbent assay
ESI	electrospay ionisation
FACS	fluorescent active cell sorting
FBS	fetal bovine serum
FCB	fluorescent cell barcode
FcγR	Fc-gamma receptor
FSC	forward scatter channel
GF	growth factor
GM-CSF	granulocyte macrophage colony-stimulating factor

gp	glycoprotein
GSK3	glycogen synthase kinase 3
GWAS	genome-wide association studies
HC	healthy control
HDL	high-density lipoprotein
HLA	human leukocyte antigen
ICD-10	International Statistical Classification of Diseases and Related Health Problems
IFITM	interferon-induced transmembrane
IFN	interferon
IgG2	immunoglobulin heavy constant γ2
IL	Interleukin
IR	integrin receptor
JAK	Janus kinase
LC	liquid chromatography
LIF	leukemia inhibitory factor
LPS	Lipopolysaccharides
LS	longitudinal study
LST8	lethal with Sec13 protein 8
MAC	membrane attack complex
MAPK	mitogen-activated protein kinase
MCP1	monocyte chemoattractant protein 1
M-CSF	macrophage colony-stimulating factor
MDD	major depressice disorder
MEK1	mitogen-activated protein kinase kinase
MFI	median fluorescent intensity
MHC	major histocompatability complex
MI	multiplexed immunoassay
mLST8	mammalian lethal with Sec13 protein 8
MRM	multiple reaction monitoring
MS	mass spectrometry
mSIN1	mammalian stress-activated protein kinase interacting protein
mTOR	mammalian target of rapamycin
mTORC1	mTOR complex 1
mTORC2	mTOR complex 2
NMDA	N-methyl-D-aspartate
NO	nitric oxide
Nos	nitric oxide synthase
NRG1	neuregulin 1
NSAID	nonsteroidal anti-inflammatory drug
OSM	oncostatin M
PANSS	positive and negative symptom scale
PBBS	peripheral benzodiazepine-binding site
PBMC	peripheral blood mononuclear cell
PBR	peripheral benzodiazepine receptor
PBS	phosphate buffered saline
PCP	phencyclidine
PDGF	platelet-derived growth factor

PDPK1	phosphoinositide-dependent kinase 1
PE	phycoerythrin
PET	positron emission tomography
PFA	paraformaldehyde
PI3k	phosphoinositide 3-kinase
PIAS	protein inhibitors of activated STATs
PKA	protein kinase A
PKC	protein kinase C
PMT	photomultiplier tube
poly I:C	polyinosinic-polycytidylic
PS	peripheral system
PTEN	phosphatase and tensin homolog
PTP	protein tyrosine phosphatase
Raptor	regulatory associated protein of mTOR
Rictor	rapamycin-insensitive companion of mTOR
ROS	reactive oxygen species
RP-LC	reverse phase liquid chromatography
RPMI	Roswell Park Memorial Institute
RTK	receptor tyrisine kinase
RT-PCR	reverse transcriptase-coupled polymerase chain reaction
SCZ	schizophrenia
SEB	Staphylococcal Enterotoxin B
SGK1	serum and glucocorticoid-induced protein kinase 1
SOCS	suppressor of cytokine signalling
SSC	side scatter channel
STAT	signal transducer and activator of transcription
T. gondii	Toxoplasma gondii
T0	time point zero
T6	after 6 weeks timepoint
TGF	transforming growth factor
tGM	total grey matter
T_H	T helper cell
TLR	Toll-like receptor
TNF	tumor necrosis factor
TREM2	Triggering receptor expressed on myeloid cells 2
TSC	tuberous sclerosis complex
TSPO	translocator protein 18kDa
TYK	tyrosine kinase
UHR	ultra high risk
v/v	volume to volume

Chapter 1
Introduction

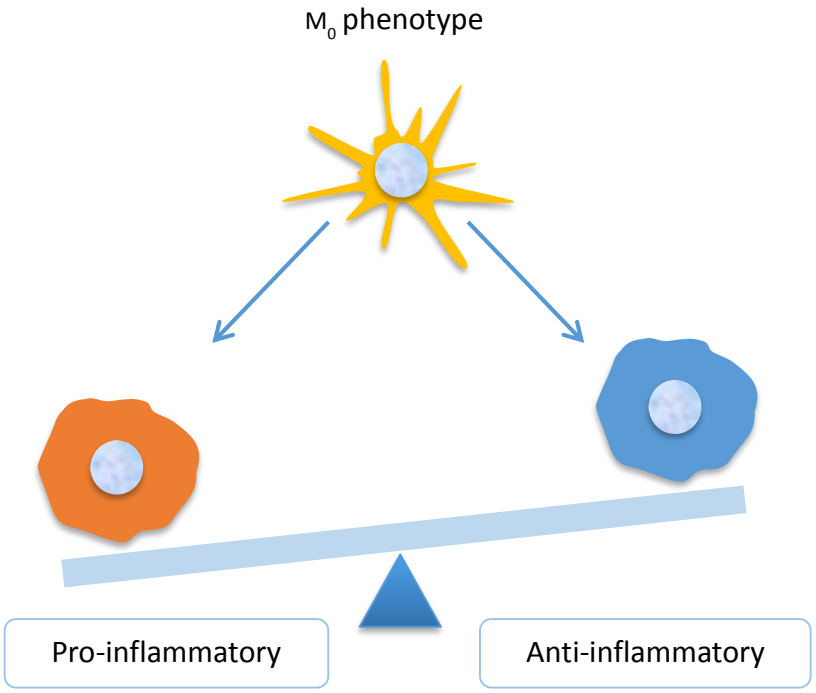

Chapter 1 | Introduction

Microglia, the brain's immune cells, have been implicated in the pathogenesis of schizophrenia. Previously, the pathophysiology of microglial activation was considered to be intrinsic to the central nervous system (CNS). However, in light of recent findings implicating the immune system's involvement in the aetiopathology of schizophrenia, combined with the microglial perivascular localization, microglial activation has been considered as a contributing factor. This chapter provides a literature overview of recent schizophrenia research findings, including clinical representation, current hypotheses and discusses the need for the development of more efficacious treatments.

1.1 Schizophrenia clinical representation

The Greek derived word *schizophrenia* translates as "splitting of the mind" and was introduced by the Swiss psychiatrist Eugen Bleuler in 1908[1]. On a global scale approximately 24 million people suffer from this severe and complex neuropsychiatric disorder. 0.3% to 0.7% of the world population is affected, although there is reported variation by ethnicity, across countries and by geographic origin (for example children of immigrants)[2]. Schizophrenia is manifested through abnormal mental functions and disturbed behaviour. The symptoms can be divided into three domains[3]. Positive symptoms include delusions, hallucinations and thought disorganization. Negative symptoms refer to loss of motivation, emotional deficits, and an inability to experience pleasure and disturbances in social interaction. The third category is impaired cognitive function, which includes symptoms such as attention and working memory deficits. Diagnosis is based on psychiatric interview, which has not changed over the last 100 years. The International Statistical Classification of Diseases and Related Health Problems 10th Revision (ICD-10) and Diagnostic and Statistical Manual of Mental Disorders (DSM) are most commonly used for diagnosis[4] (see DSM diagnostics for schizophrenia in **Table 1.1**).

Table 1.1 DSM-5 criteria for diagnosing schizophrenia. Two changes were made to Criterion A in DSM-5 compared to DSM-IV. 1) the elimination of the special attribution of bizarre delusions and Schneiderian first-rank auditory hallucination (*e.g*. two or more voices conversing), leading to the requirement of at least two Criterion A symptoms for any diagnosis of schizophrenia, and 2) the addition of the requirement that at least one of the Criterion A symptoms must be delusions, hallucinations, or disorganized speech.

Diagnostic Criteria

A. Two (or more) of the following, each present for a significant portion of time during a 1-month period (or less if successfully treated). At least one of these must be (1), (2) or (3):
   1. Delusions
   2. Hallucinations
   3. Disorganized speech (*e.g.* frequent derailment or incoherence)
   4. Grossly disorganized or catatonic behaviour
   5. Negative symptoms (*i.e.,* diminished emotional expression or avolition)

B. For a significant portion of the time since the onset of the disturbance, level of functioning in one or more major areas, such as work, interpersonal relations or self-care, is markedly below the level achieved prior to the onset (or when the onset is in childhood or adolescence, there is failure to achieve expected level of interpersonal, academic, or occupational functioning).

C. Continuous signs of the disturbance persist for at least 6 months. This 6-month period must include at least 1 month of symptoms (or less if successfully treated) that meet Criterion A (*i.e*. active-phase symptoms) and may include periods of prodromal or residual symptoms. During these prodromal or residual periods, the signs of disturbance may be manifested by only negative symptoms or by two or more symptoms listed in Criterion A present in an attenuated form (*e.g*. odd beliefs, unusual perceptual experiences).

D. Schizoaffective disorder and depressive or bipolar disorder with psychotic features have been ruled out because either 1) no major depressive or manic episodes have occurred during active-phase symptoms, or 2) if mood episodes have occurred during active-phase symptoms, they have been present for a minority of the total duration of the active ad residual periods of the illness.

E. The disturbance is not attributable to the physiological effects of a substance (*e.g*. a drug of abuse, a medication) or another medical condition.

F. If there is a history of autism spectrum disorder or a communication disorder of childhood onset, the additional diagnosis of schizophrenia is made only if prominent delusions or hallucinations, in addition to the other required symptoms of schizophrenia, are also present for at least 1 month (or less if successfully treated).

Schizophrenia affects males and females slightly differently (1.4 males to 1 female), with males (16 – 20 years) having an earlier onset than females (20 – 30 years)[2,5,6]. Also, an emphasis on negative symptoms and longer disease duration (associated with poorer outcome) shows higher incidence in males, whereas mood symptoms and a relatively shorter presentation of the disorder (better outcome) show equivalent risks for both males and females[2]. In general, the effect of age at onset is likely related with gender, with males having worse premorbid adjustment, lower educational achievement and in general a worse outcome. The course of the disorder appears to be less severe in 20% of the patients with a small number of individuals achieving a complete recovery. However, most patients will remain in need of some form of daily living support, and many remain chronically ill and impaired. Some have exacerbations and remissions of active symptoms, whilst others have a course of progressive deterioration[2].

Rates of comorbidity with substance-related disorders are high. Over half of schizophrenia patients smoke cigarettes daily. In addition, patients seem more prone to drug abuse, such as cannabis. Unfortunately, cannabis use is associated with an earlier disease onset[7,8]. Furthermore, discontinuation of cannabis use is linked to enhanced symptomatic improvement in patients with first-episode psychosis[9,10].

Life expectancy is reduced in individuals with schizophrenia due to associated medical conditions that are more common in this population, *e.g*. weight gain, diabetes, metabolic syndrome and cardiovascular and pulmonary disease. Approximately 5 to 6% of individuals with schizophrenia die through suicide, and about 20% of the patients will attempt suicide at least once. Suicide is therefore the primary reason for premature death in this patient group[2,11–13]. This fact gives an indication of the burden schizophrenia patients have to bear in their daily lives.

1.2 Aetiology

Remarkably, schizophrenia remains a neuropsychiatric disorder of largely unknown aetiology. Evidence from clinical neuroscience and genetics suggests that diagnostic categories in the DSM and ICD may not align with pathophysiological mechanisms of mental disorders[14]. This does not aid the current ongoing research for biomarker profiles and causes for schizophrenia. There is consensus that the causes of schizophrenia are multifactorial. Thus it is unlikely that a single marker will be sufficient to define all schizophrenia phenotypes. In this section existing hypotheses and theories of schizophrenia are presented.

1.2.1 Genetic predisposition

Twin studies have indicated a strong genetic involvement. The Genain quadruplets are probably the most famous example, as these four monozygotic twin sisters all developed adult schizophrenia[15]. Polygenic risk scores currently explain only a fraction of disease liability (*e.g.* 18%-23% in schizophrenia[16] relative to up to 80% heritability derived from family and monozygotic twin studies[17,18]). Another example of genetic predisposition is illustrated by foster children born to mothers with schizophrenia. Of the foster children 16.6% from a mother with schizophrenia developed the disorder, whereas none of the control foster children did[19]. Genetic studies have identified multiple genes for potential involvement in schizophrenia, such as *COMT, neuregulin-1*, and *DISC1*[20–23]. One of the most replicated genetic findings is the major histocompatibility complex (MHC) and the association with specific human leukocyte antigen (HLA) genes[21–26]. A meta-analysis of genome-wide association studies (GWAS) identified 108 schizophrenia-associated loci, of which 75% are protein-coding genes.

Notable associations are *DRD2* (dopamine receptor 2; a target of antipsychotic drugs), glutamatergic neurotransmission and voltage-gated calcium channel subunits[27]. Copy number variations are estimated to account for 2% of schizophrenia cases[28,29] and epigenetic factors might be involved as well[30]. However, although a genetic predisposition can be a risk factor for schizophrenia, it should be noted that most individuals diagnosed with schizophrenia have no family history of a psychotic disorder[2].

1.2.2 Altered neurotransmitter signalling

In *post mortem* brain tissue, many subtle morphological differences can be detected that pertain to a variety of neural systems and processes including signal transduction (glutamatergic, GABA-ergic and dopaminergic neurotransmission), synaptic density, inhibitory interneuron function and glial cells[31–34]. As a consequence, neurotransmitter based hypotheses of schizophrenia have been the leading hypothesis over the last decades[35–37]. The dopamine hypothesis proposes overactive dopaminergic signalling. It is suggested that dopaminergic signalling first becomes dysregulated at the dopamine receptor level but that this subsequently shifts towards the presynaptic level, thus regulating the amount of dopamine to be released into the synaptic cleft. Also, It is suggested that dopamine dysregulation itself is related to psychotic symptoms rather than schizophrenia[37]. The revised dopamine hypothesis, based on a meta-analysis using pharmacological MRI data, proposes hyperactive dopamine transmission in the mesolimbic areas and hypoactive dopamine transmission in the prefrontal cortex in schizophrenia patients[38]. The NMDA (N-methyl-D-aspartate) receptor hypothesis assumes NMDA receptor hypo-functioning, causing abnormal glutamatergic neurotransmission. Evidence for this hypothesis comes from *post-mortem* studies, showing abnormal glutamatergic receptor expression levels[39]. Also the use of phencyclidine (PCP), a non-competitive NMDA receptor antagonist, induces schizophrenia-like symptoms[40]. The GABAergic hypothesis involves the fine-tuning via GABAergic interneurons, which control and synchronize disparate cortical circuits. This fine-tuning may be disrupted and this may underlie some of the schizophrenic symptoms[41,42]. The serotonergic hypothesis suggests stress-induced serotoninergic overdrive in the cerebral cortex. Excessive serotonergic stimulations may thereby cause glutamatergic dysfunction, leading to neuronal hypometabolism and ultimately synaptic atrophy and grey matter loss[35,43,44]. The final neurotransmitter-based hypothesis is the cholinergic hypothesis, suggested by the high prevalence of patients smoking nicotine products. The percentage of smoking patients exceeds 70%, which is a 2- to 4-fold higher rate than in the general population[45,46]. It is believed that this high nicotine usage is an attempt of self-medication[47]. Furthermore, in controlled experiments, nicotine has been found to enhance cognitive function in schizophrenia patients[48].

1.2.3 Environmental factors

Environmental factors have also been identified as risk factors for the development of schizophrenia. Children born to mothers exposed to influenza viral infection (*e.g.* during an influenza epidemic) in the prenatal phase, had a 80% higher likelihood of developing schizophrenia compared to children born before and after the epidemic[49,50]. Maternal malnutrition has been shown to be another environmental risk factor (*e.g*. the Dutch hunger winter in 1944-1945[51] and the Chinese famine of 1959-1961[52]). These observations have led to the neurodevelopmental hypothesis of schizophrenia, suggesting that the disorder can result from altered brain development in the early stages of gestation, leading to abnormal cortical development (**Figure 1.1**)[53,54]. The theory has been supported by imaging studies showing the presence of structural brain abnormalities in first episode patients, indicating these alterations were already present before disease onset[55,56]. Furthermore, similar alterations are also present in prodromal patients, but to a lesser degree[57]. The age of schizophrenia onset peaks between 18 and 36[58,59], an age where the prefrontal cortex is still developing and synaptic pruning is ongoing[54], this provides further evidence of altered cortical development in the disorder.

The two-hit hypothesis is a derivative of the neurodevelopmental hypothesis and suggests a combination of potential genetic susceptibility coupled with a distinct developmental insult predisposing the individual to disease. A later event, the second hit, may be required to precipitate the onset of the disorder[60]. The three-hit hypothesis relates to the genetic predisposition as the first hit and therefore assumes the presence of a genetic component in schizophrenia. The second hit is represented by an early environmental insult followed by the third hit, which is a later environmental hit, causing the onset of the disorder[61]. Evidence for these neurodevelopmental insults are the

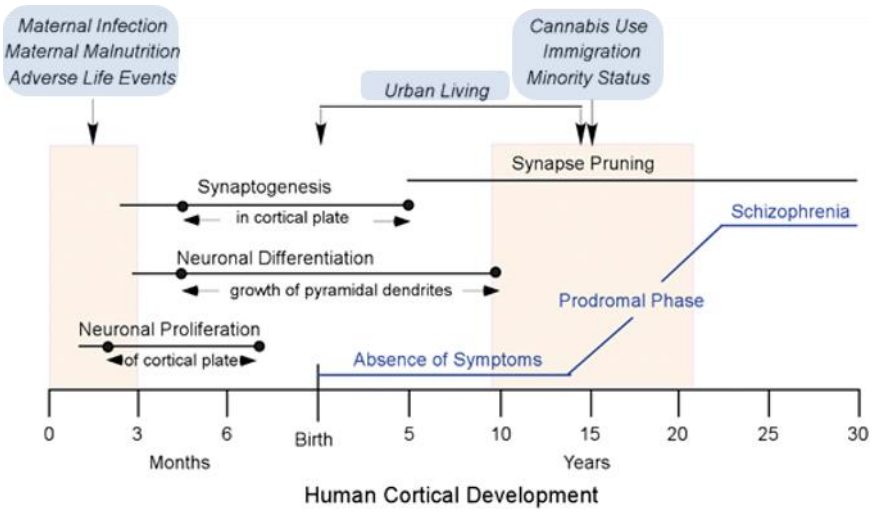

Figure 1.1 Neurodevelopmental hypothesis of schizophrenia; from Selemon & Zecevic (2015). Black lines indicate normal developmental phases. Red highlighted areas indicate developmental stages associated with abnormal cortical development. Blue highlighted areas indicate risk factors related to schizophrenia, possibly associated with altered cortical development. The blue line indicates symptom development towards schizophrenia throughout the developmental stages. *Reprinted with permission*[53]

influenza epidemic, maternal malnutrition during famine, prenatal cytokine exposure[62–64] and obstetric factors[65]. These prenatal events could prime immune components, and lead to a vulnerability to develop the disease later in life. Evidence for this comes for example from a study using neonatal dried blood spots. Individuals who developed non-affective psychosis later in life already had altered acute phase protein expression levels at birth[66]. The later environmental hit could be infection, inflammation, autoimmunity, stress or drug abuse. Another environmental risk linked to schizophrenia is season of birth (late winter, early spring). The incidence for schizophrenia is also higher for children growing up in urban environments and for some minority ethnic groups[2].

1.2.4 Immune component in Schizophrenia

There is inconsistency in the literature regarding findings for immune dysfunction in schizophrenia. However, this could be explained by small sample size, stage of the illness, treated vs. untreated patients and matching of patient and control groups. However, when focusing on meta-analyses, proper sample sizes, and first onset patients, an increase of inflammatory markers might be one of the most robust findings in schizophrenia, giving rise to many immune hypotheses such as autoimmunity[67–69], involvement of infectious agents[70], T_{H1}-T_{H2} shift[71], cytokines[72], genetic-inflammatory-vascular[73], fetal brain cytokine imbalance[74], and mild encephalitis[75].

Of interest is the overlap with autoimmune diseases. There is a high comorbidity between schizophrenia and autoimmune and chronic inflammatory conditions suggesting a common underlying immune abnormality leading to both conditions for at least a patient subgroup. For example, the immune response genes residing within the MHC region have been linked to the autoimmune disease multiple sclerosis and there is a genetic pleiotropic overlap between multiple sclerosis and schizophrenia[76]. Interestingly, a higher prevalence of NMDA receptor antibodies have been found in serum of patients with an initial diagnosis of schizophrenia, indicating autoimmunity[77,78]. Patients with autoimmune diseases like multiple sclerosis, celiac disease and systemic lupus erythematosus are more likely to develop psychosis compared to controls[67–69]. Furthermore, a 30-year population-based register study found that having had an autoimmune disease *a priori* would increase the risk of schizophrenia by 29%. In addition, any history of hospitalization with infection increased the risk of developing schizophrenia to 60%[79]

The first article on the potential infectious aetiology of schizophrenia was published in the journal "*Scientific American"* in 1896 with the article ''Is Insanity Due to a Microbe?''. Nowadays, one of the most researched infectious agents in schizophrenia is the parasite *Toxoplasma gondii (T. gondii)*, with a growing body of epidemiological evidence indicating the likelihood of an association between

exposure to *T. gondii* and increased risk of schizophrenia[80,81]. Interestingly, antipsychotic drugs have the ability to inhibit replication of *T. gondii*[82]. Apart from parasites, there are many indications in the literature for the involvement of a viral component in schizophrenia. One of the earliest findings is the effect of the influenza epidemic in 1918. Children born to mothers exposed to influenza viral infection in the prenatal phase had a 80% higher likelihood of developing schizophrenia compared to children born before and after the epidemic. This indicates that viral exposure during gestation is associated with schizophrenia in later life[49,50]. Especially dopaminergic neurons appear to be vulnerable to this type of prenatal infection[83]. A meta-analysis revealed that childhood viral infections, mainly caused by enteroviruses, increase the risk of future psychotic illness[84]. In schizophrenic patients, increased antibodies were found to animal retroviruses and human corona viruses, but this was only present in recent onset patients[85,86]. In DNA extracted from peripheral blood mononuclear cells (PBMCs) of first episode patients, traces of retroviruses were found in non-protein coding areas[87]. In *post mortem* frontal cortices and in cerebrospinal fluid (CSF) of first-onset schizophrenia patients an increase of retroviral RNA has been found[88,89]. In addition, mRNA of interferon-induced transmembrane (IFITM) protein was found to be increased in brain blood vessels of schizophrenia patients. IFITM is a viral restriction factor, which might indicate a more systemic inflammatory disturbance in schizophrenia[90]. These findings indicate a potential underlying susceptibility of the immune system, making patients more susceptible to infections, which could be a risk factor for the onset of the disorder.

When isolated T cells from healthy volunteers are exposed to patient or healthy control serum, differential effects on T-cell function can be detected[91]. The PBMC fraction of blood is composed of lymphocytes (70-90%; 45-70% T-lymphocytes, 15% B-lymphocytes), monocytes (10-30%) and dendritic cells (1-2%). After isolation, these display a different response profile when comparing isolated PBMCs from first-onset drug-naive schizophrenia patients to those of healthy matched controls, indicating a lasting change in these cells. A meta-analysis of 16 studies screening patient PBMCs shows an increase of total lymphocytes, $CD3^+$ cells (total T-lymphocytes), $CD4^+$ cells (T Helper cells; T_H) and $CD4^+$:$CD8^+$ ratio[92] ($CD8^+$ are suppressor cells ending the immune response). Changes in the $CD4^+$:$CD8^+$ ratio has been suggested to be a state marker for acute exacerbations of psychosis. Gene expression studies have shown a schizophrenia associated dysregulation of immune pathways in PBMCs, independent of treatment status[93–95]. Further proof for an altered functioning of the peripheral immune system in schizophrenia is provided by the observed shift of T_{H1} to T_{H2}, indicating a shift from a full immune response to a more regulating, humoral response[96–98]. This is further supported by an increase in B cells in acute onset schizophrenia patients but not in drug treated patients[96]. High B-lymphocyte levels are associated with antibody production and presentation. This finding corresponds to the results of a

meta-analysis including 81 studies, reporting an increased prevalence of positive titres for 20 different autoantibodies in patients with schizophrenia[99].

Cytokines are key signalling molecules that coordinate both the innate (*e.g.*, granulocytes, monocytes/macrophages, and natural killer cells) and the adaptive (*e.g.*, B- and T-lymphocytes) immune system, and exert effects in the peripheral system (PS) and the CNS. They are produced by both immune and non-immune cells, and exert their effects by binding specific cytokine receptors on a variety of target cells, thereby modulating for example the balance between humoral and cell-based immune responses. Two meta-analyses revealed significant alterations in serum cytokine levels of schizophrenia patients compared to controls. Interleukin(IL)-6, IL-1RA and sIL-2R were increased whereas IL-2 was decreased in patients[100]. The meta-analysis identified a relationship between cytokine expression and first episode or acute symptomatic relapse. Cytokines altered in both groups and normalised by treatment were IL-1β, IL-6 and transforming growth factor-β (TGF-β), suggesting that these molecules are state-related markers. IL-12, Interferon gamma (IFNγ), tumor necrosis factor alpha (TNFα) and sIL-2R were only increased in the acute relapse group. Therefore, these may be trait markers as their levels remained elevated regardless of disease phase and antipsychotic treatment[101]. In addition, the anti-inflammatory cytokine IL-10 was found to be correlated with symptom improvement[102]. Biomarker studies in patient sera[103–106] and CSF[107,108] have also supported the cytokine hypothesis of schizophrenia by reporting further changes in immune function. The identified cytokines have been the most reported as candidate biomarkers associated with schizophrenia as well as with other neuropsychiatric diseases[72,109,110], hence the specificity of the cytokine inflammatory signal for schizophrenia can be questioned. This highlights the need for the discovery of novel and specific inflammatory panels for schizophrenia.

The fetal brain cytokine imbalance hypothesis of schizophrenia assumes maternal infection during pregnancy to increase the risk of schizophrenia. This can be caused by bacterial, parasitic and viral pathogens resulting in prenatal infection, disrupting the fetal brain balance between pro –and anti-inflammatory cytokine signalling and thereby affecting postnatal brain development[74]. The influenza epidemic in 1918, as mentioned earlier, is an example of such a scenario. However, although the risk of schizophrenia increased greatly during this epidemic, it should be noted that the majority of exposed babies did not subsequently develop schizophrenia. This observation suggests an interaction with genetic and environmental risk factors that interact to mitigate schizophrenia.

The genetic-inflammatory vascular hypothesis of schizophrenia proposes the presence of a genetic predisposition to exaggerated inflammatory responses, thereby damaging the brain's microvascular network, causing metabolic disturbances[73]. The incredibly precise regulation of the delivery of energy and oxygen required for normal brain function can be disrupted. In reaction to environmental agents,

including infections, hypoxia, and physical trauma, abnormalities of CNS metabolism arise, promoted by genetically modulated inflammatory reactions. This could damage the microvascular system of the brain and further disturb CNS metabolism and allow intrusion of pathogens and peripheral system components. There are examples of psychoses resulting from micro-vascular CNS diseases, including systemic lupus erythematosus and Sjögren's syndrome[111]. This also fits with the mild encephalitis hypothesis, which assumes low level neuroinflammation leading to mild encephalitis, which could precipitate the onset of schizophrenia. This can be triggered by infections, autoimmunity, toxicity or trauma[75].

Finally, common additional factors associated with schizophrenia are weight gain[112–117], stress and hormonal related molecular changes[118,119], all with the ability to enhance inflammation. Most antipsychotic medications possess some anti-inflammatory activity, but they do not reinstate the balance between pro- and anti-inflammation[120,121].

1.3 The difference between peripheral and central nervous system inflammation

Peripheral immune modulators have the ability to induce psychiatric symptoms in both animal models and humans. Furthermore, many medical conditions (*e.g*. multiple sclerosis, diabetes, obesity) associated with chronic inflammatory and immunological abnormalities have been regarded risk factors for psychiatric disorders[79,122–124]. However, it should be noted that immunological dysregulation in the PS is substantially different compared to the CNS as both involve different molecular mechanisms. Neuroinflammation is the common term used for inflammatory reactions within the CNS and this process has been increasingly associated with psychiatric illness as well as neurodegeneration[125]. Neuroinflammation could be regarded as a response mechanism enabling the CNS to endure enhanced metabolic demands. In addition, it increases processing power and plasticity of CNS neuronal networks. However, it can become maladaptive and induce neuronal stress[126]. The immune response in the PS differs from the CNS as it can be more severe. Initially in the PS, innate immune cells, like macrophages, mast cells and dendritic cells, are activated, leading to a variety of inflammatory mediators including chemokines, cytokines and proteolytic cascades responding in a non-specific manner leading to tissue reactions ranging from mild homeostatic responses to full-scale inflammation[127]. In this aggravated PS immune response, the vasculature reacts with vasodilation and extravasation of plasma components and blood cells, resulting in redness, heat generation and swelling. Usually in this stage, antigens and activation of the complement system are involved. Dendritic cells transfer information to the adaptive immune system leading, for example, to

phagocytosis. Diverse molecular pathways link the PS immune system to the CNS, separated by the blood-brain barrier (BBB), enabling it to support defence by promoting fever, increased sleep and enhanced pain sensitivity[126,128]. However, in the CNS the immune response is not as severe as in the PS. This difference between peripheral inflammation and neuroinflammation is important, as they are associated with the activation of two distinct systems. Here, the mild inflammatory tissue reaction protects neurons whilst the peripheral inflammatory responses would result in neuronal damage. This is where the term neuroinflammation has to be distinguished from the peripheral immune response. Instead of dendritic cells, the CNS has perivascular macrophages and vascular pericytes. The innate parenchymal immune cells of the CNS are represented by astrocytes and microglia[129–131]. In the context of minor neuroinflammation, glial and vascular cells become activated in order to cope with enhanced metabolic demands[132,133]. Intensive acute or chronic activation renders microglia neurotoxic where they can produce reactive oxygen species (ROS) and recruit monocytes from the peripheral system into the CNS[134]. A transition to maladaptive forms of neuroinflammation starts with changes in the BBB, causing the release of pro- and/or anti-inflammatory mediators or cells, which facilitate the spread to neighbouring areas. Finally, a breakdown of the BBB results in an intrusion of large molecules and recruitment of immune cells into the CNS, potentially damaging neurons and other brain cells. In addition, glial cells might not be able to reduce the release of glutamate, leading to high excitotoxicity in non-injured surrounding tissues (for an overview of neuroinflammation actions and outcomes see **Figure 1.2**)[135]. Neuroinflammation, possibly microglia induced[136], could be a key pathological player in

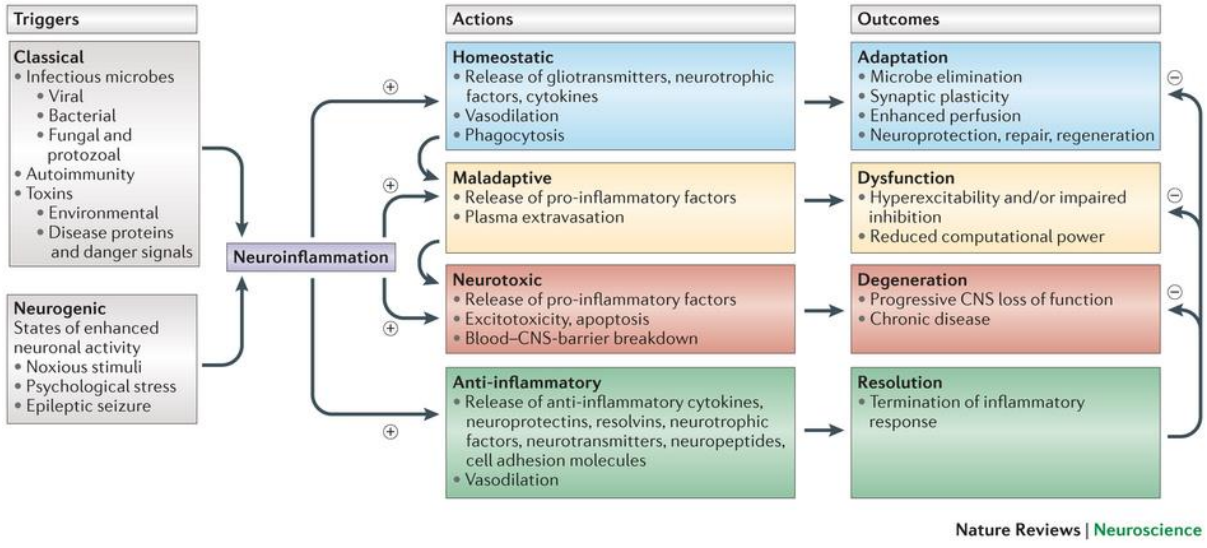

Figure 1.2 Triggers, actions and outcomes of neuroinflammation; from Xanthos & Sandkühler (2013). Neuroinflammation can be caused by 'Classical' factors (*e.g.* infectious microbes, autoimmunity, toxins) and to enhanced neuronal activity (*e.g.* noxious stimuli, psychological stress, epileptic seizure). + indicates independent and interacting responses by immune cells, vascular cells and neurons. These responses could be homeostatic, leading to adaptation, dysfunctional or neurotoxic effects, leading to pathology. – represents anti-inflammatory mechanisms triggered in parallel and are known to terminate neuroinflammation and reduce pathological outcomes. *Reprinted with permission*[104].

the schizophrenia disease process, indicated by increased serum concentrations of pro-inflammatory cytokines through the activation of monocytes and chronic humoral responses[137–139]. This neuroinflammation can be induced by infectious agents (such as viral infection) or the dysbalance in peripheral immune response[140,141].

1.4 The involvement of microglia

Schizophrenia is increasingly associated with neuroinflammation and the over-activation of the brain's resident immune cells, the microglia[136]. Microglia are derived from a myeloid precursor population in the yolk sac and migrate during embryogenesis to the CNS at the end of gastrulation[142]. Once there, they develop into a non-overlapping network throughout the brain specialized in immune surveillance. They are also involved with synaptic pruning, antigen presentation, developmental apoptosis, neuronal differentiation and in maintaining the neuronal network. Microglia comprise up to 20% of the non-neuronal network and rarely need replacement due to their longevity. They are able to develop into a range of phenotypical activation states, encompassing pro-inflammatory, anti-inflammatory and reparative phenotypes[143]. Pro-inflammatory microglia release pro-inflammatory cytokines and reactive oxygen species as a protective response against pathogens or acute CNS injury[144,145]. In contrast, anti-inflammatory microglia promote tissue restoration through the release of anti-inflammatory cytokines and trophic factors and by phagocytosis of cellular debris[144,145]. Previous studies, focused on stroke, traumatic brain injury and neurodegenerative diseases, suggest that the deleterious effects of microglial activation in the CNS are primarily mediated by the anti-inflammatory phenotype[144,145]. Nonetheless, recent data supports the concept that the balance between both anti- and pro-inflammatory phenotypes coupled with their spatial and temporal distribution post insult is the critical factor for determining the long-term consequences of brain inflammation[144,146]. However, many publications use a different categorisation with classically activated M1 or alternatively activated M2 microglia[144,145]. At the time of writing this thesis (Oct 2017) a PubMed search for "microglia M1 M2" retrieves 436 articles, of which 137 were published within the preceding 12 months. The initial M1 vs. M2 classification has been further expanded in that microglia can assume multiple intermediate phenotypes (*e.g.* M2a, M2b and M2c), each with a distinct role in mounting a regulated immune response (**Figure 1.3**)[147–150]. One of the primary reasons for the controversial interpretation of microglial activation is that the majority of data has been obtained through *in vitro* exposure to purified antigens and cytokines. These *in vitro* results are presented as if *in vivo* data can be read through this

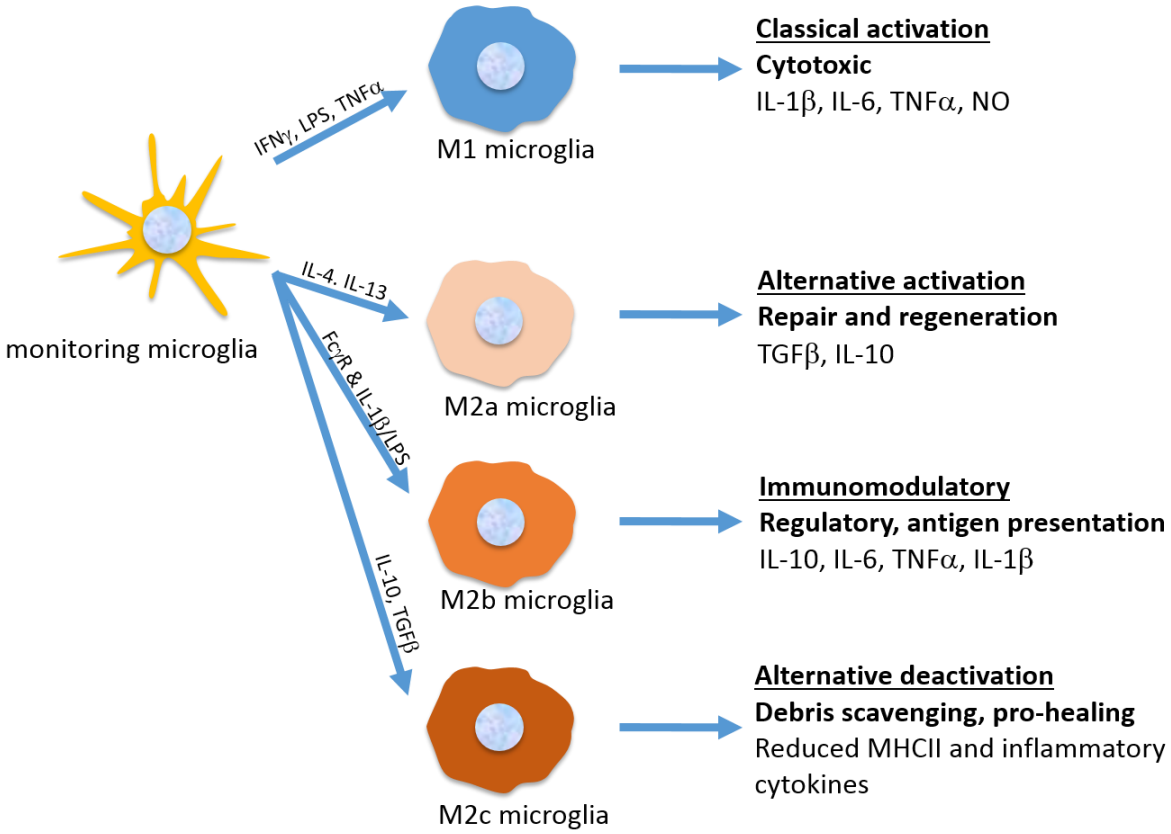

Figure 1.3 Overview of microglial M1 and M2 phenotypical repertoire. Resting microglia can be polarised through specific signalling molecules, resulting in different phenotypes with specialised functions and mechanisms. NO: nitric oxide, FcγR: Fcγ receptor for immunoglobulin G.

filter[151,152]. In addition, this concept has the limitation that the nomenclature is derived from peripheral macrophages, which come in dozens of varieties. A new classification system is required which takes into account the myeloid origin and the fact that microglia are intrinsic CNS cells[152]. Ultimately, it is likely that the ultimate functional role assumed by microglia *in vivo* represents the integration of multiple phenotypic cues derived from complex physiological mixtures, such as CSF, across multiple cell signalling pathways[144].

Evidence for the involvement of microglia in schizophrenia comes to some extent from *post-mortem* studies. A systematic review combined 22 studies reporting on microglial markers in *post-mortem* brain tissue. Out of these 22 studies, 11 studies reported an increase in microglial markers, 8 found no effect and 3 found a decrease in microglial markers[153]. Especially in paranoid patients, a pronounced increase of HLA-DR (involved with antigen presentation) in the hippocampus was reported. A meta-analysis of data obtained from genetic profiling of *post-mortem* brain tissue, using a gene co-expression network approach, found microglia marker genes to be represented in the top categories within each detected network[154]. However, it should be taken into account that *post mortem* studies may be confounded by age, lifestyle and medication effects[155] and therefore the interpretation of

disease-specific profiles is not straight forward. In addition, these studies do not present information of the pathological process at the disease onset. Therefore, in an attempt to elucidate microglia driven neuroinflammation *in vivo* positron emission tomography (PET) studies on first-episode drug-naive and antipsychotic treated patients were conducted. These PET studies use a tracer which binds specifically to activated microglia. This investigation allows to measure and compare tracer binding activity in patient and control subjects. To date results from PET studies aiming to investigate microglial activation in schizophrenia brain have been inconsistent, with some reporting an increase[156], some a decrease[157] and some detect no differences between patients and controls [158].

In line with the neurodevelopmental hypothesis of schizophrenia, Bilbo & Schwarz hypothesized that sub-populations of microglia are permanently maintained in an activated or primed state into adulthood as a consequence of perinatal infections and that a subsequent immune challenge in adulthood can cause the release of excessive levels of cytokines from primed microglia[159]. This hypothesis has been suggested and slightly altered many times thereafter and is currently also known as the microglia hypothesis of schizophrenia[160]. Fitting with this developmental microglia hypothesis, genome-wide association studies (GWAS) in schizophrenia suggest that genetic polymorphisms in secreted proteins, such as members of the complement cascade[161], potentially alter synaptic pruning by microglial cells during developmental phases critical to schizophrenia pathogenesis[162–164]. This overactive microglial pruning would thereby alter the brain's wiring and signalling routes.

The poly I:C animal model, used as neurodevelopmental model for schizophrenia[165], uses an analog for viral double-stranded RNA (polyinosinic-polycytidylic acid sodium salt; poly I:C) as a model to mimic a prenatal viral infection. Pregnant rats or mice are injected with either poly I:C or saline and offspring later develop abnormal behavioural, cognitive and pharmacological phenotypes. By creating a controlled maternal infection during embryogenesis, it was shown that in poly I:C offspring a higher amount of activated and pro-inflammatory/phagocytic microglia was present at day 30, comparable to adolescence/early adulthood in humans[166,167] which is the average age of onset for schizophrenia. This strengthens the hypothesis of prenatal insults having the ability to alter microglial functioning which persist into adulthood to cause further changes in the CNS and which could be involved in the development of schizophrenia.

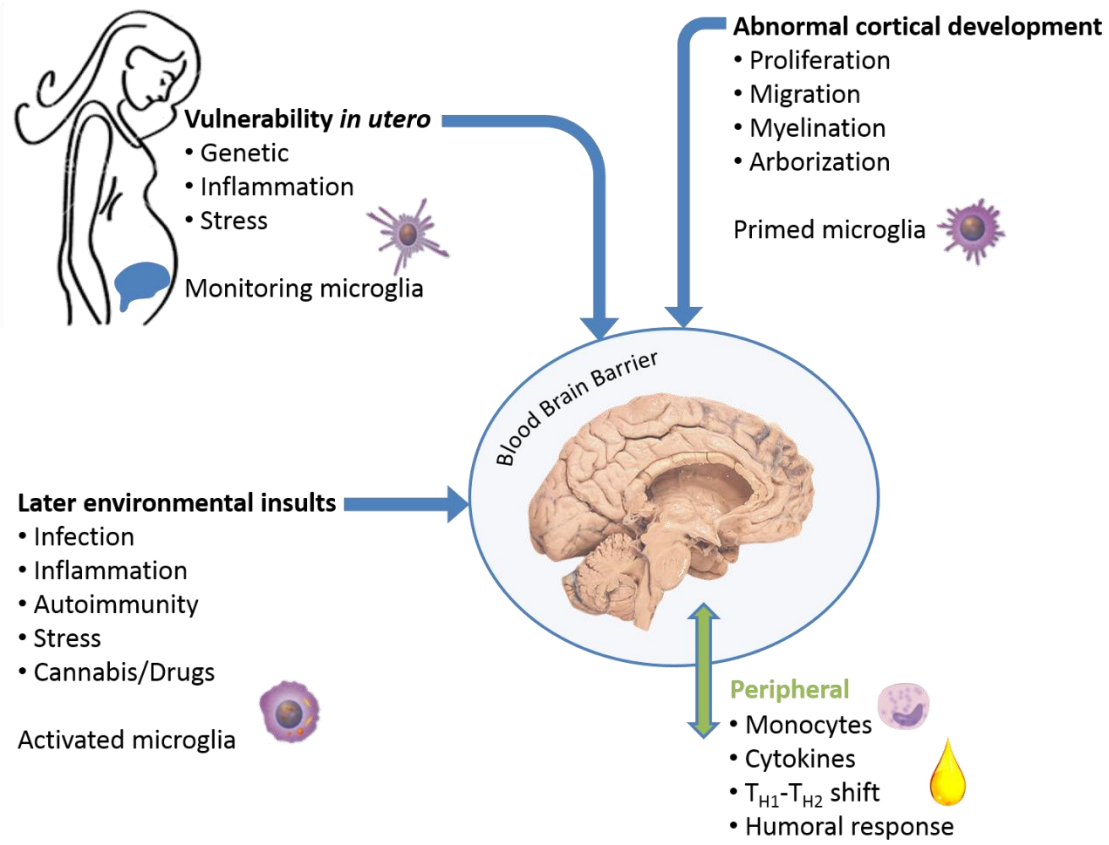

Figure 1.4 The two-hit, three-hit and microglia hypotheses of schizophrenia. During the prenatal phase the fetal brain development can be disturbed by early environmental factors, such as the inflammatory status of the mother's immune system. This predisposes the CNS to an altered developmental trajectory, continuing into adulthood, predisposing it to development of psychosis. Due to a later environmental hit, such as a viral infection, full schizophrenia can be precipitated. The blue arrows represent developmental stages/hits and green arrow represents potential exchange between the CNS and peripheral system.

Microglia can also be activated by immune signalling analytes passing through the BBB. In patients, the BBB may be more permeable, allowing a higher crossover of immune related components facilitating translocation of peripheral immune components into the CNS. Investigating the presence of plasma proteins in CSF, such as albumin and dietary antigens, allows to examine the state of the BBB. Comparing CSF to serum ratios between patients and healthy controls has pointed to a dysfunction of the BBB[108,168]. Therefore, it can be hypothesized that peripheral signalling molecules and immune proteins are more likely to enter the CNS in schizophrenia. Increased cytokine levels in the CNS may be the result of BBB disruption, causing them to travel from the PS to the CNS. Another cause could be the translocation of immune components, resulting in cytokine release from microglia.

Taken together, the microglia, two-hit and three-hit hypotheses for schizophrenia can be combined to integrate central and peripheral factors in early and later life (**Figure 1.4**). Furthermore, the most robust findings are the involvement of an immune component and prenatal infectious insults resulting in an increased disease risk. Due to a more permeable BBB, changes in the PS would have the ability to further affect brain physiology, which is already primed by neurodevelopmental disturbances. This

crossover of peripheral immune factors could then enhance the CNS immune response, such as the activation state of the microglia and thereby increasing neuroinflammation.

1.5 Imaging neuroinflammation *in vivo*

In an attempt to elucidate microglia driven neuroinflammation *in vivo,* positron emission tomography (PET) studies on first-episode drug-naive and antipsychotic treated patients have been performed. These PET studies use a tracer binding specifically to activated microglia, translocator protein 18 kDa (TSPO). TSPO is a hetero-oligomeric complex located on the outer mitochondrial membrane known to be involved in modulating immune response, in cholesterol transport, and in heme/steroid synthesis[169]. TSPO was initially described as a peripheral benzodiazepine receptor (PBR), a secondary binding site for diazepam, but has been renamed to TSPO to reflect some of these cellular functions[170]. This protein was initially found in peripheral organs (i.e., kidneys, nasal epithelium, adrenal glands, lungs, and heart), but is also expressed on microglia in healthy brains[171]. TSPO expression is suggested to be dramatically upregulated during microglia activation processes such as brain injury and repair[172]. TSPO basal expression rises in several acute and degenerative disorders, including Alzheimer's disease, Parkinson's disease, multiple sclerosis, Huntington's disease[173] and amyotrophic lateral sclerosis (ALS)[174]. As a result, TSPO has been considered a hallmark of neuroinflammation. Therefore, TSPO PET imaging has been employed for both improving the knowledge regarding the involvement of neuroinflammation in CNS diseases and to assess the efficacy of novel anti-inflammatory therapeutic compounds[174]. The most widely used TSPO PET tracer is [^{11}C](*R*)-PK11195, a labelled R-enantiomer of isoquinoline carboxamide developed in the early 1980s. However, interpretation of [^{11}C](*R*)-PK11195 PET data remains difficult, due to a number of methodological issues limiting the clinical usefulness of [^{11}C](*R*)-PK11195: i) the short half-life of carbon-11; ii) a very low signal in the normal brain which results in a poorly defined pattern of binding for healthy control groups; iii) a poor signal-to-noise ratio due to high nonspecific binding caused by its highly variable kinetic behaviour; iv) genetic polymorphisms affecting the binding affinity properties of the tracer[175,176]. To counteract these drawbacks, there has been a great amount of effort towards the development of second-generation TSPO PET radiotracers[177,178], including [^{18}F]FEPPA, [^{11}C]PBR28 and [^{11}C]DPA-713.

Table 1.2 Overview of recent publications reporting PET tracer binding potential in individuals with psychosis. The table presents a summary overview of PET tracer studies investigating microglia in schizophrenia. The Di Biase *et al.* study consists of UHR, recent onset and chronically ill patients. The Bloomfield *et al.* study consists of UHR and chronically ill patients. Red - increase of tracer binding potential (BP_{ND}), green – decrease of BP_{ND}, black - no differences detected. AP - antipsychotic, HC - healthy control, N – group size, NA - not available, PANSS - Positive and Negative Symptom Scale, SCZ - schizophrenia, UHR - ultra high risk. Modified from Howes & McCutcheon (2017)[179].

Study	N (SCZ-HC or UHR-SCZ-HC)	Mean age (UHR-SCZ - HC)	Mean PANSS (UHR-SCZ)	Mean duration of illness	First onset?	Drug naïve/ Treatment	PET tracer	Results
van Berckel *et al.* (2008)[180]	10 - 10	24 - 23	NA	3.1 years	No	AP treated	[^{11}C](R)-PK11195	Increase of BP_{ND} in total grey matter
Doorduin *et al.* (2009)[181]	7 - 8	31	74	5.3 years	No	AP treated	[^{11}C](R)-PK11195	Increase of BP_{ND} in hippocampal regions
Takano *et al.* (2010)[182]	14 - 14	43.9	77.9	18.8 years	No	AP treated	[^{11}C]DAA1106	No significant differences, cortical BP_{ND} correlates to positive symptom scores
Bloomfield *et al.* (2015)[156]	14 - 14 -14	24.3 - 47 - 28.1/46.2	49.5 - 63.7	NA	UHR/No	AP naïve/AP treated	[^{11}C]PBR28	Increased BP_{ND} in total grey matter, frontal and temporal lobes
Kenk *et al.* (2015)[183]	16 - 27	43.5 - 42.5	70.2	14.8 years	No	AP treated	[^{18}F]FEPPA	No significant differences
Coughlin *et al.* (2016)[184]	12 - 14	24.1 - 24.9	NA	2.1 years	No	AP treated	[^{11}C]DPA-713	No significant differences
van der Doef *et al.* (2016)[185]	19 - 17	26 - 26	53	1.3 years	No	15/19 AP treated	[^{11}C](R)-PK11195	No significant differences, significant correlation between BP_{ND} and age.
Holmes *et al.* (2016)[186]	16 - 16	33 - 33	85	9 years	mixed	6 AP naïve, 2 treatment free, 8 AP treated	[^{11}C](R)-PK11195	AP treated show increase in cortical BP_{ND} and correlates to negative symptoms, no difference in AP-free patients
Hafizi *et al.* (2017)[187]	19 -20	27.5 - 27.8	68.6	2.8 years	Yes	14/19 AP naïve, others <4 weeks lifetime AP exposure	[^{18}F]FEPPA	No significant differences
Collste *et al.* (2017)[157]	16 - 16	28.5 - 26.4	77.4	7.9 months	Yes	AP naïve	[^{11}C]PBR28	Decreased BP_{ND} in grey matter, frontal and temporal lobes and hippocampal regions
Notter *et al.* (2017)[188]	12 - 14	24 - 26	NA	2.1 years	No	AP treated	[^{11}C]DPA-713	Strong trend towards reduced BP_{ND} in middle frontal gyrus (P = 0.051) with suggestion of using levels of inflammatory cytokines in peripheral and central tissues alongside.
Hafizi *et al.* (2017)[189]	24 - 0 - 23	21.2 - 23.0	NA	NA	UHR	22/24 AP naïve	[^{18}F]FEPPA	No significant differences
Di Biase *et al.* (2017)[158]	10 – 18 – 15 – 27	20.7 – 20.6 – 35.2	NA	1.5 – 13.6	UHR/No	AP naïve/AP treated	[^{11}C](R)-PK11195	No significant differences

Currently 13 papers report PET brain imaging findings from individuals at ultra high risk (UHR) of, or with, schizophrenia diagnoses. This investigation allows to measure tracer binding activity to microglia in patient and control subjects. Yet, there are great inconsistencies between these studies, with some reporting an increase[156], some a decrease[157] and some detect no differences between patients and controls[158] (see **Table 1.2** for an overview). One of the major issues relating to *in vivo* microglia imaging studies of schizophrenia patients are methodological inconsistencies, resulting in different outcome measures. The earliest two studies report increased binding potential in whole brain grey matter[180] and the hippocampus[181] of antipsychotic treated schizophrenia patients. Later studies, however, have not consistently demonstrated an increase in binding potential. The inconsistent outcomes across these 13 papers may be due to the application of five different radio ligands for TSPO detection. Apart from that, sample sizes are small and a range of different patient groups were investigated, ranging from UHR individuals to antipsychotic treated schizophrenia patients. Therefore, current conclusions regarding PET imaging studies and potential microglia-driven neuroinflammation in schizophrenia are inconclusive. Experts in the field have outlined the need to combine TSPO PET imaging with an independent method to provide additional insights regarding the inflammatory status of a given patient[188]. These additional methods may provide further information about the patients' immune status and potentially aid in the interpretation of the PET tracer results.

1.6 The need for new treatments

For all psychiatric disorders, misdiagnosis remains a serious problem in modern psychiatry. Follow up of patients from first admission for psychosis for 10 years or more, an overall 50% of the diagnoses will have changed[190]. This has serious consequences for the patient's outcome, as proper early intervention has been proven to be key to later outcome[191]. Furthermore, the financial impact of schizophrenia is very substantial. The total cost to the UK society for just newly-diagnosed patients over the first 5 years comes to £862 million[192]. 49% of these costs are due to loss of productivity as patients are unable to continue with normal employment. The total societal costs for 2004/05 were approximately £6.7 billion, with £2 billion covering treatment and care. The burden of indirect costs to society amounts to £4.7 billion, and £3.4 billion for lost productivity due to unemployment, absence from work and premature mortality[193].

1.6.1 Overview of currently available antipsychotic drugs

Antipsychotic treatments were accidentally discovered in the 1950s, with chlorpromazine, originally used as an anaesthetic booster, being the first antipsychotic drug[194]. Many treatments then followed

onto the market, having a similar chemical structure (*e.g.* haloperidol, fluphenazine, thioridazine and flupenthixol). These first generation antipsychotics are capable of attenuating predominantly the positive symptoms of schizophrenia. These drugs have, however, important drawbacks. As many as 25-60% of patients either largely do not respond to treatment, or are only partially responsive. Also, these drugs often have only limited effects on the negative symptoms. Furthermore, they cause a range of acute unwanted side effects (extrapyramidal symptoms such as parkinsonism), and long term effects like tardive dyskinesia which can be irreversible. Add-on treatments attenuating these side-effects have their own range of unpleasant side-effects (*e.g*. dry mouth, constipation, delirium and memory deficits), which only further contribute to treatment non-compliance. Other side-effects include sedation, autonomic and cardiovascular effects, and weight gain, which are largely due to off-site actions at other receptors[195].

The second generation of antipsychotics, also known as atypical antipsychotics, were introduced in the 1980s. Due to the wide range of side effects, lack of efficacy for negative symptoms, cognitive deficits and other efficacy issues of the first generation antipsychotics, the second generation antipsychotic clozapine was the first to be released showing superiority to first generation antipsychotics. Other second generation antipsychotics followed soon, including olanzapine, quetiapine, ziprasidone and risperidone. Whereas the first generation agents predominantly act by blocking dopamine D_2 receptors, the second generation block both dopamine D_2 receptors and serotonin 2A receptors. Although these drugs exert less parkinsonian side effects, these treatments do increase the risk of metabolic side effects, including weight gain, hyperglycemia, dyslipidemia and type 2 diabetes. Also, these treatments still mainly treat positive symptoms, but, especially clozapine, also ameliorate the negative symptoms (or do not allow them to worsen) and cognitive symptoms. A drug which can effectively treat negative and cognitive symptoms is yet to be discovered. In addition, there is still a high rate of treatment resistance and poor adherence, making successful treatment difficult[195].

There is one approved third generation drug, aripiprazole. However, its mechanism of action still remains subject to debate. It is thought to either acts as a D_2 partial agonist or function via D_2 functional selectivity. Based on the D_2 partial agonist properties, it has been suggested to be the first 'dopamine stabilizer'. According to this view, in the presence of high extracellular dopamine the partial agonist properties of aripiprazole compete with dopamine as a partial antagonist offering clinical benefit[196]. However, in the presence of low extracellular dopamine, the drug can occupy additional receptors and cause partial activation. Others hypothesize that aripiprazole works as a functionally selective D_2 ligand where its intrinsic activity varies markedly depending on the signalling environment of the D_2 receptor[197]. This is supported by findings from other compounds with a similar profile like aripiprazole, which were found not to be effective for the treatment of schizophrenia. One example of such a

compound is bifeprunox, a full spectrum D_2 receptor partial agonist which acts as a serotonin 1A receptor agonist. Although theoretically similar to aripiprazole, it was not more effective than the placebo when testing in patients, and therefore the drug was rejected by the US FDA[198,199]. Aplindore is another partial agonist with a high affinity for D_2/D_3 receptors but with a low affinity for serotonin 1A receptors. However, this compound has been abandoned as potential treatment for schizophrenia and is being tested in a rat model for Parkinson's disease instead[200].

1.6.2 Towards new drug targets

The lack of relevant animal models for complex psychiatric disorders like schizophrenia represents a major research limitation. The obvious reason for this is that the clinical manifestation of schizophrenia includes symptoms such as hallucinations, delusions and thought disorders, which are specific to humans and impossible to ascertain in animals. Hence, it is impossible to mimic a complex human brain disorder such as schizophrenia in animals. However, the drug development seems to have stalled regarding new treatments for schizophrenia whilst the current ones are still far from perfect and treatment is not effective in 30 to 40% of the patients[201,202]. Combining the issues around misdiagnosis, treatment-resistance, side-effects, unmet treatment of negative and cognitive symptoms and a high financial burden, there is obviously a need for new treatments for schizophrenia.

Although the immune system's involvement in schizophrenia is implicated often, current available treatments do not address this observation[203,204]. A first indication for the potential efficacy of add-on anti-inflammatory treatment in schizophrenia came from a patient in Japan in 2007. This 23-year old Japanese male developed severe pneumonia during his first hospitalisation for catatonic schizophrenia. Until then, treatment had failed to diminish any of the schizophrenia related symptoms. It was decided to prescribe the tetracyclic antibiotic minocycline, which happens to have the capacity to cross the BBB. Two weeks later, his psychiatric symptoms and pneumonia were improved. Minocycline administration was stopped for one week, in which the psychiatric symptoms significantly worsened[205]. This was the first indication that anti-inflammatory treatment could be beneficial for patients. Many studies followed, using minocycline as an add-on treatment. A meta-analysis revealed that minocycline was superior to placebo and especially improved the negative symptoms in some patients[206]. Minocycline has been tested in animal models such as the poly I:C model, and it was shown that in this model minocycline shows preventive effects towards multiple behavioural abnormalities[207]. It was then shown that minocycline selectively inhibits the pro-inflammatory status of microglia[208,209]. Therefore, it is suggested that minocycline is capable to diminish microglia-driven neuroinflammation.

Another potential add-on treatment could be the cyclo-oxygenase 2 (COX-2) inhibitor celecoxib[141]. COX-2 is an enzyme expressed by activated microglia and is involved in the production and release of NO and pro-inflammatory cytokines under inflammatory circumstances. As an add-on treatment in combination with rispiridone, this inhibitor showed significant positive effects with regard to improvement of PANSS scores. In contrast to other antipsychotics, this add-on medication also improved negative symptoms[210]. Another promising add-on treatment to antipsychotics could be aspirin (acetylsalicylic acid), which was shown to reduce the production of pro-inflammatory cytokines by microglia. Aspirin is therefore suggested to protect against neuroinflammation[211]. In addition, aspirin showed beneficial effects in schizophrenia patients in a clinical trial[120]. Yet, in the same trial no beneficial effects could be found for celecoxib. Two meta-analyses focussing on nonsteroidal anti-inflammatory add-on drugs (NSAIDs; celecoxib, aspirin) showed minimal effects on the positive symptoms, however aspirin alone was significantly superior to placebo[120,212]. This research field would benefit from a better understanding of the physiopathology, *e.g.* signalling pathways associated with microglial or peripheral immune system activation. This would offer the possibility to develop novel compounds with efficacy to ameliorate the immune component of the disease. Taken together, these findings suggest that anti-inflammatory add-on treatment could have the potential to reduce schizophrenia symptom severity.

1.6.3 Circumventing the blood brain barrier

One major bottleneck in CNS drug delivery is the BBB, presenting a bottleneck for the development of new neurotherapeutics. The BBB encompasses 400 miles of capillaries, having a 20m^2 surface for exchange. However, transport of small molecules across the BBB is more an exception than the rule, as 98% of all small molecules do not cross the BBB. For a small molecule to pass the BBB, the molecular mass needs to be under 500-Da with high lipid solubility, having less than 8 to 10 hydrogen bonds with solvent water. This leaves a very small number of small molecules with the ability to cross the BBB. The only way to enter the CNS through the BBB is via lipid membranes, protein transporters, receptor mediated transcytosis or adsorptive transcytosis (**Figure 1.5**)[213]. One could say that the doctor prescribing the Japanese patient minocycline struck gold.

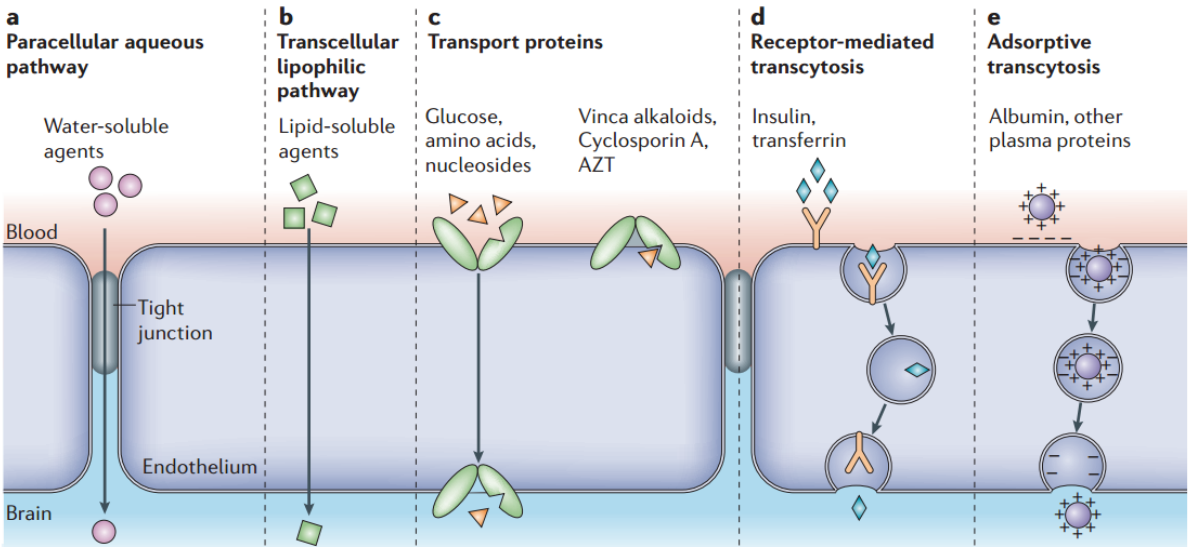

Figure 1.5 Overview of pathways across the blood brain barrier; from Abbott *et al.* (2006). Schematic overview of the endothelial cells representing the BBB. The main routes for molecular traffic across the BBB are demonstrated. **A)** The endothelial cells have tight connections between them, usually not allowing water-soluble compounds to pass, including polar drugs. **B)** The large surface area of the lipid membranes from the endothelial cells offers a diffusive route for lipid-soluble agents. **C**) The surface area contains transport carriers, targeted at specific molecules, for transfer of glucose, amino acids, purine bases, nucleosides, choline and other substances. **D)** Certain proteins can cross the BBB via specific receptors, such as insulin and transferrin. **E)** Plasma proteins, such as albumin, are poorly transported. However, cationisation can increase their uptake by adsorptive mediated endocytosis and transcytosis. Drug delivery depends on pathways illustrated in b to e. Most drugs enter via pathway b, although new drug delivery systems are aiming at using pathway d. *Modified with permission*[213].

When circumventing the BBB via trans-cranial drug delivery, the drug does not spread evenly as it relies on local diffusion. By applying bulk flow, forcing liquid through the brain, only a few more millimetres of spread can be achieved and as the brain lacks a lymphatic system it is therefore not designed for a significant volume flow. Due to demyelination, microglial activation and an astroglial reaction, there are also concerns about the long-term effects of this method. There has been a significant effort in delivering drugs to the brain by inducing a temporary BBB disruption. However, this creates the side effect of potentially toxic and unwanted plasma proteins to enter the CNS. Trans-nasal applications have been attempted as well, but the arachnoid membrane has incredibly tight junctions, not allowing much molecules to pass either. Also, any drug that does enter via the olfactory system, will exit via CSF flow tracts[214].

A more recent CNS drug delivery system in development is a Trojan horse approach, using the receptor-mediated transport system across the BBB (**Figure 1.5d**). By developing an antibody with a functional part able to bind a BBB receptor, it is able to cross-over into the CNS[215]. Another Trojan horse approach is coating liposomes, which contain the drug or protein, with a ligand able to bind a specific receptor allowing a cross-over into the CNS[216]. However, these new systems are far from the clinic as they are still in early test phases.

1.7 Phosphoflow as a discovery platform for microglial polarisation

Despite the evidence of microglial activation and altered circulatory proteins with microglial activation propensity in schizophrenia patients, the effect of circulatory protein abnormalities on microglial activation status has, as yet, not been fully explored. Previous studies relating to neuropsychiatric disorders have attempted to address this by quantifying circulating proteins and then predict their potential net effect on CNS immune cell function based on the annotated activity profile of each protein and their respective BBB permeabilities[106,153,217,218]. This therefore still does not deliver any direct evidence of the potential polarisation and involvement of microglia. To address this need, we have developed a platform with the ability of high-content screening of downstream signalling mechanisms in a human microglia cell line. The platform uses flow cytometry, fluorescent cell barcoding and automated sample preparation to enable parallel and reliable detection of big sample sizes across multiple cell signalling epitopes. Briefly, microglia cells are exposed to serum isolated from patients and healthy controls for 30 minutes and are then fixed, permeabilized and multiplexed using fluorescent cell barcoding. Responses are detected by measuring the changes in phosphorylation status of intracellular epitopes, spanning a wide variety of pathways. By comparing the cellular responses between schizophrenia and controls, altered cellular signalling cascades that are disease specific can be detected. Alternatively, it can be used to assess disease normalisation post treatment, or specific responses associated with effective treatment, by comparing patients prior and post treatment.

By using the application of phosphoflow, the activation or deactivation status of proteins can be directly measured. Phosphorylation is the addition of a phosphate group $(PO_4)^{-3}$ to a molecule, which is biologically critical to protein function and modification. This reversible process allows different amino acids within a protein to be phosphorylated or dephosphorylated, thereby altering protein activity. This mechanism forms the basis of regulating signalling pathways[219]. Furthermore, this regulatory mechanism can happen as fast as under 5 minutes for certain proteins and concentrations[220]. By applying phospho-specific state antibodies, we therefore do not just measure a single protein concentration, but the amount of activated or inhibited protein and therefore achieve a functional read-out covering multiple signalling pathways.

This is the first approach to actually apply functional testing to microglia cells and investigate their potential involvement in schizophrenia. Such a strategy allows for the discovery of disease specific alterations in cell signalling which would otherwise not be detected using gene/protein quantification techniques. Moreover, the application of a cytomics platform will facilitate the detection of changes

in homeostatic and regulatory mechanisms and potential polarisation of these cells that are associated with the disease development and treatment efficacy. As genetic studies have indicated, many different genetic mutations are contributing to schizophrenia[221]. By measuring functional alterations in cell signalling, one might detect a common disease-specific signalling hub which could represent a novel drug target. This approach allows targeting molecular phenotypes known to be disease specific, even though the molecular and genetic mechanisms might yet not be fully understood.

Many different screening platforms were previously used to investigate patient sera contents (*e.g*. mass spectrometry, immunoassay), but the outcome of these studies was limited by the capacity of the technology in hand[222]. Indeed, the use of proteomic platforms is limited by their resolution and the resulting prognostic/diagnostic panel size associated with the disorder therefore as well. By exposing human microglial cells to schizophrenia patient's sera in comparison to sera isolated from healthy controls, we are able to indirectly screen a wider spectrum in patient and control sera by looking at the effects they exert on functional cellular pathways. This in comparison to previous studies, that identified alterations in patient serum through a partial proteome readout with limited resolution and instead predict the potential net effect of the detected proteins on microglia. Previously, our group has used proteomic platforms to demonstrate that immune cells exposed to serum isolated from patients suffering from bipolar disorder or schizophrenia responded differently in comparison to immune cells isolated from healthy volunteers[91,223]. This is the first time that cytomics data will be collected to establish microglial signalling pathways when a human microglial cell line is exposed to patient derived serum. The present study will attempt to shed new light on the biological pathways underpinning microglial activation, when exposed to peripheral blood serum.

1.8 Thesis aim and outline

As outlined above, a disturbance in microglia phenotypes associated with schizophrenia may represent a surrogate disease model for novel drug discovery. However, little is known about how these cells are involved in the schizophrenia disease process and why these never-resting cells with multifaceted and highly dynamic phenotypes are differentially activated[224]. Yet, there is some evidence that anti-inflammatory treatment reducing microglial activation could be beneficial, especially with regard to addressing treatment resistant negative symptomatology common to several neuropsychiatric disorders. The main question we attempted to answer here is whether there are disease-related molecular changes in patient serum capable of causing altered microglia phenotypes and whether or not a differential microglial cell signalling phenotype represents a surrogate disease model for novel drug discovery.

The remaining chapters will be organized as follows:

- **Chapter 2** describes and discusses the experimental and statistical methods used to obtain the findings presented in the subsequent chapters. In addition, it will provide background knowledge regarding the applied techniques.

- **Chapter 3** assesses the robustness and efficacy of the high-content multi-parameter phosphoflow platform for quantification of cell signalling responses.

- **Chapter 4** investigates abnormal cell signalling responses of microglia upon serum exposure from first-onset, drug-naïve schizophrenia patients (n=60) and healthy controls (n=79). In addition, serum was screened for alterations in analyte expression levels using mass spectrometry and multiplexed immunoassays. Finally, the identified microglia signalling sites are targeted with compounds potentially enabling the normalisation of the observed changes associated with schizophrenia serum exposure. This will allow to validate the utility of the resultant microglial cellular phenotype for novel drug discovery.

- **Chapter 5** assesses the effect of *in vivo* antipsychotic treatment on normalisation of the previously identified microglial signalling profile. In addition, human PET brain imaging using a microglia activation tracer allowed for the comparison between *in vivo* neuroinflammation imaging data and *in vitro* changes in microglial intracellular signalling cascades following exposure to serum from patients and controls.

- **Chapter 6** presents a longitudinal study by exposing microglial cells to serum isolated from:
  1) an all-male cohort that consists of first-onset drug-naïve schizophrenia patients (n=9),
  2) the same patients after 6 weeks of olanzapine treatment (n=9),
  3) healthy controls (n=12).

  This study allows for validation of previously identified changes from chapters 4 and 5, as well as the detection of reversal sites associated with successful antipsychotic treatment.

- **Chapter 7** will provide an integrated summary of the findings from chapters 3 to 6 and their implications. It will also provide an outlook on where future studies should focus and how to build upon the presented findings.

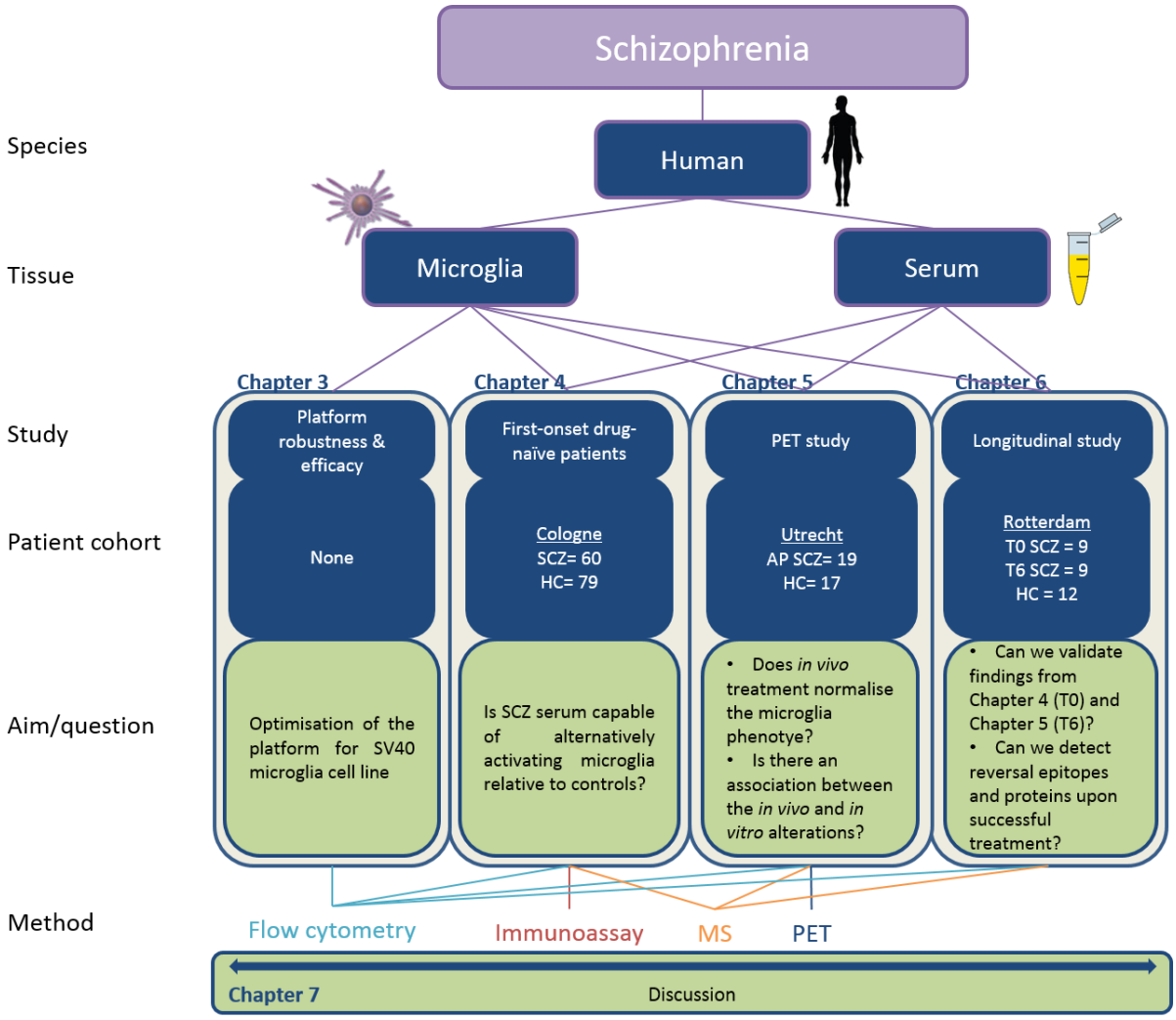

Figure 1.6 Overview of dissertation outline. AP – antipsychotic, HC – healthy controls, MS – mass spectrometry, SCZ – schizophrenia, T0 – first onset, T6 – after 6 weeks of olanzapine treatment.

Chapter 2
Methods Parameters & Backgrounds

Chapter 2 | Methods Parameters & Backgrounds

2.1 Introduction

The Materials and Methods relevant to all studies are described below. Part 1 generally introduces and highlights the principles of the main methods. Part 2 contains all experimental parameters. Methods relevant to specific sub studies are indicated by the following abbreviations where necessary: pro and anti-inflammatory microglial polarization (pro/anti), discovery cohort (DC), antipsychotic treated cohort with PET data (AP), longitudinal study with patients before and after 6 weeks of olanzapine treatment (LS).

2.2 Methods: Backgrounds

2.2.1 Multiplexed Immunoassay

The Luminex xMAP technology combines multiplexed enzyme linked immunoassay (ELISA) with a flow cytometry approach. This platform has the ability to quantify high abundant and low abundant (*e.g.* interleukins) protein concentrations.

Magnetic microspheres of 6.45µm are internally dyed with a fluorescent dye. By giving each set of beads a unique spectral signature, one can create up to 100 different sets of beads. Each type of these beads can be coated with a different antibody against a protein or metabolite. By coupling different types of antibodies to specific sets of dyed beads, one can multiplex these beads and incubate them with a solution of interest (*e.g.* serum). After an analyte is captured by the bead, a biotinylated detection antibody is introduced. The reaction mixture is then incubated with streptavidin-phycoerythrin reagent, which functions as a fluorescent reporter signal.

Upon acquisition, the beads are carried on drive fluid into the acquisition chamber. The microspheres are held in place by a magnetic plate and the beads settle in a monolayer fashion. Red light emitting diodes illuminate the chamber and a camera captures a set of images for bead identification based on their fluorescent pattern. Then green LEDs illuminate the chamber and if the analyte of interest is present the camera will capture an image (**Figure 2.1**). Once done, the magnet moves away from the chamber allowing the microspheres to move out and to flush the chamber. By overlapping the

different images, the different beads with their respective antigen of interest and the concentration can be identified.

This system allows to measure up to 50 different analytes in 50µl of patient sample. This relatively low volume is highly beneficial as patient serum samples are quite rare. However, this system is limited by the available panels set up by the providers, which are mostly focused on metabolic and immune response profiles.

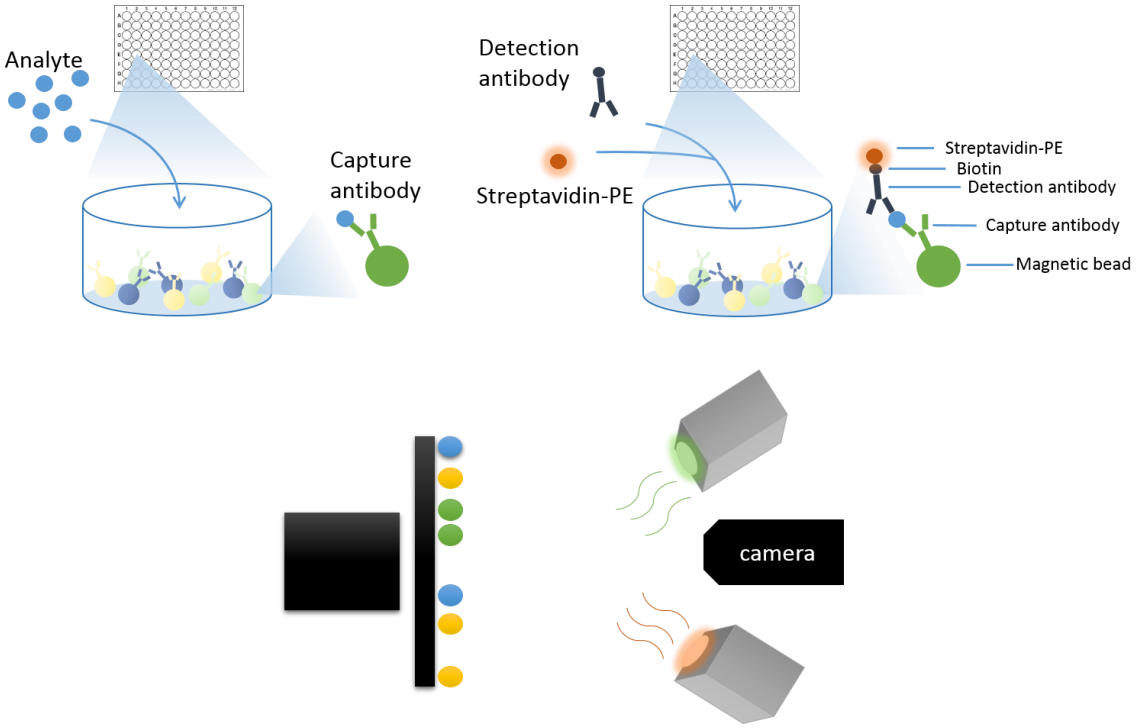

Figure 2.1 Overview of magnetic bead technology used to quantify serum concentration of proteins and small molecules. Labelling of the different magnetic bead-sets, combined with the detection of the fluorescent signal emitted from the phycoerythrin, facilitates detection of the concentration as well as the specific type of antigen. PE: phycoerythrin

2.2.2. Flow Cytometry

Flow cytometry is a laser-based technology using a fluidic system where a stream of single particles is interrogated by the machine's detection system to measure characteristics of biological particles. Flow cytometers are able to make measurements of thousands of individual cells/particles in a matter of seconds. Basically, flow cytometers function as particle analysers. There are two distinct types of flow cytometers, one type can acquire light scattering and fluorescence data from particles and the other type has the powerful addition to sort particles as well. The acronym FACS (fluorescent activated cell sorting) is often used for flow cytometry and is derived from the second type, as flow cytometers were

originally designed to sort. However, nowadays the focus shifted from particle sorting to particle analysis[225]. The following sections will focus on the particle analyser type flow cytometer.

Flow cytometers can be described as four interrelated systems. The first is a fluidic system which transports particles from a sample through the instrument for analysis. The second is an illumination system, used for particle interrogation. The third system is an optical and electronics system for direction, collection and translation of scattered light and fluorescence signals which are the result of illuminated particles. The fourth system is data storage and computer control system which allows data interpretation via the translated light and electrical signals. These signals can be collated and stored for further in-depth analysis (**Figure 2.2**)[226].

When a sample in solution is injected, the particles are randomly distributed in a three-dimensional space. In order to arrange these into a stream of single particles, the sample is injected into a central channel which is enclosed by an outer sheath that contains a faster flowing fluid, the sheath fluid. As the sheath fluid moves, it creates a drag effect on the narrowing central chamber, thereby altering the velocity of the central fluid containing the sample. This causes the central fluid's front flow to have greatest velocity at its midst whilst zero velocity at the wall, thereby creating an alignment of single particles. This process is called hydrodynamic focusing and is of importance for further detection per individual particle and to prevent blockage of the machine's nozzle[226].

After hydrodynamically aligning the particles, each particle will pass a laser interrogation point. Light from the illumination source passes through a focussing apparatus (*e.g*. a lens) before it intercepts the sample stream. The light is then focussed into a beam with an elliptical cross-section, which ensures a constant amount of particle illumination despite any positional variations within the particle stream. When the laser beam strikes a particle, it causes light scattering and fluorescent emission (if the particle is labelled with a fluorophore) which will provide information about the particle's properties[226].

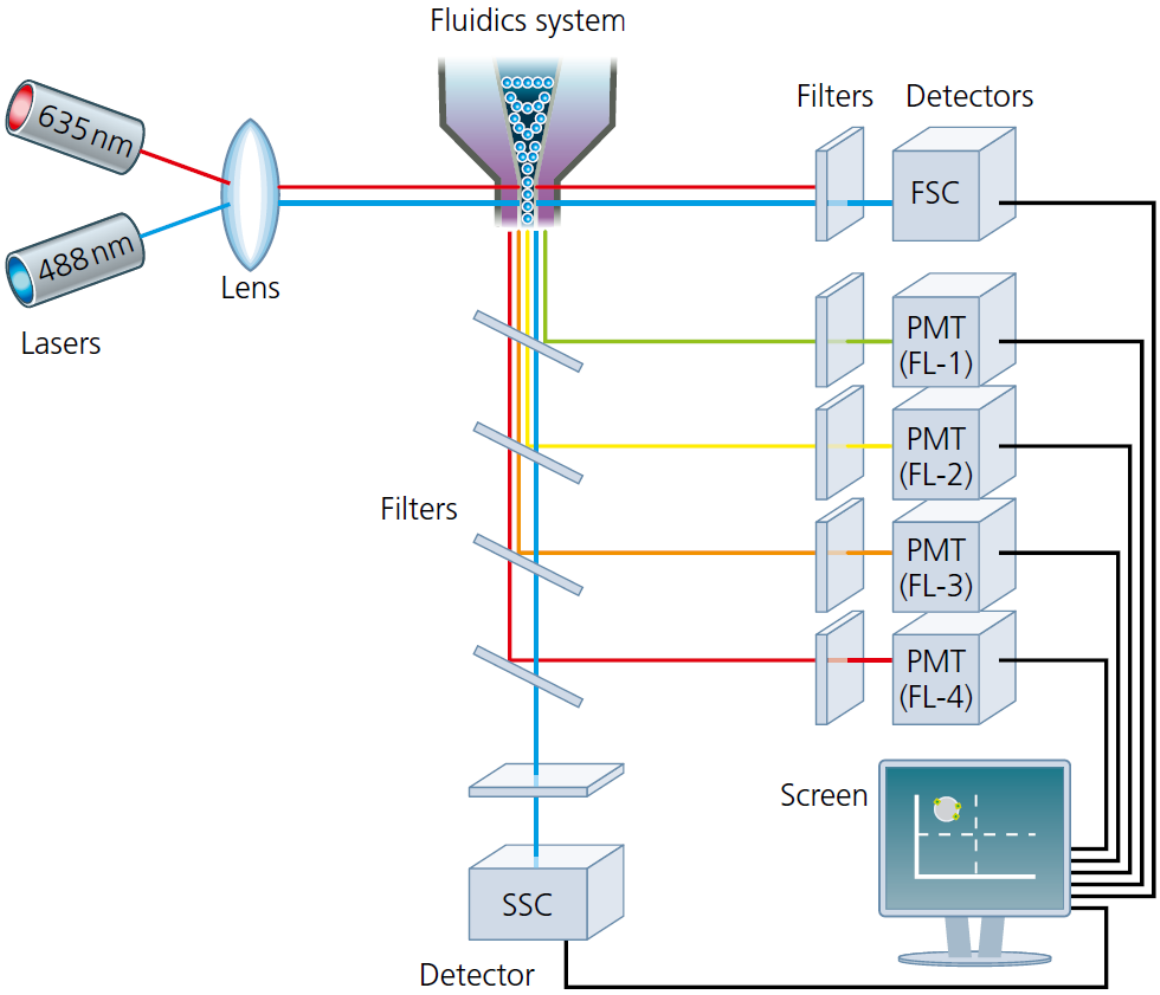

Figure 2.2 A schematic overview of a flow cytometer set up. In this example particles pass the laser detection area one by one. As they hit the laser beams, the emitted light passes multiple filters, allowing certain wavelengths to pass and deflecting others. This allows only certain wavelengths to reach the photodetectors. FSC: forward scatter channel, SSC: side scatter channel, PMT: photomultiplier tube, FL: fluorescence, nm: nanometer. Adapted from[226]

Light that scatters in the forward direction is the result of diffraction and provides information about basic morphology, such as relative cell size as larger particles scatter more light in the forward direction than smaller particles. It is collected by a lens (forward scatter channel; FSC) typically 20° offset from the laser beam axis. The side scatter channel (SSC; 90° angle lens) catches the light that is the result of refracted and reflected light. This light provides information about the granular content within a particle, as well as surface/membrane irregularities[226].

Scattered light yields valuable information about the sample under examination. Correlating FSC and SSC signals allows for the discrimination of cell subpopulations in a heterogeneous sample (*e.g.* PBMCs), viable cells, cellular debris and doublets (more than one cell measured). Usually, scattered light is monitored by the user during acquisition of the sample via computer graphics. Real-time monitoring is highly important during sample acquisition, as it gives information about changes in

scattering patterns, which allows the observation of changes in cellular morphology. Also, it gives information about the instrument, such as problems in the fluidics system[226].

The forward scattered light is first gathered by a collection lens and then directed to a photodiode. This lens collects light at approximately 0.5-10° angles. The photodiode then transmits the light into electronic pulses, proportional to the amount of forward light scattered by the cell/particle. Side scattered light is handled in a similar way as FSC. However, a fraction of the light signal is directed to a highly sensitive photodetector, a photomultiplier tube (PMT), as side scatter accounts for approximately 10% of the emitted light signal which is not as bright as the FSC light. PMTs detect and amplify weak signals and the amount of amplification can be modified by the operator in order to make the PMT more or less sensitive. The side scatter light is eventually converted into a voltage signal[226].

Light is scattered and emitted in all directions (360°) after the laser beams strike an individual cell/particle that has been hydrodynamically focused. Detection of the fluorescent signal is regulated by optical filters, allowing certain wavelengths to pass and blocking others. By placing a filter at an angle of 45° it becomes a dichroic filter/mirror. It performs two functions, one is passing specified wavelengths in the forward direction and the second function is to deflect blocked light at a 90° angle. This deflected light is then directed to a PMT, which will generate a current once the light hits it. This voltage is proportional to the light photons received by the detector. This signal is then converted via algorithms into electrical signals big enough to be plotted graphically. Each measurement within a detector can be regarded a parameter (*e.g*. forward scatter, fluorescence). The data acquired within each parameter is known as events and refers to the number of cells. Flow cytometry allows one to phenotype cells and to detect expression markers or intracellular signalling cascades within cells when using the proper epitope directed at the desired target. For example, when PBMCs are exposed to interleukin-6 (IL-6), STAT3 becomes phosphorylated at Y705. By fixating and permeabilizing the cells, this site can subsequently be stained with a fluorophore linked epitope specifically directed against STAT3 pY705. By comparing antibody read-out from the vehicle and IL-6 stimulated PBMCs, one can calculate a fold change and identify a change in activity levels of this specific epitope. Phosphorylation happens very quickly to allow fast signal processing. By using phospho-specific epitopes that are members of major intracellular signalling pathways, one has the ability to set up a phospho-flow platform to detect fast changes and activity levels in signalling cascades[226,227].

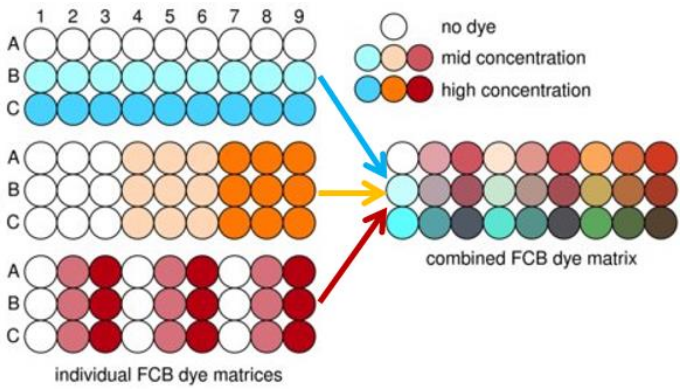

Figure 2.3 Layout of a barcode matrix to encode 27 cell populations. In this example 3 different fluorescent dyes are used to achieve 27 different barcoded populations. Each dye is used in 3 different concentrations. By applying different patterns for the dilutions per dye, a pattern emerges. When these 3 dye patterns are combined, 27 uniquely coded populations emerge. Figure adapted from[230]

This can be taken further by applying multispectral fluorescent tags, allowing multiple epitopes to be read simultaneously from one sample. For example, a sample can be stained simultaneously by three different antibodies if these antibodies have different fluorophores coupled to them. This allows to reliably retrieve read outs per fluorescence channel for the same sample. By combining this multi-parameter set up to a phosphorylation epitope specific panel, it becomes a multi-parameter phospho-flow cytometry platform[228,229].

Epitopes are not the only particles with a multiplexing possibility. The same can be achieved for different cell populations. The fluorescent cell barcode (FCB) signal facilitates high-throughput multi-parameter flow cytometry applications as it allows multiple differently treated cell samples to be combined into a single tube for further multicolour staining and analysis. The FCB signal is achieved by using a unique concentration dependent colour code system of fluorescent dyes per population (**Figure 2.3**). The dyes bind covalently to amine functional groups primarily present on protein lysine side chains and at the N-terminus[230]. This allows the different treated and coded cell samples to be distinguished by their distinct emission wavelengths and intensities once they are merged.

By combining the multi-parameter phospho-flow platform with FCB, in one sample acquisition 192 unique measurements can be achieved (64 populations, 3 epitopes). By upscaling the epitope platform to 62 antibodies, this can become 3968. This amount of unique scenario's acquired in a relatively short time frame is also regarded a high-throughput platform[231,232].

2.2.3 Mass Spectrometry based Targeted Proteomics

Mass spectrometry (MS) allows the investigator to investigate the abundance levels of proteins in a biological sample. MS is an analytical method to determine mass-to-charge ratio (*m/z*; m represents the atomic mass and z the number of elementary charges) of a given analyte. A typical mass analyser consists of three principal components, an ion source to ionise the sample, mass analysers to separate ions based on their *m/z* ratio and a detector to record the analyte signal. Nowadays, an array of MS analysers exist, each having different ionisation methods and detection strategies. Eventually the results are presented in mass spectra, plotting the *m/z* ratio of the observed ions versus ion abundance.

As human samples have a high complexity, a chromatography step is required for sufficient sample separation to reduce sample complexity. Reverse-phase liquid chromatography (RP-LC) is one of the most typically used separation methods in MS[233,234]. The peptides are in an aqueous solvent, comprising the mobile phase, which passes through LC columns coated internally with hydrophobic alkyl chains (stationary hydrophobic phase). The hydrophobic alkyl chains interact with the peptides and separate any peptide with even weak hydrophobicity from the aqueous solutions under acidic conditions. The mobile phase starts under acidic conditions and goes up into a gradient of water plus organic solvent (*e.g*. acetonitrile), for elution of the peptides. The time until a specific peptide gets eluted is called retention time, which is a unique characteristic of a peptide.

The connection between the LC and MS is provided by an electrospray ionisation (ESI) interface, which enables the ionisation and dispersion of the eluate into the mass spectrometer via an emitter needle. In ESI the sample is passed through a metal needle whilst a high voltage potential is applied (~3kV), converting neutral molecules into ions by inducing either a loss or gain of charge and forcing the spraying of charged droplets from the needle. As these droplets have the same polarity as the needle, they are pushed away from it. These droplets become smaller and smaller towards the focusing cone until they fall apart into charged analytes, due to solvent evaporation. The droplets shrink until the surface tension is unable to sustain the charge that increases in relation to the shrinking droplet surface. The droplets then explode and charged molecules enter the mass spectrometer[235] (**Figure 2.4**). This is regarded a soft approach in that there is very little residual energy retained by the peptide, therefore a lower amount of energy is necessary later on to achieve peptide fragmentation.

Depending on the aim of the study, analytical MS platforms can comprise out of two methods, global profiling (section 2.2.3.1) or targeted quantification (section 2.2.3.2). Global profiling methods employ non-direct analyses (shotgun proteomics) that yield protein inventories accompanied by quantitative measurements. In targeted MS, only specific proteins of interest are sought and quantified.

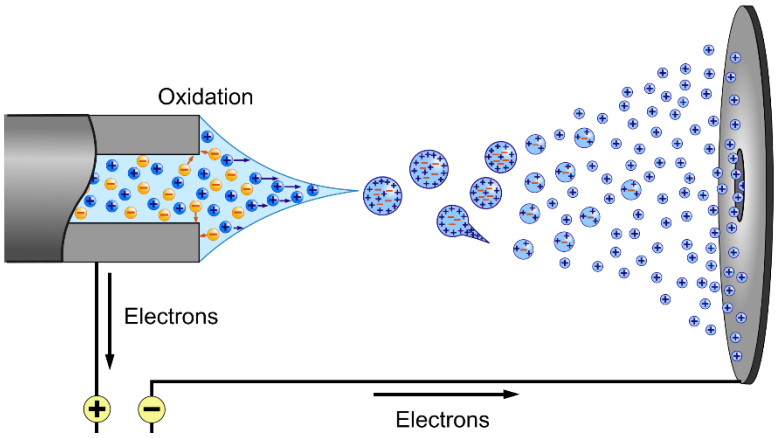

Figure 2.4 Schematic overview of the ESI interface. On the left is the needle containing the sample and on the right the sample cone and the different electric potential between them. A positive charge is applied to the needle, causing positive charges to be repelled from the needle whereas negative charges are attracted. Spray droplets consisting of analytes have positive charges on the outside surface. As they travel towards the sampling cone, solvent evaporates and the surface charge increases. Once the charge density reaches a critical limit, the droplet explodes into single charged molecules. *Figure adapted and printed with permission from Andreas Dahlin.*

2.2.3.1 Non-hypothesis driven mass spectrometry

MS can be achieved in a non-hypothesis driven way to show global protein profiling, when no analyte is primed to be measured *a priori*. One should take into account though that this method will only detect hundreds of proteins the most, whilst a complex sample such as serum, can contain up to a million different proteins (including splice variants)[236]. This type of measurement is achieved with a double quadrupole type of mass spectrometer, using a shot gun approach. This method is advantageous when one is running a discovery study to detect initial differences between different groups[237]. However, although the hypothesis free approach is great to show the overall proteomic picture, the limitation however is that quantitation is not as good as targeted methods (due to sample complexity, ion suppression etc.). However, it can be used for relative quantification.

2.2.3.2 Hypothesis driven mass spectrometry

Another approach is using targeted mass spectrometry, where one does prime the system *a priori* to screen for specific analytes of interest, a hypothesis-driven approach, in order to quantify a set of selected proteins of interest via for example multiple reaction monitoring (MRM)[238]. MRM is an exceptionally sensitive and selective method for targeted peptide abundances in a complex sample, which allows precise quantitation of the analytes of interest. MRM-MS has only recently proven to be suitable for use in pre-clinical studies to rapidly screen and measure large numbers of candidate

proteins in complex patient samples necessary for biomarker validation[237,239,240]. The basic principle typically utilises a triple quadrupole-MS (QQQ) equipped with two mass filters (Q1, Q3) and a collision cell (**Figure 2.5**).

The first quadrupole is designed to transmit only the selected precursor peptide ion (*m/z*) into the second quadrupole were the collision chamber generates fragments by collision-induced dissociation (using inert gases like helium, nitrogen or argon)[241]. The fragments containing a signature fragment ion or ions of particular *m/z* are allowed to continue into the third quadrupole for monitoring. Consequently, peptide quantitation is based on measuring the intensity of the product ions selected from the third quadrupole (**Figure 2.5**)[222]. The intensity is measured via specific precursor-fragment ion pairs of the target analyte, retention time (from the RP-LC) and signal intensity. This approach has the benefit for accurate quantitation of target peptides by including internal standards in the sample. An MRM-MS assay offers multiplexing capability of many target analytes in a single RP-LC run.

The internal standard allows to detect intensities of the analytes of interest, by spiking the endogenous sample with heavy isotope labelled peptides (*e.g.* ^{13}C and ^{15}N)[242]. These peptides are synthetically produced with identical characteristics (*e.g*. ionisation, retention time, fragmentation pattern and extraction efficiency) in comparison to the native peptide of interest with the exception of the heavy label causing a mass shift. This allows the measurement of heavy (spiked) and light (endogenous) peptides simultaneously. This aids internal standardization to correct for downstream variability in instrument sensitivity[243]. Furthermore, the targeted peptide acquisition windows and the chosen transitions can be validated by using these known heavy peptides.

A quadrupole mass analyser consists of four parallel hyperbolic rods which enable passage and filtering of ions. This is done in a vacuum environment by the use of electrically generated fields. Rods opposite to the central pathway represent either both positive or negative electrodes with a constant direct and alternating current. The ions are filtered on their mass-to-charge ratio. A positive ion will be repelled by positive rods as will a negative ion be repelled by negative rods. The chance of an ion hitting the rods depends on the *m/z* ratio, the strength of the field and the frequency of the oscillation. The positive rods only let pass high *m/z* ratio ions, whereas the negative rods only let ions with small *m/z* ratio pass. The overlap between these 2 opposites decides which distinct *m/z* ratio subset of ions can pass, thereby allowing them to reach the detector. This can be modified by a shift in the electrical parameters.

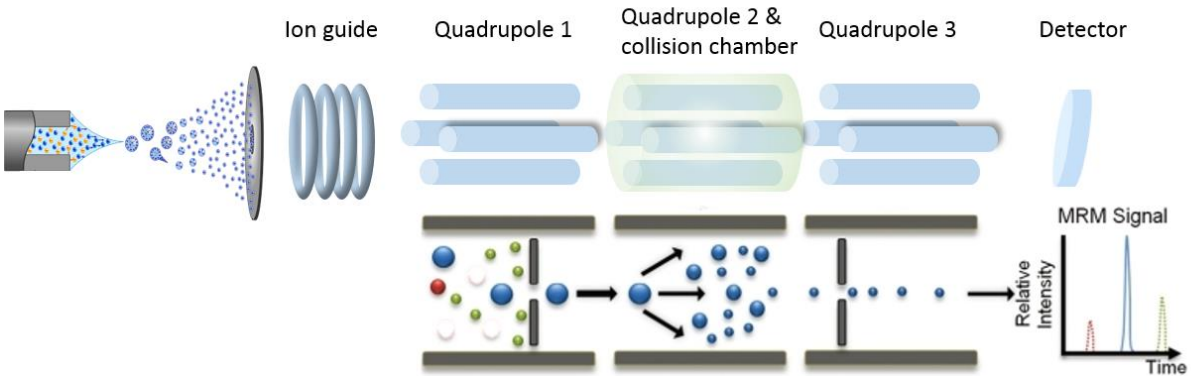

Figure 2.5 Schematic overview of analyte filtering across the three quadrupoles. In this overview ions and heavy isotope labelled peptides have been selected for charge state in the ion guide. The first quadrupole functions as a peptide selection filter, only allowing preselected, known masses pass of endogenous and heavy labelled peptides. The second quadrupole stabilizes the ion pass and functions as a collision cell, causing fragmentation. The third quadrupole filters for selected fragment ions (transition) and the peptide precursor ions are quantitated by the relative intensity of their peak area. *Bottom half of the quadrupole figure is reprinted and modified with permission*[222].

2.3 Methods: Parameters

2.3.1 Clinical sample recruitment and collection

For the DC study antipsychotic drug-naïve first-onset schizophrenia patients (n=60) and healthy control (n=79) serum donors were recruited at the Department of Psychiatry, University of Cologne, Germany. For the AP study, antipsychotic treated schizophrenia patients (n=19) and matched controls (n=17) were recruited from the Department of Psychiatry of the University Medical Center Utrecht (UMCU), Utrecht, The Netherlands, and the Department of Psychiatry of the Academic Medical Center (AMC), Amsterdam, The Netherlands. For the LS study, first-onset drug-naïve schizophrenia patients before (n=9) and after (n=9) six weeks of treatment with the atypical antipsychotic olanzapine, in addition to matched controls (n=12), were recruited from the Erasmus Medical Centre, Rotterdam, the Netherlands. The respective medical faculty ethical committees approved the study protocols. Informed consent was given in writing by all participants and clinical investigations were conducted according to the Declaration of Helsinki and Standards for Reporting of Diagnostic Accuracy[244].

Diagnoses of neuropsychiatric pathology were conducted by experienced psychiatrists and were based on the Diagnostic and Statistical Manual of Mental Disorders-IV (DSM-IV). The Positive and Negative Syndrome Scale (PANSS) was used to measure the severity of symptom subtypes. The exclusion criteria for patients and controls included additional neuropsychiatric diagnoses other than schizophrenia, other neurological disorders including epilepsy, mental retardation, multiple sclerosis, immune/autoimmune disorders, infectious disease, metabolic disorders including diabetes, obesity (body mass index above 30), cardiovascular disease, hepatic and renal insufficiency, gastrointestinal

disorders, endocrine disorders including hypo-/hyperthyroidism and hypo-/hypercortisolism, respiratory diseases, cancer, severe trauma, substance abuse including psychotropic drugs and alcohol, somatic medication with brain side-effects, somatic medication affecting the immune system including glucocorticoids, anti-inflammatory/immunomodulating drugs and antibiotics.

Blood samples were collected between 8:00 and 12:00 am into S-Monovette 7.5 mL serum tubes (Sarstedt). Samples were left at room temperature for 2 hours, according to standard protocols to allow clotting, and centrifuged at 4000g for 5 min to remove particulate material. Resulting supernatants were aliquoted and stored at -80°C in Low Binding microcentrifuge tubes (Eppendorf, Hamburg, Germany). Patients and controls were fasted for blood sample collection.

2.3.2 Microglia cell culture

The SV40 immortalized human microglial cell line (Applied Biological Materials, Richmond, Canada) was cultured at 37°C/5% CO_2 in Roswell Park Memorial Institute (RPMI) media (RPMI-1640 with sodium bicarbonate; Sigma-Aldrich, St. Louis, MO, USA) containing 10% (volume to volume; v/v) heat-inactivated fetal bovine serum FBS (Life Technologies, Waltham, MA USA), 50 U/ml penicillin and 50 µg/ml streptomycin (Life Technologies), 2 mM L-alanyl-L-glutamine dipeptide (Life Technologies)) in tissue culture polystyrene flasks (passage 1-8; Greiner Bio-One, Kremsmünster, Austria) followed by Cell Bind-treated polystyrene hyperflasks (passage 9-10; Corning, Corning, NY, USA). Cells were seeded at a density of 20,000 cells/cm^2 and reseeded when they reached 70% confluency. Detachment of the cells was achieved using 0.25 mg ml^{-1} trypsin (Lonza, Basel, Switzerland) in Dulbecco's phosphate-buffered saline solution (PBS; Sigma–Aldrich) for 10 min at 37°C followed by washing the cells twice with complete RPMI at 300g for 5 min. Cells at intermediate passages were cryopreserved at 5*10^6 cells/ml in RPMI-1640 with sodium bicarbonate (Sigma-Aldrich), 20% FBS (v/v; Life Technologies), 50 U/ml penicillin and 50 µg/ml streptomycin (Life Technologies), 2 mM L-alanyl-L-glutamine dipeptide (Life Technologies) and 10% dimethyl sulfoxide (DMSO; v/v; Sigma–Aldrich). The cells were free of mycoplasma contamination as determined by polymerase chain reaction testing.

2.3.3 Stimulation of microglia

Stimulation is defined broadly as the exposure of microglial cells to either human serum or individual chemical or biological ligands (**Table 2.1**) which have the potential to perturb resting state cell signalling dynamics by either increasing or decreasing the expression of cell signalling epitopes. All stocks and dilutions of serum and ligands were stored at -80°C and repeated freeze-thaw cycles were avoided. Microglial cells (passage 10) were resuspended in stimulation RPMI medium (stRPMI; RPMI-

1640 with sodium bicarbonate (Sigma-Aldrich), 10% (v/v) heat-inactivated fetal bovine serum FBS (Life Technologies) and 2 mM L-alanyl-L-glutamine dipeptide (Life Technologies)) at $25*10^6$ cells/ml via a 30 µm cell strainer (Partec, Görlitz, Germany). The cell suspension was distributed across a 96-well polypropylene plate (Starlab, Hamburg, Germany; $0.75*10^6$ cells/well) and rested for 45 min at 37°C. Individual clinical serum samples at 25:75 (v/v) mixture of cRPMI to serum, chemical/ biological ligands or the vehicle (stRPMI with final DMSO concentration 0.1% (v/v)) were added to different wells of the 96-well plate using a Biomek NX liquid handler (Beckman Coulter, High Wycombe, UK) with integrated compact shaker-heater-cooler system (Inheco, Martinsried, Germany) and incubated at 37°C for 30 min. The final concentration of DMSO in all conditions was 0.1% (v/v). Vehicle wells represented 40% and 13% of the total wells assayed for microglial polarization and clinical serum exposure studies respectively, and were spaced evenly across each 96-well plate. Positive controls (calyculin A and staurosporine) wells represented 13% and 6% of the total wells assayed for microglial polarization and clinical serum exposure studies respectively, and were spaced evenly across each 96-well plate. Serum samples from each clinical group were randomized across different plate positions. The concentration range for IL-4 and IL-13 dose response studies was selected to encompass the maximum and minimum physiological serum concentrations reported in healthy and disease states[245–248]. Stimulation was halted by fixation for 10 min at 37°C using paraformaldehyde (Sigma-Aldrich) in PBS at a final concentration of 1.6% (through the v/v addition from an 80 gr L^{-1} PFA stock solution).

Table 2.1. List of ligands used for incubation with SV40 microglial cells. *recombinant human protein, Conc – concentration, Pro – pro-inflammatory, anti – anti-inflammatory, DC – discovery cohort, AP – antipsychotic treated cohort, LS – follow-up study.

Ligands	Abbreviation	Function	Class	Pro vs anti	DC	AP	LS	Assay conc.	Conc. unit	CAS number	Supplier
aripiprazole	aripiprazole	3rd generation antipsychotic, D2R/5-HT1A/2CR partial agonist, 5-HT2A/7R antagonist	treatment drug			AP		10	μM	ab120764	Abcam
bone morphogenetic protein 7 *	BMP7	bone morphogenetic protein (BMP) R2 agonist	Cytokine	Anti stim				0.1	μg/ml	NA	Novus-Biotechne
calyculin A	calyculin A	protein phosphatase 1/2A (PP1/2A) inhibitor	Positive control - activator	P/A	DC	AP	AI	1	μM	101932-71-2	Tocris
clozapine	clozapine	2nd generation antipsychotic, 5-HT2R/D4R antagonist	treatment drug			AP		10	μM	0444	Tocris
haloperidol	haloperidol	1st generation antipsychotic, D2/3R inverse agonist	treatment drug			AP		10	μM	52-86-8	Sigma
interferon-γ *	IFN-γ	interferon γ (IFNγ) R agonist	Cytokine	Pro stim				0.1	μg/ml	NA	eBioscience
interleukin-13 *	IL-13	interleukin-13 (IL-13) R agonist	Cytokine	Anti stim				0.1	μg/ml	NA	Novus-Biotechne
interleukin-1β *	IL-1β	interleukin-1β (IL-1β) R agonist	Cytokine	Pro stim				0.1	μg/ml	NA	eBioscience
interleukin-23 *	IL-23	interleukin-23 (IL-23) R agonist	Cytokine	Pro stim				0.1	μg/ml	NA	eBioscience
interleukin-4 *	IL-4	interleukin-4 (IL-4) R agonist	Cytokine	Anti stim				0.1	μg/ml	NA	eBioscience
minocycline	minocycline	tetracycline antibiotic	treatment drug	Pro inh	DC			10	μM	13614-98-7	Sigma
olanzapine	olanzapine	2nd generation antipsychotic, 5-HT2AR/D2R antagonist/inverse agonist	treatment drug			AP	AI	0.02/0.2/2/20/200	μM	132539-06-1	Tocris
rapamycin	rapamycin	mammalian target of rapamycin 1 (mTORC1) inhibitor	treatment drug	Pro inh	DC			5	μM	53123-88-9	Tocris
staurosporine	staurosporine	protein kinase inhibitor	Positive control - inhibitor	P/A	DC	AP	AI	5	μM	62996-74-1	Enzo Life Sciences
transforming growth factor-β *	TGF-β	transforming growth factor (TGF) R2 agonist	Cytokine	Anti stim				0.1	μg/ml	NA	eBioscience
tumor necrosis factor-α *	TNF-α	tumor necrosis factor (TNF) R agonist	Cytokine	Pro stim				0.1	μg/ml	NA	eBioscience

2.3.4 Fluorescent cell barcoding

The multiplex fluorescent cell barcode signal facilitates high-throughput multi-parameter flow cytometry applications as it allows multiple differently treated cell samples to be combined into a single tube for further multicolour staining and analysis. The FCB signal was achieved by using a unique concentration dependent colour code system of fluorescent dyes per population. This allows the different treated and coded cell samples to be distinguished by their distinct emission wavelengths and intensities once they are merged.

Stock solutions of barcoding dyes CBD 450 (BD Biosciences, San Jose, CA, USA), CBD 500 (BD Biosciences) and DL 800 (Thermo Scientific, Waltham, MA, USA) were prepared as per the manufacturer's instructions in DMSO in polypropylene 96-well plates and stored at -80°C. Final concentrations of CBD 450 (0.000, 0.015, 0.075, 0.300 mg/ml) were combined with CBD 500 (0.000, 0.038, 0.188, 0.750 mg/ml) and DL 800 (0.000, 0.011, 0.033, 0.100 µg/ml) to resolve 64 barcoded cell populations[249,250]. Fixed cells were washed with PBS and permeabilized in 100 µl ice cold methanol (Thermo Fisher Scientific) for 20 min at 2°C using a Biomek NX liquid handler. The barcoding dyes were diluted in ice cold PBS and 100 µl/well added to the suspension of cells in methanol. The final concentration of DMSO from the barcoding dyes at this stage was 3.5% (v/v). The barcoding reaction was incubated in the dark for 30 min at 2°C and the cells were washed five times in ice cold FACS buffer (PBS with 5 gr L^{-1} bovine serum albumin (Sigma-Aldrich)). The barcoding wells were pooled, washed and resuspended at 1*10^{6} cells/ml in FACS buffer for staining.

2.3.5 Intracellular staining of cell signalling epitopes

To inhibit the non-specific Fc-gamma receptor (FcγR)-mediated binding of staining antibodies, human FcγR-binding inhibitor (eBioscience, San Diego, CA, USA) was added to the suspension of fixed-permeabilized-barcoded cells at a final concentration of 20% (v/v) and incubated for 20 min in the dark at room temperature, as per the manufacturer's instructions. The cell suspension was distributed across a 96-well polypropylene plate and stained using a Biomek NX liquid handler with fluorescently-conjugated anti-human antibodies against intracellular signaling epitopes (**Table 2.2**)[250,251] for 60 min in the dark at room temperature, as per the manufacturer's instructions. Antibodies were purchased from BD Biosciences, Cell Signaling Technology (Danvers, MA, USA), Merck Millipore (Darmstadt, Germany) and Bioss (Woburn, MA, USA). Antibodies against intracellular epitopes were used in groups of three antibodies per plex. The cells were washed twice and resuspended in FACS buffer at 2*10^{6} cells/ml for acquisition.

Table 2.2 List of antibodies used to detect intracellular cell signalling epitopes. SE* - only used in the LS study, P – pro-inflammatory, A – anti-inflammatory, SE – serum exposure

Epitopes	Clone	Isotype	Gene	Class	Fluorochrome	P/A	SE	Supplier
4EBP1 (pT36/pT45)	M31-16	Ms IgG_1, κ	EIF4EBP1	Akt	AF 488	P/A	SE	BD Biosciences
4EBP1 (pT69)	M34-273	Ms IgG_1, κ	EIF4EBP1	Akt	PE		SE	BD Biosciences
Akt (pS473)	M89-61	Ms IgG_1, κ	AKT1	Akt	AF 647 (P/A, SE, Z), PE (Z), AF 488 (Z)	P/A	SE	BD Biosciences
Akt (pT308)	J1-223.371	Ms IgG_1, κ	AKT1	Akt	PE	P/A	SE	BD Biosciences
Akt1	55/PKBa/Akt	Ms IgG_1, κ	AKT1	Akt	AF 488	P/A	SE	BD Biosciences
CD221 (pY1131)	K74-218	Ms IgG_1, κ	IGF1R	Akt	AF 647		SE	BD Biosciences
eIF4E (pS209)	J77-925	Ms IgG_1, κ	EIF4E	Akt	PE		SE	BD Biosciences
Ezrin (pY353)	I66-386	Ms IgG_1	EZR	Akt	PE		SE	BD Biosciences
GSK-3α/β	4G-1E	Ms IgG_1	GSK3B	Akt	AF 488	P/A	SE	Merck Millipore
GSK-3β (pS9)	D85E12	R IgG	GSK3B	Akt	PE	P/A	SE	Cell Signaling Technology
GSK-3β (pT390)	polyclonal	R IgG	GSK3B	Akt	PE		SE	Bioss
IRS-1 (pY896)	K9-211	Ms IgG_{2a}, κ	IRS1	Akt	AF 647		SE	BD Biosciences
mTOR (pS2448)	O21-404	Ms IgG_1, κ	mTOR	Akt	PE		SE*	BD Biosciences
mTOR (S2481)	D9C2	R IgG	mTOR	Akt	PE		SE*	Cell Signaling Technology
PDPK1 (pS241)	J66-653.44.17	Ms IgG_1, κ	PDPK1	Akt	AF 488	P/A	SE	BD Biosciences
S6 (PS235/PS236)	N7-548	Ms IgG_1, κ	RP26	Akt	AF 647	P/A	SE	BD Biosciences
S6 (PS240)	N4-41	Ms IgG_1, κ	RPS6	Akt	AF 488		SE	BD Biosciences
β-Catenin (pS45)	K63-363	Ms IgG_1, κ	CTNNB1	Akt	AF 647	P/A	SE	BD Biosciences
IRF-7 (pS477/pS479)	K47-671	Ms IgG_1, κ	IRF7	IL1R/ TLR	AF 488	P/A	SE	BD Biosciences
IκBα	25/IkBa/MAD-3	Ms IgG_1	NFKBIA	IL1R/ TLR	PE	P/A	SE	BD Biosciences
NF-κB p65 (pS529)	K10-895.12.50	Ms IgG_{2b}, κ	RELA	IL1R/ TLR	AF 647	P/A	SE	BD Biosciences
c-Cbl (pY700)	47/c-Cbl	Ms IgG_1	CBL	IR/AR	PE		SE	BD Biosciences
c-Cbl (pY774)	29/c-Cbl	Ms IgG_1	CBL	IR/AR	PE		SE	BD Biosciences
Pyk2 (pY402)	L68-1256.272	Ms IgG_{2b}, κ	PTK2B	IR/AR	PE	P/A	SE	BD Biosciences
SLP-76 (pY128)	J141-668.36.58	Ms IgG_1, κ	LCP2	IR/AR	AF 647	P/A	SE	BD Biosciences
Src (pY418)	K98-37	Ms IgG_1, κ	SRC	IR/AR	AF 488	P/A	SE	BD Biosciences
WIP (pS488)	K32-824	Ms IgG_1, κ	WIPF1	IR/AR	PE	P/A	SE	BD Biosciences
Zap70 (pY319)/Syk (pY352)	17A/P-ZAP70	Ms IgG_1	SYK, ZAP70	IR/AR	AF 647	P/A	SE	BD Biosciences
SHP2 (pY542)	L99-921	Ms IgG_1, κ	PTPN11	JAK/Stat	AF 647	P/A	SE	BD Biosciences
Stat1 (N-Terminus)	1/Stat1	Ms IgG_1	Stat1	JAK/Stat	PE	P/A	SE	BD Biosciences
Stat1 (pS727)	K51-856	Ms IgG_1, κ	Stat1	JAK/Stat	AF 488	P/A	SE	BD Biosciences
Stat1 (pY701)	4a	Ms IgG_{2a}	Stat1	JAK/Stat	AF 488 (P/A), AF 647 (SE)	P/A	SE	BD Biosciences
Stat3	M59-50	Ms IgG1, λ	Stat3	JAK/Stat	PE	P/A	SE	BD Biosciences
Stat3 (pS727)	49/p-Stat3	Ms IgG_1	Stat3	JAK/Stat	AF 488	P/A	SE	BD Biosciences
Stat3 (pY705)	4/P-Stat3	Ms IgG_{2a}, κ	Stat3	JAK/Stat	AF 647 (P/A, SE, C), PE (C), AF 488 (C)	P/A	SE	BD Biosciences
Stat4 (pY693)	38/p-Stat4	Ms IgG_{2b}	Stat4	JAK/Stat	PE	P/A	SE	BD Biosciences
Stat5 (pY694)	47/Stat5(pY694)	Ms IgG_1, κ	Stat5A, Stat5B	JAK/Stat	AF 647	P/A	SE	BD Biosciences
Stat6 (pY641)	18/P-Stat6	Ms IgG_{2a}	Stat6	JAK/Stat	PE	P/A	SE	BD Biosciences

Bcl-2 (pS70)	N46-467	Ms IgG_1	BCL2	MAPK	AF 647	P/A	SE	BD Biosciences
ERK1/2 (pT202/pY204)	20A	Ms IgG_1	MAPK1, MAPK3	MAPK	AF 647	P/A	SE	BD Biosciences
MAPKAPK-2 (pT334)	P24-694	Ms IgG_1, κ	MAPKAPK	MAPK	AF 488		SE	BD Biosciences
MEK1 (pS218)/MEK2 (pS222)	O24-836	Ms IgG_1, κ	MAP2K1, MAP2K2	MAPK	AF 647	P/A	SE	BD Biosciences
MEK1 (pS298)	J114-64	Ms IgG_1, κ	MAP2K1	MAPK	PE		SE	BD Biosciences
p38 MAPK (pT180/pY182)	36/p38 (pT180/pY182)	Ms IgG_1, κ	MAPK14, MAPK13, MAPK12	MAPK	AF 647	P/A	SE	BD Biosciences
p53 (acK382)	L82-51	Ms IgG_1, κ	TP53	MAPK	AF 647	P/A	SE	BD Biosciences
p53 (pS37)	J159-641.79	Ms IgG_1, κ	TP53	MAPK	AF 488		SE	BD Biosciences
CD140b (pY857)	J24-618	Ms IgG_1, κ	PDGFRB	Other	AF 488		SE	BD Biosciences
CrkL (pY207)	K30-391.50.80	Ms IgG_{2a}, κ	CRKL	Other	AF 488	P/A	SE	BD Biosciences
Rb (pS780)	J146-35	Ms IgG_1, κ	RB1	Other	AF 488		SE	BD Biosciences
Smad2 (pS465/pS467)/Smad3 (pS423/pS425)	O72-670	Ms IgG_1, κ	SMAD2	Other	PE	P/A	SE	BD Biosciences
CREB (pS133) / ATF-1 (pS63)	J151-21	Ms IgG_1, κ	CREB1	PKA	AF 647	P/A	SE	BD Biosciences
PKA RIIα (pS99)	I65-856.286	Ms IgG_1, κ	PRKAR2A	PKA	AF 647	P/A	SE	BD Biosciences
PKA RIIβ (pS114)	47/PKA	Ms IgG_1	PRKAR2B	PKA	AF 488	P/A	SE	BD Biosciences
p120 Catenin (pS268)	9a.390	Ms IgG_{2b}, κ	CTNND1	PKC	AF 488		SE	BD Biosciences
p120 Catenin (pS879)	K114-1011	Ms IgG_1, κ	CTNND1	PKC	PE		SE	BD Biosciences
p120 Catenin (pT310)	22/p120 (pT310)	Ms IgG_1, κ	CTNND1	PKC	AF 488	P/A	SE	BD Biosciences
PKC-α	3/PKCα	Ms IgG_{2b}	PRKCA	PKC	AF 488	P/A	SE	BD Biosciences
PKC-α (pT497)	K14-984	Ms IgG_1, κ	PRKCA	PKC	AF 647	P/A	SE	BD Biosciences
PKC-θ	27/PKCθ	Ms IgG2a, κ	PRKCQ	PKC	PE	P/A	SE	BD Biosciences
PKC-θ (pT538)	polyclonal	R IgG	PRKCQ	PKC	PE		SE	Bioss
PLC-γ1	10/PLCgamma	Ms IgG_1	PLCG1, PLCG2	PKC	PE	P/A	SE	BD Biosciences
PLC-γ1 (pY783)	27/PLC	Ms IgG_1	PLCG1	PKC	AF 647	P/A	SE	BD Biosciences
PLC-γ2	K86-1161	Ms IgG_1, κ	PLCG2	PKC	AF 488	P/A	SE	BD Biosciences
PLC-γ2 (pY759)	K86-689.37	Ms IgG_1, κ	PLCG2	PKC	AF 647	P/A	SE	BD Biosciences

2.3.6 Data acquisition using flow cytometry

Microglial cell suspensions were acquired using an eight color FACSVerse flow cytometer (BD Biosciences) with 405, 488 and 640 nm laser excitation at an average flow rate of 2 µl/sec and an average threshold event rate of 1,000-2,000 events/sec. Multicolor Cytometer Setup and Tracking (CST) beads (BD Biosciences) were used for quality control and standardization of photomultiplier tube (PMT) detector voltages across multiple experimental runs. Fluorescence compensation for cell signaling epitopes was conducted using anti-mouse IgGκ antibody capture beads (Bangs Laboratories, Fishers, IN, USA) labelled separately with anti-human STAT3 (pY705) (4/P-STAT3) Alexa Fluor 488 (AF488; BD Biosciences), anti-human STAT3 (pY705) (4/P-STAT3) phycoerythrin (PE; BD Biosciences) and anti-human STAT3 (pY705) (4/P-STAT3) Alexa Fluor 647 (AF647; BD Biosciences) alongside single stain controls with maximum and minimum concentrations of each barcoding dye.

2.3.7 Multiplexed immunoassays

A targeted panel of 17 immunomodulatory serum proteins previously linked to schizophrenia and involved in P/A microglial signalling was measured via multiplex magnetic bead-based immunoassays according to manufacturer's instructions (Milliplex MAP, Merck Millipore, **Table 2.3**). The serum analytes were chosen from Human High Sensitivity T Cell Panel (HSTCMAG-28SK), Human Complement Panel 2 (HCMP2MAG-19K) and the TGF-β Magnetic Bead 3 Plex Kit (TGFBMAG-64K-03). Briefly, serum samples, analyte standards, background and quality control samples were distributed on 96-well plates. After incubation with magnetic beads, samples were washed and incubated with detection antibodies, followed by addition of the streptavidin-phycoerythrin reagent. Data was acquired on a MAGPIX instrument (Merck Millipore) and analysed with xPONENT software version 4.2.1324.0 (Merck Millipore). The inter-assay coefficient of variation was <10% for the Human Complement Panel 2, <5% for the Human High Sensitivity T Cell Panel and <5% for the TGF-β Magnetic Bead 3 Plex multiplex assays respectively.

.

Table 2.3 List of analytes measured in clinical serum samples by multiplexed immunoassays. Proteins are ordered alphabetically. Proteins are labelled as not applicable (NA) where the protein target is not associated to a unique 'Uniprot ID' or is the metabolic product of more than one 'Uniprot ID'.

Protein	Uniprot Entry	Uniprot ID	Milliplex panel
Complement C1q	NA	NA	HCMP2MAG-19K
Complement C3	CO3_HUMAN	P01024	HCMP2MAG-19K
Complement C3b	NA	NA	HCMP2MAG-19K
Complement C4	NA	NA	HCMP2MAG-19K
Granulocyte macrophage colony-stimulating factor	CSF2_HUMAN	P04141	HSTCMAG-28SK
Interferon-γ	IFNG_HUMAN	P01579	HSTCMAG-28SK
Interleukin-10	IL10_HUMAN	P22301	HSTCMAG-28SK
Interleukin-12(p70)	NA	NA	HSTCMAG-28SK
Interleukin-13	IL13_HUMAN	P35225	HSTCMAG-28SK
Interleukin-1β	IL1B_HUMAN	P01584	HSTCMAG-28SK
Interleukin-2	IL2_HUMAN	P60568	HSTCMAG-28SK
Interleukin-4	IL4_HUMAN	P05112	HSTCMAG-28SK
Interleukin-6	IL6_HUMAN	P05231	HSTCMAG-28SK
Transforming growth factor-β1	TGFB1_HUMAN	P01137	TGFBMAG-64K-03
Transforming growth factor-β2	TGFB2_HUMAN	P61812	TGFBMAG-64K-03
Transforming growth factor-β3	TGFB3_HUMAN	P10600	TGFBMAG-64K-03
Tumor necrosis factor-α	TNFA_HUMAN	P01375	HSTCMAG-28SK

2.3.8 Mass spectrometry based targeted proteomics

Serum proteins were extracted and digested in a 96-well plate format using a Biomek NX Liquid handler as described[252,253]. Briefly, serum samples were diluted 22 times in 50 mM ammonium bicarbonate (Sigma-Aldrich) solution in low-bind Eppendorf 96-well plates (Scientific Laboratory Supplies, West Bridgford, UK). Disulphide bonds were reduced using 5 mM dithiothreitol (Sigma-Aldrich) for 30 min at 60°C. Subsequently, cysteine alkylation was achieved by incubation with 10 mM iodoacetamide (Sigma-Aldrich) for 30 min at room temperature in the dark. Serum samples were then digested overnight for 17 hours using trypsin (Promega, Madison, WI, USA) at a 1:50 enzyme to protein ratio. The reaction was stopped with 0.03% formic acid (v/v; Sigma-Aldrich). A mixture of stable isotope-labelled peptides, containing heavy (^{13}C and ^{15}N) lysine (K) or arginine (R) residues (JPT Peptide Technologies) corresponding to each targeted peptide, was spiked into the digested serum samples as an internal standard prior to the multiple reaction monitoring (MRM) based targeted protein analysis.

A panel of 77 proteins previously linked to neuropsychiatric disorders was selected for the targeted proteomic analysis (**Table 2.4**). The corresponding 147 peptides were monitored using an Agilent 6495 LC QQQMS coupled with an Agilent 1290 UPLC system operated in dynamic MRM mode. Peptide selection was determined using the following criteria: (i) unique sequence identity as verified using

Protein BLAST (http://blast.ncbi.nlm.nih.gov/Blast.cgi), (ii) less than 18 amino acids in sequence length, (iii) no missed cleavages, (iv) no glycosylation sites, (v) no potential ragged ends. Peptides containing amino acids prone to modifications were avoided and only selected when no alternative options were available. Instrument parameters were optimized for all peptides and their transitions as described[253,254]. A minimum of three interference-free transitions were selected and monitored for both the targeted peptide and the corresponding heavy isotope-labelled internal standard peptide, in a 0.8 min retention time window. Peptide separation was performed on an Agilent AdvanceBio Peptide Map column (2.1 x150mm 2.7-micron) at 50°C. Mobile phases used were A (0.1% formic acid in water; v/v) and B (0.1% formic acid in 100% acetonitrile; v/v) with a linear gradient from 3% to 35% B in 45 min at a flow rate of 300 nl/min.

Table 2.4 Complete list of analytes measured in clinical serum samples by MRM mass spectrometry.

Protein	*Uniprot Entry*	*Uniprot ID*	*Peptide sequence*
Angiotensinogen	ANGT_HUMAN	P01019	SLDFTELDVAAEK
Angiotensinogen	ANGT_HUMAN	P01019	FMQAVTGWK
Angiotensinogen	ANGT_HUMAN	P01019	ALQDQLVLVAAK
Antithrombin-III	ANT3_HUMAN	P01008	FDTISEK
Antithrombin-III	ANT3_HUMAN	P01008	LPGIVAEGR
Apolipoprotein A-I	APOA1_HUMAN	P02647	EQLGPVTQEFWDNLEK
Apolipoprotein A-I	APOA1_HUMAN	P02647	ATEHLSTLSEK
Apolipoprotein A-II	APOA2_HUMAN	P02652	SPELQAEAK
Apolipoprotein A-IV	APOA4_HUMAN	P06727	IDQNVEELK
Apolipoprotein A-IV	APOA4_HUMAN	P06727	ISASAEELR
Apolipoprotein A-IV	APOA4_HUMAN	P06727	ALVQQMEQLR
Apolipoprotein C-I	APOC1_HUMAN	P02654	EFGNTLEDK
Apolipoprotein C-I	APOC1_HUMAN	P02654	EWFSETFQK
Apolipoprotein C-II	APOC2_HUMAN	P02655	ESLSSYWESAK
Apolipoprotein C-II	APOC2_HUMAN	P02655	TAAQNLYEK
Apolipoprotein C-III	APOC3_HUMAN	P02656	GWVTDGFSSLK
Apolipoprotein C-III	APOC3_HUMAN	P02656	DALSSVQESQVAQQAR
Apolipoprotein C-IV	APOC4_HUMAN	P55056	AWFLESK
Apolipoprotein D	APOD_HUMAN	P05090	VLNQELR
Apolipoprotein E	APOE_HUMAN	P02649	LEEQAQQIR
Apolipoprotein E	APOE_HUMAN	P02649	ALMDETMK
Apolipoprotein E	APOE_HUMAN	P02649	AATVGSLAGQPLQER
Apolipoprotein E	APOE_HUMAN	P02649	LGPLVEQGR
Apolipoprotein E	APOE_HUMAN	P02649	SELEEQLTPVAEETR
Apolipoprotein F	APOF_HUMAN	Q13790	SLPTEDCENEK
Apolipoprotein L1	APOL1_HUMAN	O14791	VNEPSILEMSR
Apolipoprotein L1	APOL1_HUMAN	O14791	LNILNNNYK
Apolipoprotein L1	APOL1_HUMAN	O14791	VTEPISAESGEQVER
Apolipoprotein M	APOM_HUMAN	O95445	SLTSCLDSK
Apolipoprotein M	APOM_HUMAN	O95445	AFLLTPR
C4b-binding protein α chain	C4BPA_HUMAN	P04003	EDVYVVGTVLR
C4b-binding protein α chain	C4BPA_HUMAN	P04003	YTCLPGYVR
C4b-binding protein α chain	C4BPA_HUMAN	P04003	FSAICQGDGTWSPR
Carbonic anhydrase 1	CAH1_HUMAN	P00915	ADGLAVIGVLMK
Carboxypeptidase B2	CBPB2_HUMAN	Q96IY4	YPLYVLK
Carboxypeptidase B2	CBPB2_HUMAN	Q96IY4	DTGTYGFLLPER
CD5 antigen-like	CD5L_HUMAN	O43866	EATLQDCPSGPWGK
Ceruloplasmin	CERU_HUMAN	P00450	NNEGTYYSPNYNPQSR

Ceruloplasmin	CERU_HUMAN	P00450	EVGPTNADPVCLAK
Clusterin	CLUS_HUMAN	P10909	FMETVAEK
Clusterin	CLUS_HUMAN	P10909	IDSLLENDR
Coagulation factor XII	FA12_HUMAN	P00748	CFEPQLLR
Coagulation factor XII	FA12_HUMAN	P00748	VVGGLVALR
Complement C1q subcomponent subunit C	C1QC_HUMAN	P02747	TNQVNSGGVLLR
Complement C1r	C1R_HUMAN	P00736	YTTEIIK
Complement C1r subcomponent-like protein	C1RL_HUMAN	Q9NZP8	GSEAINAPGDNPAK
Complement C1s subcomponent	C1S_HUMAN	P09871	TNFDNDIALVR
Complement C1s subcomponent	C1S_HUMAN	P09871	LLEVPEGR
Complement C2	CO2_HUMAN	P06681	HAIILLTDGK
Complement C3	CO3_HUMAN	P01024	VYAYYNLEESCTR
Complement C3	CO3_HUMAN	P01024	AGDFLEANYMNLQR
Complement C4-A	CO4A_HUMAN	P0C0L4	VLSLAQEQVGGSPEK
Complement C4-A	CO4A_HUMAN	P0C0L4	ITQVLHFTK
Complement C4-A	CO4A_HUMAN	P0C0L4	DFALLSLQVPLK
Complement component C6	CO6_HUMAN	P13671	TLNICEVGTIR
Complement component C6	CO6_HUMAN	P13671	SEYGAALAWEK
Complement component C8 α chain	CO8A_HUMAN	P07357	MESLGITSR
Complement component C9	CO9_HUMAN	P02748	VVEESELAR
Complement component C9	CO9_HUMAN	P02748	LSPIYNLVPVK
Complement factor B	CFAB_HUMAN	P00751	EELLPAQDIK
Complement factor B	CFAB_HUMAN	P00751	DISEVVTPR
Complement factor B	CFAB_HUMAN	P00751	YGLVTYATYPK
Complement factor B	CFAB_HUMAN	P00751	DLLYIGK
Complement factor H	CFAH_HUMAN	P00751	CFEGFGIDGPAIAK
Corticosteroid-binding globulin	CBG_HUMAN	P08185	ITQDAQLK
Corticosteroid-binding globulin	CBG_HUMAN	P08185	GTWTQPFDLASTR
Fibronectin	FINC_HUMAN	P02751	YSFCTDHTVLVQTR
Ficolin-3	FCN3_HUMAN	O75636	YGIDWASGR
Gelsolin	GELS_HUMAN	P06396	AGALNSNDAFVLK
Gelsolin	GELS_HUMAN	P06396	SEDCFILDHGK
Haptoglobin	HPT_HUMAN	P00738	DYAEVGR
Haptoglobin	HPT_HUMAN	P00738	VTSIQDWVQK
Haptoglobin	HPT_HUMAN	P00738	VGYVSGWGR
Hemoglobulin subunit α	HBA_HUMAN	P69905	MFLSFPTTK
Hemoglobulin subunit α	HBA_HUMAN	P69905	FLASVSTVLTSK
Hemoglobulin subunit γ-1	HBG1_HUMAN	P69891	MVTAVASALSSR
Hemopexin	HEMO_HUMAN	P02790	VDGALCMEK
Hemopexin	HEMO_HUMAN	P02790	NFPSPVDAAFR
Heparin cofactor 2	HEP2_HUMAN	P05546	IAIDLFK
Heparin cofactor 2	HEP2_HUMAN	P05546	FAFNLYR
Histidine-rich glycoprotein	HRG_HUMAN	P04196	ADLFYDVEALDLESPK
Histidine-rich glycoprotein	HRG_HUMAN	P04196	DSPVLIDFFEDTER
Igα-1 chain C region	IGHA1_HUMAN	P01876	DASGVTFTWTPSSGK
Igα-1 chain C region	IGHA1_HUMAN	P01876	TPLTATLSK
Igα-2 chain C region	IGHA2_HUMAN	P01877	DASGATFTWTPSSGK
Igγ-1 chain C region	IGHG1_HUMAN	P01857	FNWYVDGVEVHNAK
Igγ-2 chain C region	IGHG2_HUMAN	P01859	GLPAPIEK
Igγ-2 chain C region	IGHG2_HUMAN	P01859	TTPPMLDSDGSFFLYSK
Igγ-3 chain C region	IGHG3_HUMAN	P01860	DTLMISR
Igγ-3 chain C region	IGHG3_HUMAN	P01860	NQVSLTCLVK
Igμ chain C region	IGHM_HUMAN	P01871	YAATSQVLLPSK
Igμ chain C region	IGHM_HUMAN	P01871	QIQVSWLR
Inter-α-trypsin inhibitor heavy chain H1	ITIH1_HUMAN	P19827	LDAQASFLPK
Inter-α-trypsin inhibitor heavy chain H1	ITIH1_HUMAN	P19827	GSLVQASEANLQAAQDFVR
Inter-α-trypsin inhibitor heavy chain H2	ITIH2_HUMAN	P19823	FYNQVSTPLLR
Inter-α-trypsin inhibitor heavy chain H2	ITIH2_HUMAN	P19823	IQPSGGTNINEALLR
Inter-α-trypsin inhibitor heavy chain H4	ITIH4_HUMAN	Q14624	GPDVLTATVSGK
Inter-α-trypsin inhibitor heavy chain H4	ITIH4_HUMAN	Q14624	ETLFSVMPGLK
Kininogen-1	KNG1_HUMAN	P01042	DFVQPPTK
Kininogen-1	KNG1_HUMAN	P01042	DIPTNSPELEETLTHTITK

Lumican	LUM_HUMAN	P51884	SLEDLQLTHNK
N-acetylmuramoyl-L-alanine amidase	PGRP2_HUMAN	Q96PD5	GCPDVQASLPDAK
N-acetylmuramoyl-L-alanine amidase	PGRP2_HUMAN	Q96PD5	TFTLLDPK
Phosphatidylinositol-glycan-specific phospholipase D	PHLD_HUMAN	P80108	NQVVIAAGR
Pigment epithelium-derived factor	PEDF_HUMAN	P36955	LQSLFDSPDFSK
Pigment epithelium-derived factor	PEDF_HUMAN	P36955	TVQAVLTVPK
Pigment epithelium-derived factor	PEDF_HUMAN	P36955	ELLDTVTAPQK
Pigment epithelium-derived factor	PEDF_HUMAN	P36955	DTDTGALLFIGK
Plasma kallikrein	KLKB1_HUMAN	P03952	LSMDGSPTR
Plasma protease C1 inhibitor	IC1_HUMAN	P05155	TNLESILSYPK
Plasma protease C1 inhibitor	IC1_HUMAN	P05155	FQPTLLTLPR
Plasminogen	PLMN_HUMAN	P00747	FVTWIEGVMR
Protein AMBP	AMBP_HUMAN	P02760	TVAACNLPIVR
Protein AMBP	AMBP_HUMAN	P02760	ETLLQDFR
Prothrombin	THRB_HUMAN	P00734	SGIECQLWR
Prothrombin	THRB_HUMAN	P00734	ELLESYIDGR
Retinol-binding protein 4	RET4_HUMAN	P02753	YWGVASFLQK
Retinol-binding protein 4	RET4_HUMAN	P02753	QEELCLAR
Serotransferrin	TRFE_HUMAN	P02787	EGYYGYTGAFR
Serum albumin	ALBU_HUMAN	P02768	AAFTECCQAADK
Serum albumin	ALBU_HUMAN	P02768	ETYGEMADCCAK
Serum albumin	ALBU_HUMAN	P02768	QNCELFEQLGEYK
Serum amyloid P-component	SAMP_HUMAN	P02743	IVLGQEQDSYGGK
Sex Hormone-binding globulin	SHBG_HUMAN	P04278	IALGGLLFPASNLR
Tetranectin	TETN_HUMAN	P05452	EQQALQTVCLK
Transthyretin	TTHY_HUMAN	P02766	AADDTWEPFASGK
Transthyretin	TTHY_HUMAN	P02766	VLDAVR
Vitronectin	VTNC_HUMAN	P04004	DVWGIEGPIDAAFTR
Vitronectin	VTNC_HUMAN	P04004	DWHGVPGQVDAAMAGR
α-1-antichymotrypsin	AACT_HUMAN	P01011	EQLSLLDR
α-1-antichymotrypsin	AACT_HUMAN	P01011	EIGELYLPK
α-1-antichymotrypsin	AACT_HUMAN	P01011	ADLSGITGAR
α-1-antitrypsin	A1AT_HUMAN	P01009	LSITGTYDLK
α-1-antitrypsin	A1AT_HUMAN	P01009	SVLGQLGITK
α-1-antitrypsin	A1AT_HUMAN	P01009	SPLFMGK
α-1B-glycoprotein	A1BG_HUMAN	P04217	CLAPLEGAR
α-1B-glycoprotein	A1BG_HUMAN	P04217	ATWSGAVLAGR
α-1B-glycoprotein	A1BG_HUMAN	P04217	SGLSTGWTQLSK
α-2-antiplasmin	A2AP_HUMAN	P08697	FDPSLTQR
α-2-antiplasmin	A2AP_HUMAN	P08697	DFLQSLK
α-2-antiplasmin	A2AP_HUMAN	P08697	DSFHLDEQFTVPVEMMQAR
α-2-HS-glycoprotein	FETUA_HUMAN	P02765	HTLNQIDEVK
α-2-HS-glycoprotein	FETUA_HUMAN	P02765	FSVVYAK
α-2-macroglobulin	A2MG_HUMAN	P01023	NEDSLVFVQTDK
α-2-macroglobulin	A2MG_HUMAN	P01023	AIGYLNTGYQR
β-2-glycoprotein 1	APOH_HUMAN	P02749	EHSSLAFWK
β-2-glycoprotein 1	APOH_HUMAN	P02749	VSFFCK

2.3.9 Statistical data analysis

Statistical analysis was conducted using R (version 3.3.1; R Core Team) and GraphPad Prism (version 5.00; GraphPad Software, Inc.). Clinical groups were determined using the conditional Wilcoxon rank-sum test for continuous variables[255] and Fisher's exact test for categorical variables[256] to ensure that there were no significant differences in gender, age, body mass index, cannabis and nicotine use and ethnicity for available clinical data between groups.

2.3.9.1 Statistical approach for flow cytometry data analysis

Flow cytometry data was analyzed in FCS 3.0 file format using Flow Jo v.10.0.8 (Tree Star, Ashland, OR, USA) and Kaluza Analysis v.1.3 (Beckman Coulter) software. Samples containing less than 100 cell counts were excluded from further analysis.

Quality control assessment was conducted using principal component analysis to check for experimental artifacts in the data related to positional effects within and across 96-well plates, barcoding dye fluorescence spillover, sample viability, cell counts and clinical group. Z' factor analysis was used to demonstrate that the functional assay was robust for high-throughput screening independently of the position of a stimulant within the multiplexing array and the antibody detection fluorophore (Z' factor values of 0.5-1.0 indicate excellent robustness of the assay for high-throughput screening)[257].

For the determination of stimulant activity, the MFIs per stained epitope (n= 62) for clinical serum samples and positive controls were compared between each stimulant and the vehicle treatment across experimental replicates (n=3) using the conditional Wilcoxon rank-sum test, employing the exact distribution for obtaining the *P*-value[258]. The same test was also applied for each stimulant per functional fluorescence channel (AF647, AF488 and PE) in the unstained condition in order to ascertain that the observed stimulant activity was not an artefact of stimulant auto-fluorescence or fluorescence spill over from adjacent channels (collectively termed 'background fluorescence'). For instances where the unstained comparison of stimulant MFI to vehicle MFI was found to be significantly changed for a particular fluorescence channel, the epitopes labelled in the corresponding fluorescent channel were only regarded as being active if the stained MFI response had a 10% greater fold-change, or was in the opposite direction, compared to the unstained MFI response[250].

Response ratios were computed for stimulant activity which was both significant (conditional Wilcoxon rank-sum test, $P<0.05$) and did not represent a construct of background fluorescence. The response ratio was calculated as the median stimulant MFI divided by the median vehicle MFI across all three

replicates. If the response ratio was <1, *i.e.* the stimulant resulted in a decrease in MFI with respect to the vehicle, the response is reported as a negative fold change (-1/response ratio). Epitopes which did not show significant responses for serum samples in at least one clinical group were excluded from subsequent analysis. Stain indices of the antibodies were calculated across the replicates, in the absence of stimulation, as the median MFI of the antibody stained sample divided by the median MFI of the corresponding unstained control.

Differences in epitope expression, following serum exposure, between clinical groups were investigated using a linear mixed effects model with a random intercept to account for different samples and their replicate measurements. The model was adjusted for optional covariates, age and gender, which were selected in a stepwise procedure for each epitope individually using Bayesian Information Criterion. To account for the unknown distribution of the data, the null distribution was computed for the test statistic by randomly permuting sample labels 10,000 times in order to determine the *P*-value for each epitope.

For the compound analysis, the response ratio was calculated per epitope as the median compound MFI divided by median vehicle MFI across all experimental replicates. The significance of the observed compound activity was computed using a one-tailed Wilcoxon rank-sum test to evaluate the hypothesis of expected compound directionality relative to the vehicle. Measures described above were used to ascertain that compound activity was not an artefact of background fluorescence.

2.3.9.2 Statistical approach for multiplexed immunoassay analysis

For multiplexed immunoassay data, quality control assessment was conducted using principal component analysis to identify data artefacts. Positional effects between assay plates for each analyte measurement were identified using a student's T test ($P < 0.05$) and subsequently normalized using median scaling between plates. A linear regression model was used to analyse differences in protein concentration between clinical groups. Differences in protein abundance between clinical groups were investigated using a linear regression model, adjusting for covariates age and gender via stepwise selection as described above.

2.3.9.3 Statistical approach for mass spectrometry data analysis

For the MRM, raw data files were imported to Skyline (version 3.1.0) software for data analysis[259]. Peptide transition peak integration was achieved using Savitzky–Golay smoothing[260] and data was

manually inspected to confirm the correct peak identification. The area ratios of the endogenous peptide transition peaks to the corresponding internal standard heavy peptide transition peaks were exported for subsequent analysis. Following log_2-transformation to stabilize data variance, the overall abundance of each peptide was determined by selecting the most abundant transition between corresponding peptide isotopes across samples. Technical variation across sample measurements was controlled for using median scaling normalization based on the heavy isotope internal standard. Two control samples were identified as outliers using principal component analysis and excluded from further analysis. Differences in peptide abundance between clinical groups were investigated using a linear regression model, adjusting for covariates age and gender via stepwise selection and applying permutation testing as described above.

2.3.9.3 Statistical approach for positron emission tomography data analysis

Pre-processing was done by filtering samples on specific activity of the tracer (>1.5 standard deviation below mean) combined with tracer activity based on the ratio of specifically bound radioligand to that of non-displaceable radioligand in tissue, in order to guarantee reliable tracer scan data. Differences in tracer binding potential between healthy controls and patients were assessed using a one-way analysis of variance (ANOVA) with group as between-subjects factor and brain region as within-subjects factor, followed by *post-hoc* correction Tukey's honest significant difference test. Correlations were measured by Pearson's r (two-tailed).

Data was visualized using Flow Jo v. 10.0.8, R software, GraphPad Prism 5, Excel 2016 and Adobe Illustrator.

Chapter 3
Platform Robustness, Sensitivity & Efficacy

Chapter 3 | Platform Robustness, Sensitivity & Efficacy

3.1 Introduction

To construct a platform capable of identifying cell signalling responses to human serum in the human SV40 microglia cell line, fluorescent cellular barcoding was employed[249] to multiplex up to 64 independent microglial stimulation reactions. In addition, multi-parameter phospho-specific flow cytometry[251] was employed to simultaneously measure the activation status of up to 62 intracellular signalling epitopes spanning key microglial cell signalling pathways[261]. Therefore, the high-content platform performance was tested for its robustness with respect to its multiplexing abilities and reproducibility in terms of reliable detection of altered cellular signalling responses. The potential of these cells to function as a sensor when exposed to complex mixtures (*e.g.* serum) will be evaluated. In addition, the actual sensitivity towards microglial polarization will be evaluated in terms of specific cytokine responses based on previously well characterized microglia signalling networks[262].

Details of this platform and its application to primary human PBMCs have been reported previously[250]. Whereas PBMCs are small non-sticky cells which grow in suspension, which is optimal for flow cytometry, the SV40-microglia cell line is a slightly larger sticky, adherent cell type. Therefore, the platform had to be adjusted and optimised to this specific cell characteristic. Furthermore, the sensitivity and multiplexing capacity of these cells had to be determined. Some of the work presented in this chapter including specific figures and text is based on a collaborative paper, drafted by Dr. Santiago Lago[263].

3.2 Results

3.2.1 Multiplexing different cell populations

In order to achieve the measurement of 64 differently treated microglia populations across the phospho-specific antibody panel by flow cytometry, the fluorescent cell barcoding (FCB) technology was utilised. By applying FCB, reproducible antibody staining across differently stimulated cell populations can be achieved whilst cell numbers will not be compromised. Initially, SV40 microglia cells were dispensed into 64 wells of a 96 well plate and each well was treated identically. First, the cells were fixed and permeabilized.

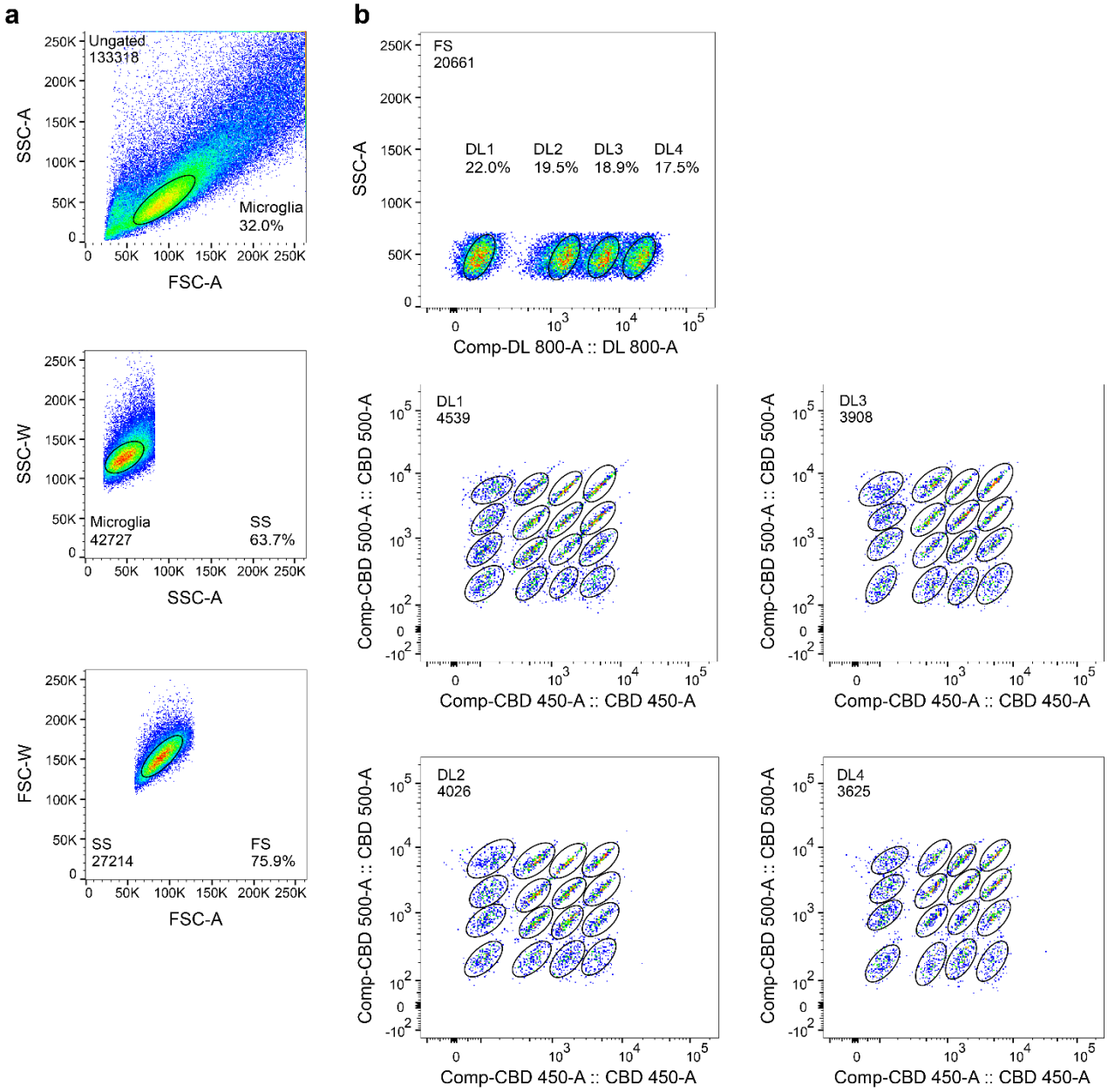

Figure 3.1 Gating structure for the functional analysis of 64 fluorescently cell barcoded populations of SV40 microglia cells. **(a)** Viable SV40 microglial cells were gated (FSC-A vs SSC-A), followed by single-cell discrimination (SSC-A vs SSC-W and FSC-A vs FSC-W). **(b)** 64 barcoded cell populations were resolved within the single-cell microglial gate using DL 800, CBD 450 and CBD 500 dyes. Single-cell microglia were first gated for DL800 populations (DL1 – DL4). Within each DL 800 population, microglia were gated for CBD 450 vs CBD 500 populations (16 populations per single DL 800 gate). Each population corresponds to a different treatment or vehicle condition. For each of the 64 populations, cell count and median MFI values across Alexa Fluor 488, phycoerythrin and Alexa Fluor 647 fluorescence detection channels were exported. MFI - median fluorescence intensity.

The microglia were subsequently stained with the FCB dye mixture. This mixture was plated in advance in a 96-well plate containing 64 uniquely colour coded populations across the wells, each with its unique set of different concentrations of three fluorescent dyes (CBD 450, CBD 500 and DL 800). As each cell population received a unique fluorescent colour code, all the cells could be pooled into a single falcon. The FCB dyes bind covalently to amine functional groups primarily present on protein lysine side chains and at the N-terminus[230]. This fluorescent label allows the 64 differently treated and coded cell samples to be distinguished by their distinct emission wavelengths and intensities once they are merged (**Figure 3.1**).

Next, the same experimental set up was repeated, but this time with different stimulants and plate lay outs. As the full antibody panel depends on the read-out of three different fluorescent channels, the 64 pooled microglia populations were stained with three antibodies. Each antibody targeted the same epitope and is from the same clone, but the difference is in the three different fluorescent tags labelled to the epitope for the detection of reproducible and accurate readout of the antibody signal across the three different fluorescent channels. Based on previous experiments on this panel[250], it was decided to employ 30 minute incubations. This is a time frame consistent with other publications showing time courses regarding inducing phosphorylation changes in cellular signalling cascades[264]. One full plate of 64 populations was stimulated with vehicle, whereas another plate of microglia was stimulated with 50ng/ml IL-6. Both plates were fixed, permeabilized and barcoded. Each pooled set of 64 populations was then stained with anti-human STAT3 pY705 in phycoerythrin (PE; **Figure 3.2a**), Alexa Fluor 647 (AF 647; **Figure 3.2b**) and Alexa Fluor 488 (AF 488; **Figure 3.2c**). All antibodies came from the same clone. The Coefficient of Variations (CVs) across the 64 wells were 7.9% for PE, 8.7% for AF 647 and 6.5% for AF 488, respectively.

To test the reproducibility of the panel further, 1μM of calyculin A or vehicle was dispensed in either a horizontal or vertical alternating pattern with respect to the barcode matrix (**Figure 3.3 a, b**). Each pooled set was then stained with anti-human AKT (pS473) AF 488 (**Figure 3.3 c, d**), anti-human AKT (pS473) AF 647 (**Figure 3.3 e, f**) and anti-human AKT (pS473) PE (**Figure 3.3 g, h**). All antibodies came from the same clone. After unravelling the barcoded populations, the original horizontal and vertical stimulation lay outs could be reliably and accurately traced back through the AKT (pS473) read outs. The Z' factor values were 0.72 and 0.69 for PE, 0.76 and 0.77 for AF 647 and 0.77 and 0.76 for AF 488 for horizontal and vertical orientations respectively, putting the assay in the category of an excellent assay[257]. This indicates that calyculin A (1 μM) at Akt (pS473) could be measured in a reproducible manner and with a sufficient dynamic range independently of the position of the stimulant within the multiplexing array and the antibody detection fluorophore used.

a

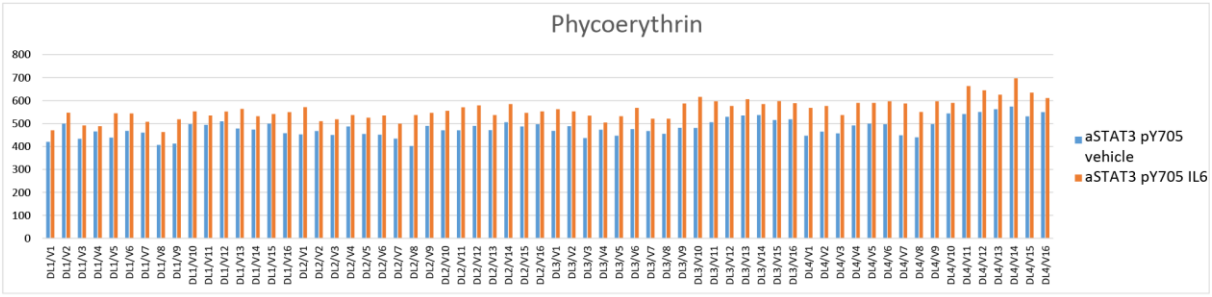

b

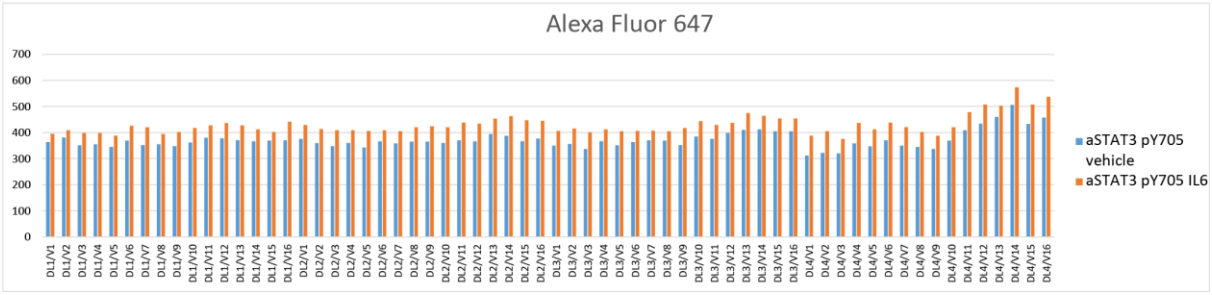

c

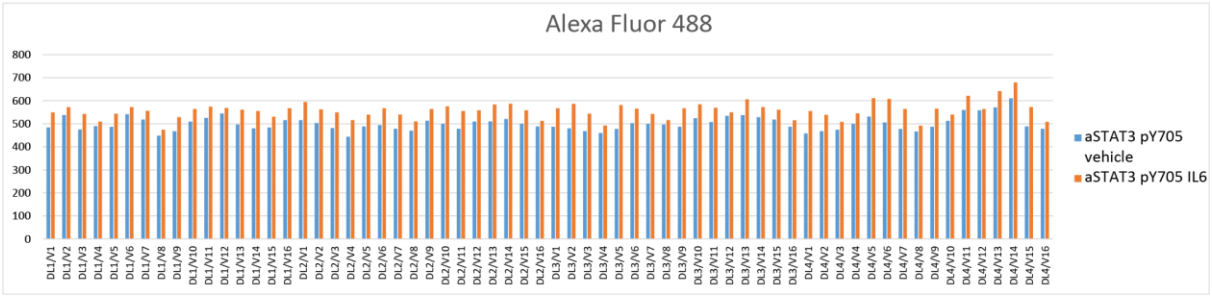

Figure 3.2 Median fluorescence intensities across 64 barcoded microglia populations for each functional fluorescence channel. 64 wells in one 96 well plate were exposed for 30 minutes to 50ng/ml IL-6 and 64 wells in another 96 well plate were exposed to a vehicle. Each plate was barcoded and pooled separately. Each plate was stained with anti-human STAT3 pY705 conjugated to **(a)** Phycoerythrin, **(b)** Alexa Fluor 647 or **(c)** Alexa Fluor 488. Plots show median fluorescent intensity (MFI) values on the y-axis and all 64 fluorescent barcode populations on the x-axis.

. .

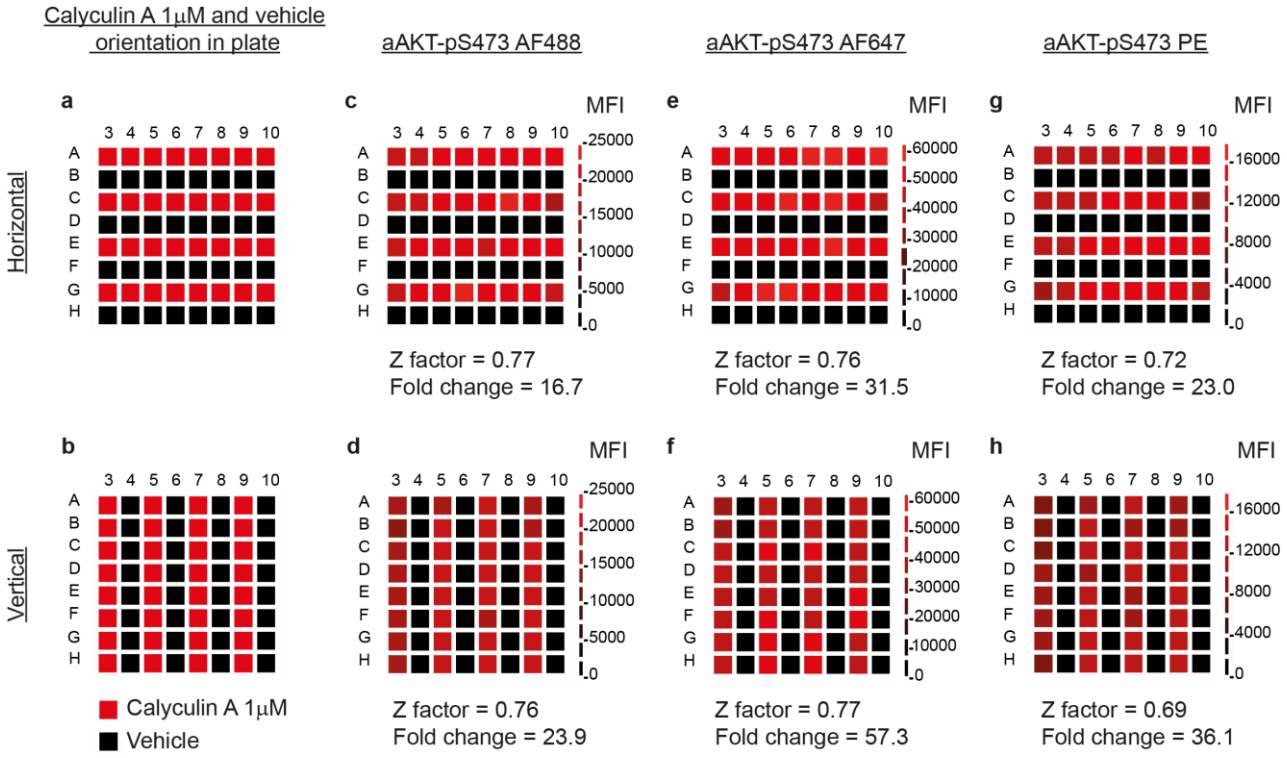

Figure 3.3 Z factor analysis across 64 barcoded SV40 microglial cell populations for each functional fluorescence channel. Microglia were stimulated for 30 minutes with 1 μM calyculin A or vehicle arranged in either a horizontal **(a)** or vertical **(b)** alternating pattern. MFIs for each barcoded population were used to calculate the Z factor and fold change (mean MFI Calyculin A/ mean MFI vehicle) for each stimulant orientation pattern after staining with anti-Akt (pS473) Alexa Fluor 488 **(c,d)**, anti-Akt (pS473) Alexa Fluor 647 **(e,f)** and anti-Akt (pS473) phycoerythrin (PE) **(g,h)** antibodies. MFI - median fluorescence intensity.

3.2.2 Proof of Concept Studies

As the eventual goal was to serum expose microglia, it was first necessary to assess whether the sensitivity and responsiveness of the SV40 microglia cell line towards complex mixtures and phospho-specific flow cytometry is detectable. In order to create a representative complex mixture for serum, human peripheral blood mononuclear cells (PBMCs) were cultured for 72 hours with a mixture of 1μg/ml Staphylococcal Enterotoxin B (SEB), 1μg/ml CD28 and 0.1μg/ml Lipopolysaccharides (LPS). The supernatant was collected and titrated in RPMI. Due to technical constraints of the robotic platform and clinical sample volumes, 75% was the highest feasible concentration which could be tested. Microglia were exposed for 30 minutes to either supernatant or vehicle, barcoded, pooled and redistributed across 24 wells. From these 24 wells, 2 remained unstained, leaving 22 wells for antibody staining. By multiplexing the three functional fluorescent channels, one well containing 64 differently treated cell populations can be stained for three different epitopes. The epitopes spanned a wide variety of cell signalling pathways, broadly including protein kinase A (PKA), protein kinase C (PKC), protein kinase B/mammalian target of rapamycin 1 (Akt/mTORC1), mitogen-activated protein kinase

(MAPK), IL-1 receptor/Toll-like receptor (IL-1R/TLR), Janus kinase/STAT (JAK/STAT) and integrin receptor/antigen receptor (IR/AR).

The results of the supernatant exposure (**Figure 3.4a**) show an increase in response ratio (treatment median fluorescence intensity/vehicle median fluorescence intensity) associated with an increase in supernatant concentration. This provided confidence in the stability of the platform and the responsiveness of microglia. Serum was collected from an individual with acute common cold symptoms and was used for a proof of concept study. Using serum at 75% concentration resulted in activation of the highest number of epitopes (N=36) compared to 5% (N=23), 26% (N=27) and 48% (N=28) serum concentrations ($P<0.05$, Wilcoxon rank-sum test, minimum 5%-fold change; **Figure 3.4b**). In addition, in contrast to the other serum concentrations tested, 75% concentration was sufficient to induce significant effects across all measured signalling pathways, including the IL-1R/TLR pathway.

In order to compare both experiments, the response ratios were plotted for both the supernatant (from the exposed PBMC culture) and the serum responses at the 75% exposure concentration (**Figure 3.5**). The responses were ranked first on changes in serum inducing a fold change of at least 10%, followed by changes caused by the supernatant of at least 10%. This revealed a very distinct pattern for the serum exposure compared to the supernatant. Yet, the ratio intensities did not differ across the two different scenarios. After fully filtering the 10% fold changes in epitope response, 19 epitopes were left for the serum exposure and 43 for the supernatant. This difference in the number of active epitopes can be explained by the fact that the PBMCs were stimulated with a rather strong pro-inflammatory mixture over a long time, probably causing a strong secreted inflammatory signal in the supernatant which also could have contained traces of the original stimulant mixture. Therefore, this stimulant was probably much more potent compared to serum obtained from a person suffering from a common cold. However, in both scenarios a distinct signalling profile was detected. This strengthened the confidence in the sensitivity of the platform and the ability to detect physiologically relevant response profiles.

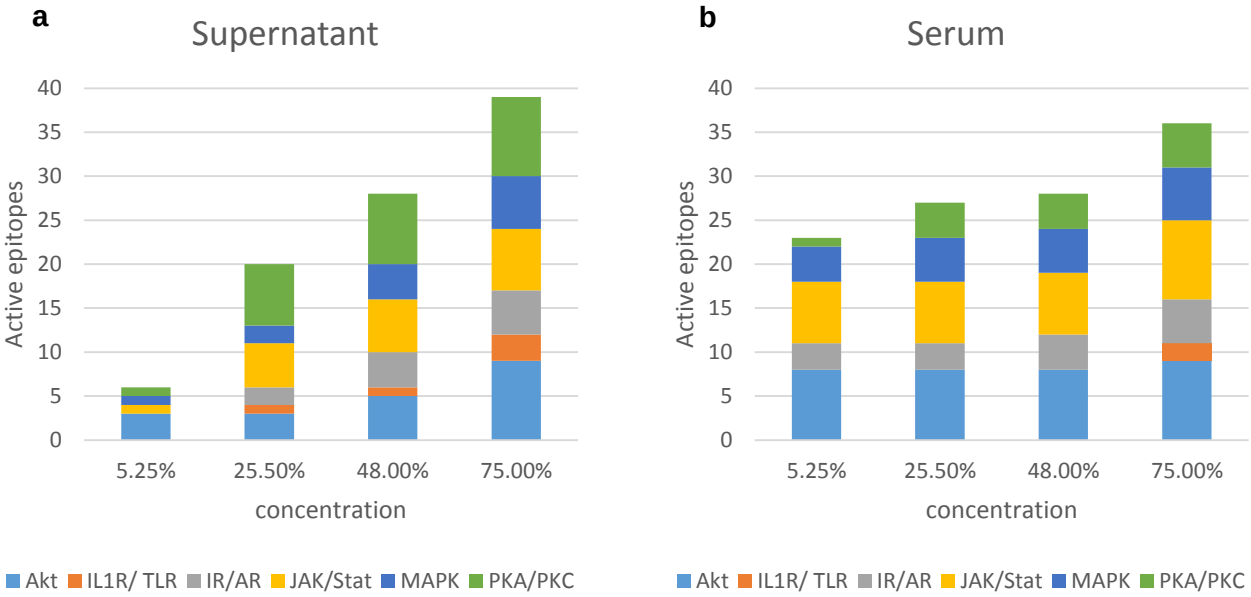

Figure 3.4 Cell culture supernatant and serum titration. The graphs show the number of epitopes ('Active epitopes', Y axis) significantly changed ($P<0.05$, Wilcoxon rank-sum test; minimum 5% fold change) after 30 min exposure of the SV40 human microglial cell line to **(a)** cell culture supernatant (from 72 h stimulation of human peripheral blood mononuclear cells with 1 µg/ml staphylococcal enterotoxin B, 1 µg/ml anti-CD28 and 0.1 µg/ml lipopolysaccharides from Escherichia coli O55:B5) and **(b)** serum from an individual suffering from severe cold, per concentration (X axis) and epitope category (colour-coded). Epitopes are grouped into classes: protein kinase B (Akt; total number of measured epitopes n=16), IL-1 receptor/Toll-like receptor (IL-1R/TLR; n=3), integrin receptor/antigen receptor (IR/AR; n=7), Janus kinase/STAT (JAK/Stat; n=10), mitogen-activated protein kinase (MAPK; n=8) and protein kinase A (PKA)/protein kinase C (PKC; n=14). Due to technical constraints of the robotic platform and the clinical sample volumes, the highest feasible concentration which could be tested was 75%.

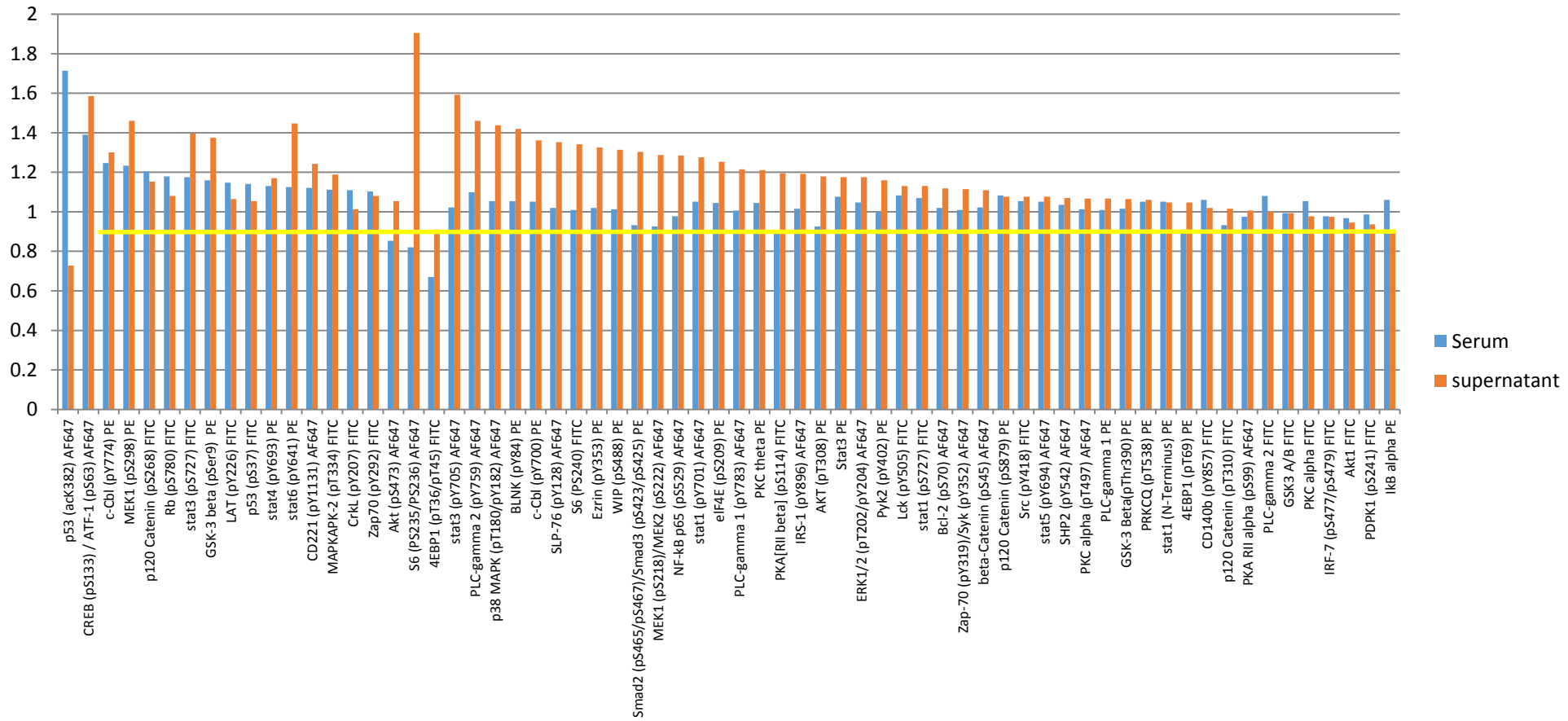

Figure 3.5 Comparison between 75% serum from a person suffering from a common cold and 75% exposure to stimulated PBMC supernatant. Epitopes (x-axis) are arranged at highest change in response ratio (ratio>10%, y-axis) in serum first, followed by highest change in response ratio in the supernatant (ratio>10%). The yellow line is placed at a ratio of 1, indicating the value at which no difference was detected in epitope expression between stimulant and vehicle. Ratios are calculated by (MFI of the treatment/MFI of the vehicle) per epitope.

3.2.3 Functional characterization of intracellular pro- and anti-inflammatory microglial reactive states

As the aim was to use the microglia as a sensor to differentiate between different inflammatory phenotypes when exposed to patient serum, we first needed to determine whether inflammatory related intracellular signalling cascades could be distinguished and how refined these profiles would be. Therefore, four proinflammatory ligands (IFN-γ[151,265], IL-23[266,267], TNF-α[144,151]and IL-1β[151,268]) and four anti-inflammatory ligands (IL-4[144,151,265], IL-13[269,270], TGF-β[144,151,271] and BMP-7[144,272]) were selected and each ligand was measured in three different concentrations, each in triplicate. In addition, the positive controls calyculin A (1 μM; phosphatase inhibitor) and staurosporine (5 μM; non-specific kinase inhibitor) were included. For this assessment a subset of the antibody array (targeting 42 intracellular signalling epitopes) was selected to determine whether it was possible to detect characteristic signalling responses at 30 min to ligands known to specifically induce either pro- or anti-inflammatory microglial phenotypes[144,145].

After accounting for background fluorescence, potentially caused by the ligands, a significant response to a ligand was defined as an increase or decrease within a specific epitope relative to the vehicle control (unpaired Wilcoxon $p<0.05$, fold change>10%). In addition to widespread activity of the positive controls calyculin A and staurosporine, we observed responses specific to the proinflammatory ligands at Stat1 (pY701), Stat4 (pY693), NF-κB p65 (pS529) and IκBα and to anti-inflammatory ligands at Akt (pS473), Stat6 (pY641), Smad2 (pS465/pS467)/Smad3 (pS423/pS425) and PKA RIIα (pS99) (**Figure 3.6a**). The platform also identified convergent cell signalling responses within each ligand class such as IκBα downregulation induced by proinflammatory ligands (IL-23, TNF-α and IL-1β) or Stat6 (pY641) phosphorylation evoked by anti-inflammatory ligands (IL-4 and IL-13). Furthermore, it was possible to discriminate the activity of ligands which are known to signal through the same receptor heterodimers (*e.g.* IL-4 and IL-13)[273] by divergent responses at secondary epitopes such as Akt (pS473).

To further test the sensitivity of the SV40 microglia cells towards a physiological concentration range of serum, one proinflammatory ligand and one anti-inflammatory ligand were selected for a dose-response evaluation. Titration of prototypical pro- and anti-inflammatory responses to IFN-γ at Stat1 (pY701) (EC_{50} 2.85 ng/ml) and IL-13 at Stat6 (pY641) (EC_{50} 13.81 ng/ml), respectively, suggested that the platform was capable of detecting microglial polarization phenotypes at physiologically relevant ligand concentrations (**Figure 3.6b, c**).

Finally, epitopes were ranked by their respective stain indices (mean MFI of the stained samples/mean MFI of the unstained samples) within the vehicle condition (**Figure 3.7**).

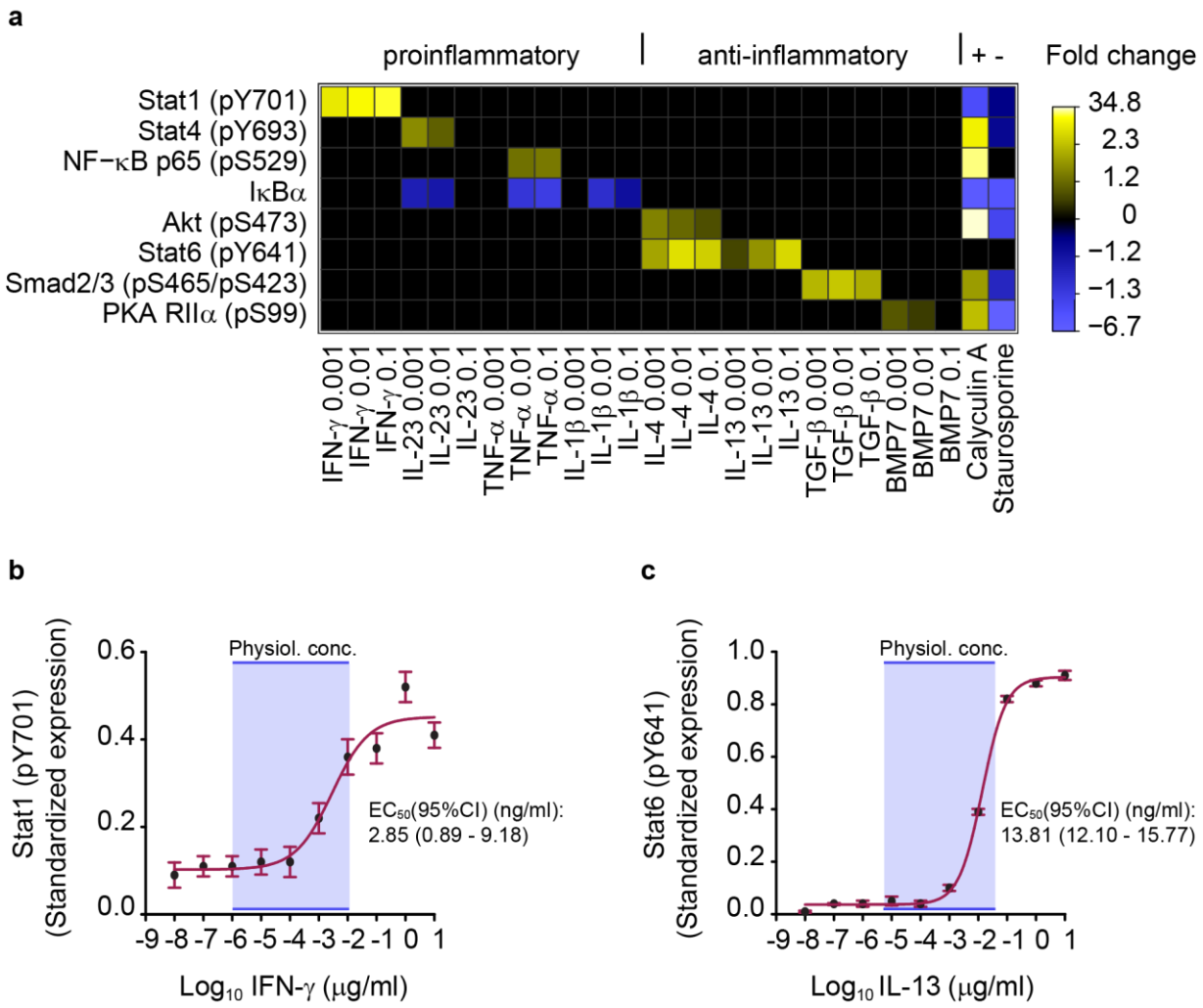

Figure 3.6 Functional characterization of SV40 human microglial cells as a sensor for early signalling events induced by pro- and anti-inflammatory microglial stimuli. (a) Characteristic responses at selected cell signalling epitopes (y axis) following 30 min incubation with different concentrations (μg/ml) of secreted ligands (x axis) which specifically induce either proinflammatory (IFN-γ, IL-23, TNF-α, IL-1β) or anti-inflammatory (IL-4, IL-13, TGF-β, BMP7) microglial phenotypes. Broad spectrum phosphatase inhibitor (calyculin A, 1 μM) and kinase inhibitor (staurosporine, 5 μM) are shown as positive controls for up- (+) and down-regulation (-) of cell signalling epitope expression, respectively. Only significant responses (Wilcoxon rank-sum test, $P<0.05$; adjusted for background fluorescence) which were sustained in the same direction for a minimum of two consecutive doses are shown. Legend shows mean fold change in epitope expression calculated as mean median fluorescence intensity (MFI) of the ligand treatment/mean MFI of the vehicle treatment across triplicate experiments. For down-regulated epitopes, the legend shows -1/fold change. Legend labels are distributed evenly across the quantile range for negative and positive fold changes separately. Ligands and epitopes are grouped by association to either pro- or anti-inflammatory signalling pathways. Smad2 (pS465/pS467)/Smad3 (pS423/pS425) is abbreviated as Smad2/3 (pS465/pS423). **(b, c)** Dose response sensitivity to prototypical proinflammatory (IFN-γ) and anti-inflammatory (IL-13) ligands at Stat1 (pY701) and Stat6 (pY641) respectively. Mean values from triplicate experiments (points) with standard error of the mean (vertical bars) and fitted 4-parameter logistic curves are shown. Y axis represents the MFI standardized as a proportion of minimum and maximum values. The physiological concentration range (physiol. conc.) for each cytokine (blue window) represents maximum and minimum values reported in serum across healthy and disease states[245–248].

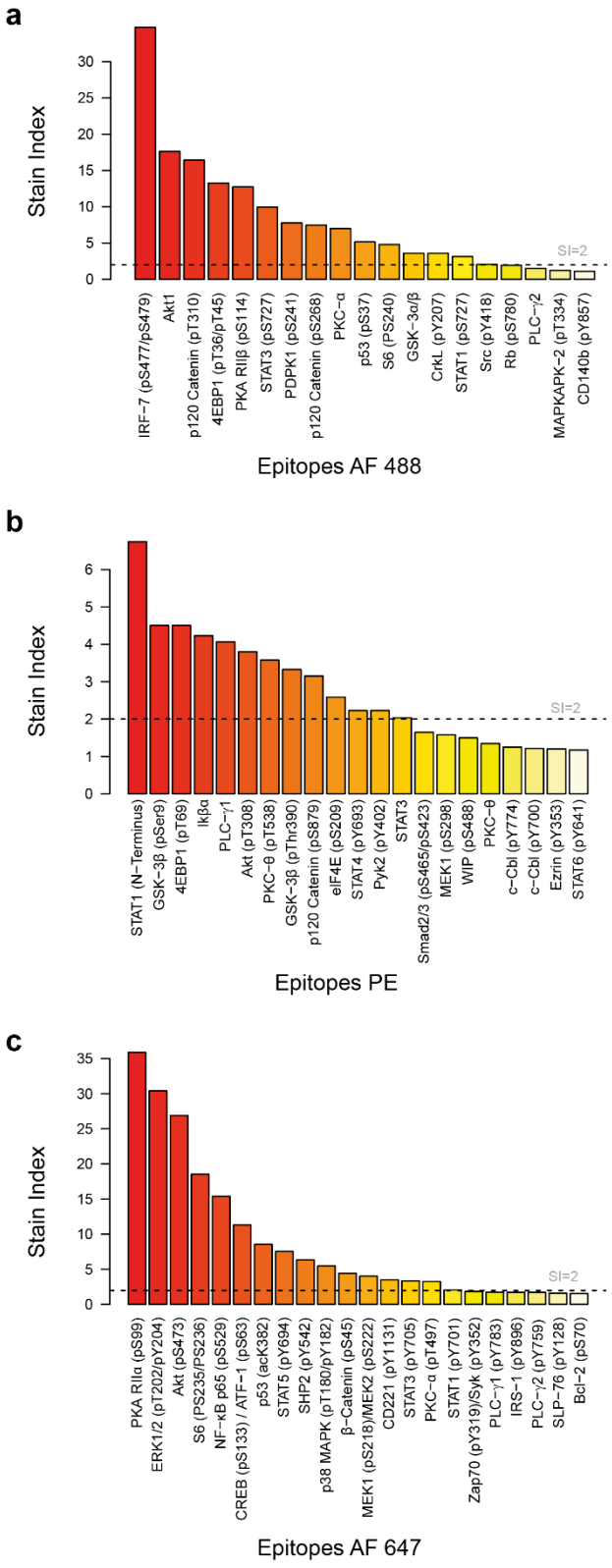

Figure 3.7 Stain indices of antibody clones against SV40 microglial cell signalling epitopes. Histograms show the stain index (mean MFI of the stained samples/mean MFI of the unstained samples, across triplicate measurements in the vehicle condition) for each epitope. Stain indices are ranked per functional fluorescent channel and labelled with a representative fluorophore: Alexa Fluor 488 (AF 488) **(a)**, phycoerythrin (PE) **(b)** and Alexa Fluor 647 (AF647) **(c)**. Smad2 (pS465/pS467)/Smad3 (pS423/pS425) is abbreviated as Smad2/3 (pS465/pS423). The dashed line marks a stain index of 2. MFI - median fluorescence intensity.

3.3 Discussion

In this chapter the development and validation of the cytomics platform application to the adhering microglia cell line was presented. First, the establishment of the platform with respect to its multiplexing capacity and read out stability was achieved, allowing high-content screening. Second, the application of the platform for detection of changes in intracellular signalling cascades was verified. And lastly, early specific signalling events related to microglial phenotypic polarization were detected at physiologically relevant concentrations. The discussion will focus on the comparison between our newly developed cytomics platform and the currently used methodologies used to investigate microglial functioning. Finally, we will focus on establishing the sensitivity of the newly developed platform in regard to detecting differential microglial signalling profiles following exposure to serum isolated from patients suffering from schizophrenia (+/- therapeutic intervention).

3.3.1 Comparison of the multi-parameter phospho-specific flow cytometry platform to conventionally used methods to functionally profile microglia

Currently, the field of microglia research is largely limited to findings obtained through methodologies using *in vitro* microglia culture, *post-mortem* brain slices, genomics, proteomics and PET brain imaging studies.

The bulk of findings used to functionally profile microglia were obtained from *post-mortem* brain tissue. One of the most widely used methods for such analyses is immunohistochemistry, both in rodent and human brain tissue. In contrast to, for example, RNA analysis and reverse transcriptase-coupled polymerase chain reaction (RT-PCR), immunohistochemistry or Western blot allows for protein detection, which is more functionally relevant than mRNA. And unlike other immunoassays, immunohistochemistry allows for localisation of proteins to specific cell types and regional differentiation. Furthermore, when combined with high-resolution techniques, subcellular localization can be accomplished providing functional information. For example, stimulus-dependent transcription factors translocate to the nucleus upon ligand engagement of upstream receptors. Therefore, detection of specific transcription factors in nuclei could imply ligand binding of specific cytokine receptors[148]. Although this is a widely used and accepted technique, concluding causal relations between specific markers and functional events remains difficult. For example, detecting microglial involvement in schizophrenia using *post-mortem* brain tissue is difficult to interpret, as these individuals underwent chronic antipsychotic drug-treatment. Hence, it is not clear whether microglial

changes are related to the disease pathophysiology or are a side effect of a lifelong exposure to drug treatment.

Given the marked limitations of *post-mortem* microglia studies, *in vitro* microglia culture studies have provided the opportunity to explore many aspects of microglial biology. However, by removing primary microglia from their microenvironment, the *in vivo* environmental signals will be lacking. This causes the absence of environmental signalling cues which play a critical role in defining the microglia phenotype[274]. Therefore, these cells should either be promptly analysed post isolation or the researcher has to attempt to mimic the microglial microenvironment, which in itself could yield information about factors associated with microglia phenotype regulation[148]. This is illustrated by growing isolated microglia on top of an astrocyte monolayer, with microglia developing a highly ramified morphology associated with downregulated NF-κB[275]. The co-culture of both type of cells highlights the importance of astrocyte-microglia interactions. Another significant hindrance in using this microglia cell model is the lack of a single unique microglia marker, as the identification of microglia *in vivo* is defined by a combination of morphology and a lack or low expression of multiple macrophage antigens. Therefore, it is challenging to isolate, culture and maintain a pure primary microglia phenotype in culture. Another issue with establishing primary microglia cell models is that the cells are isolated, and sometimes even expanded, from neonatal brain tissue and investigated as a cellular model for resident microglia function[148]. However, such an assumption is flawed as at that stage the microglia have not yet been exposed to the mature CNS environment within an intact BBB. This is illustrated by studies reporting poor or even immature antigen presentation abilities for these cells due to their trans-differentiation. When co-cultured with granulocyte macrophage colony-stimulating factor (GM-CSF), isolated microglia develop more into dendritic cell like phenotypes[276]. When treating the cells with macrophage colony-stimulating factor (M-CSF), the surviving cells develop a modestly ramified morphology that can be maintained for weeks[277], consistent with macrophage-like survival and phenotype. To avoid losing the microglial microenvironment, brain slices and organotypic cultures have been investigated. However, in contrast to isolated microglia, the slicing process itself could facilitate microglia activation. This is illustrated, for example, by the induction of the expression of a distinct ion channel in slice cultures compared to cells *in vitro*[278].

One of the disadvantages of many high-resolution imaging techniques is photobleaching, a photochemical reaction leaving the used fluorophore permanently unable to fluoresce. However, some publications used two-photon imaging instead, an imaging technique allowing prolonged imaging sessions without creating photobleaching or photodamage. Two groups have previously imaged mice microglial cells in which a specific chemokine receptor had been replaced with enhanced green fluorescent protein. They both reported that microglia cells in an intact, healthy CNS are

continuously remodelling their processes, thereby constantly probing their extracellular environment[279,280]. This finding suggests that resting microglia do not actually exist, as their dynamic surveillance includes monitoring the entire tissue without moving the soma but through branching processes[281]. However, the disadvantage lies with the genetic modification of the microglia, by assuming the expression of a specific receptor to be unique to microglia within the CNS. Both studies used the transgenic *Cx3cr1*$^{EGFP/+}$ mouse model, in which brain microglia selectively express enhanced green fluorescent protein (EGFP) under control of the fractalkine receptor (CX3CR1) promoter. Yet, success of this model depends on which promoter-reporter has been used and on detailed knowledge of promoter activity under physiological and pathological conditions. It should be noted that so far no microglia-specific promotor has been identified, therefore these results might not be reflecting an accurate microglia specific phenotype.

Some studies have attempted to compare cell lines from different species to primary human microglia via a genetic and proteomic approach[274,282], whereas others tried to compare isolated primary microglia to macrophages and brain tissue via direct RNA sequencing in mice[283]. Yet, the problem here lies with these publications having mainly used rodent or murine material, but not a human microglia cell line. Thereby they did not allow a full comparison from human primary microglia to the range of available microglia cell lines across species, nor did they compare it to primary microglia from rodents. And although many experimental animal studies do present a lot of opportunities, the overlap between rodent and human microglial cellular models remains to be determined[282,284].

Whilst many methodologies have been applied to microglia characterization, there is a lack of understanding of the signalling pathways associated with microglial polarization. To this day very little is known about specific microglia pathway signalling cascades in general, especially how they interact with environmental signals. This makes this multi-parameter phospho-specific flow cytometry panel unique, as it provides insights into changes in a broad range of signalling pathways in microglia. As we used phosphoflow, we do not just measure protein concentrations, but changes in pathway activity via alterations in phosphorylation status.

Our approach also looks at a much shorter stimulation time scale than the majority of published data. This allows us to investigate immediate and direct changes linked to environmental challenges. Such a strategy will facilitate the identification of the most common changes in signalling pathways leading to further downstream modulation associated with microglial activation.

3.3.2 Detection of changes in homeostatic equilibrium

Extracellular cues trigger a cascade of information flow, in which signalling molecules; i) become chemically/physically modified or translocate; ii) gain new functional capabilities; iii) affect subsequent molecules in the cascade, culminating in a phenotypic cellular response[261]. By exposing microglia *in vitro* to a stimulant, such as IL-6 or calyculin A, the normal monitoring state of the microglia cell is perturbed. As illustrated in section **3.2.1**, direct exposure to IL-6 induced STAT3 protein-modification through phosphorylation resulting in the detection of altered STAT3 (pY705) levels. However, as illustrated by the microglia treated with vehicle, proteins always have basal levels of phosphorylation. Therefore, the detected change in phosphorylation does not represent a fully activated or deactivated protein, but is involved with the modification of the protein's basal activity. For example, the increase of phosphorylated STAT3 (pY705) is commonly associated with an increase of the STAT3 activity. However, the activity of STAT3 is modulated through other phosphorylation sites as well, such as regulatory site S727. This phosphorylation site is capable of regulating the STAT3 activity by either stimulating or diminishing the STAT3 protein activity. The STAT3 (pS727) phosphorylation site can be modified through intracellular components, regulated through other signalling pathways[285]. Before, pathways were often conceptualized as distinct entities responding to specific triggers. But, as illustrated with these two different STAT3 phosphorylation sites, inter pathway cross-talk and other properties of networks reflect underlying complexities that cannot be explained by the consideration of individual pathways or model systems in isolation[261].

By identifying the perturbed change in phosphorylation patterns, we will be aiming to detect a common signalling hub that could become a potential new drug site. This newly discovered drug site would allow further drug screening for the discovery of potential new treatments for schizophrenia. However, such a strategy does present another issue, so far very little has been published on the effects of antipsychotics on changes in microglial signalling. Mostly, publications mention the exposure and the outcome, but not what happened in between (*i.e.* at the cell signalling level). Indeed, we do not know which signalling pathways are involved when atypical antipsychotics are administered and eventually lower levels of TNFα and NO are measured as secreted products[286,287]. Here we are aiming to modify a drug target's phosphorylation status that would allow us to further examine that particular pathway and its symptomatic involvement.

3.3.3 Detection of early, specific microglia signalling cascades

The presented data indicates great microglial sensitivity towards the environment. Furthermore, the detected changes in intracellular signalling responses and phosphorylation changes were highly specific depending on the ligand (**Figure 3.8**). This gives confidence for these cells to be used as a sensor in response to patient serum. So far, there have been many serum profiling studies using single or multiplexed immunoassays and/or mass spectrometry approaches. Yet, the resolution of these approaches is limited by either antibody availability, specificity or equipment screening capacity. Via the proposed approach here, we will be able to indirectly screen changes in serum capable of inducing altered microglial signalling profiles. This is the first dataset to indicate such specific and fast signal responses in microglia post exposure to complex mixtures can be detected by microglia.

3.3.3.1 Distinct pro-inflammatory signalling cascades not always depending on STAT1

The functional polarization characterization shows specific early events related to the ligand. Within the proinflammatory ligands, the STAT1 phosphorylation by IFN-γ is one of the most classical signal transduction pathways among the proinflammatory stimulants[288]. This particular JAK/STAT mediated signalling pathway results in increased transcription of NOS2, IL-12 and many pro-inflammatory cytokines[289]. This classical activation will lead to anaerobic glycolysis, increased production of pro-inflammatory cytokines, synthesis of reactive oxygen species and nitrogen species, enabling efficient killing of engulfed threats[290]. However, microglia can control their own polarization too, through autocrine and paracrine means[291]. In most cases this response is protective and is downregulated once the threat or damage has been dealt with. Yet when unregulated, long-term or chronic inflammation could lead to tissue destruction[292].

Of interest are the signalling pathways of TNF-α, IL-1β and IL-23, that all converge on NF-κB. Yet, these three ligands all do so in their own distinct ways as they all signal through different receptors with different strengths and efficiencies. All three end up inhibiting IκBα, but only TNF-α is potent enough in doing so to upregulate NF-κB (**Figure 3.6a**). In addition, IL-23 shows a decrease in STAT4 signalling upon higher IL-23 concentrations, regulating the proinflammatory response as it does facilitate and support NF-κB signalling. Another reason for this observed decrease could be that a stronger IL-23 stimulation can result in a mixed activation of STAT1, STAT3, STAT4 and STAT5. Some pathways are more sensitive than others, and therefore become activated on lower concentrations. In the higher IL-23 concentration range other interacting pathways could become activated and inhibit the STAT4

signal. In addition, due to other pathways becoming active at the higher concentration range, multiple STAT proteins could have become activated. But, by applying a 10% fold change cut off in our analysis, this spread out signal might have been too weak for detection[293].

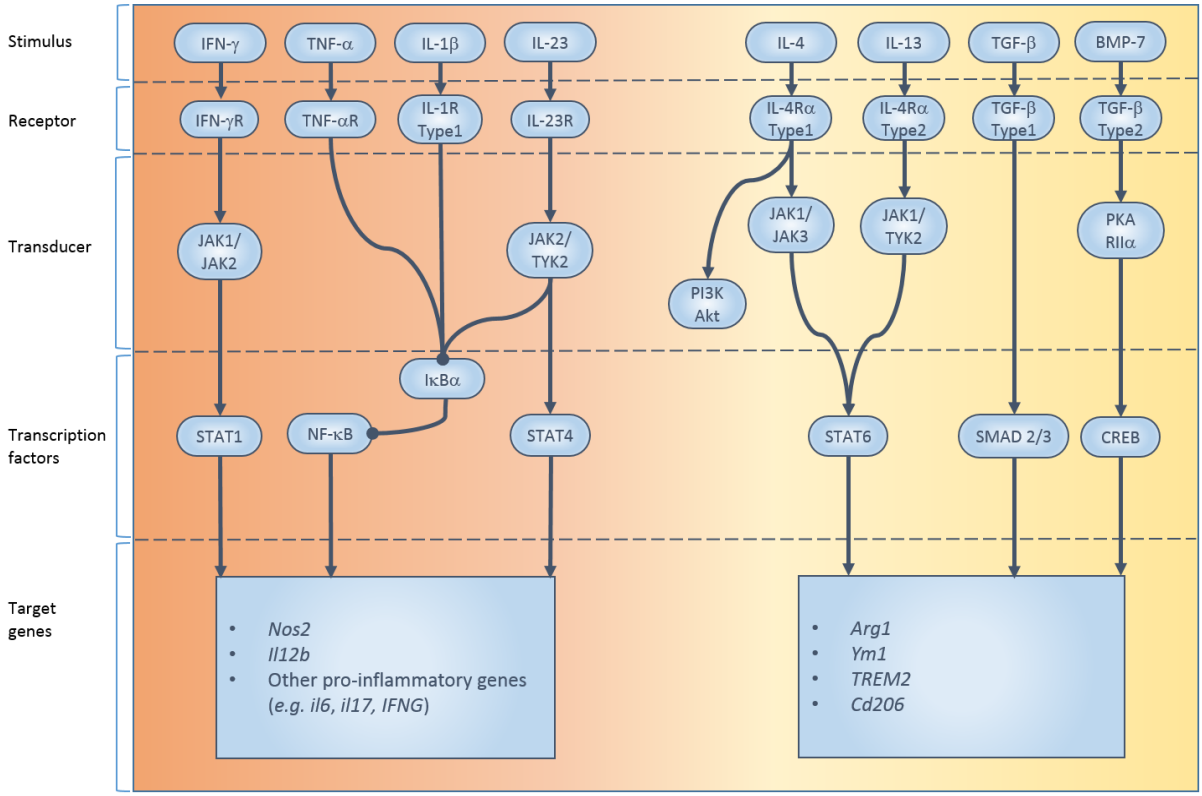

Figure 3.8 Overview of signal transduction pathways from the functional characterization. Ligands from the functional characterization are ordered per polarization pole with proinflammatory on the left (orange background) and anti-inflammatory on the right (yellow background). An initial stimulus will eventually lead to sequence-specific transcription factors that mediate the changes in the transcriptional output. Although some of the used stimuli converge onto similar transcription factors, they still have divergent effects. Three out of four proinflammatory ligands downregulate IκBα, thereby disinhibiting NF-κB, but only one, TNF-α, is potent enough to upregulate NF-κB signal transduction. Within the four anti-inflammatory ligands 2 receptor families are stimulated, but different heterodimers within those families. Subsequently, the signal transduction pathways, as with the TGF-β family, the responses are substantially different. With the IL-4 receptors the responses are subtler compared to the TGF-β pathways. The proinflammatory target genes result in cytokine secretion, nitric oxide (Nos2) and IL12b, a strong pro-inflammatory inducer. In contrast, the anti-inflammatory target genes result in counterbalancing the nitric oxide production and upregulating anti-inflammatory cytokines (Arg1) and induced expression of mannose receptor (Cd206), a lectin preventing further degradation of the extracellular matrix components (Ym1) and debris clearance (TREM2). Arrows represent increased activation, spheres decreased. R: receptor, JAK: Janus kinase, TYK: tyrosine kinase, STAT: signal transducer and activator of transcription, PKA: protein kinase A, PI3K: phosphoinositide 3-kinase, CREB: cAMP response element-binding protein, Nos2: nitric oxide synthase 2, il12b: interleukin 12b, Arg1: arginase 1, TREM2: triggering receptor expressed on myeloid cells 2.

3.3.3.2 Sensitivity towards different receptor subtype signalling cascades

Whereas STAT1 is regarded an essential mediator of proinflammatory macrophage polarization in the presence of IFN-γ, so is STAT6 to drive anti-inflammatory activation in the presence of IL-4 or IL-13[294–296]. In general, these cytokines are required for the generation of high-affinity IgE antibodies and are involved in supressing unrestricted inflammation, thereby maintaining homeostasis[297]. In microglia, they are able to achieve a phenotypical shift by shifting the cellular response away from the pro-inflammatory cytokine generation and nitric oxide production towards the synthesis of anti-inflammatory and tissue repair factors, thereby causing a profound metabolic shift. Even though IL-4 and IL-13 both signal through the IL-4Rα receptors, the subtypes are connected to different transducers causing different downstream signalling activities[298].

TGF-β and BMP-7 are both members of the TGF-β superfamily, yet signal via very distinct pathways. TGF-β1 signals through the TGF-β type 1 receptor which will phosphorylate Smad2/3. BMP-7 ligates at the type 2 receptor, a Smad-independent pathway, causing cAMP-dependent auto-phosphorylation of the PKA regulatory RII α subunit, resulting in CREB phosphorylation[299–301]. TGF-β has been implicated in blocking microglial migration within the CNS and impairing BBB crossing into the CNS, thereby creating a more protective environment[302]. In addition, TGF-β is known to be involved in tissue remodelling and matrix deposition once inflammation has been downregulated[265]. BMP-7 is capable of significantly downregulating inflammatory cytokines and driving the microglial phenotype towards an anti-inflammatory one[303].

3.3.4 Outlook

So far, most of the publications regarding microglia polarization have mainly focused on single ligand stimulated cell cultures over longer periods of time, using restricted detection panels on genetic read out or secreted cytokines[148,151]. Here we present the first evidence for fast acting, specific changes in microglial signalling pathways *in vitro* post exposing human microglial cells to inflammatory stimulants whilst having screened on a panel allowing a broad detection range. Furthermore, we have shown that even when using ligands that act via the same receptor family, they still have distinctive signalling cascades. When signalling cascades from different ligands do converge on the same downstream protein, different effects can still be detected based on the expression of the sequential proteins in that cascade. This fine tuning detection level allows us to continue using these cells as a sensor for complex sample exposure, such as serum.

Although many publications hypothesize the involvement of microglia in schizophrenia, there is no direct evidence of the involvement of these cells in schizophrenia. Little is known with regard to the

role of microglia in the disease onset and/or progression and whether or not they play a primary role in the pathology or a mere by-product to other changes associated with the physiopathology of neuropsychiatric diseases such as schizophrenia. These questions are of major importance to unravel and establish the potential role of these microglial cells in the disease pathology. Although the proposed study will not be able to answer all these questions, it will be the first step towards gaining more knowledge of how these cells respond to the exposure of serum derived from schizophrenic patients. Due to their perivascular location, they will be the first cells to encounter serum products upon BBB disruption[304]. Therefore, this will give us a better indication of the potential of deviant microglia responses in schizophrenia. By using the proposed approach, where microglia cells become a sensor to patient-derived serum, we are also establishing: i) not only an insight into the potential polarization of the microglia; ii) changes in patient serum leading to altered microglial signalling responses and therefore the discovery of potential new drug targets. The mutual exclusivity between prototypical pro- and anti-inflammatory signalling pathways might be a crucial factor in microglial polarization and could potentially be utilised as a tipping point for the modulation of polarization leading to therapeutic efficacy.

Chapter 4
Drug Target Discovery in Microglia

Chapter 4 | Drug Target Discovery in Microglia

4.1 Introduction

One of the primary reasons for the controversial interpretation of microglial activation is that the majority of data has been accrued through *in vitro* exposure to specific antigens and cytokines[151,152]. However, it is likely that the ultimate functional role assumed by microglia *in vivo* represents the integration of multiple phenotypic cues derived from complex physiological mixtures, such as serum and CSF, across multiple cell signalling pathways[144]. Despite the suggested involvement of microglial activation and the presence of altered circulatory proteins with microglial activation propensity in schizophrenia patients, the effect of circulatory protein abnormalities on microglial activation status has, as yet, not been explored. Studies have suggested that microglia play a key role in responding to blood-borne components at perivascular sites within the CNS[304].

Previous studies relating to neuropsychiatric disorders have attempted to address this by quantifying circulating proteins and then imputing their potential net effect on CNS immune cell function. Most of the reports have attempted to annotate the activity profile of each protein in relation to their respective blood brain barrier permeabilities[106,153,217,218]. Furthermore, a growing body of clinical and experimental evidence indicates that neurovascular endotheliopathy and BBB hyperpermeability occur in schizophrenia patients, which could facilitate interactions between brain innate and peripheral adaptive immunity[305]. A recent study has identified a list of microglia gene expression and their corresponding regulatory elements which are modulated by the environment and therefore maintaining microglia identity and function[274]. As microglia play a key role in responding to blood-borne components at perivascular sites within the CNS[304], we propose here a reverse approach in which human microglial cells are exposed directly to native serum samples from schizophrenia patients and healthy controls. A high content functional single-cell screening study was performed to dissect the cell signalling pathways which may be associated with phenotypic switching of microglia cells. Subsequently, we conduct an exploratory analysis of which serum proteins previously linked to neuropsychiatric disorders are altered in the disease state and whether new drug target microglial cell signalling phenotype is amenable to new drug discovery.

The work presented in this chapter including specific figures and text is based on a collaborative paper, drafted by Dr. Santiago Lago[263].

4.2 Results

4.2.1 Serum from first-onset drug-naïve schizophrenia patients induced pro-inflammatory microglia activation *in vitro*

To determine whether serum from schizophrenia patients can differentially regulate the cell signalling phenotype of microglial cells, we incubated SV40 microglial cells with serum from 60 symptomatic (95.54 ± 20.49 Positive and Negative Syndrome Scale (PANSS) total score) first-onset antipsychotic drug-naïve schizophrenia patients and 79 matched healthy controls (**Table 4.1**) for 30 min and subsequently assessed changes in expression of 62 intra-cellular signalling epitopes (**Table 2.2**). Six epitopes showed significant (linear mixed effects model, $P<0.05$) differential responses between schizophrenia and healthy control serum (**Figure 4.1a**; **Table 4.2**) and were clustered on adjacent proteins in either the mTORC1 or STAT3 pathways. Sites on mTORC1 pathway proteins included direct mTORC1 substrates 4EBP1 (pT36/T45) and 4EBP1 (pT69) in addition to 4EBP1 substrate eIF4E (pS209). Sites on STAT3 pathway proteins included the activation site STAT3 (pY705), the regulatory site SHP2 (pY542) and total STAT3 (independent of phosphorylation). Responses to serum from schizophrenia patients at these sites reflected either potentiation of positive expression changes or attenuation of negative expression changes resulting in a net functional increase in the activation status of both pathways relative to controls (**Figure 4.1b**). The activation of STAT3 and mTORC1 pathways has been implicated as a key molecular switch governing the phenotypic conversion of resting microglia to the deleterious proinflammatory activated microglia in animal models of neurodegeneration, stroke and traumatic brain injury[144,306–308]. The role of STAT3 signalling is primarily associated with a positive feedback loop in which the activation of STAT3 transcription factors downstream of proinflammatory cytokine receptors (*e.g.* IL-6, IL-23, IFN-γ and GM-CSF receptors) triggers the further synthesis and secretion of characteristic pro-inflammatory cytokines (*e.g.* IL-6, IL-23, IL-1β, TNF-α)[144,306]. Concurrently, mTORC1 pathway activation at the level of 4EBP1 and eIF4E represents a metabolic shift towards the translation of proteins implicated in microglial reactivity (*e.g.* TNF-α, IL-1β, iNOS, MCP-1, and CCL-22)[307,308]. Taken together, these findings suggest that the over-activation of STAT3 and mTORC1 pathways in response to schizophrenia patient serum could represent a cellular phenotype in which discrete signalling motifs are synergistically geared towards pro-inflammatory activation.

Table 4.1 Demographic characteristics of clinical samples used in the microglial serum exposure study. The clinical groups of first-onset drug-naïve schizophrenia patients (SCZ) and healthy control (HC) samples were matched. The Wilcoxon rank-sum test (*) for continuous variables and Fisher's exact test (^{o}) for categorical variables were exmployed to determine significant differences in the demographic variables between clinical groups. The table shows mean values ± standard deviation. BMI - body mass index. PANSS - Positive and Negative Syndrome Scale. NA – not applicable. ($^{+}$) BMI data only available for 54 patients and 70 control samples.

	SCZ	HC	P
	60	79	NA
Gender (male/female)	31/29	43/36	0.864 ^{o}
Age (years)	30.72 ± 10.46	31.15 ± 8.32	0.298 *
BMI (kg/m2)	24.21 ± 5.56 $^{+}$	23.15 ± 3.50 $^{+}$	0.492 *
Smoking (yes/no/not known)	26/19/15	22/57/0	**0.002 ^{o}**
Ethnicity (white/other)	56/4	57/1	0.365 ^{o}
Cannabis (yes/no/not known)	24/21/15	27/48/4	0.086 ^{o}
PANSS Positive	22.96 ± 5.91	NA	NA
PANSS Negative	23.20 ± 7.34	NA	NA
PANSS General	49.37 ± 9.95	NA	NA
PANSS Total	95.54 ± 20.49	NA	NA

Table 4.2 Alterations in microglial cell signalling epitope expression in response to serum from first-onset drug-naive schizophrenia patients relative to healthy controls. Sample numbers in each clinical group include 60 schizophrenia (SCZ) and 79 healthy control (HC). *'Number of data points'* refers to the number of data points available per epitope across triplicate measurements for each clinical group after data preprocessing (terms in 'italics' represent column headings). Linear mixed effects model was used to account for the replicate measurements. Only epitopes for which there was a statistical difference in expression (*'permuted P'*<0.05) following incubation with SCZ relative to HC serum are shown. No covariates (age or gender) were selected for the epitopes shown following stepwise application of Bayesian Information Criteria in the linear mixed effects model. '*Serum response*' represents median MFI of the serum treatment/median MFI of the vehicle treatment within the respective clinical group. Only epitopes that displayed a significant '*serum response*' (Wilcoxon rank-sum test, permuted *P*<0.05; adjusted for background fluorescence) in either clinical group are shown. '*Response direction*' refers to the increase (↑) or decrease (↓) in epitope expression in response to serum. '*Response ratio*' refers to (1-*'SCZ serum response'*)/(1-*'HC serum response'*). This represents a means of expressing the relative potentiation or attenuation of response independently of its direction. This is expressed in the following column as '*potentiation/attenuation fold change*' (*'response ratios'* between 0 and 1 are converted to -1/*'response ratio'*), whereby a positive value represents potentiation and a negative value represents attenuation of response. '*Stain index*' refers to the median MFI of the stained samples/median MFI of the unstained samples within the vehicle treatment. MFI - median fluorescence intensity.

	Number of data points			Serum response					
Epitope	**SCZ**	**HC**	**Permuted P value**	**SCZ**	**HC**	**Response direction**	**Response ratio**	**Potentiation/ attenuation fold change**	**Stain index**
4EBP1 (pT36/pT45)	177	233	0.0001	0.963	0.934	↓	0.56	-1.79	13.3
4EBP1 (pT69)	177	233	0.0001	1.061	1.038	↑	1.61	1.61	4.5
Stat3 (pY705)	176	234	0.0012	0.988	0.970	↓	0.41	-2.46	3.4
SHP2 (pY542)	175	233	0.0049	0.951	0.933	↓	0.73	-1.37	6.3
eIF4E (pS209)	176	233	0.0384	1.027	1.010	↑	2.65	2.65	2.6
Stat3	176	234	0.0357	1.062	1.051	↑	1.22	1.22	2.0

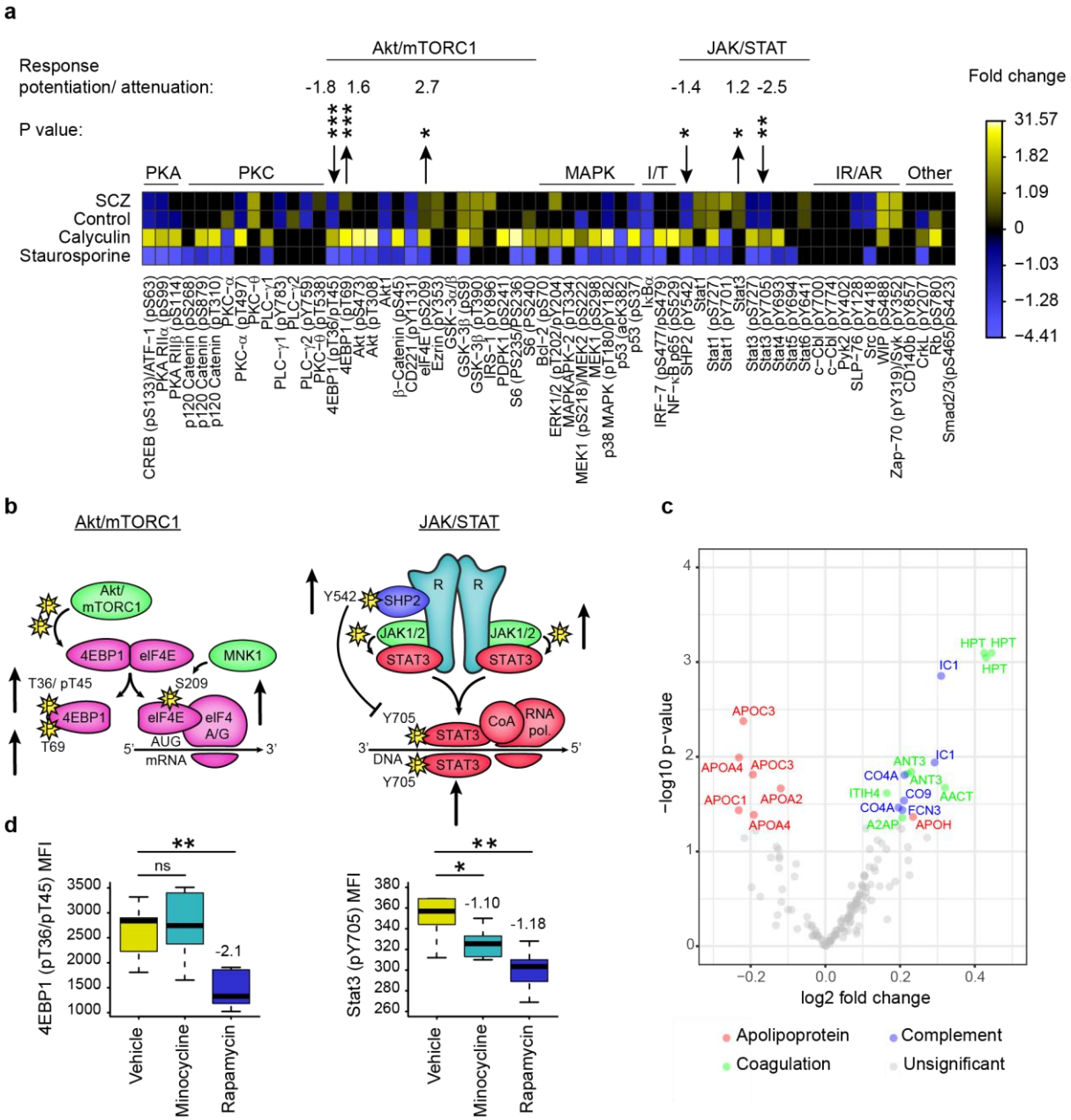

Figure 4.1 Phenotypic alteration of microglial cell signalling in response to serum from drug-naïve schizophrenia patients. Differential responses at 30 min to serum from 60 first-onset antipsychotic drug-naïve schizophrenia patients (SCZ) and 79 matched healthy controls across 62 functionally diverse cell signalling epitopes grouped by pathway (top) in SV40 human microglial cell line. Responses to positive control ligands which induce widespread up-regulation (calyculin A, 1 μM) or down-regulation (staurosporine, 5 μM) are included for comparison. Only responses in which cellular treatments (serum or ligand exposure) provoked a significant difference (Wilcoxon rank-sum test, permuted $P<0.05$; adjusted for background fluorescence) in epitope expression relative to the vehicle are shown. Legend shows mean fold change in epitope expression calculated as mean median fluorescence intensity (MFI) of the treatment/mean MFI of the vehicle across triplicate experiments. For down-regulated epitopes, the legend shows -1/fold change. Legend labels are distributed evenly across the quantile range for negative and positive fold changes separately. Epitopes which showed a significant difference (linear mixed effects model, permuted, $*P<0.05$, $**P<0.005$, $***P<0.0005$) in response to SCZ patient serum relative to healthy controls are marked by arrows which show the direction of the response. 'Response potentiation/ attenuation' refers to (1-median response to SCZ serum)//(1-median response to healthy control serum); resulting values between 0 and 1 are converted to -1/value. This represents a means of expressing the relative potentiation (positive values) or attenuation (negative values) of response to serum from SCZ patients independently of its direction. Smad2 (pS465/pS467)/Smad3 (pS423/pS425) is abbreviated as Smad2/3 (pS465/pS423).

(b) Epitopes from **panel a** (n=6) which responded differently to SCZ patient serum relative to healthy controls are shown in the mechanistic context of adjacent proteins in Akt/mTORC1 and JAK/STAT signalling pathways. Vertical arrows (↑) represent net functional increase in the activation status of each epitope (i.e. potentiation of positive expression changes or attenuation of negative expression changes) in response to SCZ serum relative to healthy controls, indicative of M1 microglial activation. In the Akt/mTORC1 pathway, mTORC1 phosphorylates 4EBP1 at residues T36 and T69, which triggers the dissociation of eIF4E. eIF4E is then phosphorylated by MNK1 at residue S209 and associates with eIF4A and G to initiate cap-dependent translation. In the JAK/STAT pathway, activation of cytokine or growth factor receptors induces the phosphorylation of STAT3 at residue Y705 by JAK1/2 kinases. Subsequent dimerization of STAT3 pY705 recruits transcriptional co-activators which enhance the activity of RNA polymerase at specific genomic loci. Phosphorylation of SHP2 at Y542 negatively regulates STAT3 Y705 phosphorylation. Proteins are coloured with respect to their cellular function: green (kinase), blue (phosphatase), pink (translation), red (transcription) and turquoise (receptor). P - phosphate group. **(c)** Volcano plot representing the relationship between $\log_2$ fold change (x-axis) and statistical significance (y-axis, linear mixed effects model) for peptide abundances in SCZ serum relative to healthy controls, as measured through multiplexed reaction monitoring (MRM) analysis. Peptides significantly (linear mixed effects model, $P<0.05$) altered in SCZ patient serum are labelled and coloured in terms of protein classes which are associated with pro-inflammatory microglial activation (apolipoproteins (red), coagulation factors (green) and the complement cascade (blue)). **(d)** Effect of microglial polarization inhibitors (minocycline, 10 μM[208], and rapamycin, 5 μM[264]) on phosphorylation status of the most significant activation epitopes per pathway, 4EBP1 (pT36/pT45) and STAT3 (pY705), from **panel a**. Box plots show interquartile range with the median (horizontal line) and the minimum and maximum values (whiskers). Significance (Wilcoxon rank-sum test, *P<0.05, **P<0.005, ns - P≥0.05) and fold changes (FC) in epitope MFI for each inhibitor relative to the vehicle are shown. Data reflects mean of 6 experimental replicates.

4.2.2 Detection of changes in patient serum capable of inducing altered microglia phenotype

To explore whether the putative activation phenotype could be explained by differences between the two clinical groups in the relative concentrations of serum proteins previously linked to schizophrenia (n=94; **Table 2.3**, **Table 2.4**), we employed targeted multiple reaction monitoring mass spectrometry (for medium-high abundance proteins) and targeted multiplexed immunoassays (for low abundance proteins). This revealed alterations in several proteins from the apolipoprotein family (AII, AIV, CI, CIII and H subtypes), the complement cascade (C1 inhibitor, C4a, C9 and ficolin-3), coagulation factors (haptoglobin, antithrombin-III, haptoglobin, inter-α-trypsin inhibitor heavy chain H4, α-1-antichymotrypsin and α-2-antiplasmin) and cytokines IFN-γ and TGF-β (**Figure 4.1c**; **Table 4.3**). These findings are consistent with previous reports of alterations of these proteins in serum from schizophrenia patients (summarized in **Table 4.4** including functional pathways and microglia activation capacity). In the CNS, microglia are the primary cell type expressing receptors for complement factors (CR1, CR3 and CR4)[161], apolipoprotein (TREM2)[309] and haptoglobin (CD163)[310]. These protein classes have been associated with microglial activation in the form of increased synaptic pruning and inflammatory responses to cellular debris at critical neurodevelopmental stages[161,309,310]. Likewise, cytokines IFN-γ and TGF-β are considered mediators of pro- and anti-inflammatory microglial polarization, respectively[144]. Taken together, these findings indicate that the activated cell signalling phenotype induced by circulatory proteins in the present study may be associated with the pathogenic mechanisms underlying brain physiopathology associated with schizophrenia.

4.2.3 Exploration of sensitivity towards drug screening on activation epitopes

Finally, we attempted to explore whether the most significant putative changes in microglial epitopes induced by schizophrenia patient serum on the mTORC1 and STAT3 pathways were amenable to drug discovery. We subsequently incubated SV40 microglia cells with prototypic compounds known to inhibit a targeted phenotype *in vivo* such as an mTOR inhibitor (rapamycin)[307,311] and a tetracycline antibiotic (minocycline)[208]. The expression of phosphorylated mTORC1 substrate site 4EBP1 (pT36/45) was inhibited by rapamycin (5 μM) only, while the expression of the phosphorylated STAT3 (pY705) activation site was inhibited by both minocycline (10 μM) and rapamycin (5 μM) (**Figure 4.1d**). These findings show that the epitopes which are over-activated by schizophrenia patient serum can be targeted and modulated with microglial pro-inflammatory inhibitors. Such a finding is suggesting that the microglial endo-phenotypes identified by the present methodology could form a platform for CNS novel drug discovery approaches.

Table 4.3 Altered serum analytes in first-onset drug-naive schizophrenia patients) relative to healthy controls. '*Assay*' refers to the analyte detection method including multiplex immunoassay (MI) or multiple reaction monitoring (MRM) mass spectrometry (terms in 'italics' represent column headings). *'Proteins'* are ordered by *'assay'* and then alphabetically. Analytes are defined as proteins or peptide sequences for MI or MRM assays, respectively. Sample numbers in each clinical group include 60 schizophrenia (SCZ) and 79 healthy control (HC). *'Number of data points'* refers to the number of data points available per analyte for each clinical group after data pre-processing. Only analytes for which there was a statistical difference in expression (linear mixed effects model, *'P P'*<0.05) in SCZ relative to HC serum are shown. '*Covariates*' refer to clinical variables (age or gender) selected for each analyte by stepwise application of Bayesian Information Criteria in the linear mixed effects model. '*Fold change*' between clinical groups (derived from the regression coefficient) refers to the peptide abundance (MRM) or analyte concentration (MI); resulting values between 0 and 1 converted to -1/'*Fold change*'). FC – fold change, NA - not applicable, P P – permuted P-value.

			Data points				
Protein	**Peptide sequence**	**Assay**	**HC**	**SCZ**	**Covariates**	**P P**	**FC**
Interferon-γ (IFN-γ)	NA	MI	79	59	-	0.018	-1.07
Transforming growth factor-β1 (TGF-β1)	NA	MI	79	59	-	0.045	-1.05
Antithrombin-III	FDTISEK	MRM	77	60	gender + age	0.014	1.26
Antithrombin-III	LPGIVAEGR	MRM	77	60	gender + age	0.015	1.25
Apolipoprotein A-II	SPELQAEAK	MRM	77	60	-	0.022	-1.13
Apolipoprotein A-IV	IDQNVEELK	MRM	77	60	gender	0.010	-1.26
Apolipoprotein A-IV	ISASAEELR	MRM	77	60	-	0.041	-1.21
Apolipoprotein C-I	EFGNTLEDK	MRM	77	60	age	0.037	-1.26
Apolipoprotein C-III	GWVTDGFSSLK	MRM	77	60	gender	0.004	-1.25
Apolipoprotein C-III	DALSSVQESQVAQQAR	MRM	77	60	-	0.015	-1.21
Apolipoprotein H	EHSSLAFWK	MRM	77	60	-	0.043	1.26
Complement C4-A	VLSLAQEQVGGSPEK	MRM	77	60	age	0.016	1.24
Complement C4-A	ITQVLHFTK	MRM	77	60	age	0.034	1.22
Complement component C9	VVEESELAR	MRM	77	60	-	0.029	1.23
Ficolin-3	YGIDWASGR	MRM	77	60	-	0.037	1.23
Haptoglobin	DYAEVGR	MRM	77	60	age	0.001	1.56
Haptoglobin	VTSIQDWVQK	MRM	77	60	age	0.001	1.54
Haptoglobin	VGYVSGWGR	MRM	77	60	age	0.001	1.53
Inter-α-trypsin inhibitor heavy chain H4	GPDVLTATVSGK	MRM	77	60	gender	0.024	1.18
Plasma protease C1 inhibitor	TNLESILSYPK	MRM	77	60	gender + age	0.001	1.36
Plasma protease C1 inhibitor	FQPTLLTLPR	MRM	77	60	gender + age	0.012	1.34
α-1-antichymotrypsin	EQLSLLDR	MRM	77	60	gender + age	0.021	1.38
α-2-antiplasmin	FDPSLTQR	MRM	77	60	gender + age	0.044	1.23

Table 4.4 Common functional pathways of altered serum analytes from Table 4.3 and Figure 4.1C. All identified serum proteins have been previously associated with schizophrenia (SCZ; 'SCZ references'). The microglia section gives an overview of current literature available indicating whether microglia are capable of responding to that particular analyte and, if known, how it can affect microglia polarization. NA – not available

Uniprot ID	*Abbreviation*	*Gene*	*Protein ID*	*Direction*	***Biological processes***						*SCZ references*	***Microglia***		
					Blood Coagulation	*Complement Activation*	*Metabolic Process*	*Acute Phase/ Inflammatory Response*	*Metal/Ion Binding*	*Lipid Binding/ Transport*		*Microglia references*	*Pro-inflammatory*	*Anti-inflammatory*
P08697	A2AP	*SERPINF2*	α-2-antiplasmin	↑	✓			✓			252	NA		
P01011	AACT	*SERPINA3*	α-1-antichymotrypsin	↑	✓		✓	✓			312–314	315,316	✓	
P01008	ANT3	*SERPINC1*	Antithrombin-III	↑	✓			✓	✓		252,317	NA		
P02652	APOA2	*APOA2*	Apolipoprotein A-II	↓			✓	✓		✓	252,318	309		✓
P06727	APOA4	*APOA4*	Apolipoprotein A-IV	↓			✓	✓		✓	252,318–320	NA		
P02654	APOC1	*APOC1*	Apolipoprotein C-I	↓			✓			✓	252,318	321		✓
P02656	APOC3	*APOC3*	Apolipoprotein C-III	↓			✓			✓	252	NA		
P02749	APOH	*APOH*	Apolipoprotein H	↑			✓			✓	106	NA		
P0C0L4	CO4A	*C4A*	Complement C4-A	↑		✓		✓			161	161	✓	
P02748	CO9	*C9*	Complement component C9	↑		✓					322	NA		
O75636	FCN3	*FCN3*	Ficolin-3	↑		✓			✓		322	NA		
P00738	HPT	*HP*	Haptoglobin	↑			✓	✓			319,323,324	325		✓
P05155	IC1	*SERPING1*	Plasma protease C1 inhibitor	↑	✓	✓		✓			314	NA		
P01579	IFNG	*IFNG*	Interferon-γ (IFN-γ)	↓				✓			71,101,326	148,327	✓	
Q14624	ITIH4	*ITIH4*	Inter-α-trypsin inhibitor heavy chain H4	↑			✓	✓			22,328,329	330		✓
P01137	TGFB1	*TGFB1*	Transforming growth factor-β1 (TGF-β1)	↓				✓			71,101	148,282,302		✓

4.3 Discussion

This chapter presents a comprehensive investigation on how changes in first-onset drug-naïve schizophrenia serum are capable of inducing microglial signalling responses. This is the first study attempting to demonstrate that circulating blood serum from schizophrenia patients can have a direct effect on activating the intracellular activation phenotypes of resident brain immune cells *in vitro*. The changes in downstream signalling cascades have been presented as well as the detected changes in patient serum potentially causing these intracellular phenotypes. Furthermore, the central epitopes known to be involved in the activated signalling pathway have been investigated for their response to targeted drug screening. In the next section the main signalling cascades that have been identified through serum exposure will be discussed in more detail. The specificity of the emerging phenotype signature associated with the exposure of microglial cells to serum from schizophrenia patients will be compared to major depressive disorder (MDD).

4.3.1 Altered STAT3 signalling in microglia cells following patient serum exposure

Patient serum exposure resulted in less of a decrease of STAT3 (pY705) and SHP2 (pY542) in microglia compared to exposure to healthy control serum, while total STAT3 protein expression (independent of phosphorylation) increased compared to controls. The STAT pathways have been found across many multicellular organisms (e.g. worms, flies and vertebrates) and are critical for developmental regulation, growth control and homeostasis[285]. The JAK–STAT pathway transmits information received from extracellular polypeptide signals (such as growth factors and cytokines), through transmembrane receptors, directly to target gene promoters in the nucleus, providing a mechanism for transcriptional regulation without second messengers. Usually, STAT proteins are inactive as transcription factors in the absence of specific receptor stimulation and are localized in the cytoplasm of unstimulated target cells. They are activated rapidly in response to receptor-ligand coupling and are recruited to the intracellular domain of the receptor[285]. JAK-STAT3 signalling pathways are regulated by a vast array of stimuli, such as cytokines (e.g. IL-2, IL-6, IL-10, IL-11, IL-22 and IFN-γ). Although activation of STAT3 is best known to happen through the cytokine receptor subunit gp130, many routes lead to STAT3 activation other than cytokine stimuli, such as leptin, leukemia inhibitory factor (LIF), ciliary neurotrophic factor (CNTF), oncostatin M (OSM)[298], HDL and haem oxygenase 1[331,332]. Once STAT3 is activated through phosphorylation at tyrosine 705, the protein will homo- or heterodimerize and translocate to the nucleus. In the nucleus, STAT3 binds to specific DNA sequences to regulate mRNA expression from its target genes[333].

The JAK-STAT signalling pathways do not usually function autonomously. Next to environmental stimuli, they can be regulated by intrinsic stimuli. Diverse protein kinases phosphorylate STATs on serine residue 727, including several mitogen-activated protein kinases (MAPKs)[334], allowing additional cellular signalling pathways to potentiate the primary STAT-activating stimulus. Similarly, it is possible that additional sites of regulated serine phosphorylation or other posttranslational modifications may regulate attenuation of STAT activity[285].

Negative regulation of the JAK-STAT pathway can be accomplished through receptor internalization to endocytic vesicles and subsequent receptor degradation. Inhibition of phosphorylated STAT dimers can be achieved via protein inhibitors of activated STATs (PIAS) or by protein tyrosine phosphatases (PTP), such as SHP2. The JAKs have their own inhibitors, called suppressor of cytokine signalling (SOCS) proteins. The most prototypical STAT3 regulator is SOCS3, which creates a loop from the nucleus to the JAKs. Expression of SOCS genes can be stimulated by the same cytokines that enhance STAT activation, so the SOCS proteins can act in classic feedback inhibition loops (**Figure 4.2**) [285,335,336].

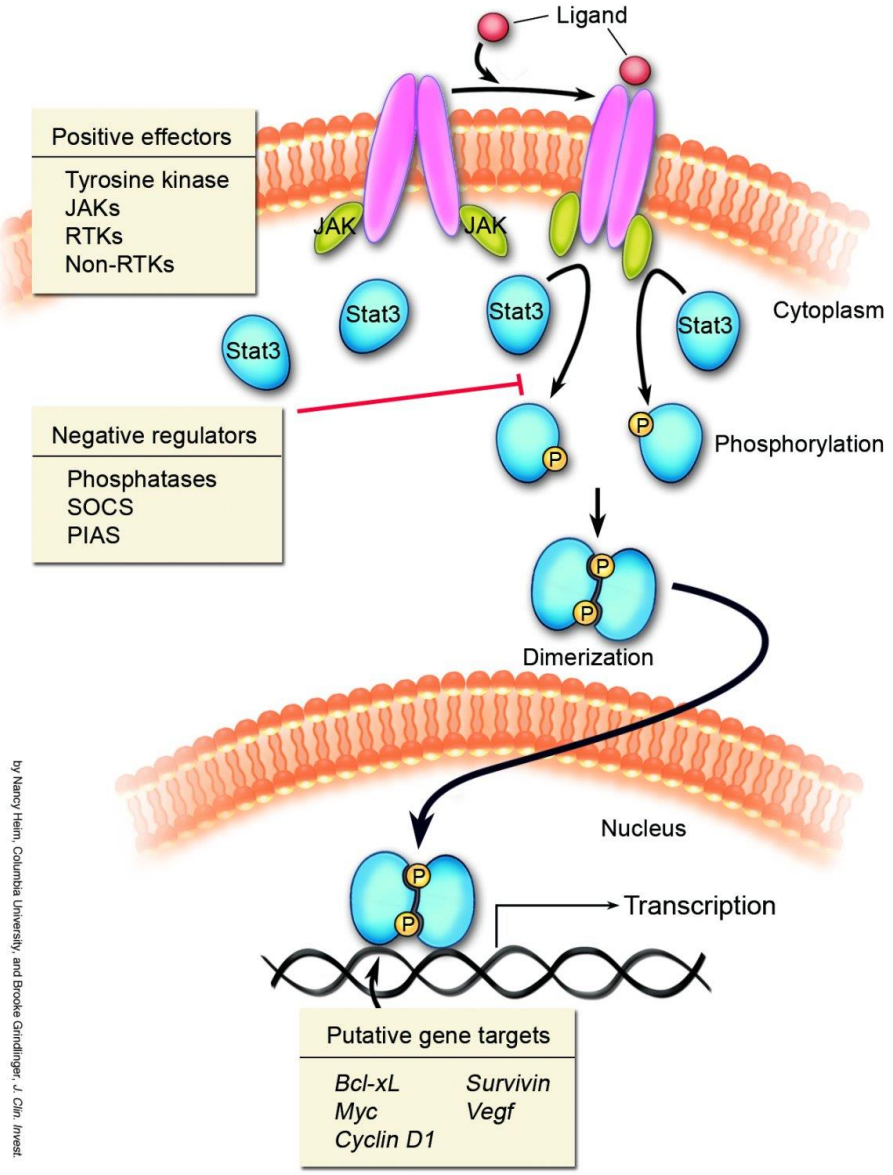

Figure 4.2 Model for Stat3 signalling. Stat3 is a transcription factor, which is activated in response to many cytokines and growth factors that bind to specific receptors. Upon ligand-receptor binding, Stat3 is recruited to the plasma membrane, where it becomes activated via phosphorylation of a tyrosine residue either directly by receptor tyrosine kinases (RTKs), such as the PDGF receptor and EGF receptor, or by non-RTKs, such as Src and JAK. Stat3 activation induces dimerization via reciprocal phosphotyrosine–SHP2 interaction between two Stat3 molecules. The Stat3 dimers then translocate to the nucleus where they bind to consensus sequences on the promoter of target genes and activate their transcription. Stat3 activation is tightly regulated by different negative regulators of phosphorylation, such as phosphatases, suppressor of cytokine signalling (SOCS), and protein inhibitor of activated Stats (PIAS). In many cancer-derived cell lines and primary tumors Stat3 is constitutively activated either as a consequence of deregulated signalling from positive effectors (*e.g*. overexpression of growth factor receptors and their ligands) or by abnormal activity of negative effectors. *Reprinted with permission*[337].

4.3.2 Implication of cytokine signalling pathway in microglia following schizophrenia patient serum exposure

The combination of SHP2 and STAT3 is known to be involved with signalling cascades initiated by the IL-6/glycoprotein(gp)130 family receptor, which is associated with signal transduction of cytokines. The gp130 receptor serves as a signal-transducing receptor subunit for the IL-6-type or gp130 cytokines consisting of IL-6, IL-11, LIF, OSM, CNTF, cardiotrophin-1 (CT-1), and the cardiotrophin-like cytokine (CLC). However, the gp130 receptor unit can also interact with 5 other different receptor units, facilitating transduction of a wide range of cytokines[338]. Although we did not identify the presence of increased pro-inflammatory cytokines in patient serum (**Table 4.3**), the applied panel for cytokine detection (n=10) did not allow for the detection of a full cytokine-profile. Therefore, the identified STAT3 (pY705) phosphorylation could be associated with increased circulating cytokine levels in patient serum. Two meta-analyses, one combining 23 and one 62 studies, report the presence of increased proinflammatory IL-6 levels in first-onset schizophrenia patients, which is the prototypical ligand for STAT3 pY705 activation[100,339]. Furthermore, another meta-analysis, using 40 studies, identified IL-6 levels to normalize upon successful treatment[101]. Although we did not identify a significant difference in IL-6 levels (**Table 4.3**), the STAT3 pY705 activation could have been a result of increased levels of other IL-6 family cytokine members signalling through the gp130 receptor. Furthermore, the reported increase in unphosphorylated STAT3 further supports the potential signalling processes via the gp130 receptor. It is well known that gp130-linked cytokines stimulate the phosphorylation of STAT3 at Y705, which subsequently either: i) activates many genes associated with inflammatory responses; ii) or results in an increase of unphosphorylated STAT3 levels which will in turn initiate a second wave of promoting a wider gene expression that does not respond directly to phosphorylated STAT3[340]. Such a process is usually facilitated by unphosphorylated STAT3 binding to NF-κB and the resulting complex will be transferred to the nucleus to activate a subset of NF-κB-dependent proinflammatory genes[340]. Thus, unphosphorylated STAT3 can sustain a longer cytokine-dependent profile not via the conventional signalling mechanism used by phosphorylated STAT3.

However, although changes in STAT3 signalling patterns could have been due to the effect of altered cytokine levels in serum, it could also reflect an alteration in other cell signalling pathways. As explained in section **4.3.1**, STAT3 signalling can be fine-tuned via many modulators. The present finding could therefore also reflect the activity of a parallel pathway capable of modifying the STAT3 response in microglia. Also, although most STAT3 cytokines are pro-inflammatory, it is noteworthy to mention that the anti-inflammatory cytokine IL-10 is mediated by STAT3 (pY705)[144]. Therefore, future studies should include a separate line of investigation to measure the full cytokine spectrum.

4.3.3 Altered 4EBP1 signalling in microglia upon schizophrenia patient serum exposure

Patient serum exposure resulted in less of a decrease of 4EBP1 (pT36/pT45) and an increase in both 4EBP1 (pT69) and eIF4E (pS209) in microglia, compared to exposure to healthy control serum. Both the 4EBP1 phosphorylation sites are involved with inhibition of 4EBP1 activity, thereby diminishing the inhibition of 4EBP1 on eIF4E. The 4EBP1 proteins compete with eIF4G and eIF4A for a common binding site on eIF4E. The phosphorylation of 4EBP1 prevents its binding to eIF4E, allowing eIF4E to assemble into the EIF4F complex and therefore promote translation as the eIF4F complex binds the mRNA cap structure at the 5' end. This 4EBP1 translational control is part of the phospho-inositide 3-kinase (PI3K)/mammalian target of rapamycin (mTOR) signalling pathway[341]. mTOR is a protein serine/threonine kinase that belongs to the PI3K-related family. mTOR signalling is involved in a variety of biological processes, such as protein synthesis, lipid synthesis, transcription, actin dynamics, autophagy and neuronal morphology. Two structurally and functionally different mTOR complexes have been identified. The first one, mTOR complex 1 (mTORC1), contains regulatory associated protein of mTOR (Raptor), which is replaced by rapamycin-insensitive companion of mTOR (Rictor) in mTOR complex 2 (mTORC2). In addition to mTOR, both complexes share the proteins lethal with Sec13 protein 8 (LST8), DEP domain containing mTOR-interacting protein (Deptor) and scaffold proteins Ttil1 and Tel2 which regulate the complexes' assembly and stability[342–345]. As illustrated in **Figure 4.3**, mTORC1 signalling is most likely involved in microglia exposed to schizophrenia patient serum.

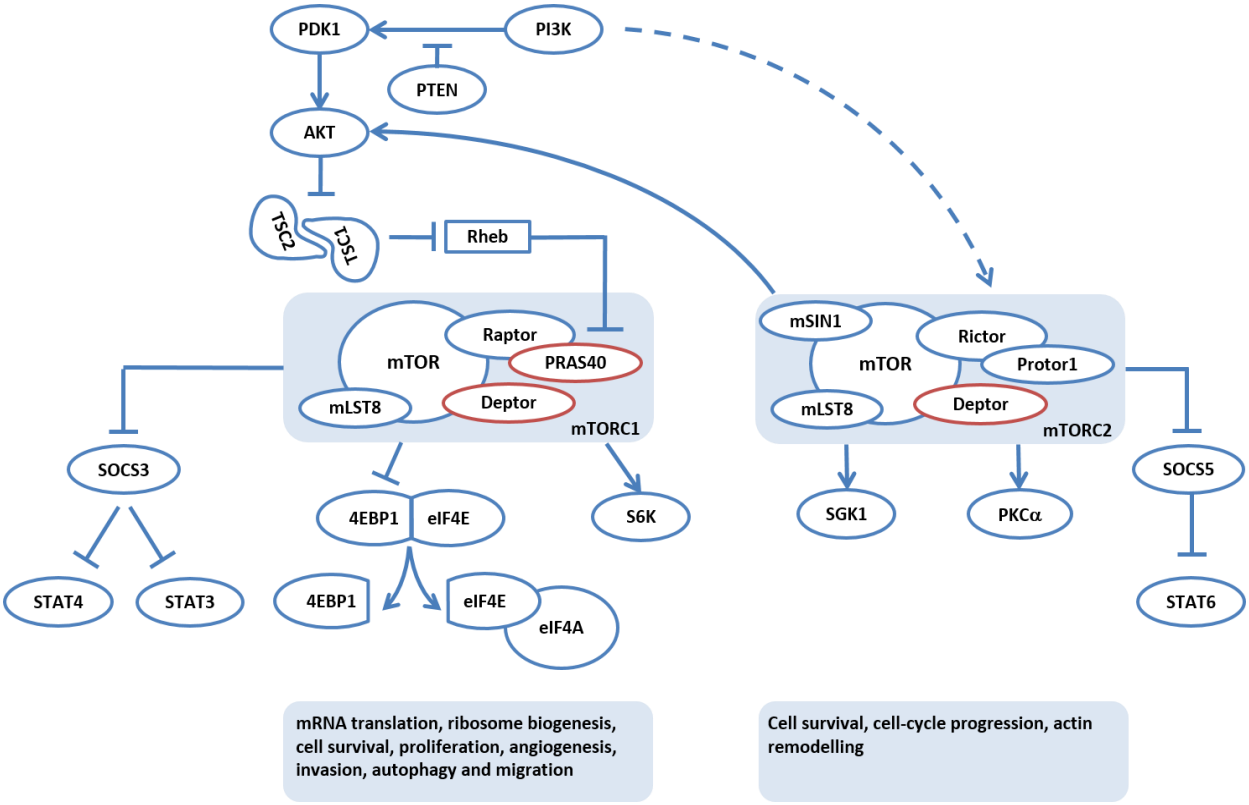

Figure 4.3 Overview of mTORC1 and mTORC2 signalling pathways. Upon activation through neurotrophins, glutamate, or growth factors, Akt activated through PI3K will phosphorylate TSC2, rendering the TSC complex inactive. This results in activation of Rheb which will deactivate the endogenous mTORC1 inhibitors. 4EBP1 is then phosphorylated by mTORC1, releasing the competition with eIF4A, allowing eIF4E to form the eIF4F complex by binding 4eIF4A. Regarding mTORC2, the mechanism underlying this complex remains elusive and very little is known about its upstream regulation. Potent activators are neurotrophins, glutamate, and in neurons changes that induce long-lasting alterations in synaptic strength. It is suggested that assembled ribosomes directly bind to mTORC2 in a PI3K dependent manner. In addition, protein synthesis is not required *per se* for the ribosome-mediated association and activation of mTORC2. mTORC2 activation will result in phosphorylation of AGC kinases, a protein group of 60 members including PKA, PKB and PKC but also enzymes such as SGK1[343–345]. 4EBP1: Eukaryotic translation initiation factor 4E-binding protein 1, AKT: protein kinase B, Deptor: DEP domain containing mTOR-interacting protein, eIF4: Eukaryotic translation initiation factor 4, mLST8: mammalian lethal with Sec13 protein 8, mSIN1: mammalian stress-activated protein kinase interacting protein, mTOR: mammalian target of rapamycin, PDK1: phosphatidylinositol-dependent kinase 1, PI3K: phospho-inositide 3-kinase, PKCα: protein kinase Cα, PTEN: phosphatase and tensin homolog, SGK1: serum and glucocorticoid-induced protein kinase 1, SOCS: suppressor of cytokine signalling, TSC: tuberous sclerosis complex. Red colour indicates endogenous inhibitors to mTOR. Dashed lines indicate that the exact mechanism is unknown.

4.3.4 Implication of increased mTORC1 signalling in microglia following schizophrenia patient serum exposure

In contrast to STAT3, mTORC1 signalling has been suggested to be disrupted in schizophrenia[346]. This comes from studies reporting dysfunctions of diverse upstream activators and environmental stressors, previously implicated in schizophrenia, that have the ability to over-activate or inhibit mTORC1 signalling[346]. Furthermore, inhibition of the *DISC1* gene product, one of the most common genes associated with schizophrenia, results in increased phosphorylation of Akt and S6 (two components of the mTOR pathway), neuronal hypertrophy, abnormal dendritic morphology and hyper excitability. These changes are associated with learning and memory deficits and depressive-like behaviour in rodents[347,348]. Rapamycin, a prototypical inhibitor of mTORC1 signalling, is capable of reversing these biochemical and behavioural effects in the *DISC1* knock-down model[347]. Additionally, multiple publications have presented data regarding the inhibition of mTORC1 signalling and the association of neuronal protection from inflammatory responses via the modulation of microglial activation[307,311,349–352], suggesting that the *DISC1* knockout effects may be limited to overactive mTORC1 signalling cascades in microglia.

Activation of the mTORC1 pathway has repeatedly been associated with the deleterious consequences of microglial pro-inflammatory polarization in preclinical models of ischaemia and neurodegeneration[307,311,349–351]. Interestingly, increased mTORC1 signalling is also associated with an impaired autophagic response[353]. Impairments in autophagy have been proposed to contribute to neuropsychiatric pathogenesis following reports of decreased autophagic regulator beclin-1 expression in *post-mortem* brains of schizophrenia patients, relative to controls[354], and behavioural abnormalities linked to autism spectrum disorder in myeloid cell-specific Atg7 knockout mice[355]. Induction of autophagy has also been proposed to mediate the efficacy of antidepressant and mood stabilizing treatments in MDD and bipolar disorder respectively[356–358]. Future investigations should therefore aim to better characterize the potential relative contributions of metabolic priming and altered autophagic responses in determining the functional consequences of microglial mTORC1 activation in schizophrenia.

Interestingly, mTOR signalling has been suggested to be a biomarker for the autoimmune disease systemic lupus erythematosus[359], an autoimmune disease associated with a higher risk of developing schizophrenia. As a consequence, mTORC1 inhibitor rapamycin has been recently proposed to be a safe and effective treatment for this autoimmune disorder[360]. The immunosuppressive abilities of mTOR inhibitors are further strengthened by the application of these drugs for the prevention of organ transplant rejection[361]. Such an immunosuppressive compound could be of interest to test as an add-

on treatment for schizophrenia and would have to be further tested for its efficacy towards symptom improvement.

4.3.5 Potential crosstalk between STAT3 and mTORC1 signalling pathways

Of interest is the potential crosstalk between the JAK-STAT3 and mTORC1 signalling pathways. Recent data suggests that while mTORC1 signalling alone is not sufficient to trigger microglial activation, it represents a metabolic primer of key translational proteins which subsequently lead to an exaggerated response in the presence of specific proinflammatory stimuli[362]. In this respect, the observed alterations in mTORC1 signalling may act synergistically with those reported for STAT3 to induce pro-inflammatory polarization. Further indications for the STAT3-mTOR crosstalk come from studies showing that STAT3 requires phosphorylation on tyrosine and serine residues by independent protein kinase activities for maximal activation of target gene transcription[363]. Members of the JAK/Tyk family of tyrosine kinases mediate phosphorylation of STAT3 at Tyr705 during CNTF signalling; however, phosphorylation at STAT3 Ser727 appears to depend on both the extracellular stimulus and the cellular context. For example, in CNTF stimulated neuroblastoma cells, STAT3 is phosphorylated at regulatory site Ser727. Subsequently it has been shown that the CNTF-induced phosphorylation at Ser727 is mTOR dependent as phosphorylation was prevented by the mTOR inhibitor rapamycin[364]. Further evidence comes from RHEB-/- mice, in which an increase of SOCS3 can be identified due to the lack of inhibition by mTORC1 as the mTORC1 endogenous inhibitors will not be inhibited by Rheb. Furthermore, in mice treated with specific mTORC1 inhibitors, microglia will not polarise towards a pro-inflammatory, but rather an anti-inflammatory-like phenotype following stroke[307]. STAT3 (pY705) is needed for STAT3 activation, and it is suggested that the synergistic combination of mTORC1 phosphorylating STAT3 at S727 simultaneously stimulates pro-inflammatory differentiation. In this context, it is suggested that mTORC1 integrates signals to promote pro-inflammatory microglial differentiation[365,366]. Although this research presents a comprehensive overview of a STAT3-mTOR mechanism, this context has only been investigated in the presence of CNTF, therefore this finding can easily be different in the presence of other stimulants.

The STAT3-mTORC crosstalk has been suggested to specifically regulate immune responses, yet there is no data published about this potential crosstalk in microglia. An indication for mTOR's immune regulating involvement comes from T cells. It was shown that rapamycin inhibits mTOR and thereby inhibits T cell fate, promoting anergy[367]. mTOR inhibitors are being more and more recognized for their immunosuppressive activities, with them recently even being applied to prevent organ transplant rejection[368,369]. However, the lack of published data with regard to the role of mTOR in regulating pro-

and anti-inflammatory differentiation in microglia does not allow to elucidate this pathway's involvement in microglial polarization. Some research has been done in PBMCs, but the reported outcomes have caused more confusion rather than clarification regarding the potential immune regulating STAT3-mTORC1 crosstalk[370–372]. It would be of interest to examine this more closely in cell lines and rodents after genetic ablation of either one of these distinct pathways, allowing a unique investigation towards mTOR dependent phenotypic polarization[373].

4.3.6 Changes in schizophrenia serum may be linked to pro-inflammatory polarization in microglia

The finding of increased complement components ficolin[374], C4 and C9 in patient serum aligns with previously published data regarding the involvement of the complement cascade (illustrated in **Figure 4.4**[164]; **Table 4.4**) in schizophrenia[161,221,375]. Although the BBB protects the CNS from plasma-derived immune components, many complement components can be locally produced within the CNS, most often in response to injury or inflammatory signals, but they are also involved with guiding synaptic pruning[376–378]. However, when the BBB becomes leaky, the usual tight regulation of transport is lost. This can be caused by a number of mediators, such as complement activation products[379]. The complement activation by-product C5a is amongst others involved in increasing BBB permeability during neuroinflammatory states[380]. C4 is involved in microglial synaptic pruning[377,378], a process that has been hypothesized to be involved with the prodromal phase and onset of schizophrenia during adolescence[53,159,179]. Mice with increased C4 production show elevated synaptic pruning during the neurodevelopmental phase[161], something that continues into adulthood as shown by other rodent studies[381–383]. Microglial over-activity has not only been linked to excessive synaptic loss, but also cognitive decline, as shown in animal models of Alzheimer's disease[384].

Interestingly, a link between pro-inflammatory auto-immune diseases and neuropsychiatric disorders has been suggested. Patients with autoimmune diseases like multiple sclerosis, celiac disease and

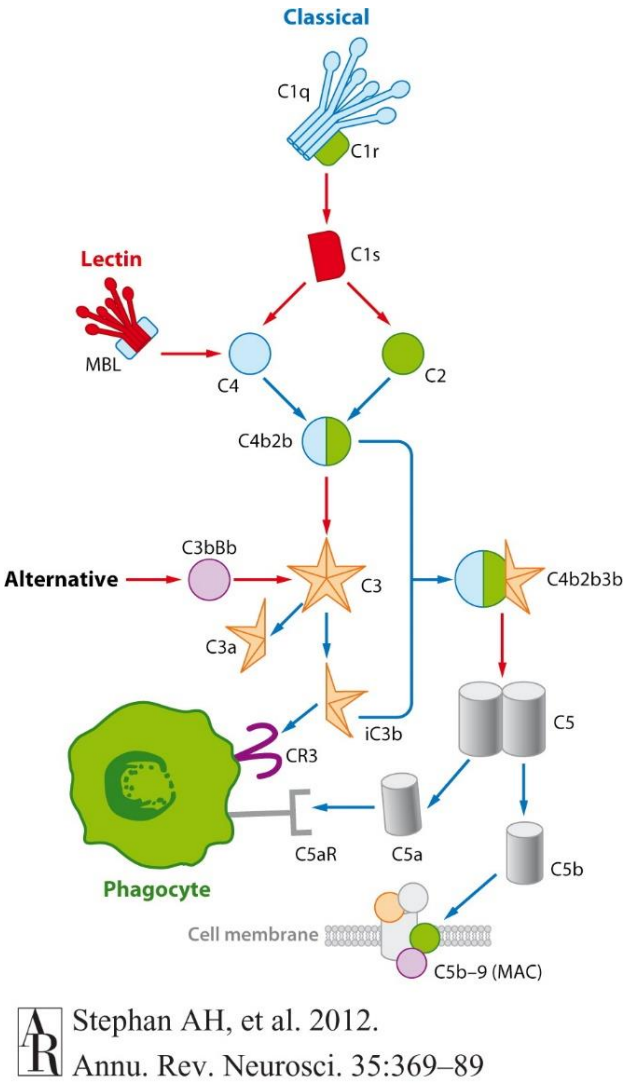

Figure 4.4 Overview of complement signalling cascades; from Stephan *et al.* (2012). Complement is activated by three major routes: the classical, the alternative, and the lectin pathways, all of which converge on complement component C3, a central molecule in the complement system that ultimately drives complement effector functions, including the elimination of pathogens, debris, and cellular structures. The **classical pathway** is induced when C1q interacts with antibodies or one of its many binding partners or apoptotic cells. The C1q tail region of C1q binds proteases C1r and C1s to form the C1 complex. Binding of the C1q complex to an antibody/receptor on the cell surface induces a conformational change in the C1q molecule, which leads to activation of an autocatalytic enzymatic activity in C1r; C1r then cleaves C1s to generate the active serine protease. Once activated, C1s cleaves C4 and C2 to generate the C3 convertase, C3b2b, which in turn cleaves C3 and activates downstream cascade components. The **lectin pathway** is triggered by the binding of mannose binding lectin (MBL) or ficolin to mannose residues on the cell surface[374]. This activates the MBL-associated proteases mannose binding lectin serine protease 1 (MASP1) and MASP2, which then cleave C4 to generate the C4 convertase, C4b2b. The **alternative pathway** is spontaneously and continuously activated (via spontaneous C3 hydrolysis), which serves to amplify the cascade triggered by classical and lectin pathways. All three cascades converge on major complement component C3. Cleavage of C3 generates the anaphylactic peptide C3a and the opsonin C3b. Opsonisation with C3b/iC3b leads to elimination of target structures by phagocytes that express C3 receptors (*e.g.* C3R/Cd11b). C3b later joins with C4b2a (the C3 convertase) to form the C5 convertase (C4b2a3b complex) that generates the anaphylatoxin C5a, which binds to C5a receptors (C5aR) on phagocytic/effector cells. Robust activation of complement can trigger activation of the terminal complement cascade, resulting in cell lysis through the insertion of the pore-forming C5b-C9 complex into the membrane, termed membrane attack complex (MAC). *Reprinted with permission*[164].

systemic lupus erythematosus are more likely to develop symptoms related to schizophrenia (*e.g.* psychosis) compared to controls[67–69]. Furthermore, similar complement components and complement-related genetic polymophisms have been identified as altered in serum from these patients suffering from auto-immune disorders as we identify in this study[385–388]. However, although we identify the presence of pro-inflammatory proteins in serum from schizophrenia patients overlapping to proteins identified in serum from patients suffering from auto-immune diseases, those patients suffering from auto-immune diseases linked to schizophrenia do most of the time not suffer from schizophrenia. Therefore, it remains questionable whether this observation is related to the pathophysiology of neuropsychiatric disorders.

Although the pathogenesis of schizophrenia remains unknown, increasing evidence from genomic, transcriptomic and proteomic studies support a role for both coagulation and inflammation related processes in the pathophysiology[66,317,389]. Furthermore, meta-analyses have consistently shown that ischemic cardiovascular disease reduces the life expectancy of schizophrenia patients, which is about

15 years less than that of the general population[390,391]. This increased cardiovascular risk has been ascribed to antipsychotic treatment side effects, smoking and inactivity[392]. Interestingly, a case study recently showed the potential benefits of chronic warfarin (used for the treatment of deep-vein thrombosis), indicating that changes in the modulation of coagulation pathways might contribute to schizophrenia pathogenesis[393]. Furthermore, neuroimaging of patients revealed brain atrophy indicated by whole brain volume deficits, but ischemic lesions are not typically present[56,389]. All coagulation factors we identified are involved with inhibiting clot formation, and this could also affect BBB integrity.

The decrease of apolipoprotein levels are in line with the observed proinflammatory shift, due to less binding to the anti-inflammatory stimulating microglial TREM2 receptor[309,394,395], a receptor highly and exclusively expressed by microglia within the CNS[396,397]. TREM2 has been shown to be linked to neuroprotection. The selective overexpressing of TREM2 in microglia in the brain of P301S mice has been shown to stimulate a protective profile[394]. Furthermore, a study in schizophrenia patients has shown that alterations in serum apolipoprotein levels correlate to poorer cognitive performances and lower hippocampal volumes[252]. As we detected a decrease in apolipoproteins, this would have caused less interaction with TREM2, allowing a proinflammatory polarization. This further strengthens the involvement in microglial pruning in schizophrenia. Therefore, inhibition of microglial activity in this instance could reduce the extent of pathological synaptic loss.

Although these proteins do elucidate some of the potential interactions between serum components and observed microglia signalling, it should be taken into account that we applied a targeted platform. We measured a total of 90 proteins in patient serum relative to healthy controls, whilst there are much more serum proteins that could have interacted with the microglia that we did not measure. Therefore, future studies using a much wider screening platform investigating both low and high abundance proteins would be beneficial to get an understanding of other interactions that could have occurred too.

Chapter 5
Pet Study

Chapter 5 | *In vivo* Microglia Activation

5.1 Introduction

As microglia are embedded in a dense network of neuronal interactions, they are intimately associated with neurons. Due to this network nature, the CNS exhibits unique pathological patterns, in contrast to other tissues[126]. Whether a neuron's axon is damaged or a nerve cell loses input due to elimination of a distant projecting neuron, it will cause a reaction from a neighbouring microglia that will interrogate the altered situation. In this regard, PET scanning has been useful in investigating affected regions of the brain in neurodegenerative disorders. PET tracer [^{11}C](*R*)-PK11195 binds selectively to TSPO. This binding activity is only expressed by myeloid cells within the CNS, as indicated by immunohistochemistry and autoradiography studies[171,398,399]. Furthermore, it is suggested that this translocator protein is greatly increased in activated glial cells in states of brain injury and repair[172]. Therefore, PET imaging studies have taken advantage of this specific radio ligand for identification of microglia induced neuroinflammation.

Two meta-analyses of *post-mortem* data provide evidence for microglial activation in schizophrenia[153,400], but *post-mortem* tissue studies do not present information of the pathological process at the disease onset. Therefore, schizophrenia patients have been investigated using *in vivo* PET studies in an attempt to elucidate microglia driven neuroinflammation. Yet, the PET results to date remain inconsistent, with some studies reporting an increase in microglial activation in first-onset drug-naïve patients[156], some report a decrease[157] and others detect no significant differences between patients and controls (see **Table 1.2** for an overview). Furthermore, the TSPO marker used in PET imaging has recently even been suggested not to be specific to microglia[188,401,402] nor to distinguish between different microglial activation states[403].

One of the major issues relating to *in vivo* microglia imaging studies are methodological inconsistencies, resulting in different outcome measures. Currently 13 papers report PET data from individuals with ultra high risk (UHR) of, or with, schizophrenia diagnoses. The earliest two studies report increased binding potential in whole brain grey matter[180] and the hippocampus[181] of antipsychotic treated schizophrenia patients. Later studies, however, have not consistently demonstrated an increase in binding potential. The inconsistent outcomes across these 13 papers could possibly be explained by the application of five different radio ligands that should be specific for TSPO detection. Apart from that, sample sizes are small and a range of different patient groups were investigated, ranging from UHR individuals to antipsychotic treated schizophrenia patients. The most

commonly used tracer is [^{11}C](*R*)-PK11195, which in three out of five studies has been reported to show a significant increase of binding potential in antipsychotic treated patients[180,181,186]. One of the studies not reporting a significant difference using this particular tracer investigated a heterogeneous group of patients with most patients being on antipsychotic treatment but not all of them[185]. However, the other study, which is also the most recently published study, used this tracer in UHR, recent onset and chronically ill patients and did not identify any differences relative to controls[158].

One of the major disadvantages of the currently published PET studies is the lack of an independent line of investigation providing information regarding an individuals' inflammatory profile, such as cytokines in serum. Furthermore, there is little knowledge about the CNS environment with the propensity of affecting microglial functioning, making interpretation of these PET studies difficult. Here, we present the first PET tracer study in schizophrenia patients combined with an investigation of changes in serum proteins which have previously been implicated in the disease process of neuropsychiatric diseases[253]. Furthermore, a human microglia cell line was exposed to schizophrenia patient serum followed by high-content functional single-cell screening to investigate the cell signalling pathways which predispose microglia to phenotypic switching. This allows for the comparison of PET data to blood analytes of a given patient, which may yield functional information regarding microglia signalling.

5.2 Results

5.2.1 PET study design

The cohort presented is identical to the patients and healthy controls from van der Doef *et al.* (2017)[185]. Most patients were on antipsychotic treatment at the time of the PET brain imaging, except for three patients who were not on medication and one drug-naïve patient. Demographics of recent onset schizophrenia with (n=15) and without treatment (n=4) and matched healthy controls (n=17) are shown in **Table 5.2**. The PANSS scores place the patients in the mildly psychiatrically ill category (53 ± 10 PANSS total score)[404].

A human microglia cell line was exposed to serum collected at the time of brain imaging for 30 minutes. Subsequently, the cells were fluorescently barcoded and changes in microglia signalling evoked by serum exposure were measured across 62 cell signalling epitopes. The epitopes spanned a wide variety of cell signalling pathways broadly including Akt/GSK-3β, PKA, PKC, MAPK, JAK/STAT, IL-1R/TLR and antigen/integrin (A/I) receptor signalling (**Chapter 2; Table 2.2**). This allowed monitoring 2232 unique cell signalling responses, in addition to positive controls and vehicles, all measured in triplicate.

We further explored the composition of the serum for the presence of analytes (**Chapter 2; Table 2.4**), with the potential to activate microglia, using a targeted mass spectrometry approach. We also examined the direct effects of five different antipsychotics on the identified epitopes, to answer the question whether the observed changes in cell signalling represented direct effects of drug traces in serum or complex changes in patient physiology.

Table 5.1 Demographic characteristics of the schizophrenia patients and controls. The Wilcoxon rank-sum test (*) was used for continuous variables and Fisher's exact test (º) for categorical variables, so that there were no significant differences in the demographic variables between clinical groups. The table shows mean values ± standard deviation. Other antipsychotic treatment includes flupentixol, paliperidone, aripiprazole, quetiapine and zuclopentixol. AF – antipsychotic free. AP – antipsychotic treated. HC – healthy control. SCZ – schizophrenia. PANSS - Positive and Negative Syndrome Scale. NA – not applicable. Y - yes. N - no. M - male. F - female.

					P value	
		SCZ AF	SCZ AP	HC	SCZ AF vs. HC	SCZ AP vs. HC
		4	15	17	-	-
		4/0	12/3	14/3	1.000 º	1.000 º
Age (years)		28 ± 2.16	25.13 ± 4.05	25.82 ± 3.66	0.192 *	0.569 *
Smoking (Y/N)		3/1	7/8	5/12	0.253 º	0.467 º
Cannabis (Y/N)		1/3	1/14	0/17	0.191 º	0.469 º
Injected dose (MBq)		392 ± 123	420 ± 46	420 ± 49	0.875 *	0.840 *
Specific activity (GBq/µmol)		85 ± 21	91 ± 33	80 ± 21	0.875 *	0.121 *
Injected mass (µg)		1.7 ± 0.6	1.9 ± 0.8	2.0 ± 1.0	0.875 *	0.252 *
Disease duration (years)		0.8 ± 0.65	1.10 ± 0.61	-	-	-
PANSS	**Positive**	16 ± 7	11 ± 3			
	Negative	14 ± 5	14 ± 3			
	General	28 ± 8	27 ± 6			
	Total	57 ± 16	53 ± 9			
Antipsychotic treatment	**Clozapine**		3			
	Risperidone		2			
	Olanzapine		5			
	Other		5			

5.2.2 Detection of increased [^{11}C](*R*)-PK11195 in temporal brain region of antipsychotic treated patients

[^{11}C](*R*)-PK11195 binding potential (BP_{ND}) represents the ratio at equilibrium of specifically bound radioligand to that of non-displaceable radioligand in tissue. Upon inspection for detection of specific tracer activity levels and BP_{ND} one schizophrenia patient was identified as an outlier as specific tracer activity was below filtering level combined with extreme low BP_{ND} levels, indicating unreliable tracer data due to a too high signal-to-noise ratio. No significant differences in mean [^{11}C](*R*)-PK11195 BP_{ND} between schizophrenia patients versus controls were observed in either total grey matter or for regional [^{11}C](*R*)-PK11195 BP_{ND} (**Figure 5.1a, Table 5.3**). However, visual inspection of the data, with patient groups separated regarding treatment status, suggested BP_{ND} to be higher in the antipsychotic treated group. Pairwise comparisons showed a trend in treated patients for mean BP_{ND} (ANOVA; P=0.063), with an average increase of 20%. On the other hand, in the comparison of antipsychotic free patients to controls no difference was detected (P=0.263). The visual impression was further strengthened by the finding of a non-significant interaction of clinical group (treated patients, untreated patients and controls) and brain region (F1,5=0.290, P=0.918), indicating that the BP_{ND} differences between groups do not differ across all the regions. Therefore, it was decided to test the BP_{ND} for individual brain regions further post-hoc by t-test (one-tailed). BP_{ND} was found to be only significantly increased in medicated schizophrenia patients in the temporal cortex (P<0.05, FC=1.54) and a trend was observed for increased BP_{ND} in total grey matter (P=0.139, FC=1.22) (**Table 5.4**; **Figure 5.1b**).

Correlation analysis with PANSS revealed two significant correlations within the antipsychotic treated patient group, which were PANSS general and temporal cortex (P=0.039, r=0.56) and PANSS general and total grey matter (P=0.046, r=0.54) (**Figure 5.2**).

Table 5.2 Overview of [^{11}C](*R*)-PK11195 binding potential across different brain regions using the combined patient group. The table shows tracer binding potential from 18 schizophrenia patients (SCZ) and 17 healthy controls (HC) across different brain regions and for total grey matter volume. There were no significant differences detected between SCZ and HC binding potential. The table shows mean values ± standard deviation.

Region	Data points		BP_{ND}		
	HC	**SCZ**	**HC**	**SCZ**	**P value**
Frontal	17	18	0.12 ± 0.09	0.12 ± 0.07	0.849
Temporal	17	18	0.08 ± 0.09	0.13 ± 0.08	0.213
Parietal	17	18	0.15 ± 0.07	0.15 ± 0.07	0.931
Striatum	17	18	0.09 ± 0.11	0.11 ± 0.10	0.555
Thalamus	17	18	0.20 ± 0.12	0.23 ± 0.12	0.553
Total grey matter	17	18	0.14 ± 0.09	0.18 ± 0.08	0.313

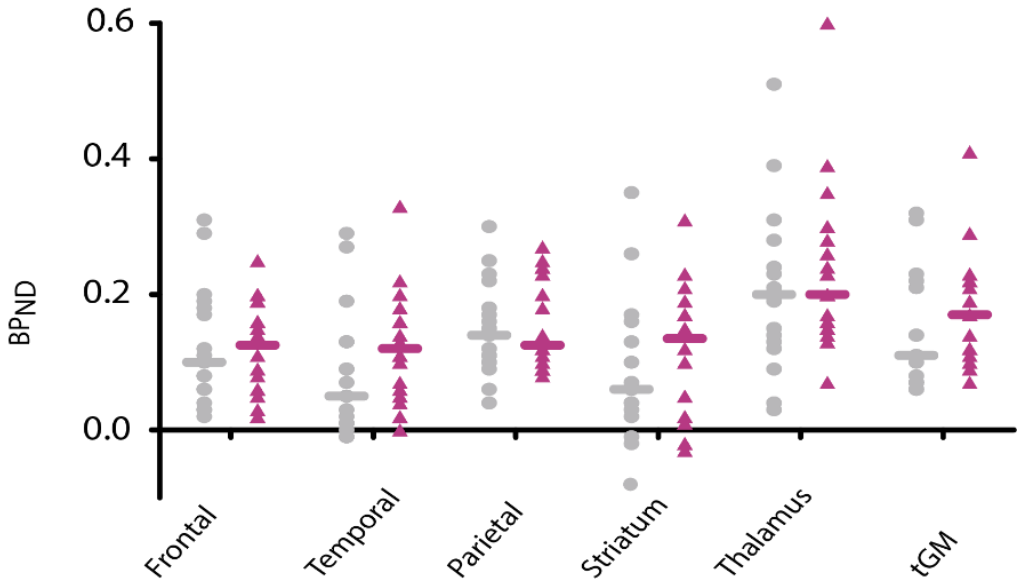

Figure 5.1 Overview of BP_{ND} across the different brain regions in combined patient group. The scatterplots show individual BP_{ND} values in total grey matter (tGM) and each of the studied regions of interest (frontal cortex, temporal cortex, parietal cortex, striatum, and thalamus) between patients (triangle) and controls (grey circle). Bars indicate median group BP_{ND} values.

Table 5.3 Overview of [^{11}C](*R*)-PK11195 binding potential across different brain regions with patients separated according to treatment status. The table shows mean BP_{ND} from 14 antipsychotic treated schizophrenia patients (SCZ AP), 4 untreated SCZ patients (AF) and 17 healthy controls (HC) across different brain regions and for total grey matter volume. The table shows mean values ± standard deviation. Significant P values (*post hoc* Tuckey test; P<0.05) are in bold font. AP – antipsychotic, AF – antipsychotic free, tGM – total grey matter.

Region	**Data points**			**BP_{ND}**			**P value**		
	HC	**SCZ AP**	**SCZ AF**	**HC**	**SCZ AP**	**SCZ AF**	**SCZ AP vs HC**	**SCZ AF vs HC**	**SCZ AP vs SCZ AF**
Frontal	17	14	4	0.12±0.07	0.13±0.07	0.11±0.07	0.365	0.409	0.320
Temporal	17	14	4	0.08±0.09	0.13±0.06	0.12±0.15	**0.038**	0.322	0.452
Parietal	17	14	4	0.15±0.07	0.16±0.07	0.13±0.07	0.348	0.317	0.246
Striatum	17	14	4	0.09±0.11	0.10±0.10	0.14±0.11	0.392	0.226	0.274
Thalamus	17	14	4	0.20±0.12	0.13±0.13	0.23±0.11	0.193	0.328	0.442
tGM	17	14	4	0.14±0.09	0.15±0.06	0.20±0.15	0.139	0.249	0.361

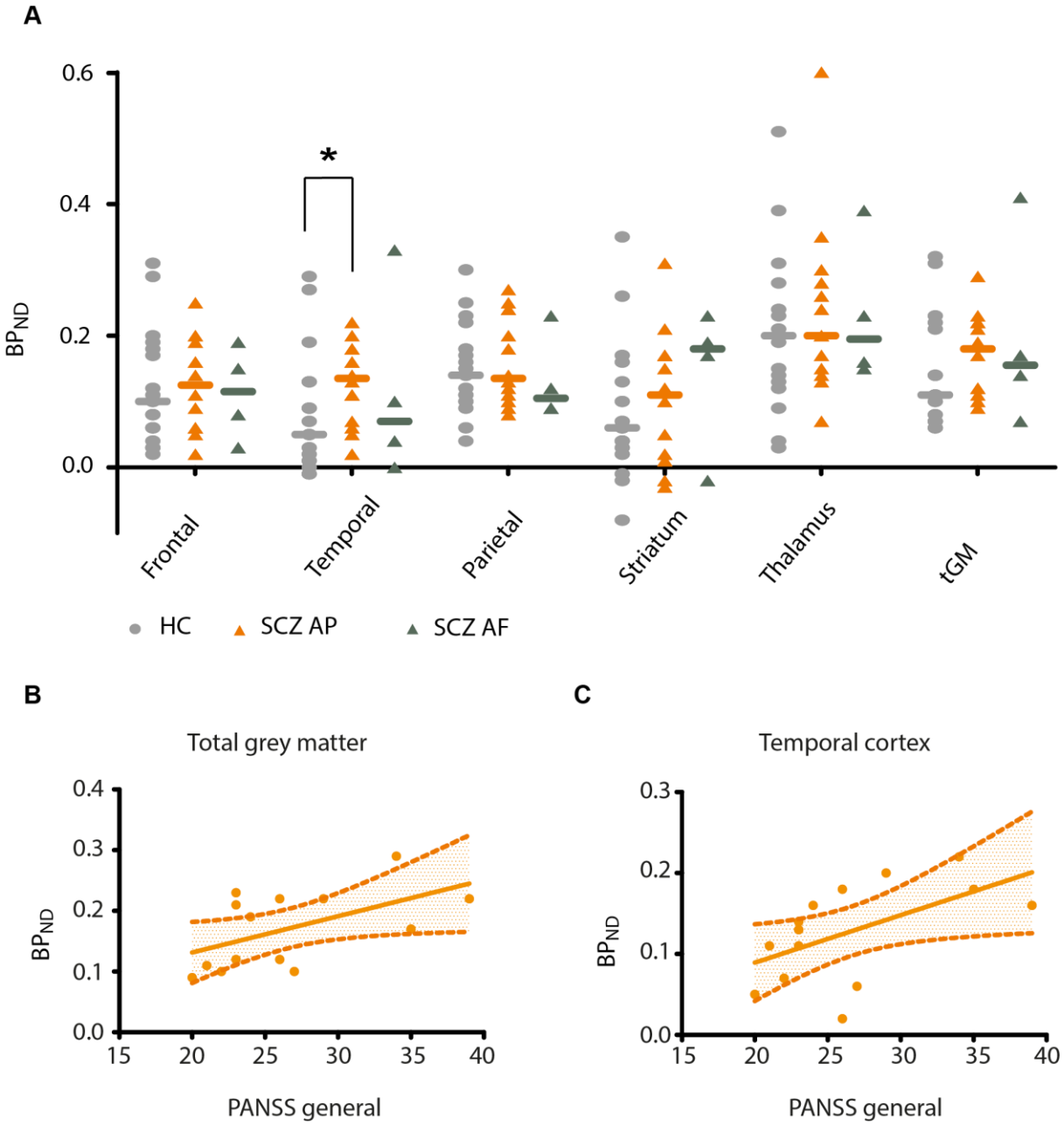

Figure 5.2 Overview of BP_{ND} across the different brain regions for separated patient sub-groups and controls. (A) The scatterplot shows individual BP_{ND} values in total grey matter (tGM) and each of the studied brain regions (frontal cortex, temporal cortex, parietal cortex, striatum, and thalamus) between patients (triangle) and controls (grey circle). A significant increase of BP_{ND} in treated patients was identified in the temporal region (*post hoc* Tuckey test; *P<0.05). Orange triangles represent antipsychotic treated patients, green triangles antipsychotic free patients. Bars indicate median group BP_{ND} values. **(B,C)** Overview of significant BP_{ND} correlations to PANSS general within the treated patient group. The scatterplots show individual PANSS general scores (x-axis) and BP_{ND} (y-axis) for total grey matter (P=0.046, r=0.54) (b) and the temporal cortex (P=0.039, r=0.56) (c). Dotted lines with orange fill indicate the 95% confidence interval. AP – antipsychotics. AF – antipsychotic free. PANSS - Positive and Negative Syndrome Scale.

5.2.3 Microglial exposure to serum from treated schizophrenia patients does not indicate normalisation of microglial activation phenotype

To investigate antipsychotic treatment effects, SV40 microglia cells were incubated with serum from antipsychotic free schizophrenia patients (n=4), antipsychotic treated schizophrenia patients (n=15) and matched controls (n=17) for 30 min. Subsequently, changes in the expression of 62 intra-cellular signalling epitopes (Chapter 2; **Table 2.2**) were investigated. Two epitopes showed significant (linear mixed effects model, $P<0.05$) differential microglial responses between treated schizophrenia and healthy control serum exposure and were clustered on the JAK/STAT and Other pathways (**Figure 5.3A**; **Table 5.3**), whereas the antipsychotic free vs. healthy control comparison resulted in the identification of only one significantly changed epitope response. This epitope was identical to the previously identified JAK/STAT pathway epitope from the treated patient vs. control comparison, which corresponds to the regulatory site of STAT3 (pS727). This suggests an attenuation of negative expression changes resulting in a net functional increase in the activation status of the JAK/STAT pathway in both antipsychotic free and antipsychotic treated patient groups relative to controls. The other identified epitope, CrkL (pY207), resulted in a net functional decrease in activation status within the antipsychotic treated patient group only.

As these serum samples from drug-treated patients might contain traces of antipsychotic compounds, we additionally screened a range of antipsychotic compounds for effects on the identified epitopes (**Figure 5.3B, C**).

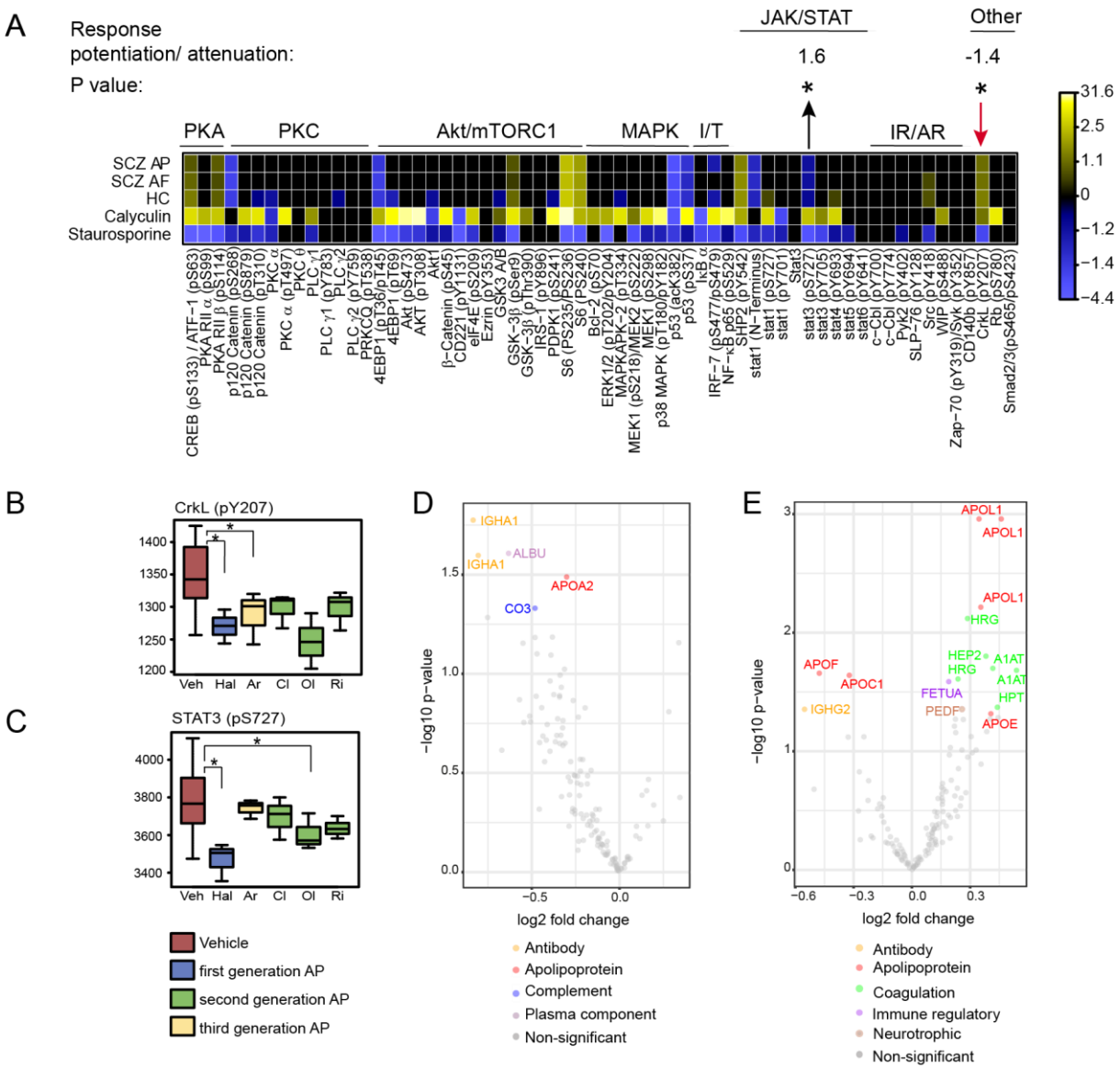

Figure 5.3 Differential responses in microglia signalling pathways upon serum exposure from schizophrenia patients and matched controls. (A) The heatmap shows differential responses at 30 min exposure to serum from 15 drug-treated schizophrenia patients (SCZ AP), 4 antipsychotic free schizophrenia patients (SCZ AF) and 17 matched controls (HC) across 62 functionally diverse cell signalling epitopes, grouped by pathway (on top) in the SV40 human microglia cell line. Responses to positive control ligands which induce widespread up-regulation (calyculin A, 1 μM) or down-regulation (staurosporine, 5 μM) are included for comparison. Only responses in which cellular treatments (serum or ligand) provoked a significant difference (Wilcoxon rank-sum test, permuted $P<0.05$; adjusted for background fluorescence) in epitope expression relative to the vehicle are shown. Legend shows mean fold change in epitope expression calculated as mean median fluorescence intensity (MFI) of the treatment/mean MFI of the vehicle across triplicate experiments. For down-regulated epitopes, the legend shows -1/fold change. Legend labels are distributed evenly across the quantile range for negative and positive fold changes separately. Epitopes which showed a significant difference (linear mixed effects model, permuted, *P<0.05, in response to SCZ patient serum relative to healthy controls are marked by arrows which show the direction of the response (black arrow – significant in SCZ AP vs. HC and SCZ AF vs. HC, red arrow significant in SCZ AP vs. HC). 'Response potentiation/attenuation' refers to (1-median response to SCZ serum)//(1-median response to healthy control serum); resulting values between 0 and 1 are converted to -1/value. This represents a means of expressing the relative potentiation (positive values) or attenuation (negative values) of response by serum from SCZ patients independently of its direction. Smad2 (pS465/pS467)/Smad3 (pS423/pS425) is abbreviated as Smad2/3 (pS465/pS423).

(B, C) The boxplots show responses to typical (blue), atypical (green) and third generation (yellow) antipsychotic compounds across the two identified cell signalling epitopes from the SCZ AP vs. HC comparison, CrkL (pY207) and STAT3 (pS727), in the SV40 human microglia cell line after a 30 min exposure. Responses are in mean median fluorescence intensity (MFI) on the y-axis with Haloperidol (Hal), Aripiprazole (Ar), Clozapine (Cl), Olanzapine (Ol) and Rispiridone (Ri) on the x-axis. Vehicle (Veh; red) is included for comparison to basal phosphorylation levels of the respective epitope. Bars indicate median responses; whiskers indicate the maximum and minimum, however when outliers are present they represent 1.5x the interquartile range. **(D, E)** Volcano plots representing the relationship between $\log_2$ fold change (x-axis) and statistical significance (y-axis) for peptide abundances for SCZ AF vs. HC (**D**) and SCZ AP vs. HC (**E**). Peptides were measured through multiplexed reaction monitoring (MRM). Peptides significantly (linear mixed effects model, $P<0.05$) altered in SCZ patient serum are labelled and coloured in terms of protein classes, which are associated with directing microglial polarization, antibody (orange), apolipoproteins (red), coagulation factors (green), complement (blue), immune regulatory (purple), neurotrophic (brown), plasma component (lilac) and non-significant (grey).

Table 5.4 Alterations in microglial cell signalling epitope expression in response to serum exposure of antipsychotic free and treated schizophrenia patients relative to healthy controls. Sample numbers in each clinical group include 4 antipsychotic free schizophrenia patients (SCZ AF), 15 antipsychotic treated patients (SCZ AP) and 17 healthy controls (HC), each sample was measured in triplicate. *'data points'* refers to the number of data points available per epitope across triplicate measurements for each clinical group after data preprocessing (terms in 'italics' represent column headings). Linear mixed effects model was used to account for the replicate measurements. Only epitopes for which there was a statistical difference in expression (*'permuted P'*<0.05) following incubation with SCZ relative to HC serum are shown. No covariates (age or gender) were selected for the epitopes shown following stepwise application of Bayesian Information Criteria in the linear mixed effects model. '*Serum response*' represents median MFI of the serum treatment/median MFI of the vehicle treatment within the respective clinical group. Only epitopes that displayed a significant '*serum response*' (Wilcoxon rank-sum test, permuted *P*<0.05; adjusted for background fluorescence) in either clinical group are shown. '*Response direction*' refers to the increase (↑) or decrease (↓) in epitope expression in response to serum. '*Response ratio*' refers to (1-*'SCZ serum response'*)/(1-*'HC serum response'*). This represents a means of expressing the relative potentiation or attenuation of response independently of its direction. This is expressed in the following column as '*potentiation/attenuation fold change*' (*'response ratios'* between 0 and 1 are converted to -1/*'response ratio'*), whereby a positive value represents potentiation and a negative value represents attenuation of response. '*Stain index*' refers to the median MFI of the stained samples/median MFI of the unstained samples within the vehicle treatment. MFI - median fluorescence intensity. P P – permuted P value.

		Data points			Serum response					
	Epitope	**SCZ**	**HC**	**P P**	**SCZ**	**HC**	**Response direction**	**Response ratio**	**Potentiation/ attenuation fold change**	**Stain index**
SCZ AF vs. HC	STAT3 (pS727)	12	51	0.0497	0.878	0.924	↑	1.61	1.61	7.1
SCZ AP vs. HC	CrkL (pY207)	45	51	0.0361	1.103	1.148	↓	0.69	-1.45	2.3
	STAT3 (pS727)	45	51	0.0245	0.881	0.924	↑	1.57	1.57	7.1

5.2.4 Changes in expression of serum proteins in antipsychotic treated patients relative to controls.

To explore whether the microglia activation phenotype could be explained by differences in the relative concentrations of serum proteins previously linked to neuropsychiatric disorders (n=77; **Chapter 2**, **Table 2.4**), we employed targeted multiple reaction monitoring mass spectrometry (for medium-high abundance proteins). Within the antipsychotic free patient group alterations were identified in proteins from the apolipoprotein family (A-II), Immunoglobulin G (IgGα1), complement (C3) and plasma protein family (albumin) (**Figure 5.3D; Table 5.6**). Within the treated patient group, alterations were identified in several proteins from the apolipoprotein family (C-I, F and L-I subtypes), immune regulatory (α-2-HS-glycoprotein), coagulation factors (α1-antitryspin, haptoglobin, heparin cofactor 2, histidine-rich glycoprotein) and the neurotrophic protein pigment epithelium-derived factor (**Figure 5.3E; Table 5.6**).

Table 5.5 Altered serum analytes between schizophrenia patients relative to healthy controls. Schizophrenia patients (SCZ) were divided into sub-groups according to treatment status, which was either antipsychotic free (AF) or antipsychotic treated (AP), for the comparison to healthy controls (HC). Terms in 'italics' represent column headings. *'Protein'* is ordered alphabetically. Analytes are defined as proteins or peptide sequences, respectively. *'Data points'* refers to the number of data points available per analyte for each clinical group after data pre-processing. Only analytes for which there was a statistical difference in expression (linear mixed effects model, *'P P'*<0.05) in SCZ relative to HC serum are shown. '*Covariates*' refer to clinical variables (age or gender) selected for each analyte by stepwise application of Bayesian Information Criteria in the linear mixed effects model. '*Fold change*' between clinical groups (derived from the regression coefficient) refers to the peptide abundance; resulting values between 0 and 1 converted to -1/*FC*). Abbr – abbreviation, FC – fold change, P P – permuted P.

					Data points				
	Protein	**Abbr**	**Uniprot ID**	**Peptide sequence**	**HC**	**SCZ**	**Covariates**	**P P**	**FC**
SCZ AF vs. HC	**Albumin**	ALBU	P02768	ETYGEMADCCAK	17	4	-	0.025	-1.88
	Apolipoprotein A-II	APOA2	P02652	SPELQAEAK	17	4	-	0.033	-1.35
	complement C3	CO3	P01024	AGDFLEANYMNLQR	17	4	-	0.047	-1.62
	Immunoglobulin heavy constant α1	IGHA1	P01876	TPLTATLSK	17	4	gender	0.017	-2.30
	Immunoglobulin heavy constant α1	IGHA1	P01876	DASGVTFTWTPSSGK	17	4	-	0.025	-2.24
SCZ AP vs. HC	**α1-antitrypsin**	A1AT	P01009	SPLFMGK	17	15	gender	0.020	1.52
	α1-antitrypsin	A1AT	P01009	SVLGQLGITK	17	15	-	0.021	1.71
	Apolipoprotein C-I	APOC1	P02654	EWFSETFQK	17	15	gender + age	0.023	-1.38
	Apolipoprotein E	APOE	P02649	AATVGSLAGQPLQER	17	15	-	0.048	1.50
	Apolipoprotein F	APOF	Q13790	SLPTEDCENEK	17	15	-	0.022	-1.61
	Apolipoprotein L-I	APOL1	O14791	VTEPISAESGEQVER	17	15	-	0.006	1.43
	Apolipoprotein L-I	APOL1	O14791	VNEPSILEMSR	17	15	-	0.001	1.41
	Apolipoprotein L-I	APOL1	O14791	LNILNNNYK	17	15	-	0.001	1.58
	α2-HS-glycoprotein	FETUA	P02765	HTLNQIDEVK	17	15	-	0.026	1.21
	Heparin cofactor 2	HEP2	P05546	IAIDLFK	17	15	-	0.016	1.46
	haptoglobin	HPT	P00738	VGYVSGWGR	17	15	gender + age	0.043	1.55
	Histidine-rich glycoprotein	HRG	P04196	DSPVLIDFFEDTER	17	15	-	0.008	1.33
	Histidine-rich glycoprotein	HRG	P04196	ADLFYDVEALDLESPK	17	15	-	0.025	1.27
	Immunoglobulin heavy constant γ2	IGHG2	P01859	GLPAPIEK	17	15	-	0.044	-1.74
	Pigment epithelium-derived factor	PEDF	P36955	TVQAVLTVPK	17	15	-	0.044	1.29

5.2.5 Correlations across the identified microglia signalling epitopes, serum MRM peptides and PET brain regions.

In order to aid the interpretation of the brain imaging data, we applied targeted mass spectrometry for the detection of changes in serum. For this purpose, a human microglia cell line was exposed to schizophrenia and healthy control serum (obtained from the same cohort which underwent PET imaging) for detection of changes in serum capable of inducing alterations in cell signalling pathways. After analysing each dataset, we correlated the results from PET imaging, mass spectrometry and serum exposure as an exploratory step, using the healthy control and antipsychotic treated patient subgroups. The aim was to gain further knowledge of pathophysiological mechanisms aiding the interpretation of PET imaging data. In addition, these correlations could provide potential novel insights into the reconstruction of the biological regulation network involved with schizophrenia.

Within the control group, the correlation analysis revealed multiple correlations to BP_{ND} across the PET regions. Microglia signalling epitope STAT3 (pS727) was found to have strong inverse correlations with BP_{ND} across all brain regions (**Figure 5.4**). The haptoglobin peptide (VGYVSGWGR) was found to correlate with BP_{ND} from the frontal (r=-0.65, p=0.006), temporal (r=-0.68, p=0.002), striatum (r=-0.50, p=0.041), thalamus (r=-0.60, p=0.010) and total grey matter (r=-0.61, p=0.009) regions (**Table 5.7**).

Within the treated patient group, both the identified correlations of STAT3 (pS727) to all brain regions and haptoglobin to most regions, as identified in the control group, could not be identified (**Table 5.8**). However, there were some other correlations identified. The first one was between CrkL (pY207) and total grey matter (r=-0.55, p=0.043) and the other one between the apolipoprotein E peptide (AATVGSLAGQPLQER) and STAT3 (pS727) (r=-0.56, p=0.030). STAT3 (pS727) also correlated with disease duration (r=0.52, p=0.047). And, PANSS total was found to have an inverse correlation with the same haptoglobin peptide as identified in the control group to correlate with most brain regions (r=-0.53, p=0.040).

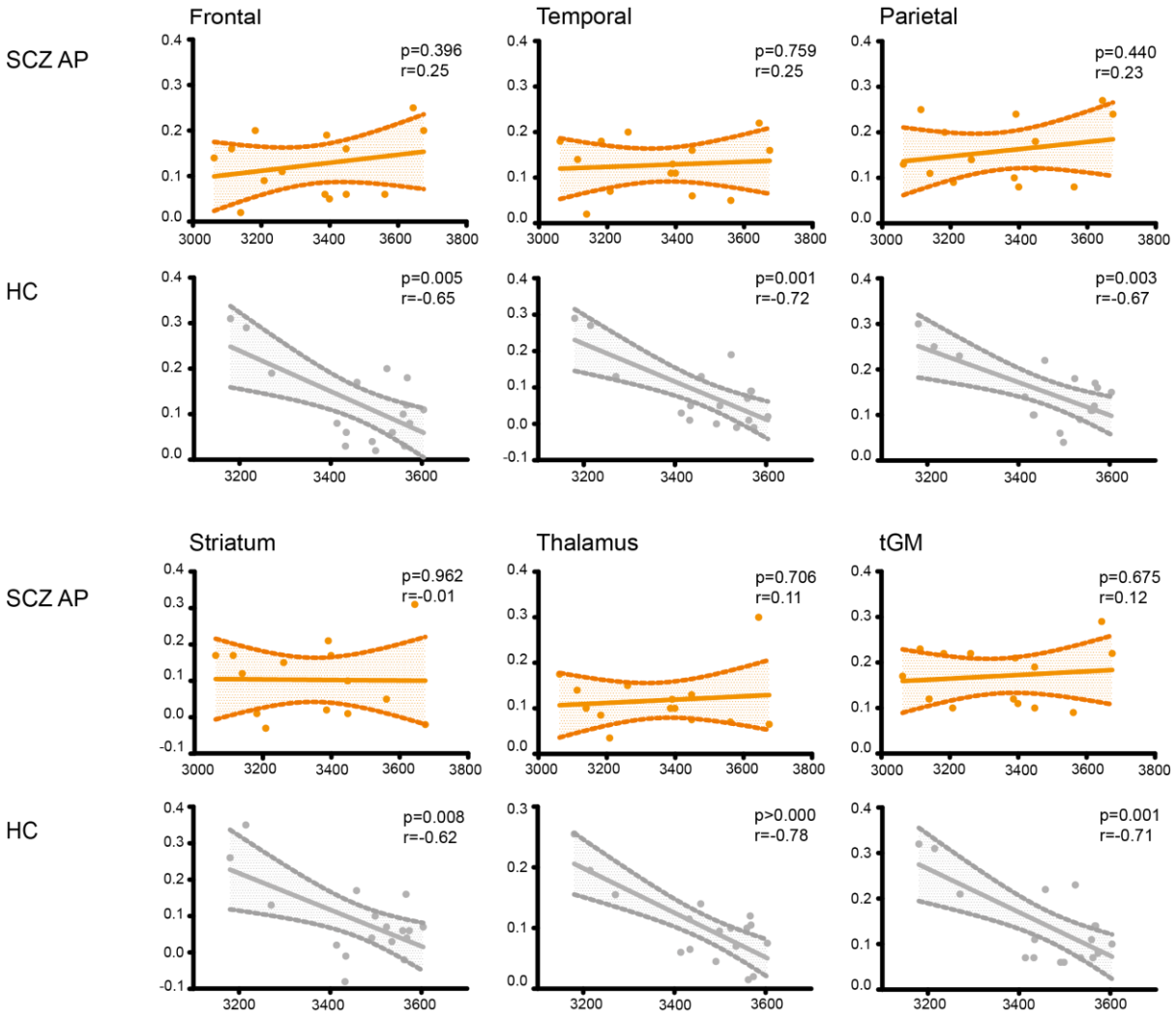

Figure 5.4 Correlation plots for the brain regions of interest between BP_{ND} and STAT3 (pS727). Correlation analyses for antipsychotic treated schizophrenia patients (SCZ AP) and healthy controls (HC) were performed for each brain region of interest between STAT3 pS727 (x-axis) and BP_{ND} (y-axis). Each plot contains its respective p-value (p) and correlation coefficient (r). Dotted lines with orange fill indicate the 95% confidence interval.

Table 5.6 Correlation matrix from the correlation analysis across PET tracer, microglia signalling epitopes and serum analytes for the healthy control group. The table presents the correlation values for all possible interactions across the three detection methods. Correlation values are highlighted if significant (P<0.05 – yellow, P<0.01 – green). The peptide correlating to BP_{ND} across multiple PET regions corresponds to the haptoglobin protein.

	PET						MRM													
	Frontal	Temporal	Parietal	Striatum	Thalamus	tGM	VNEPSILEMSR	LNILNNNYK	VTEPISAESGEQVER	DSPVLIDFFEDTER	IAIDLFK	SPLFMGK	SVLGQLGITK	SLPTEDCENEK	EWFSETFQK	ADLFYDVEALDLESPK	HTLNQIDEVK	VGYVSGWGR	TVQAVLTVPK	GLPAPIEK	AATVGSLAGQPLQER
VNEPSILEMSR	-0.19	-0.20	-0.18	0.01	-0.10	-0.14															
LNILNNNYK	-0.31	-0.31	-0.31	0.02	-0.14	-0.29															
VTEPISAESGEQVER	-0.06	0.00	-0.19	0.18	0.12	-0.04															
DSPVLIDFFEDTER	-0.07	-0.09	0.00	-0.08	0.04	-0.08															
IAIDLFK	-0.29	-0.29	-0.09	-0.30	-0.22	-0.23															
SPLFMGK	0.25	0.12	0.28	0.32	0.04	0.22															
SVLGQLGITK	-0.04	-0.09	-0.05	0.11	0.01	-0.04															
SLPTEDCENEK	0.33	0.25	0.43	0.22	0.26	0.26															
EWFSETFQK	-0.16	-0.08	-0.24	-0.27	0.18	-0.15															
ADLFYDVEALDLESPK	-0.05	-0.02	-0.05	0.01	0.12	-0.03															
HTLNQIDEVK	0.17	0.18	0.17	0.27	0.30	0.19															
VGYVSGWGR	-0.64	-0.68	-0.48	-0.50	-0.60	-0.61															
TVQAVLTVPK	-0.28	-0.19	-0.25	-0.15	-0.06	-0.18															
GLPAPIEK	-0.22	-0.35	-0.18	-0.41	-0.37	-0.34															
AATVGSLAGQPLQER	-0.14	-0.15	-0.13	-0.05	0.14	-0.12															
CrkL pY207	-0.21	-0.36	-0.03	-0.34	-0.32	-0.21	-0.20	-0.24	-0.41	-0.13	0.24	-0.22	-0.40	0.10	0.15	-0.22	-0.13	0.29	-0.24	-0.11	0.14
stat3 pS727	-0.65	-0.72	-0.67	-0.62	-0.78	-0.71	0.00	0.03	-0.06	-0.19	-0.14	-0.18	-0.09	-0.25	-0.07	-0.18	-0.47	0.30	0.03	0.48	-0.18

Table 5.7 Correlation matrix from the correlation analysis across PET tracer, microglia signalling epitopes and serum analytes for the antipsychotic treated schizophrenia patients. The table presents the correlation values for all possible interactions across the three detection methods. Correlation values are highlighted if significant (P<0.05 – yellow, P<0.01 – green). The peptide correlating to Stat3 (pS727) corresponds to the apolipoprotein E protein.

	PET						MRM													
	Frontal	Temporal	Parietal	Striatum	Thalamus	tGM	VNEPSILEMSR	LNILNNNYK	VTEPISAESGEQVER	DSPVLIDFFEDTER	IAIDLFK	SPLFMGK	SVLGQLGITK	SLPTEDCENEK	EWFSETFQK	ADLFYDVEALDLESPK	HTLNQIDEVK	VGYVSGWGR	TVQAVLTVPK	GLPAPIEK	AATVGSLAGQPLQER
VNEPSILEMSR	0.00	0.19	-0.09	0.32	0.30	0.05															
LNILNNNYK	0.07	0.23	-0.05	0.22	0.25	0.14															
VTEPISAESGEQVER	-0.12	0.08	-0.07	0.19	0.23	0.14															
DSPVLIDFFEDTER	-0.24	-0.08	-0.37	-0.06	-0.09	-0.27															
IAIDLFK	0.12	0.15	0.11	0.52	0.49	0.19															
SPLFMGK	0.27	0.19	0.31	0.14	0.20	0.21															
SVLGQLGITK	0.24	0.16	0.27	0.15	0.23	0.24															
SLPTEDCENEK	-0.47	-0.34	-0.49	-0.02	-0.20	-0.48															
EWFSETFQK	0.02	0.11	-0.09	0.46	0.25	-0.01															
ADLFYDVEALDLESPK	-0.15	-0.40	-0.14	-0.23	-0.30	-0.33															
HTLNQIDEVK	-0.11	-0.13	-0.05	0.33	0.14	-0.04															
VGYVSGWGR	-0.11	0.00	-0.16	0.46	0.32	-0.01															
TVQAVLTVPK	-0.20	-0.09	-0.23	0.34	0.38	-0.10															
GLPAPIEK	-0.28	-0.08	-0.41	0.26	0.10	-0.27															
AATVGSLAGQPLQER	0.05	-0.04	-0.03	0.37	0.23	0.03															
CrkL pY207	-0.41	-0.42	-0.51	-0.15	-0.21	-0.55	-0.08	0.11	-0.33	0.38	0.35	0.13	0.08	0.15	-0.05	0.29	0.39	0.17	0.08	0.02	-0.05
stat3 pS727	0.25	0.09	0.22	-0.01	0.11	0.12	-0.07	0.08	-0.08	0.13	0.36	-0.02	-0.13	-0.40	-0.32	0.21	0.18	-0.08	0.17	-0.39	-0.56

5.3 Discussion

To our knowledge, this is the first PET study, to combine the investigation of *in vivo* microglia driven neuroinflammation in antipsychotic treated schizophrenia patients using PET imaging, alongside the investigation of changes in microglial intracellular signalling cascades following patient serum exposure. We have found evidence for increased TSPO in the temporal region of drug-treated patients only, suggesting abnormalities in microglial activity in this patient group. In addition, TSPO binding in the temporal cortex also correlates to the PANSS general score. Furthermore, the exposure of a human microglia cell line to serum obtained from the same schizophrenia patients who also underwent PET imaging revealed alterations in STAT3 signalling. An association between the *in vivo* and *in vitro* alterations is further supported by the strong inverse correlations between STAT3 (pS727) and BP_{ND} across all PET regions which were identified within the control group only, indicating changes in STAT3 signalling in the patient group. We also identified changes in serum previously linked to schizophrenia[253,263].

Previous findings in PET studies using TSPO have been inconsistent, raising questions in terms of the specificity of TSPO to detect microglial activation[188] or the ability to distinguish between different microglial activation states[403]. Experts in the field have outlined the need to combine TSPO PET imaging with an independent method to provide additional insights regarding the inflammatory status of a given patient[188]. We combined TSPO PET imaging findings with targeted multiple reaction monitoring mass spectrometry to identify changes in circulatory proteins in schizophrenia patients. Furthermore, we exposed a human microglia cell line to serum obtained from schizophrenia patients who also underwent PET imaging, followed by high-content functional single-cell screening to dissect the cell signalling pathways which may be involved in the phenotypic switching of microglia. These two additional methods provide further information about the patients' immune status and potentially aid in the interpretation of the PET tracer results.

Our previous study (**Chapter 4**) identified changes in the mTORC1 and STAT3 pathways in microglia exposed to serum from drug-naïve first-onset schizophrenia patients. Here, we present the identification of dysfunctional STAT3 signalling upon serum exposure from antipsychotic treated schizophrenia patients. Thereby indicating that although these patients are receiving treatment, treatment does not result in the normalisation of microglial responses to serum.

5.3.1 Detection of increased TSPO in the temporal brain region of schizophrenia patients treated with antipsychotic medication

Following separation of the patients into treated and non-treated groups, increased TSPO was detected in the temporal region within the antipsychotic treated patient group. However, as the PET tracer is not capable of differentiating between anti- and pro-inflammatory microglia, the interpretation of this finding is not straightforward. As discussed in several recent publications, findings obtained using TSPO PET imaging have been inconsistent in terms of whether the technique is able to measure neuroinflammation *in vivo.* The combination of TSPO PET imaging with an independent method to assess the inflammatory profile could help to strengthen findings.

TSPO is an 18kDa high affinity cholesterol- and drug-binding protein and it has been suggested that the PKCε – ERK1/2 – STAT3 signal transduction pathway is the primary regulator of *Tspo* gene expression in normal and pathological tissues expressing high levels of TSPO[405]. Therefore, due to its high affinity drug-binding properties, traces of antipsychotics could also interact with TSPO. Thus, it cannot be excluded that the detection of increased TSPO binding in schizophrenia could be associated with drug treatments.

On the other hand, if antipsychotics were a confounding factor for TSPO binding, it would be expected that differences should be observed between all brain regions across drug-treated patients and controls. PET imaging studies have attempted to measure TSPO binding in UHR and drug-naïve schizophrenia patients, but these findings have been inconsistent and therefore do not allow us to validate the current identified change in temporal tracer activity[157,158,186–189,406]. Other *in vivo* imaging studies have identified decreased grey matter connectivity[407], attenuated signal processing abilities[408] and decreased brain volume[409,410] in the temporal cortex of schizophrenia patients. Numerous imaging studies implicated the medial temporal lobe, as well as the frontal cortex, to be a key area of alteration in schizophrenia. Especially volumetric alterations in the hippocampal area have been characterized as one of the hallmark features of schizophrenia[410–412]. These alterations have been detected in those at risk[413], first-episode antipsychotic-naïve patients[414,415] and in chronically treated patients[416]. Although the current finding of increased binding potential in the temporal cortex supports these findings, we cannot rule out the potential interaction of antipsychotics. Interestingly, a recent study investigating brain morphometry, showed that no significant changes in volume could be detected between recent onset patients before and after 12 months of minocycline add-on treatment relative to controls, but they could in the placebo patient group which showed significantly lower grey matter volumes[417]. As minocycline is an anti-inflammatory antibiotic capable of affecting the microglia phenotype, this study could indicate that inhibition of microglia induced neuroinflammation can ameliorate morphological changes in schizophrenia patients. Further work using different doses and modes of administration of

antipsychotics combined with and without add-on anti-inflammatory treatment is needed to determine the potential influence of antipsychotics for microglial activity and brain morphometrical changes in patients and healthy controls.

5.3.2 Changes in STAT3 (pS727) signalling in microglia following patient serum exposure

We present evidence for increased activity at regulatory site STAT3 (pS727) in microglia after exposure to serum from drug-treated patients. This could be associated with the schizophrenia pathophysiology, as this trend is also observed in the antipsychotic free patient group. However, as the drug-free group consists of 4 patients, we can only interpret that result as an indication. The STAT3 dysfunction is further strengthened by the lack of correlations to BP_{ND} as identified in the control group. Previously, we also identified altered STAT3 signalling in first-onset drug-naïve schizophrenia patients. Therefore, drug-treatment does not appear to fully normalise altered STAT3 signalling in schizophrenia patients. Altered activation of STAT3 upon microglial exposure to patient serum could reflect altered circulatory cytokine levels[418]. However, the functions of STAT3 are diverse, involving both IL-10 stimulated anti-inflammatory polarization[419] and IL-6 stimulated pro-inflammatory polarization[306]. Apart from these cytokines, other factors have the ability to influence the microglia phenotype via the SOCS-JAK-STAT pathway[331,332] (**See section 4.3.1**). Recently, a study demonstrated that microglia-specific STAT3 knockout mice showed antidepressive-like behaviour, suggesting STAT3 to be a potential target for the treatment of negative symptomology[420]. This is indicative that dysfunctional STAT3 might be underlying some of the negative symptoms and may have utility as a potential new drug target for schizophrenia.

5.3.3 Identification of decreased CrkL (pY207) activity in microglia associated with serum exposure from drug-treated patients

Next to dysfunctional STAT3 (pS727), altered phosphorylation levels of CrkL (pY207) were identified in microglia after exposure to serum from antipsychotic treated patients relative to controls. The finding of CrkL (pY207) might be an effect of antipsychotic drug traces in serum as it was identified in the treated patient group only. Yet, it is still of importance to mention this finding as *CRKL* is implicated as a genetic risk for schizophrenia[421,422]. However, alterations in the phosphorylation of CrkL (pY207) have as yet not been extensively investigated. There is currently one other paper investigating and identifying this specific phosphorylation site in schizophrenia patients, using PBMCs from patients before and after 6 weeks of olanzapine treatment. They could not detect a change in this particular

phosphorylation in PBMCs from first-onset drug-naïve patients relative to controls, but they could in PBMCs from those same patients 6 weeks after olanzapine treatment[250]. This further strengthens the notion that this is potentially caused by antipsychotic treatment effect.

Here, we show that antipsychotic drugs induce a decrease of CrkL (pY207) phosphorylation compared to basal phosphorylation levels in microglia (**Figure 5.2c**). Combined with the identification that serum exposure from treated schizophrenia patients caused a diminished response relative to controls (**Figure 5.2a**), our finding might be explained by an effect of antipsychotic drug traces in serum. Whether this treatment effect is beneficial for the patients remains unanswered.

5.3.4 Altered serum proteins in drug-treated schizophrenia patients

Whereas we previously identified a pattern of downregulated apolipoproteins in first-onset drug-naïve schizophrenia patients[263], we now identify a partial shift towards an increase of apolipoproteins in treated patients. Apolipoproteins have been previously reported to be altered in serum of schizophrenia patients relative to controls[252,317,318,423] and have been found to correlate with cognitive deficits and alterations in hippocampal brain volume[252]. Selective overexpression of microglial apolipoprotein receptor TREM2[309] in the neurodegenerative P301S mouse model induces a neuroprotective phenotypic shift in microglia with concurrent reduction in proinflammatory cytokine production[394]. Therefore, the shift in directionality of the apolipoproteins in patient serum relative to controls may reflect a partial normalisation of this protein class in relation to antipsychotic drug treatment. This shift could potentially be aiding a shift towards a neuroprotective profile in the CNS too.

The immune regulatory protein group consists of α2-HS-glycoprotein (also known as fetuin-A). This protein is associated with insulin resistance and fat accumulation in the liver in humans, which may link it with the alteration in apolipoproteins found in this study[424]. This specific protein has been previously reported to be altered in serum of schizophrenia patients relative to controls[318,423].

Within the coagulation protein group, haptoglobin has been previously identified as one of the most upregulated proteins in first-onset drug-naïve schizophrenia patients[263,324]. Here, we identify the presence of increased haptoglobin in antipsychotic treated patients as well. Furthermore, altered haptoglobin functioning is further illustrated by the lack of correlations to BP_{ND} as identified in the control group (**Table 5.7**), which are missing in the schizophrenia patient group (**Table 5.8**). Although haptoglobin is categorized into the coagulation protein group, this protein also modulates many aspects of the acute phase response. A study using a rodent model showed that haptoglobin deficiency worsens, whereas overexpression alleviates, brain injury during stroke. It was therefore suggested that

haptoglobin has neuroprotective properties[325]. Furthermore, it was shown that oligodendrocytes secrete this protein within the CNS for neuroprotection. In the CNS, microglia are the primary cell type expressing receptors for haptoglobin (CD163)[310]. Therefore, the increased expression of haptoglobin in patient serum might be a coping mechanism to stimulate a protective environment.

5.3.5 Limitations

After separating the patients in treated and untreated groups, the antipsychotic free patient group was represented by only 4 patients. This did not allow us to draw firm conclusions, and the data from these patients should be interpreted as potential trends that will need to be investigated further. Also, the interpretation of PET data could be affected by antipsychotic drug treatment. The interpretation of PET data is further complicated due to the inability of the tracer to distinguish between different microglial activation states. As recently suggested by Notter and Meyer (2017)[425], future schizophrenia PET studies should aim to define which particular microglia phenotypes are dysfunctional in schizophrenia and at what stage of the disease this happens.

Finally, we would like to raise awareness to the need to characterize microglia-specific phenotypes to develop an improved classification structure, instead of using the macrophage derived M1 and M2 phenotypes[152]. This would potentially aid the interpretation of studies like ours, as at the moment we are trying to fit results to phenotypes that probably do not represent microglia populations.

CHAPTER 6
LONGITUDINAL STUDY

Chapter 6 | Longitudinal Study

6.1 Introduction

The previous two results chapters investigated patient cohorts with either drug-naïve first-onset schizophrenia patients or antipsychotic treated recent onset patients. Although results gained from these two cohorts provide new insights concerning changes in, and potential involvement of, microglia in schizophrenia, they do not present information regarding treatment dependent reversal.

The findings presented in this chapter focus on the identification of microglia signalling responses which were altered following exposure to serum collected from individuals with first onset schizophrenia, relative to healthy controls, and normalized by *in vivo* antipsychotic therapy. Furthermore, it presents the opportunity to use the findings for identification of treatment dependent normalisation indicating effective treatment. This could be helpful in drug response prediction and may aid in the identification of new drug targets. Moreover, these reversal responses can be correlated to improvements in PANSS scores related to the 6 weeks' follow-up time-point following a clinical course of olanzapine treatment.

6.2 Results

6.2.1 Follow-up study design

Serum exposed microglia cell signalling responses were obtained from an all-male cohort of drug-naïve schizophrenia patients before (SCZ T_0, n=9) and after 6 weeks (SCZ T_6, n=9) of treatment with the atypical antipsychotic olanzapine. The patient and control samples (HC, n=12) were matched for age, gender, BMI, ethnicity and cannabis use, but not for smoking (**Table 6.1**). Patients before treatment were moderately to markedly ill, whereas after treatment their PANSS scores put them in the category of mildly to moderately ill. After 6 weeks of treatment, the total PANSS reduction was 20%, indicating minimal symptomatic improvement (**Figure 6.1**)[404]. In order to investigate changes related to schizophrenia, the measurement of relative expression in microglial signalling epitopes was achieved through exposure to serum from drug-naïve schizophrenia patients and to healthy controls. In order to identify microglial signalling hubs indicative of drug-dependent normalisation, microglia were exposed to serum from drug-naïve schizophrenia patients before and after 6 weeks of olanzapine treatment. By comparing the results from these two comparisons, microglial signalling epitopes indicative of reversal drug targets could be identified.

A human microglia cell line was exposed to serum from each clinical group (SCZ T_0, SCZ T_6 and HC) for 30 minutes. Subsequently, the cells were fluorescently barcoded and changes in microglia signalling evoked by the serum were measured across 64 cell signalling epitopes. The epitopes spanned a wide variety of cell signalling pathways broadly including Akt/GSK-3β, PKA, PKC, MAPK, JAK/STAT, IL-1R/TLR and antigen/integrin (A/I) receptor signalling (**Chapter 2 Table 2.2**). This created 1920 unique cell signalling responses, in addition to positive controls and vehicle, all responses were measured in triplicate.

As this study was underpowered, we decided to include findings with a P-value below 0.1 for exploratory purposes and to increase the opportunity for identification of potential new drug targets. We contrast to the findings at standard P<0.05 threshold. Drug targets were identified through the overlap in identified alterations from the comparison between patients before treatment and controls versus the identified alterations from the comparison between patients before and after treatment. The overlap of identified significant changes between these two data sets allowed for the identification of drug targets.

Patient and control sera were also investigated using targeted MRM mass spectrometry (n=77 proteins, **Chapter 2 Table 2.4**), to identify serum analytes with the potential to alter microglia phenotype. We also examined the effects of olanzapine on the epitopes identified in the serum exposure comparison between patients before and after treatment, to answer the question whether the observed changes in cell signalling represented direct effects of the drug or complex changes in patient physiology.

Table 6.1 Demographic characteristics of the drug-naïve schizophrenia patients before and after 6 weeks olanzapine treatment and controls. The Wilcoxon rank-sum test was used for continuous variables and Fisher's exact test for categorical variables, so that there were no significant differences in the demographic variables (P>0.05; except smoking, in bold font) between patient and control groups. There was no serum available at T6 from two patients at T0, therefore two different patients were added at the T6 group. All patients and controls were male; therefore, the variable gender is not included in the table. The table shows mean values ± standard deviation. HC – healthy control. SCZ – schizophrenia. T0 – before treatment. T6 – after 6 weeks of olanzapine treatment. Y - yes. N - no.

	SCZ T0	**SCZ T**	**HC**	**P**
Number	9	9	12	-
Age	28.33± 5.94	27.00 ± 6.63	28.25 ± 7.66	0.900
BMI	23.30 ± 4.69	23.35 ± 3.19	23.89 ± 1.66	0.589
Smoking (Y/N)	6/3	7/2	2/10	**0.011**
Ethnicity (Caucasian/other)	4/5	4/5	9/3	0.254
Cannabis (Y/N)	2/7	1/8	4/8	0.490

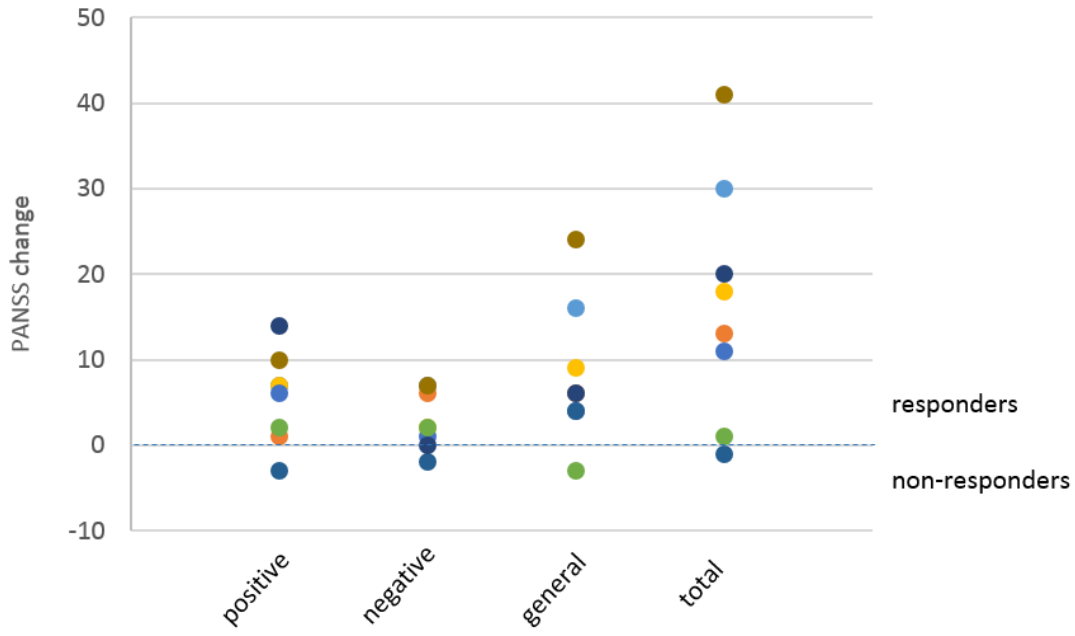

PANSS	positive	negative	general	total
Before treatment	19.63 ± 4.72	21.63 ± 6.52	39.13 ± 6.24	80.38 ± 15.31
After olanzapine treatment	14.72 ± 4.90	18.50 ± 4.60	31.25 ± 7.55	64.38 ± 15.84
Difference	5.50 ± 5.37	2.88 ± 3.40	8.25 ± 8.29	16.63 ± 14.07

Figure 6.1 Clinical response of schizophrenia patients at the 6 weeks' time point of antipsychotic treatment with olanzapine. The graph shows improvements in positive, negative and general symptom subscales. Based on the total PANSS, two patients did not show overall improvements. For two patients, samples were only available from the T_0 time point as they dropped out at T_6. Therefore, two different patients did not provide blood samples at T_0, were included in the T_6 sub-group. As the two patients at T_0 who did not undergo PANSS assessment at T_6, these scores are missing in the graph. Different coloured spheres represent individual patients. PANSS - Positive and Negative Syndrome Scale.

6.2.2 Signature for effects of disease and clinical antipsychotic treatment on microglia signalling

To investigate alterations in microglia signalling induced by serum components, SV40 microglia cells were incubated with serum from healthy controls (HC, n=12), drug-naïve schizophrenia patients before (SCZ T_0, n=9) and after 6 weeks (SCZ T_6, n=9) of treatment with the antipsychotic olanzapine. In total, across both group comparisons (SCH T_0 vs. HC and SCZ T_0 vs. SCZ T_6), 15 epitopes were identified to be altered (linear mixed effects model, P<0.1; **Table 6.2**). Five epitopes (**Figure 6.2; Table 6.2** blue fill) were identified to be within conventional significance levels (P<0.05). Within these five epitopes, one epitope was identified from the SCZ T_0 vs. HC group comparison, PKA RIIα (pS99), with an increased activity in microglia exposed to serum from SCZ T_0. In contrast, the SCZ T_0 vs. SCZ T_6 group comparison identified a range of epitopes across different signalling pathways, including PKC (p120 Catenin pS268), Akt/mTORC (CD221 pY1131) and MAPK (MEK1 pS298 and p53 acK382). Almost each of these changes in epitope expression represented increased activity, except for p53 (acK382) which showed a change in opposite direction (*i.e*. down- in place of up-regulation) upon exposure to serum from T_6 patients.

As one of the aims of this study was to identify signalling epitopes indicative of potential reversal drug targets, we assessed which of the cell signalling alterations, detected in both SCZ T_0 vs. HC and SCZ T_0 vs. SCZ T_6 comparisons, were reversed following *in vivo* treatment. In order to identify epitopes to be reversed, epitopes had to be within the exploratory range in both comparisons (SCZ T_0 vs. HC and SCZ T_0 vs. SCZ T_6; P<0.1), were changed in opposite directions ('reverse'), and had a minimum 10% difference in potentiation/attenuation fold change. Two epitopes were identified to be reversed, which were GSK3β (pSer9) and PDPK1 (pS241), both members of the Akt/mTORC pathway (**Figure 6.2**, **Table 6.2**; orange highlight).

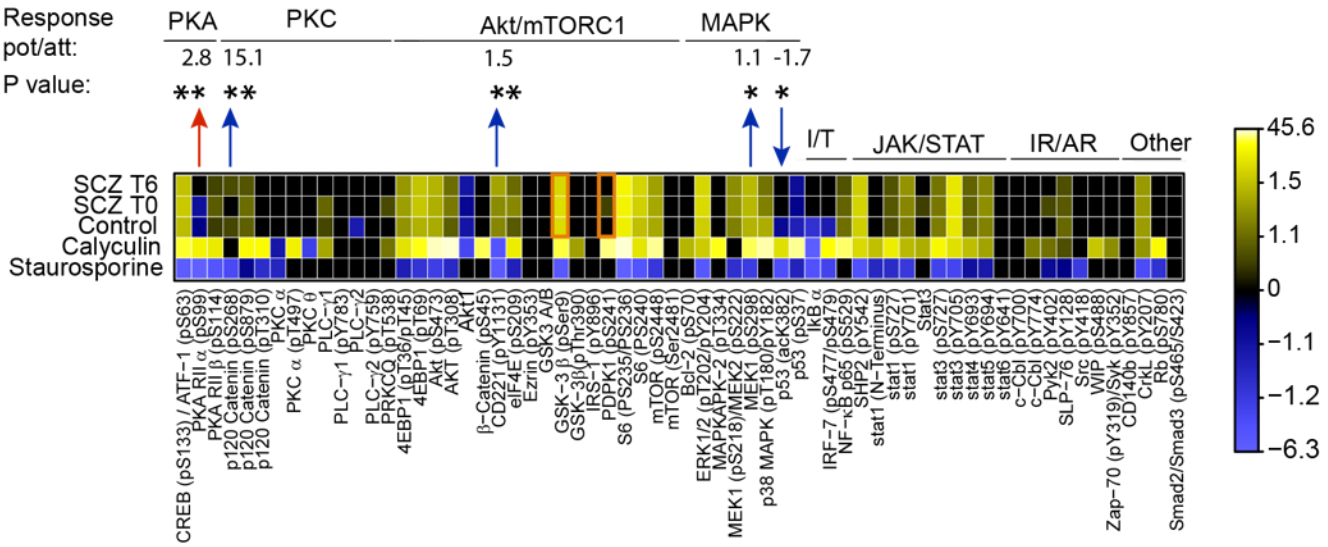

Figure 6.2 Differential responses in microglia signalling pathways following exposure to serum from olanzapine-treated schizophrenia patients at treatment time-points T0 and T6 and matched controls. The heatmap shows differential responses at 30 min exposure to serum from 9 drug naïve (T0) and olanzapine treated (T6) schizophrenia patients (SCZ) and 12 matched controls across 64 functionally diverse cell signalling epitopes, grouped by pathway (on top) in the SV40 human microglia cell line. Responses to positive control ligands which induce widespread up-regulation (calyculin A, 1 μM) or down-regulation (staurosporine, 5 μM) are included for comparison. Only responses in which cellular treatments (serum or ligand) provoked a significant difference (Wilcoxon rank-sum test, permuted $P<0.05$; adjusted for background fluorescence) in epitope expression relative to the vehicle are shown. Legend shows mean fold change in epitope expression calculated as mean median fluorescence intensity (MFI) of the treatment/mean MFI of the vehicle across triplicate experiments. For down-regulated epitopes, the legend shows -1/fold change. Legend labels are distributed evenly across the quantile range for negative and positive fold changes separately. Epitopes which showed a significant difference (linear mixed effects model, permuted, $*P<0.05$, $**P<0.01$) in response to SCZ patient serum relative to healthy controls, or before and after treatment, are marked by arrows which show the direction of the response. Red arrows indicate a significant difference between SCZ T0 and HC. Blue arrows indicate significant differences between SCZ T0 and SCZ T6. 'Response pot/att' refers to (1-median response to SCZ T0vserum)/(1-median response to healthy control serum) or (1-median response to SCZ T6 serum)/(1-median response to SCZ T0 serum) in the SCZ T0 vs. HC and SCZ T0 vs. SCZ T6 comparisons, respectively; resulting values between 0 and 1 are converted to -1/value. This represents a means of expressing the relative potentiation (positive values) or attenuation (negative values) of response by serum from SCZ patients, relative to the HC group or baseline SCZ measurement, independently of its direction. Epitopes that were included in the exploratory phase ($P<0.1$), which were changed in opposite directions ('reverse'), in both comparisons $P<0.1$ and differed at least 10% are highlighted by orange squares to indicate putative normalisation of SCZ serum induced signalling alterations. Smad2 (pS465/pS467)/Smad3 (pS423/pS425) is abbreviated as Smad2/3 (pS465/pS423). Pot/att – potentiation/attenuation.

Table 6.2 Alterations in microglia signalling pathways following exposure to serum from olanzapine-treated schizophrenia patients at treatment time-points T0 and T6 and matched controls. Sample numbers in each clinical group include 9 schizophrenia patients (SCZ) before treatment (T0), 9 SCZ after 6 weeks of olanzapine treatment (T6) and 12 healthy controls (HC). *'data points'* refers to the number of data points available per epitope across triplicate measurements for each clinical group after data preprocessing (terms in 'italics' represent column headings). Linear mixed effects model was used to account for the replicate measurements. Only epitopes for which there was a statistical difference in expression (P P<0.05 – blue fill, P P<0.1 – yellow fill) following incubation with SCZ relative to HC serum, or SCZ T0 relative to SCZ T6 serum, are shown. No covariates (age or gender) were selected for the epitopes shown following stepwise application of Bayesian Information Criterion in the linear mixed effects model. '*Serum response*' represents median MFI of the serum treatment/median MFI of the vehicle treatment within the respective clinical group. Only epitopes that displayed a significant '*serum response*' (Wilcoxon rank-sum test, permuted *P*<0.05; adjusted for background fluorescence) in either clinical group are shown. '↕' refers to the response direction, of either an increase (↑) or decrease (↓) in epitope expression in response to serum. '*Ratio*' refers to (1-median response to SCZ T0vserum)/(1-median response to healthy control serum) or (1-median response to SCZ T6 serum)/(1-median response to SCZ T0 serum) in the SCZ T0 vs. HC and SCZ T0 vs. SCZ T6 comparisons, respectively. This represents a means of expressing the relative potentiation or attenuation of response independently of its direction. This is expressed in the following column as '*pot/att fold FC*' (potentiation/attenuation fold change; *'response ratios'* between 0 and 1 are converted to -1/*'response ratio'*), whereby a positive value represents potentiation and a negative value represents attenuation of response. Orange marking indicates epitopes with P<0.1 in both comparisons, which are changed in opposite directions ('reverse') and differed at least 10%. MFI - median fluorescence intensity. P perm – permuted P-value.

	Data points			Serum response			SCZ T0-HC				SCZ T0-T6			
Epitope	SCZ T0	SCZ T6	HC	SCZ T0	SCZ T6	HC	P perm	↕	ratio	Pot/Att FC	P perm	↕	ratio	Pot/Att FC
PKA RIIα (pS99)	24	20	28	0.923	0.921	0.972	0.001	↑	2.778	2.778	0.490	↑	1.034	1.034
4EBP1 (pT36/pT45)	23	22	28	1.224	1.201	1.185	0.060	↑	1.211	1.211	0.744	↓	0.898	-1.114
4EBP1 (pT69)	23	22	28	1.519	1.503	1.324	0.063	↑	1.604	1.604	0.319	↓	0.969	-1.032
GSK3β (pSer9)	24	21	28	1.812	1.768	1.777	0.063	↑	1.045	1.045	0.078	↓	0.946	-1.057
IkBα	26	24	28	0.913	0.921	0.854	0.057	↓	0.598	-1.672	0.375	↓	0.906	-1.103
p38 MAPK (pT180/pY182)	26	21	28	1.144	1.123	1.284	0.085	↓	0.509	-1.966	0.532	↓	0.854	-1.171
p53 (pS37)	22	18	29	0.949	0.936	0.901	0.070	↓	0.518	-1.929	0.912	↑	1.247	1.247
PDPK1 (pS241)	24	20	30	1.030	1.009	1.012	0.070	↑	2.507	2.507	0.070	↓	0.298	-3.360
PRKCQ (pT538)	25	22	30	1.047	1.015	0.997	0.077	↓	-13.667	-13.667	0.413	↓	0.317	-3.154
CD221 (pY1131)	22	20	28	1.169	1.252	1.153	0.211	↑	1.104	1.104	0.004	↑	1.491	1.491
MEK1 (pS298)	24	20	28	1.348	1.396	1.331	0.729	↑	1.051	1.051	0.038	↑	1.138	1.138
p120 Catenin (pS268)	24	21	32	1.003	1.051	1.042	0.114	↓	0.081	-12.286	0.006	↑	15.086	15.086
p53 (acK382)	22	18	29	1.050	0.915	0.938	0.243	↓	-0.801	-0.801	0.011	↓	-1.711	-1.711
stat3 (pS727)	24	19	29	1.127	1.124	1.143	0.594	↓	0.890	-1.124	0.075	↓	0.972	-1.029
stat3 (pY705)	24	19	29	2.431	2.429	2.381	0.993	↑	1.036	1.036	0.078	↓	0.999	-1.001

6.2.3 Comparison of *in vitro* effects of olanzapine exposure on identified cell signalling epitopes to changes associated with T6 serum exposure

In order to verify whether the detected changes associated with SCZ T_6 serum exposure in microglia represented traces of olanzapine in serum or changes in serum related to the disease, we investigated the drug effects in microglia *in vitro*. We screened five different olanzapine concentrations (0.02 μM, 0.2μM, 2.0μM, 20μM and 200μM; in triplicate for each concentration) for 30 minutes for the putative drug targets GSK3β (pS9) and PDPK1 (pS241) (**Figure 6.3A**) and epitopes identified from the SCZ T_0 vs. SCZ T_6 comparison (**Figure 6.3B**).

GSK3β (pS9) was found to be increased in microglia exposure to T_0 serum, but its fold change reversed in microglia exposed to T_6 serum. Olanzapine stimulation does indicate a trend towards increasing this epitope's activity at the three lower concentrations. The highest olanzapine concentration of 200μM might have been too high. Some antipsychotics can become toxic from 50μM to 100μM onwards, and therefore the higher concentrations should be interpret with caution[426]. Therefore, the identification of GSK3β (pS9) might be a result of disease-related changes in serum. PDPK1 (pS241) showed a similar directionality in change of fold change as GSK3β (pS9), with microglial activity levels increased post T_0 serum exposure, and reversed after T_6 serum exposure (**Table 6.2**). The activity of this epitope was decreased by direct exposure to olanzapine, as the four lower olanzapine concentrations caused a decrease of this epitope relative to vehicle. Therefore, the reversal of this epitope might reflect olanzapine traces in serum.

Next, we focused on the epitope changes specifically identified in the SCZ T_0 vs. SCZ T_6 comparison. Upon SCZ T_6 serum exposure, three epitopes were identified to be increased following exposure to serum collected at T_6, which were CD221 (pY1131), MEK1 (pS298) and p120 catenin (pS268). Whereas there was an indication for olanzapine increasing the activity of the MEK1 (pS298) epitope, it showed a decreasing effect on the other two epitopes relative to vehicle. An interesting change was observed at CD221 (pY1131), also known as insulin-like growth factor 1 receptor, which showed an even bigger response following exposure to T_6 serum compared to T_0. On the contrary, exposure to olanzapine *in vitro* appeared to decrease the expression of this epitope. A similar effect could be detected at p120 catenin (pS268). Although this epitope normalised more towards control serum exposure levels when exposed to T_6 serum, due to an increase in epitope activity, direct exposure to olanzapine caused an opposite effect at this epitope by decreasing its levels. Therefore, the identification of these epitopes is most likely due to disease-related changes in serum.

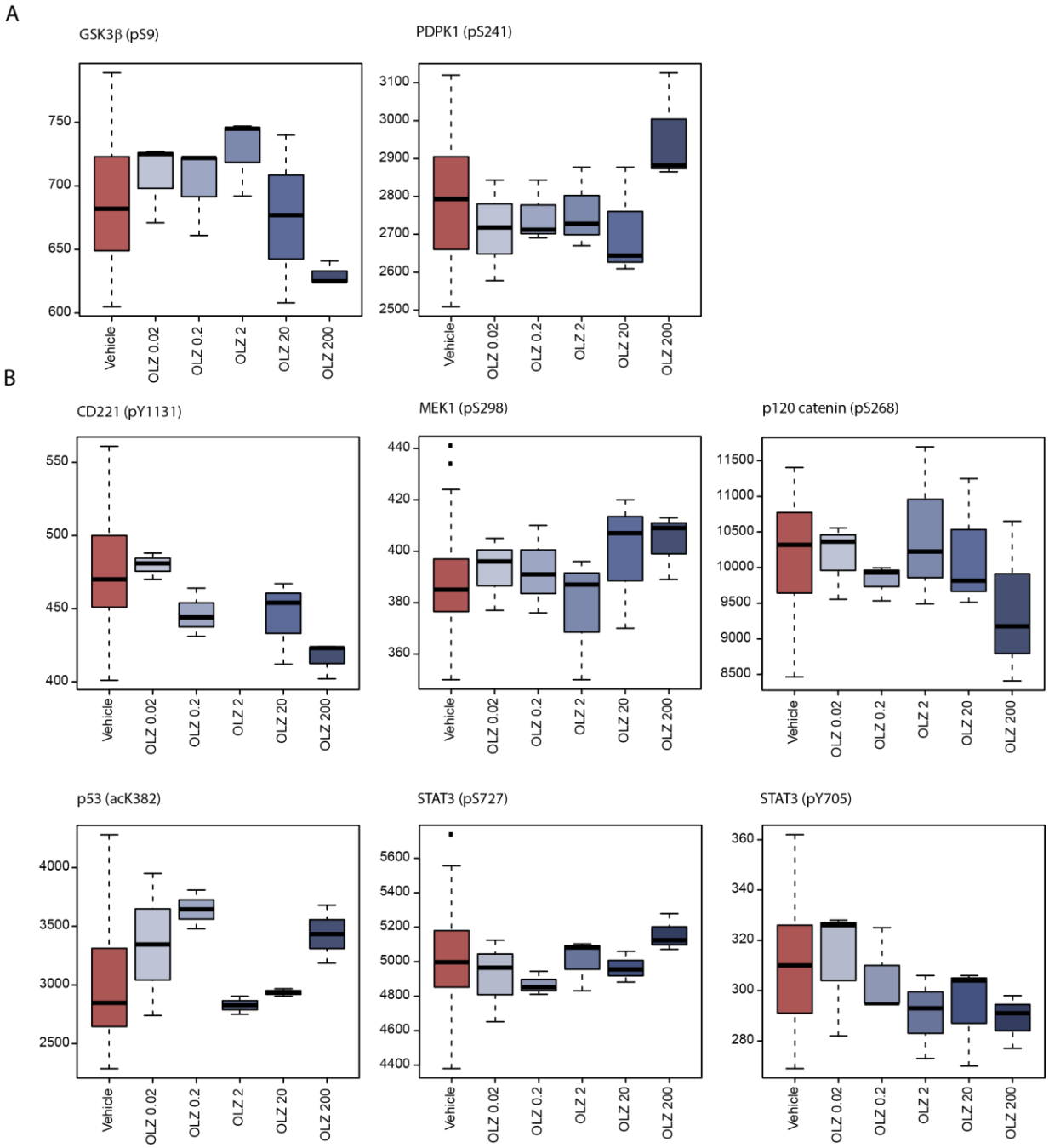

Figure 6.3 Olanzapine responses in microglia relative to vehicle across the identified reversal and T6 epitopes. The boxplots show differential responses at 30 min exposure to five different olanzapine concentrations (0.02μM, 0.2μM, 2.0μM, 20μM and 200μM; each measured in triplicate) across identified cell signalling epitopes in the SV40 human microglia cell line with **(A)** showing reversal epitopes and **(B)** epitopes identified from the SCZ T_0 vs. SCZ T_6 comparison. Responses are in median fluorescence intensity (MFI) on the y-axis with different concentrations of olanzapine (OLZ; blue) on the x-axis. Vehicle (red, n=45) is included as a baseline comparison for the respective epitope. Bars indicate first, second (median) and third median quartiles of responses; whiskers indicate maximum and minimum values, except for when outliers were present in which case they represent 1.5x interquartile range. Olanzapine responses are not included if there were two or less measurements left after pre-processing.

From the SCZ T_0 vs. SCZ T_6 comparison, three epitopes showed a decrease in activity at P<0.1, which were STAT3 (pY705), STAT3 (pS727) and p53 (acK382). Direct exposure of olanzapine revealed that the two different STAT3 epitopes reacted in opposite ways. Whereas levels of the STAT3 (pY705) epitope decreased, STAT3 regulatory site pS727 showed a small increased effect upon olanzapine stimulation. The epitope p53 (acK382) responded differently to olanzapine exposure. The lower olanzapine concentrations (0.02 μM and 0.2 μM) initially caused an increase in p53 (acK382) levels relative to vehicle. This was followed by a strong decrease upon the 2.0 μM olanzapine concentration, followed by a slow increase upon incrementing concentrations (20 μM and 200 μM). This effect might be due to another interacting pathway that became activated on the higher olanzapine concentrations. This pathway might be able to exert an inhibiting effect at the activity of the p53 (acK382) epitope.

6.2.4 Identification of disease-related serum changes potentially involved in inducing altered microglia signalling

To explore whether the alterations in microglia signalling cascades could be explained by differences between the clinical groups (SCZ T_0 n=9, SCZ T_6 n=9, HC n=12) in the relative concentrations of serum proteins previously linked to neuropsychiatric disorders (n=77 proteins; **Chapter 2 Table 2.4**)[253], we employed targeted multiple reaction monitoring mass spectrometry (for medium-high abundance proteins). The SCZ T_0 vs. HC comparison revealed alterations in several proteins from the antibody family (immunoglobulin heavy constant γ2; IgG2), apolipoprotein family (AII, AIV, CI, CII, CIII and J subtypes; clusterin is also known as apolipoprotein J), cell adhesion (vitronectin) and the complement cascade (C9). The SCZ T_0 vs. SCZ T_6 comparison revealed alterations in coagulation factors (carboxypeptidase B2, hemopexin) and apolipoprotein C-I (Apo C-I) (**Figure 6.4**; **Table 6.3**).

Proteins identified in the SCZ T_0 vs. HC comparison were consistent with previous reports of alterations of these proteins in serum from schizophrenia patients. There was overlap with proteins we identified before in first-onset drug-naïve patients, especially the apolipoprotein and complement cascade protein groups (**Chapter 4; Table 4.4**). Some proteins were identified that did not overlap, but had been identified in other schizophrenia patient studies which are vitronectin[423,427], clusterin[329,428] and IgG2. IgG2 is usually reported to be increased in first-onset schizophrenia patients[429], yet we identify a decrease.

For the identification of treatment-dependent reversal proteins, the same peptide had to be within the exploratory significance range in both comparisons (P<0.10, SCZ T_0 vs. HC and SCZ T_0 vs. SCZ T_6), the fold change had to change direction and the difference in fold change between the two

comparisons had to be at least 10%. This left one peptide, belonging to the Apo C-I protein (**Table 6.3**, orange highlight).

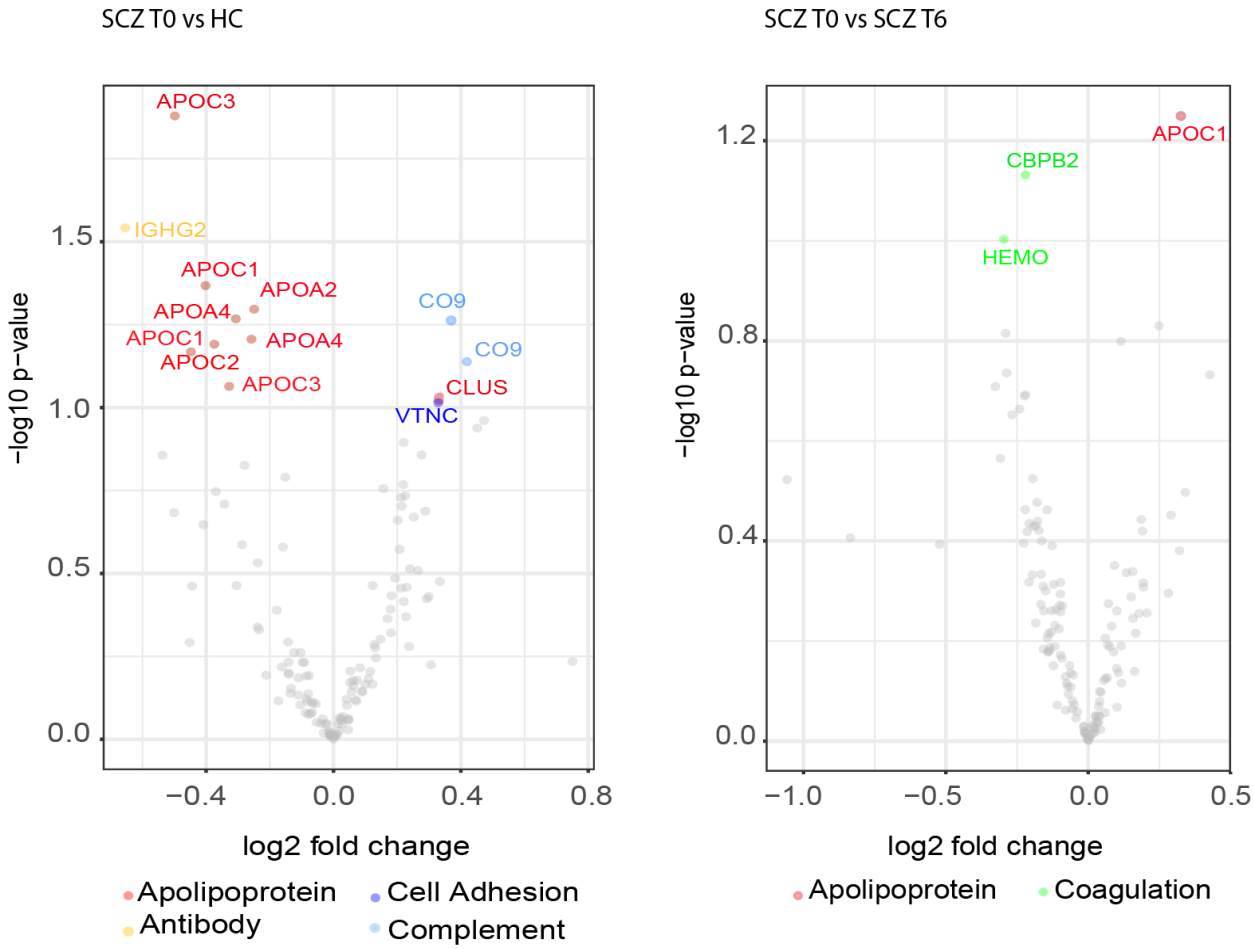

Figure 6.4 Volcano plots showing differences in serum peptides in patients relative to controls and to patients after 6 weeks of olanzapine treatment. The volcano plots represent the relationship between $\log_2$ fold change (x-axis) and statistical significant (y-axis). Peptides were measured through multiplexed reaction monitoring (MRM). Peptides significantly (linear mixed effects model, P<0.10) altered in SCZ patient serum are labelled and coloured in terms of protein classes, which are associated with directing microglial polarization, apolipoproteins (red), coagulation factors (green), cell adhesion (dark blue), complement (light blue), antibody (orange) and non-significant (grey). The left volcanoplot presents peptide changes for drug naïve SCZ patients (T0) relative to HC. The right plot presents peptide changes for SCZ after 6 weeks of olanzapine treatment (T6) compared to baseline (T0).

Table 6.3 Altered serum analytes in drug naïve schizophrenia patients relative to healthy controls or patients after 6 weeks of olanzapine treatment. Terms in 'italics' represent column headings. Analytes are defined as peptide sequences. Peptides are ordered on smallest P-value within the SCZ T0 vs. HC comparison, followed by smallest P-value in the SCZ T0 vs. SCZ T6 comparison. Sample numbers in each clinical group include 9 SCZ T0, 9 SCZ T6 and 12 healthy controls (HC). Only analytes for which there was a statistical difference in expression (linear mixed effects model, P-value<0.10) in relative expression are shown. '*Cov*' refers to clinical variables (age or gender) selected for each analyte by stepwise application of Bayesian Information Criterion in the linear mixed effects model. '*FC*' between clinical groups (derived from the regression coefficient) refers to the peptide abundance; resulting values between 0 and 1 were converted to -1/'*Fold change*'). Orange marking indicates peptides with P<0.1, which are changed in opposite directions ('reverse') and differed at least 10%. Yellow fill – P<0.1, blue fill – P<0.05, green font – decreased fold change, red font – increased fold change, grey font – non-significant fold change. SCZ – schizophrenia, BC – blood coagulation, CA – complement activation, MP – metabolic process, AP/IR – acute phase/immune response, M/IB – metal/ion binding, LB/T – lipid binding/transport, Abbr – abbreviation, Cov – covariates, FC – fold change.

Biological process										$SCZ T_0$ - HC			$SCZ T_0$ - $SCZ T_6$		
BC	CA	MP	AP/IR	M/I B	LB/T	Uniprot ID	Abbr	Protein	Peptide	Cov	P-value	FC	Cov	P-value	FC
		✓			✓	P02654	APOC1	Apolipoprotein C-I	EWFSETFQK	age	0.043	-1.49	age	0.056	1.38
		✓			✓	P02656	APOC3	Apolipoprotein C-III	DALSSVQESQVAQQAR		0.013	-1.65		0.458	1.17
	✓		✓			P01859	IGHG2	Immunoglobulin heavy constant γ2	GLPAPIEK		0.029	-1.92		0.655	-1.17
		✓	✓		✓	P02652	APOA2	Apolipoprotein A-II	SPELQAEAK		0.051	-1.28		0.159	1.12
		✓	✓		✓	P06727	APOA4	Apolipoprotein A-IV	IDQNVEELK		0.062	-1.29		0.749	1.06
		✓	✓		✓	P06727	APOA4	Apolipoprotein A-IV	ISASAEELR		0.054	-1.36		0.648	1.08
		✓			✓	P02654	APOC1	Apolipoprotein C-I	EFGNTLEDK	age	0.064	-1.45	age	0.148	1.28
		✓			✓	P02655	APOC2	Apolipoprotein C-II	ESLSSYWESAK		0.068	-1.56		0.483	1.21
		✓			✓	P02656	APOC3	Apolipoprotein C-III	GWVTDGFSSLK		0.086	-1.39		0.747	1.07
✓	✓		✓		✓	P10909	CLUS	Clusterin (Apolipoprotein J)	FMETVAEK		0.095	1.39	age	0.217	-1.27
	✓					P02748	CO9	Complement component C9	LSPIYNLVPVK		0.073	1.52		0.184	-1.33
	✓					P02748	CO9	Complement component C9	VVEESELAR		0.055	1.45		0.223	-1.31
✓	✓		✓			P04004	VTNC	Vitronectin	DWHGVPGQVDAAMAGR		0.097	1.39		0.364	-1.19
✓	✓			✓		Q96IY4	CBPB2	Carboxypeptidase B2	DTGTYGFLLPER		0.623	1.05		0.074	-1.25
✓			✓	✓		P02790	HEMO	hemopexin	VDGALCMEK		0.219	1.22		0.099	-1.34

6.2.5 Symptom subscale correlations to identified microglial reversal epitopes and serum reversal protein Apo C-I

To determine whether improvement of schizophrenia symptoms is related to the detected normalisation changes in cellular responses and serum proteins, we correlated changes (δ) in the identified normalized microglia epitopes (PDPK1 pS241 and GSK3β pS9) and serum peptides (Apo C-I) to changes in PANSS scores. Due to limited sample numbers and data pre-processing, Spearman's correlation was only run in scenarios containing enough data points ($n \geq 7$). There was a significant correlation between δPDPK1 (pS241) and δGSK3β (pS9) ($p=0.015$, $rho=0.85$) (**Figure 6.5**), supporting the link between these epitopes as members of the same signalling cascade. There were no significant correlations identified between changes in epitope and δ syndrome subscales ($P<0.05$), however trends (at $P<0.1$) were observed. δPDPK1 (pS241) showed a borderline correlation with δPANSS general ($p=0.060$, $rho=0.73$) and δPANSS total ($p=0.079$, $rho=0.70$). Another trend was observed for the correlation between δGSK3β (pS9) and δPANSS general ($p=0.086$, $rho=0.69$). Both trends indicate increased epitope activity accompanying improvement in symptoms. However, due to small sample numbers, these correlations need to be validated with a bigger sample size. There were no significant correlations identified between changes in δApo C-I and δPANSS or between δApo C-I and changes of the normalised epitopes.

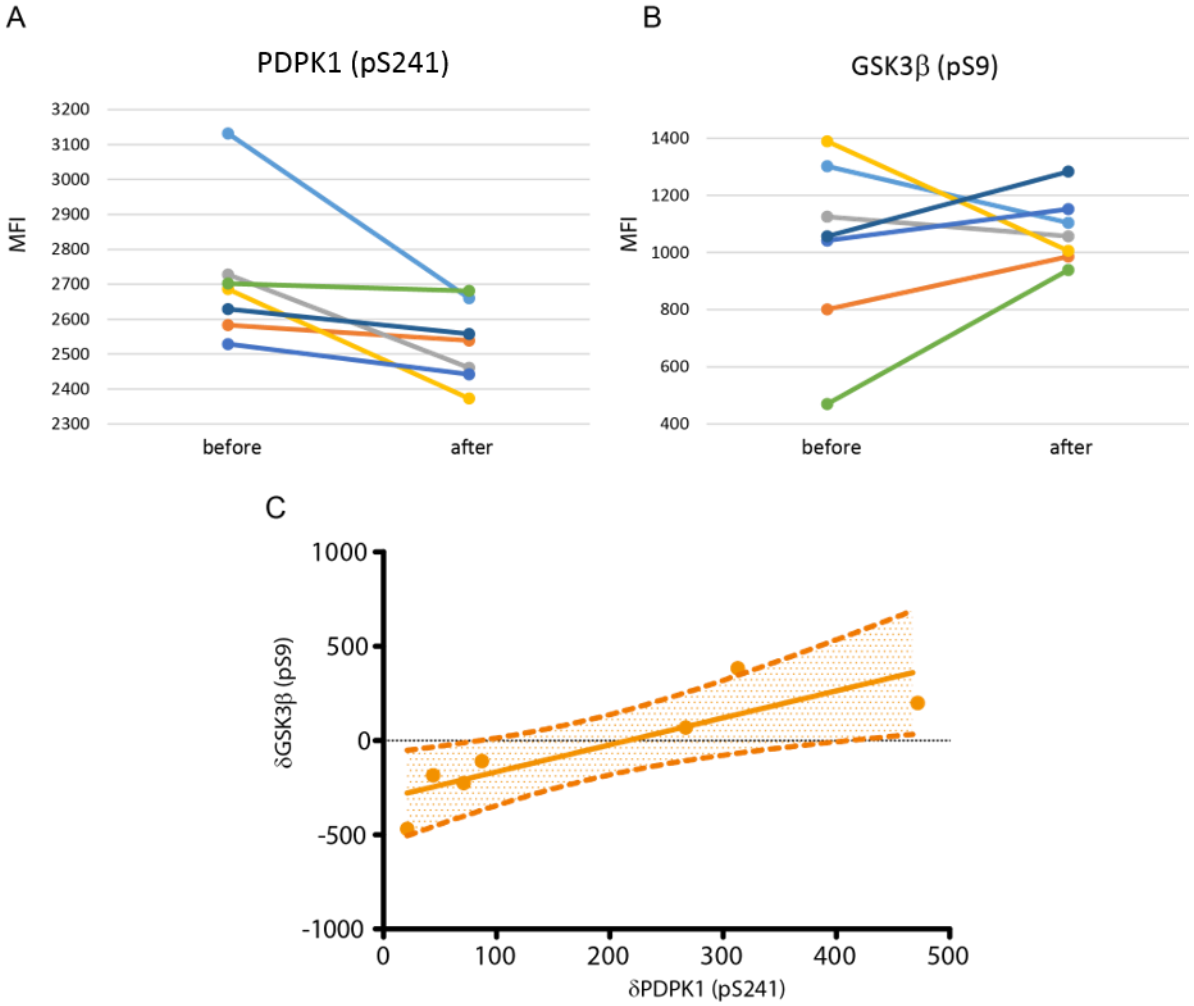

Figure 6.5 Overview of significant correlation between changes in PDPK1 (pS241) and changes in GSK3β (pS9). (A,B) The top two plots show epitope activity levels (y-axis) in microglia exposed to T0 serum (before) and to serum from the same patients at the 6 weeks' time-point (after). The plots represent the identified normalised epitopes **(A)** PDPK1 (pS241) and **(B)** GSK3β (pS9). All individuals are represented by different coloured lines. **(C)** Overview of significant correlation between δPDPK1 (pS241) and δGSK3β (pS9). The scatterplot shows changes in microglial epitope levels following serum exposure from individuals before and after olanzapine treatment, with δPDPK1 (pS241) on the x-axis and δGSK3β (pS9) on the y-axis (p=0.015, rho=0.85). Dotted lines with orange fill indicate the 95% confidence interval. MFI – median fluorescent intensity.

6.3 Discussion

One of the major issues regarding the patient cohort investigated in this chapter is the limited number of samples. This resulted in an increase of the significant P-value threshold, in order to allow an exploratory phase for the detection of treatment-dependent reversal nodes whilst accepting that chances for false positive discoveries increased to 10% instead of the commonly applied 5%. Epitopes and proteins were categorised as reversal when they were found to be altered between schizophrenia patients and controls and subsequently normalised by *in vivo* treatment with olanzapine. In addition, when comparing the data to the previously presented data sets, we may be able to strengthen the current observations. Therefore, this discussion will focus on the validation of previously identified changes in microglia signalling epitopes and serum proteins via comparison to previously presented data in Chapters 4 and 5. In addition, the identified treatment-dependent reversal epitopes and proteins will be discussed. Finally, the findings will be discussed in the context of the current knowledge from existing literature. However, the findings presented here would need validation by using a similar study design with a larger sample size.

6.3.1 Partial validation by comparison of current results to those of different schizophrenia patient cohorts and same patient PBMC data

Patient serum exposure led to the identification of 15 altered microglial signalling epitopes ($P<0.1$), of which 9 were identified in the SCZ T_0 vs. HC comparison and 8 in the SCZ T_0 vs. SCZ T_6 comparison. Of these 15 altered microglial signalling epitopes, two were identified to overlap between the two comparisons. Due to the limited number of samples and the extended P-value, changes in epitopes were compared to the previously presented patient cohorts with respect to the matching comparison, which is for the SCZ T_0 vs. HC comparison to Chapter 4 (**Table 4.2**) and for SCZ T_0 vs. SCZ T_6 to Chapter 5 (**Table 5.5**). Of interest are the two epitopes that almost reached significance ($P<0.05$) in the SCZ T_0 vs. HC comparison, which are 4EBP1 (pT36/pT45) and 4EBP1 (pT69). These two epitopes were identified to be the most significantly altered in serum exposed microglia in Chapter 4 presenting a first-onset drug-naïve schizophrenia cohort, and showed borderline P-values of 0.060 and 0.063, respectively, in the present comparison. If the patient and control groups presented in this chapter would have contained more samples, these two epitopes could possibly have reached significance. The third most significantly altered microglia epitope presented in Chapter 4 was STAT3 (pY705). Although we did not identify this epitope to be altered in the SCZ T_0 vs. HC comparison, it was identified in the SCZ T_0 vs. SCZ T_6 comparison. Interestingly, serum exposure from *in vivo* olanzapine treated patients indicated a decrease in levels of this particular epitope. The need to achieve a similar directional effect was identified in patient serum exposed microglia from Chapter 4. Patient serum caused less of a

decrease of STAT3 (pY705) relative to control serum in exposed microglia, and a correction for this was achieved via exposure to potential drug candidates. Therefore, the *in vivo* olanzapine treatment might be efficient in aiding towards the desired normalisation pattern identified in Chapter 4. However, altered STAT3 (pS727) signalling in microglia, found here in the exploratory range of the SCZ T_0 vs. SCZ T_6 comparison, was also identified in Chapter 5, which presents an antipsychotic treated schizophrenia cohort. Although the change of direction is not similar between these two cohorts, in both comparisons serum exposed microglia revealed altered STAT3 (pS727) signalling. Therefore, *in vivo* treatment does not appear to fully normalise components in serum capable of inducing altered STAT3 signalling in schizophrenia patient serum exposed microglia, suggesting the need for targeting these disease-related changes with adjunctive medications.

Interestingly, a study using the same patients and controls as the study presented in this chapter, but investigating amongst others changes in basal expression levels in isolated PBMCs from these patients, showed similarities with some of the epitopes identified here in serum exposed microglia. They found altered STAT3 (pY705) in both SCZ T_0 vs. HC and SCZ T_0 vs. SCZ T_6 comparisons, with the latter showing a similar change of direction as identified in serum exposed microglia. Other similarities in epitope expression from the SCZ T_0 vs. SCZ T_6 microglia epitopes to those identified in PBMCs were PDPK1 (pS241), STAT3 (pS727) and p53 (acK382)[250]. Yet these three epitopes are opposite in fold change direction in comparison to the identified expression levels in patient PBMCs. This difference in fold change direction might be explained by the fact that the primary PBMCs have been continuously exposed to serum *in vivo,* which could have caused PBMCs to adjust to their environment and adjust signalling cascades concurrently. In contrast, microglia had not been exposed to these components before and therefore show an initial signalling response without having had the time to adjust to the continuous presence of those same serum components. Another possible explanation is the fact that these are different cell types. Therefore, it is likely that these cells respond differently to the same stimulant.

6.3.2 Identification of reversal epitopes PDPK1 (pS241) and GSK3β (pS9) indicative of effective *in vivo* treatment

In order to identify which of the epitopes represented potential drug targets for schizophrenia, we assessed which of the signalling epitopes reversed over the course (6 weeks) of clinical olanzapine treatment. Microglia epitopes were categorised as reversed when they were found to be altered between schizophrenia patients and controls and subsequently normalised by *in vivo* treatment with the antipsychotic olanzapine. Two out of 64 epitopes were identified as reversed, which are GSK3β

(pS9) and PDPK1 (pS241). Interestingly, it is the combination of these two epitopes which strengthens this finding. This is because the identification of GSK3β (pS9) could be a direct result of increased PDPK1 (pS214) signalling, as both epitopes are members of the Akt signalling pathway. This assumption is further strengthened by the strong correlation between these two epitopes. For PDPK1, phosphorylation at serine 214 has been proven vital for full signalling activity, which is achieved via autophosphorylation[430]. PDPK1 plays a central role in the activation of the Akt pathway, which is the prime route for GSK3β regulation[431].

GSK3β signalling was originally associated with the regulation of glycogen synthesis in response to insulin. Yet, the broader function of GSK3β was later proven, via Akt signalling which is capable of inhibiting GSK3β, to be involved with multiple hormones and growth factors (*e.g*. BDNF, IGF, and insulin)[431]. The GSK3β kinase is constitutively active and can be inactivated through the phosphorylation of a single serine residue, serine 9. Converging evidence suggests that the regulation of the Akt-GSK3β pathway might be of importance for the pathophysiology of schizophrenia[432]. Two commonly associated genetic mutations with schizophrenia, *DISC1* and neuregulin 1 (*NRG1*), are suggested to play a role in the development and susceptibility for schizophrenia[433]. Furthermore, it has been shown that mutations in these two genes are capable of affecting Akt phosphorylation in different cell culture systems[434,435], thus suggesting that the Akt/GSK3 signalling pathway also contributes to the complex set of pathological events induced by mutant gene products in schizophrenia. Another gene expression study, using a similar study design as presented in this chapter with PBMCs from schizophrenia patients before and after 6 weeks of antipsychotic treatment, identified abnormalities in biological pathways involving Akt, which are subsequently normalised by antipsychotic treatment[436]. Moreover, Akt knockout mouse models have shown an association between Akt deficiency and depression-like behaviour in mice[437,438]. It was subsequently shown that antipsychotics alter the GSK3β protein expression levels in the rat medial prefrontal cortex and striatum. Moreover, the authors suggested that GSK3 may represent one of the mechanisms through which antipsychotics are able to exert behavioural changes[439]. In order to elucidate these findings, cell culture systems have been used to clarify the effects antipsychotics exert on the Akt-GSK3 signalling pathway. Atypical antipsychotics have been shown to either activate Akt or to mimic Akt activity by increasing the phosphorylation of its substrates GSK3α and β. The atypical antipsychotic clozapine has been shown to act as an enhancer of Akt/GSK3 signalling [440]. *In vivo*, acute or subchronic administration of several atypical antipsychotics, including olanzapine, risperidone, quetiapine, clozapine, and ziprasidone, results in an inhibition of GSK3β, that reproduces the action of Akt, in different brain regions[439,441]. Taken together these studies suggest the Akt-GSK3β pathway to be involved in the

aetiopathophysiology of schizophrenia and is associated with effective treatment resulting in partial symptomatic relief[442–445].

6.3.3 Validation of serum proteins in comparison to previous schizophrenia patient sample cohorts

Mass spectrometry was employed to explore whether the alterations in microglia signalling cascades could be explained by differences in the relative concentrations of serum proteins previously linked to neuropsychiatric disorders[253]. Due to the limited number of samples, the P-value threshold was increased ($P<0.10$) for exploratory reasons. Therefore, changes in peptides were compared to the previously presented results with respect to the matching comparison, which is for SCZ T_0 vs. HC to Chapter 4 (**Table 4.3**) and for SCZ T_0 vs. SCZ T_6 to Chapter 5 (**Table 5.6**). In addition, next to the overlap in detected proteins, direction of fold change was taken into account. The comparison from the SCZ T_0 vs. HC results to serum proteins identified in Chapter 4 left two protein groups post filtering, which are the apolipoproteins (A-II, A-IV, C-I and C-III) and complement cascade (C9). The comparison between identified proteins from the SCZ T_0 vs. SCZ T_6 comparison to serum proteins identified in the antipsychotic treated patient group from Chapter 5 did not yield any proteins. When similar directionality of fold change is excluded from the criteria, one protein is identified which is Apo C-I.

The finding of increased C9 in patient serum aligns with previously published data regarding the involvement of the complement cascade in schizophrenia[161,162,375]. C9 is involved in the final phase of the complement cascade, as part of the membrane attack complex (MAC), causing lysis of a target cell or pathogen[162] (see **Figure 4.3**). Interestingly, in an animal model of Alzheimer's disease, microglia were shown to be reactive before any obvious amyloid plaque formation had occurred. This early microglial response occurs through yet unknown triggers. However, complement factors have been suggested to be such a trigger. Furthermore, complement activation and activated microglia have been associated with early neuropathological events in Alzheimer's disease brains[446].

Apolipoproteins have also been reported to be altered in serum of schizophrenia patients relative to controls and have been found to correlate with cognitive deficits and alterations in hippocampal brain volume[252]. Interestingly, selective overexpression of microglial apolipoprotein receptor TREM2[309] in the neurodegenerative P301S mouse model induced a neuroprotective phenotypic shift in microglia towards the anti-inflammatory state with concurrent reduction in proinflammatory cytokine production[394]. This raises the possibility that the reduction in apolipoproteins observed in schizophrenia T_0 relative to control serum in the present study may reflect a compromised neuroprotective profile.

Altered cholesterol metabolism and polymorphisms within the apolipoprotein genes have been associated with several neurological and psychiatric conditions, thus emphasizing the important role these factors play in CNS physiology. Apolipoprotein signalling within the CNS facilitates tightly regulated delivery of lipids and substrates to specific cells in the brain, as well as regulating signal transduction pathways[447]. The majority of apolipoprotein signalling is related to myelin sheaths and, to a lesser degree, plasma membranes of glial and neuronal cells[448]. Furthermore, apolipoprotein polymorphisms have been associated with adverse outcomes in several CNS pathological states, including traumatic brain injury and stroke[449]. Therefore, the observed decrease of apolipoproteins in SCZ T_0 serum could imply altered lipid metabolism which could affect, for example, myelin sheaths and thereby signal transduction.

6.3.4 Identification of the normalisation of serum protein apolipoprotein C-I

The brain is the most lipid-rich organ in the body and, owing to the impermeable nature of the BBB, lipid and lipoprotein metabolism within this organ is distinct from the rest of the body. Yet, recent research suggests that some brain apolipoproteins are synthesized outside the CNS. For example, the transit of peripherally derived apolipoproteins into the CNS has been suggested for Apo A-I and Apo A-II, as they may enter the CSF via the choroid plexus[447,450]. Apolipoproteins play a well-established role in the transport and metabolism of lipids within the CNS. However, evidence is emerging that they also fulfil a number of functions that extend beyond lipid transport and are critical for healthy brain function[447]. The importance of apolipoproteins in brain physiology is highlighted by genetic studies, where apolipoprotein gene polymorphisms have been identified as risk factors for several neurological diseases (*e.g.* Alzheimer's and Parkinson's disease) and outcome of pathological states, such as stroke and spinal cord injury[447].

Here, we identify serum Apo C-I to normalise following effective treatment of patients with olanzapine. Expression of Apo C-I decreases with age and Apo C-I is known to block Apo E receptor interaction[451–453]. Polymorphisms of the Apo C -I gene are associated with altered Apo C-I transcription and an increased incidence of Alzheimer's disease[454]. Furthermore, Apo C-I levels are found to vary with APOE genotype in humans and in mice carrying the human *APOE* gene. Due to potent reduction of microglial derived pro-inflammatory cytokine secretion, Apo C-I was found to be immunosuppressive[321]. And indeed, *APOC1*$^{-/-}$ mice show impaired hippocampal-dependent memory formation with no major changes in brain morphology or brain cholesterol levels and increased expression of the proinflammatory marker TNFα[455]. However, mice overexpressing human Apo C-I also display impaired learning and memory[456].

Changes in Apo C concentrations have been demonstrated by several authors and have been linked to the physiopathology of schizophrenia[252,318,319]. Furthermore, direct associations between cognitive impairments, underlying structural abnormalities and altered protein expression in Apo C proteins could be observed[252]. Changes in apolipoproteins in elderly individuals with mild cognitive impairment were found to be associated with cognitive function and brain volumetric MRI measures. In addition, changes in apolipoproteins were found to be predictive of cognitive impairment in cognitively normal subjects[457]. Moreover, Apo C-I polymorphisms have been implied to be genetic risk factors for dementia and cognitive impairment in the elderly[458]. Therefore, it has been suggested that there is a connection between Apo C-I, neuronal changes and cognitive deficits. Hence, the presented normalisation of serum Apo C-I levels in schizophrenia patients following antipsychotic drug-treatment might be involved with an improvement of the cognitive symptoms as observed in schizophrenia patients.

It should be noted that in our study, Apo C-I normalisation following antipsychotic patient treatment was identified in serum and not in CSF. Therefore, we cannot conclude that the alterations in microglia signalling would occur *in vivo* too, as too little research has investigated the ability of apolipoproteins to cross the BBB into the CNS. Therefore, the concentration of Apo C-I in CSF could be different to serum levels. In addition, the fact that there is an interaction between different *APOE* genotypes and Apo C-I, suggests that Apo C-I may be an *APOE* genotype-dependent suppressor of glial activation. However, any of the referenced studies in this section did not account for *APOE* genotype or for its interaction with Apo C-I. Therefore, the Apo C-I related findings from those particular studies might change once the *APOE* genotype is accounted for.

Chapter 7
Conclusion

Chapter 7 |Conclusion

This thesis presented the results from microglial serum exposure studies, using serum from schizophrenia patients and healthy controls, to investigate whether changes in serum are capable of inducing an altered microglia signalling phenotype. In addition, via the application of mass spectrometry, a panel of serum proteins which have been previously linked to neuropsychiatric disorders was monitored for alterations. The aim of this chapter is to summarize the main findings from chapters 3-6 and highlight their significance to the field of schizophrenia research. Subsequently, the limitations of the current studies and implications for future research will be discussed.

7.1 Overview of main findings

7.1.1 Summary

Abnormal activation of the brain's resident immune cells, microglia, has been hypothesized to be involved in the pathogenesis of schizophrenia. Despite the suggested involvement of microglial activation and the reported changes in circulatory proteins with microglial activation propensity in schizophrenia patients, the effect of circulatory protein abnormalities on microglial activation status has, as yet, not been explored. In the present study, we show a reverse approach in which human microglial cells were directly exposed to native serum samples from schizophrenia patients and healthy controls. We build on previous evidence that the peripheral immune system can signal through the BBB and alter the phenotype of brain-resident microglia[459–461].

We used a high-content screening platform (**Chapter 3**) for the functional characterization of changes in signalling pathways at the single-cell level in a human microglia cell line following exposure to serum obtained from schizophrenia patients and controls. We demonstrate that peripheral blood serum isolated from schizophrenia patients, independent of their treatment status, is sufficient to trigger microglial cell signalling network responses *in vitro*, which are indicative of altered STAT3 signalling (**Chapters 4-6**). An association between the *in vivo* and *in vitro* alterations is further supported by strong inverse correlations between STAT3 (pS727) and BP_{ND} across all PET imaging brain regions which were identified within the control group only, indicating changes in STAT3 signalling in the patient group (**Chapter 5**). In addition, using a longitudinal study design, several of the identified alterations in microglia signalling were normalized following a clinical course (6 weeks) of olanzapine treatment (PDPK1 pS241 and GSK3β pS9; **Chapter 6**).

To explore whether the putative microglial activation phenotype could be explained by differences between the clinical groups in the relative concentrations of serum proteins previously linked to neuropsychiatric disorders, we employed targeted multiple reaction monitoring mass spectrometry. This revealed relative changes in apolipoprotein, coagulation and complement protein groups in schizophrenia patients relative to controls (**Chapters 4-6**). One of the identified alterations in serum proteins was normalized *in vivo* (Apo C-I) at the 6 weeks' follow-up time-point of a clinical course of olanzapine treatment (**Chapter 6**).

To our knowledge, this is the first study to suggest that circulating blood serum from schizophrenia patients can have a direct effect on the intracellular activation phenotypes of resident brain immune cells *in vitro*. This provides a new perspective on the potential direction of causality between peripheral and CNS disease mechanisms. While alterations in circulating factors have often been considered secondary effects of CNS abnormalities, the present data suggests that they may in fact be sufficient, or at least reciprocal, in provoking pathogenic cell signalling alterations in key CNS cell subpopulations.

7.1.2 Identification of altered STAT3 phosphorylation state in microglia after exposure to serum from schizophrenia patients

We identified alterations in the phosphorylation of STAT3 in microglia exposed to serum from schizophrenia patients (**Chapters 4-6**), independent of treatment status. Furthermore, an association between *in vivo* and *in vitro* alterations is supported by strong inverse correlations between STAT3 (pS727) and BP_{ND} across all PET imaging brain regions which were identified within the control group only (**Chapter 5**), indicating changes in STAT3 signalling in the patient group.

As discussed extensively in **section 4.3**, the identification of altered STAT3 (pY705) signalling could reflect altered circulating cytokines (both pro- and anti-inflammatory)[144] in serum from schizophrenia patients. However, the STAT3 regulatory site S727 can be phosphorylated through many different kinases, including MAPK and mTOR[364]. Depending on the extracellular stimulus and the intracellular context, the phosphorylation of STAT3 at S727 can either result in: i) translocation to the nucleus through maximal STAT3 activation when combined with STAT3 (pY705) or ii) result in dephosphorylation of STAT3 (pY705), thereby limiting STAT3 activity[334,364]. This is suggesting that the STAT3 signalling pathway can be fine-tuned via this STAT3 (pS727) phosphorylation site. Therefore, the current observation of altered microglial STAT3 signalling could also reflect the activity of a parallel pathway capable of modifying the STAT3 response in microglia. Nonetheless, the identification of altered microglial STAT3 activation following exposure to patient serum provides new perspectives with regard to the development of new drug targets for schizophrenia.

However, the question remains whether the observed altered STAT3 signalling in microglia exposed to serum is the result of for example altered circulating cytokines in schizophrenia patient serum or is due to other factors in serum capable of inducing parallel pathways with the ability to modulate STAT3 signalling (**Figure 7.1**).

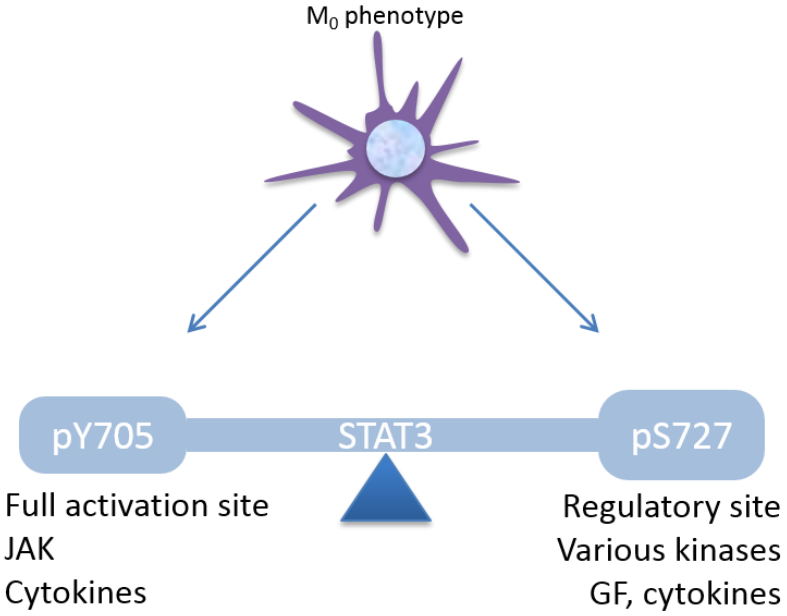

Figure 7.1 Identified altered STAT3 phosphorylation sites in microglia exposed to schizophrenia patient serum. An altered microglia phenotype was identified following exposure to serum from schizophrenia patients compared to controls. This phenotype contains changes in STAT3 phosphorylation patterns via the activation site Y705 and the regulatory site S727. STAT3 (pY705) can be phosphorylated via JAK, while STAT3 (pS727) can be phosphorylated through various kinases, such as MAPK and mTOR. Therefore, whereas STAT3(pY705) can only be phosphorylated through direct ligand-receptor interactions (usually cytokine related), STAT3 (pS727) can be regulated indirectly through many different ligands, depending on the kinase (de-)phosphorylating it. For example, neuropoietic cytokines are capable of inducing phosphorylation of STAT3 (pS727) via the mTOR pathway[364,463]. GF – growth factor. JAK – Janus kinase. STAT – signal transducer and activator of transcription.

7.1.3 Changes in apolipoprotein expression in patient serum may indicate altered microglial TREM2 signalling

A targeted mass spectrometry approach was employed to explore whether the identified alterations in microglia signalling cascades could be explained by differences in the relative concentrations of serum proteins previously linked to neuropsychiatric disorders[253]. Members of the apolipoprotein family were found to be altered in all studies carried out in this thesis (**Chapters 4-6**). When exact overlap of proteins across the different chapters is taken into account, apolipoproteins A-II, A-IV, C-I and C-III were revealed to be decreased in serum from first-onset drug-naive schizophrenia patients when compared to control serum (**Chapters 4 and 6**). Antipsychotic treatment was associated with a shift in direction of the fold change of certain serum apolipoproteins, with some proteins going from a decrease to an increase in schizophrenia serum relative to controls whilst other apolipoprotein fold changes did not change (**Chapters 5 and 6**). Furthermore, the only protein which was found to normalise following antipsychotic drug-treatment was an apolipoprotein, Apo C-I (**Chapter 6**). Therefore, the treatment-related changes in the levels of apolipoproteins in schizophrenia patient serum may reflect a partial normalisation of this protein class associated with effective antipsychotic drug treatment. A recent comprehensive meta-analysis showed that the add-on treatment of statins (lipid-lowering medication) in schizophrenia patients was associated with significant superiority over placebo, resulting in improvement of total PANSS scores. Although the mechanism and the effectiveness of this treatment in clinical practice requires future investigation, the apolipoproteins might be an attractive drug target for further testing[464].

In the CNS, microglia are the primary cell type expressing receptors for apolipoproteins (TREM2)[309]. TREM2 has been reported to be critical for the microglial response to injury and has been implicated in Alzheimer's Disease pathology. TREM2 has also been reported to affect overall microglial cell survival, proliferation, phagocytosis and inflammation[465–467]. However, until recently, the TREM2 intracellular signalling mechanisms in microglia have been elusive. Ulland *et al.*[468] have suggested an explanation for why TREM2 deficient microglia are unable to respond to neurotoxic environments. Studying isolated microglia from a *Trem2*$^{-/-}$ Alzheimer's disease mouse model, they identified decreased mTOR signalling along with markers for altered energy production and anabolic metabolism, suggesting TREM2 in microglia to be involved with both mTOR signalling and glycolysis. In addition, microglial TREM2 deficiency results into autophagy. During *in vitro* settings of stress, TREM2-expressing microglia cells were more capable to sustain mTOR activation and suppress autophagy in a PI3K-dependent way, compared to microglia cells lacking TREM2. Furthermore, under stress, TREM2 deficient microglia show mTOR pathway dysfunction combined with anabolic and energetic metabolism, which induces compensatory autophagy. Therefore, the authors conclude that TREM2 is

helping microglia ''sense'' stress through the mTOR pathway[469]. In the absence of TREM2, microglia were shown to display changes in energy metabolism and were thus unable to protect the CNS from stress[468,469]. Although there is no indication in the literature for altered microglial TREM2 expression in schizophrenia patients, there is for the TREM2 ligand, the apolipoproteins. The observed decrease of a number of different apolipoproteins in schizophrenia patient serum could be associated with a decrease in ligand-receptor interactions with TREM2. This reduced TREM2 interaction could thereby induce a diminished microglial protective phenotype through altered microglial mTOR signalling. Evidence for altered microglial mTOR signalling is presented in **Chapter 4**. Following the exposure of microglia to serum from first-onset drug-naïve schizophrenia showed altered 4EBP1 (pT36/pT45), 4EBP1 (pT69) and eIF4E (pS209) responses. The epitopes 4EBP1 (pT36/T45) and 4EBP1 (pT69) are direct mTORC1 substrates, whereas eIF4E (pS209) is a direct 4EBP1 substrate. Therefore, the exposure of microglia to serum containing a decrease in apolipoproteins could have precipitated the cells towards a less protective phenotype through potentially altered TREM2-mTOR signalling. Combining these findings, the identified microglia signalling changes following serum exposure could have been the result of altered mTORC1 signalling through changes in the levels of serum apolipoproteins. As the STAT3 pathway signalling activity can be modified via, amongst others, mTOR signalling[364], the affected microglial mTORC1 signalling could be associated with the observed changes in microglial STAT3 signalling (**Figure 7.2**).

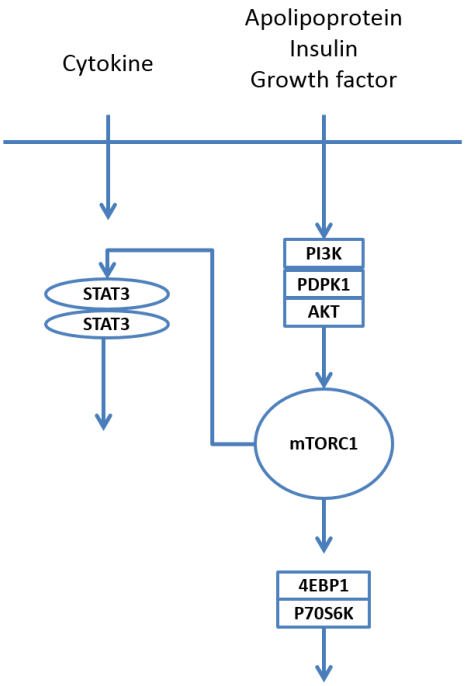

Figure 7.2 Schematic representation of altered STAT3 signalling pathway in microglia upon exposure to serum from schizophrenia patients. The overview presents a potential signalling cascade in microglia exposed to serum from schizophrenia patients relative to controls. Potentially altered circulatory cytokine levels are capable of inducing STAT3 signalling via for example the gp130 receptor. However, the STAT3 pathway activity can be fine-tuned by other parallel pathways, such as the mTOR pathway which can be activated by growth factors, glutamate, insulin and apolipoproteins. mTORC1 – mammalian target of rapamycin complex 1. STAT – signal transducer and activator of transcription.

However, it should be taken into consideration that the results from the *Trem2*$^{-/-}$ Alzheimer's disease mouse model would need validation, as this is the first, and currently only study to report on TREM2 signalling in microglia. Future studies are needed to validate these findings and to further characterize this pathway and its specific effects on the microglia phenotype. Therefore, although the detected changes in apolipoproteins could affect microglial mTOR signalling, further research is necessary to fully characterize the effects of apolipoprotein signalling in microglia

7.2 Identification of common microglial signalling hub as novel drug target

Amongst the limiting factors across the studies presented in the chapters in this thesis were patient cohorts comprised of small sample numbers. Schizophrenia is regarded a heterogeneous disease due to a range of symptoms which are never manifested in the same way across different patients. Furthermore, almost every affected patient has a unique underlying pathological mechanism that defines the disorder (*e.g.* genetic, epigenetic, environmental, as reviewed in **Chapter 1**). Therefore, one would expect the need for much bigger sample sizes compared to the ones presented in this thesis, in order to be able to identify a common target. Hence, given the limited sample sizes representing such a heterogeneous patient population, one would not expect the identification of peripheral markers capable of affecting one common pathway. However, this is exactly what we were able to demonstrate across these various studies. This section will discuss the utility of the identified microglial phenotype as a new drug target with the potential for the treatment of negative symptoms.

7.2.1 Cellular phenotype screening approach for the identification of new drug targets

Major programs in psychiatric genetics have identified over 150 risk loci for psychiatric disorders[17,221]. These loci converge on a small number of functional pathways, which span conventional diagnostic criteria, suggesting a partly common biology underlying schizophrenia and other psychiatric disorders[470]. Nevertheless, the cellular phenotypes that capture the fundamental features of psychiatric disorders are only starting to become determined[462]. Genetic variants may confer risk for schizophrenia by affecting the same molecular pathway. This disease pathway hypothesis implies a polygenetic variation affecting the same pathway and the alteration of a transcriptional network associated with an increased schizophrenia risk. Genetic risk variants for schizophrenia can also influence similar regions in the brain, suggesting that environmental and intrinsic factors may converge onto the same neural circuit[471]. The lack of new approved drugs in the past decade has been partially

attributed to failures in discovery and validation of new targets. Evaluation of recently approved new drugs has revealed that the number of approved drugs discovered through phenotypic screens has exceeded those discovered through the molecular target-based approach[472]. Therefore, the identification of altered pathway activity in microglia following exposure to serum from schizophrenia patients could be considered as a phenotypic screening approach for drug discovery. As suggested by the results presented in this thesis, this would include testing compounds that are known to directly affect JAK/STAT and mTOR signalling pathways, but also parallel pathways known to be involved indirectly and capable of fine-tuning the identified microglia signalling phenotype. When the identified drug target is taken forward into drug screening, it should be taken into account that the current detected microglial signalling alterations are changes in phosphorylation status. Therefore, future drug screenings would have to aim to bring the phosphorylation status of the respective epitope back to a phosphorylation state resembling the state as observed in the control group.

7.2.2 Altered microglial STAT3 signalling overlaps with signalling changes in MDD

In animal models of related neuropsychiatric disorders, such as MDD, microglia-specific knockout of STAT3 resulted in increased synaptic plasticity and anti-depressive like behavior[420]. In general, STAT3 involvement in MDD has been more often reported compared to schizophrenia. For example, many studies reported an increase of cytokines in MDD patients[473,474], similar to cytokine alterations reported in schizophrenia[475]. Furthermore, elevated IL-6, a cytokine often reported to be increased in schizophrenia patients[100,101,103–106], has been correlated with depressive symptoms in schizophrenia patients[476]. The detected elevated IL-6 levels in MDD have been suggested to signal through JAK-STAT3, and this mechanism of action has been associated with depression-like behaviour in animal models of MDD[477,478]. Moreover, mice lacking STAT3 specifically in microglia show anti depressive-like behaviour, indicating an involvement of neuroinflammation by microglia STAT3 activation towards depressive symptoms[420]. Although these publications involve IL-6, there has been little, if any, research published examining the broad downstream effects of the full IL-6 family and their effects regarding patient symptomology. It would be of interest to investigate how these findings would replicate when exploring the full range of IL-6 family cytokines.

The identification of microglial STAT3 activation following exposure to patient serum provides new evidence for the role of STAT3 signalling with regard to the aetiology of negative symptoms in schizophrenia. So far, STAT3 involvement in schizophrenia has been rarely reported. A study crossing the neuropsychiatric spectrum using patient derived PBMCs showed that apart from schizophrenia, The only other disorder to show altered STAT3 phosphorylation patterns was MDD[462]. Taken together,

these *ex vivo* findings, in conjunction with the well documented role of IL6-STAT3 signalling in MDD, suggests that altered STAT3 signalling in microglia may be an important target for future investigations regarding negative symptoms in both schizophrenia and MDD.

While the precise time point at which respective alterations in synaptic plasticity and pruning may contribute to the aetiology of schizophrenia are still a matter of intense debate[54], the current results suggest that the activation of STAT3 by circulating factors during critical neurodevelopmental stages should be further investigated. Moreover, the implication of microglial STAT3 signalling in MDD, together with the correlation of microglial activation markers and cognitive deficits in schizophrenia[217], suggests that STAT3 in microglia may represent a target for the treatment of negative symptomatology common to several neuropsychiatric disorders.

7.2.3 Altered microglial STAT3 signalling phenotype as new drug target for the treatment of negative symptoms

Although there were no significant correlations between the identified significant epitopes and the PANSS scores, there is a substantial overlap between the identified pathways, the negative symptomology and MDD. The overlap in altered STAT3 signalling profiles between schizophrenia and MDD is suggested by the well documented role of IL6-STAT3 signalling in MDD (**section 7.2.2**), which may be an important target for future investigations regarding negative symptoms in both schizophrenia and MDD. MDD is a psychiatric disorder characterized by several symptoms, including low mood, low self-esteem, and loss of interest or pleasure in normally enjoyable activities (anhedonia) and has a prevalence of 5.2 to 6.6%[479,480]. In addition to these impairments, this disorder is also associated with an increased lifetime suicide risk of 3.5% in affected patients[481]. MDD is currently regarded as the fourth leading cause of disability worldwide and is expected to be the second leading cause of disability worldwide by 2030[482]. The negative symptoms that accompany schizophrenia include diminished emotional expression, avolition, loss of motivation, emotional deficits and anhedonia. Both disorders typically have an onset in young adulthood. Furthermore, depression, anxiety and substance abuse are often comorbidities of schizophrenia, further complicating the clinical picture. For example, depression can cause secondary negative symptoms, panic attacks and is capable of aggravating paranoia whereas cannabis abuse can worsen positive and disorganisation symptoms. The measured range of depressive experiences in schizophrenia varies widely due to heterogeneous study populations and varying time intervals over which depressive occurrences were considered (for full overview see Table 4 in Buckley *et al.* 2009[483]). Nonetheless, it has been shown that schizophrenia patients are prone to increased rates of depression with a modal frequency of 25%[484]. Therefore, the discovery of the altered microglia signalling phenotype post schizophrenia serum exposure combined

with the overlap in signalling pathways and negative symptomology to reported changes in MDD could suggest that STAT3 may be a transdiagnostic drug target for the treatment of negative symptoms. Therefore, microglial STAT3 might represent a shared substrate for negative symptoms present in both schizophrenia and MDD, and could be considered for future investigation as a potential drug target for the treatment of negative symptoms.

Currently, negative symptoms are insufficiently, if at all, treated by available treatments. Schizophrenia patients are also prone to general medical morbidities and substance abuse, some of which may also produce depressive symptoms. Demoralization, disappointment or loneliness following a psychotic episode may worsen depressive symptoms[483]. Although over 10 years ago improved treatments for negative symptoms were promised[485], this still has not happened. Use of adjunctive agents might be the most promising option to emerge as a strategy for negative symptoms, yet the pharmaceutical industry has not joined in the search for these agents. Combining this lack of involvement and a decade of accumulated data from intervention studies revealing inconsistencies in the pattern of responsiveness of negative symptoms, the field is left disappointed with the current modest treatment efficacy.

7.2.4 Final thoughts on the utility of the identified microglial phenotype

The presented findings also allow us to re-evaluate the previously simplified dichotomy between pro- and anti-inflammatory activation states[152]. For example, although STAT1 activation is recognized as a prototypical proinflammatory polarization marker, this cellular response is not necessarily engaged by all putative proinflammatory ligands**.** Instead, patient derived native serum induces unique response profiles at discrete sites within the cell signalling network. The ability to resolve each of these responses through application of high content analysis is vital to understanding how microglia process competing secreted signals to produce complex cellular phenotypes possibly associated with schizophrenia pathogenesis. It also provides a functional basis for understanding the cellular mechanisms of microglial specialization, which can be employed to generate physiologically relevant conditional knockout animal models, novel drug screening assays and transplantation reprogramming strategies across a range of CNS disorders. The *in vivo* implications of the relatively rapid *in vitro* kinetic responses, presented in the present studies, will ultimately depend on their long-term spatial and temporal distributions in the CNS, in addition to the permeability of the respective secreted proteins across the blood brain barrier. Several of the altered serum proteins in the present study (*e.g.* apolipoproteins) are themselves associated with increased BBB permeability in subgroups of schizophrenia patients[110], suggesting that the impact of peripheral tissue alterations on the CNS, and

the potential for therapeutic intervention thereof, may be more profound than originally expected for schizophrenia.

The effectiveness of psychiatric treatments has been questioned in recent literature, resulting in the question whether pharmacotherapy or psychotherapy should be primarily used. A systematic overview of meta-analyses revealed that pharmacotherapies and psychotherapies are effective, but the medium effect sizes suggest that there is room for improvement. In addition, there is still a high rate of treatment resistance and poor adherence, making successful treatment difficult[195,201]. Despite the pressing medical need, current drug development efforts have failed to provide the mechanistic diversity necessary to address treatment resistance[195,214,486,487]. Furthermore, although many treatments induce a reduction of overall symptom scores, they usually only aid symptomatic improvement with regard to specific symptom subgroups (*e.g.* positive symptoms). [201,202,488]. Therefore, there is a compelling need for a better understanding of disease mechanisms, and in this regard microglia and the inflammatory response presents an attractive target**.** The fact that microglia are increasingly implicated in both neuropsychiatric pathogenesis[146,489] and treatment response[120,286,490] suggests that they could provide an underexploited target for novel treatments with the potential for modification of the disease course as opposed to solely symptomatic improvement[179].

Importantly, the presented novel therapeutic targets may also have utility for treating negative symptoms which are largely unaddressed by current medications[488,491–493]. This is supported by findings in the present study that epitopes which are over-activated by schizophrenia patient serum can be targeted with microglial proinflammatory inhibitors (**Chapter 4**). Rapamycin has been proposed as a potential schizophrenia treatment based on clinical trials in related disorders with high schizophrenia comorbidity (*e.g.* autism and tuberous sclerosis complex)[492] while minocycline[491] and other JAK/STAT inhibitors (*e.g.* withaferin A and pravastatin)[333] are currently being tested for efficacy in schizophrenia clinical trials. Importantly, a recent meta-analysis of minocycline efficacy as an add-on treatment for schizophrenia revealed that minocycline improves negative symptomatology[206] which is notoriously under-addressed by existing treatments[488,494,495]. Furthermore, minocycline selectively inhibits the pro-inflammatory status of microglia[208,209].

Although the modification of microglial functioning could be used as a treatment target, it should be taken into account that microglia have a vital physiological role and attempts at modifying their activity could have deleterious consequences in the long-term. Due to the fact that multiple microglia activation phenotypes are likely to exist simultaneously within the CNS *in vivo*[148,152], effective treatments would serve to rebalance the relative spatial and temporal distributions of microglial phenotypes as opposed to simply ablating their function. Moreover, recent data suggests that many of the pathological changes attributed to microglial dysfunction, such as altered synaptic refinement,

occur early in the course of the illness[496] and likely only in a subset of patients[217,312]. Therefore, it would be vital to identify the optimal time point for early intervention in addition to the biomarkers which best characterize patient sub groups with microglial pathology[496]. This would potentially allow to prevent the secondary loss of synapses due to altered synaptic pruning by microglial cells.

A unique opportunity to validate the roles of STAT3 and 4EBP1 in microglia would be by reprogramming human somatic cells obtained from schizophrenia patients in a clinical setting to microglia-like cells[497]. By validating these microglia-like cells against primary microglia, this approach would provide the opportunity for patient-specific high-throughput modelling of microglia dysfunction.

7.3 Limitations and future work

7.3.1 Clinical samples

One of the limitations of the presented work is that there were sometimes significant differences in the demographics between schizophrenia patient and control groups. Although there were no significant differences between the patient and control groups with regard to gender, age, cannabis and body mass index, there sometimes was a significant difference in smoking behaviour (patient and control samples presented in **Chapters 4 and 6**). Therefore, traces of nicotine in serum could be linked to the observed changes in microglial signalling cascades. Schizophrenia patients are known to consume more nicotine and alcohol, as well as being predisposed to substance abuse[498]. The percentage of smoking patients exceeds 70%, which is a 2- to 4-fold higher rate than in the general population[45,46]. It has been suggested that this high nicotine usage is an attempt of self-medication[47]. Furthermore, in controlled experiments, nicotine has been found to enhance cognitive function in schizophrenia patients[48]. The possibility that the significant difference in smoking behaviour might have confounded the results cannot be excluded. Another important consideration is the unknown nutritional status of the study participants. The possibility that this might have confounded the results cannot be excluded, as nutrition can impact certain serum parameters[499]. However, individuals suffering from conditions which may require dietary intervention, such as metabolic, cardiovascular, gastrointestinal or endocrine diseases, were excluded from the study at the stage of patient recruitment. Additional factors decreasing the likelihood of dietary intervention in the study population include the relatively young age of participants and Body Mass Index within the standard range. Nevertheless, this variable cannot be entirely ruled out, in the absence of patient specific information. Therefore, future validation studies would benefit from preventing such differences in the demographics.

Chapter 5 revealed altered STAT3 signalling in microglia post exposure to serum from antipsychotic treated schizophrenia patients. This finding was further supported by the identification of an association between the *in vivo* and *in vitro* alterations through strong inverse correlations between STAT3 (pS727) and BP_{ND} across all PET brain regions within the control group only. However, TSPO as microglia marker in PET imaging studies comes with many limitations. Some of these limitations are: i) similar expression of TSPO across different microglia activation phenotypes; ii) potential expression of TSPO by other CNS cells than microglia; iii) genetic polymorphisms affecting tracer binding potential; iv) the high binding affinity of the tracer for compounds; and v) high binding affinity of the tracer for certain plasma proteins, such as acute phase protein α1-acid glycoprotein[176,500]. These factors affect the results, and are therefore a potential confounding factor in TSPO PET imaging studies[176,500]. Therefore, it will be important to develop new microglia-specific molecular targets for PET imaging studies. The development of these new tracers needs to take into account tracer selectivity for microglia expression and polarization. The search for a new microglia specific tracer would have to consider the mechanisms by which microglia actively participate in both toxic and neuroprotective functions in brain diseases.

In addition, it would be of interest to repeat the PET imaging study presented in **Chapter 5** using first-onset schizophrenia patients and prodromal patients. This would allow for elucidation of potential microglia driven neuroinflammation involved in early pathological processes at the disease onset of schizophrenia. Furthermore, such a study would provide the opportunity to investigate a larger patient group, as recent PET imaging studies were limited in their sample size, which could have resulted in the reported inconsistencies in PET imaging findings. Similarly, **Chapter 6** was underpowered due to limited sample numbers as well.

7.3.2 Experimental design

Microglia were exposed directly to serum, which is not the most ideal way to simulate the micro-environment of brain resident microglia. In addition, microglia are usually not in direct contact with serum components given that the BBB is intact. However, serum is an easily accessible patient sample, compared to for example CSF, which requires a lumbar puncture. In addition, there is substantial evidence from previous studies that peripheral immune activation can influence microglial activation phenotypes in the CNS[501–503] and modify the course of inflammatory processes in the brain which are thought to be mediated by microglia[460,502,504]. This crosstalk between peripheral and CNS immune activation is attributed to circulatory factors which are secreted by peripheral immune cells and which enter the CNS[503,505]. This process is reviewed by Dantzer *et al*. (2008) and Perry *et al*. (2010)[459,461].

Furthermore, in the context of schizophrenia, previous work has shown an overlap between CNS and blood serum biomarker profiles in schizophrenia in CSF and serum derived from the drug-naïve first onset patients, including consistent alterations in certain protein levels compared to the control group[506,507]. However, future studies will have to validate these findings by exposing microglia to CSF to investigate changes in protein expression between CSF and peripheral serum to fully compare disease-specific changes in protein profiles. Furthermore, microglial exposure to CSF would represent a CNS specific micro-environment.

One of the most common issues surrounding the application of fluorochromes is fluorescent quenching, a phenomenon capable of compromising the interpretation of immunofluorescence carried out on a laser instrument[508,509]. Therefore, many studies optimised their materials and methods in order to prevent quenching as much as possible. For example, it has been shown that by keeping cells at 4°C post fixation, irrespective of cell type, a stable fluorescent signal can be achieved with increasing linearity within the range of concentrations tested[510]. Here, microglia were handled on an integrated compact shaker-heater-cooler system throughout the flow cytometry sample preparation, allowing continuous temperature control. Therefore, once the cells were fixed, they were continuously kept at 2°C. Other factors involved with fluorescent quenching are high concentrations of fluorescent dyes capable of compromising other fluorescent signals[508]. Therefore, the FCB signal was optimized first (**Chapter 3**) to allow for a reliable read-out of both the FCB signal and the other applied fluorochromes. This was achieved by washing the cells five times post FCB staining in ice cold FACS buffer, allowing for the removal of any excess dye. The dataset depends on the final read-out of the multi-parameter platform, consisting of six distinct emission wavelengths (CBD450, CBD500, AF488, PE (wavelength 578), AF647 and DL800). These six fluorochromes have been selected for their brightness and separation across the wavelength spectrum. As explained in **section 2.2.2**, within a flow cytometer, the appropriate ranges of excitation and emission wavelengths are selected by bandpass filters. Yet, spillover (physical overlap among the emission spectra of used fluorochromes) can still occur through for example degradation of the dye. This can be prevented by analysing the samples as soon as possible after staining, minimizing exposure to light and keeping the samples away from elevated temperatures. However, sometimes the fluorescence from more than one fluorochrome may still be detected by overlap of emission spectra. This spectral overlap can be corrected through fluorescence compensation, as the amount of spillover is a linear function. Fluorescence compensation for cell signalling epitopes was conducted using anti-mouse IgGκ antibody capture beads labelled separately with anti-human STAT3 (pY705) AF488, anti-human STAT3 (pY705) PE and anti-human STAT3 (pY705) AF647 alongside single stain controls with maximum and minimum concentrations of each barcoding dye. Finally, multicolour CST beads were used for quality control and

standardization of PMT detector voltages across multiple experimental runs, ensuring stable sample acquisition across replicate measurements and different cohorts. Although much effort went into the prevention of fluorescent spillover (*e.g*. temperature control, keeping samples covered, immediate sample acquisition once sample preparation was finished), fluorescent compensation was always a necessary step before continuing with further data analysis.

These results could have been validated through microscopy. For example, it would allow STAT3 localization within microglia, as STAT3 can be present in the cytoplasm but following phosphorylation can translocate to the nucleus and initiate DNA transcription. A decrease of an epitope could also have been investigated through monitoring ubiquitination[335]. This would aid further functional assessments of the detected alterations in signalling pathways. In addition, microglial responses to an inflammatory profile, such as inflammasome formation and autophagic responses, could have been monitored[511].

Among the limitations of the presented work are the limited amounts of clinical patient material as well as that the analysis of microglial activation inhibitors and antipsychotics were conducted in the absence of patient serum. However, it did allow us to show a mechanistic interaction between known antagonists of inflammatory microglial phenotypic switching [208,307,311] and the target epitopes detected following exposure to schizophrenia patient serum. This served as a means to validate the phenotypic implications of the epitopes detected and highlight the potential to offset disease-associated changes in future experiments. However, the potential of these drugs to ameliorate disease-associated changes remains to be determined in future experiments.

7.3.3 The need for the investigation of microglial pathways

One of the major issues in the microglia research field is the difficulty to differentiate pro- and anti-inflammatory microglial activation states. The different microglial states have been defined in analogy to *in vitro* macrophage activation, as classically activated M1 or alternatively activated M2 phenotypes respectively[144,145]. Yet, there is no definition specifically for these brain resident immune cells. The adoption of the M1 and M2 phenotype terminology represents an attempt to simplify data interpretation at a time when microglia had not yet been characterized. Now, this classification, suggesting established meaningful pathways of M1 and M2 microglial polarization, hinders rather than aids research progress and should be discarded[152]. **Chapter 3** demonstrated the wide signalling diversity within these cells. The platform identified convergent cell signalling responses within each ligand class such as IκBα downregulation induced by proinflammatory ligands (IL- 23, TNF-α and IL-1β) or Stat6 (pY641) phosphorylation evoked by anti-inflammatory ligands (IL-4 and IL-13). Yet, it was also possible to discriminate the activity of ligands which are known to signal through the same receptor

heterodimers (*e.g*. IL-4 and IL-13) by the detection of different responses at secondary epitopes such as Akt (pS473). Furthermore, we identified high microglial sensitivity towards a complex mixture like serum, leading to the identification of highly specific changes in intracellular signalling pathways (**Chapter 4-6**).

Although earlier (section **7.1.3**) it is suggested that the decreased TREM2 receptor interaction with apolipoproteins could have affected STAT3 signalling via the mTOR signalling pathway, there could have been other pathways involved as well. Even though altered apolipoprotein levels in schizophrenia patient serum have been consistently reported, microglia might process these signals via multiple pathways. Little is known about how microglia pathways are processing these signals. This is also true with regard to microglial STAT3 signalling. For example, although the microglial cell-specific $Stat3^{-/-}$ knockout mouse model is indicative of antidepressive-like behaviour, this is the first and for now only publication regarding microglial STAT3 effects. Therefore, more studies are necessary to validate the current findings and to further characterize the biological effects of these pathways in microglia.

Among the constraints of the presented work, it should be taken into account that microglia were exposed to serum containing a disease specific profile. However, the disease associated changes in serum, discovered by the current methodology, do not reveal any of the underlying mechanisms causing these changes. For example, it does not explain the underlying mechanism of the detected relative changes in serum proteins, such as the apolipoproteins. In addition, future studies would have to determine whether a specific marker contributes to a psychiatric disorder definition, classifies a disease subgroup, is linked to a shared symptom of multiple disorders, or can only be interpreted in the context of additional environmental or psychometric findings. Similarly, the ultimate causality between the observed clinical features relating to microglia in schizophrenia and the onset of psychotic symptoms remains to be proven. It is not known whether altered microglial functioning is pathophysiologically involved in the development of schizophrenia or is a side-effect of other ongoing changes. Nonetheless, preclinical studies have indicated the benefit of using an add-on anti-inflammatory treatment capable of inhibiting the pro-inflammatory microglial status, such as minocycline, to improve the negative symptoms in patients[206–209]. In addition, we provided evidence in **Chapter 4** that microglia could have utility for drug screening purposes. Furthermore, the identified schizophrenia-associated microglia signalling profile could be investigated as a new drug target for the identification of potential new treatments for schizophrenia.

Acknowledgements & Collaborations

I am deeply grateful to my supervisor Prof. Sabine Bahn, director of the Cambridge Centre for Neuropsychiatric Research, Department of Chemical Engineering and Biotechnology, University of Cambridge, for giving me the opportunity to conduct my PhD in her laboratory and for her support, motivation and immense knowledge throughout the years. I have been able to work in an extraordinary research environment with the fundamental access to clinical samples, which have been essential for this study. It has been an amazing experience.

A very special gratitude goes out to Dr. Santiago Lago for his support, expertise and advice. Having been taught into the art of flow cytometry within a relatively short period, allowed me to work quickly on such a complex cytomics platform. His expertise truly helped me getting propelled into the field of flow cytometry. I consider it a privilege to have been able to share in his knowledge. In addition, figures and written sections of the results and discussion in Chapter 3 and 4 and written sections throughout are based on the paper accepted at *Brain, Behavior and Immunity,* which was the result of collaborative work with Dr. Santiago Lago, who drafted the paper.

Statistical analysis has been extensively supported by David Cox, for which I am extremely grateful. This project would not have been possible without the contributions and statistical wisdom of Dr. Jakub Tomasik, Dr. Jason Cooper and Dr. Jordan Ramsey. I am thankful for the mass spectrometry expertise and support of Dr. Sureyya Ozcan. Moreover, I would like to thank all members of the Bahn lab, past and present, with whom I have had the privilege of their company, for their support, friendship and the many unforgettable moments throughout my years in Cambridge.

I wish to thank Nitin Rustogi for the many hours spending time with me doing sample plating, sample preparation and especially for his friendship.

I would like to thank our external collaborators for providing clinical samples, I am very grateful to all patients and controls who participated in these studies. I would like to thank Dr. Lot de Witte and Dr. Thalia van der Doef for sharing their PET imaging data with us. I am thankful to the funding bodies which have supported this work, including the Engineering and Physical Sciences Research Council, the Virgo consortium and the Stanley Medical Research Institute.

I would like to give my heartfelt thanks to my family and friends, for their understanding, believe in me, continuous love and never-ending support in all respects.

And finally, to my ever so proud late-grandmother who was always keen to know what I was doing and how I was proceeding (even though it is very likely she did not grasp any of it!), I will miss your excitement whenever a significant momentous moment was reached and also just your general positivity in life.

Thanks for all your encouragement!

References

1. Fusar-Poli, P. & Politi, P. Paul Eugen Bleuler and the birth of schizophrenia (1908). *Am. J. Psychiatry* **165,** 1407 (2008).

2. American Psychiatric Association. *Diagnostic and Statistical Manual of Mental Disorders, DSM-5*. (American Psychiatric Association, 2013).

3. Lewis, D. & Lieberman, J. Catching up on schizophrenia: natural history and neurobiology. *Neuron* **28,** 325–34 (2000).

4. Reed, G. M., Mendonça Correia, J., Esparza, P., Saxena, S. & Maj, M. The WPA-WHO Global Survey of Psychiatrists' Attitudes Towards Mental Disorders Classification. *World Psychiatry* **10,** 118–31 (2011).

5. Abel, K. M., Drake, R. & Goldstein, J. M. Sex differences in schizophrenia. *Int. Rev. Psychiatry* **22,** 417–428 (2010).

6. Angermeyerl, M. C. & Kiihn, L. Sciences Gender Differences in Age at Onset of Schizophrenia. *Eur. Arch. Psychiatry Neurol. Sci.* **237,** 351–364 (1988).

7. Stone, J. M. *et al.* Cannabis use and first-episode psychosis: relationship with manic and psychotic symptoms, and with age at presentation. *Psychol. Med.* **44,** 499–506 (2014).

8. Large, M. *et al.* Cannabis Use and Earlier Onset of Psychosis. *Arch. Gen. Psychiatry* **68,** 555–561 (2011).

9. Kuepper, R. *et al.* Continued cannabis use and risk of incidence and persistence of psychotic symptoms: 10 year follow-up cohort study. *BMJ* **342,** 1–8 (2011).

10. Faber, G., Smid, H. G. O. M., Van Gool, A. R., Wiersma, D. & Van Den Bosch, R. J. The effects of guided discontinuation of antipsychotics on neurocognition in first onset psychosis. *Eur. Psychiatry* **27,** 275–280 (2012).

11. Hor, K. & Taylor, M. Review: Suicide and schizophrenia: a systematic review of rates and risk factors. *J. Psychopharmacol.* **24,** 81–90 (2010).

12. Taiminen, T. *et al.* The Schizophrenia Suicide Risk Scale (SSRS): development and initial validation. *Schizophr. Res.* **47,** 199–213 (2001).

13. Kreyenbuhl, J. A., Kelly, D. L. & Conley, R. R. Circumstances of suicide among individuals with schizophrenia. *Schizophr. Res.* **58,** 253–261 (2002).

14. Insel, T. *et al.* Research Domain Criteria (RDoC): Toward a New Classification Framework for Research on Mental Disorders. *Am. J. Psychiatry* **167,** 748–751 (2010).

15. Mirsky, A. F. *et al.* A 39-Year Followup of the Genain Quadruplets. *Schizophr. Bull.* **26,** 699–708 (2000).

16. Kahn, R. S. *et al.* Schizophrenia. *Nat. Rev. Dis. Prim.* **1,** 1–23 (2015).

17. Lee, S. H. *et al.* Genetic relationship between five psychiatric disorders estimated from genome-wide SNPs. *Nat. Genet.* **45,** 984–994 (2013).

18. Cardno, A. G. *et al.* Heritability Estimates for Psychotic Disorders; The Maudsly Twin Psychosis Series. *Arch. Gen. Psychiatry* **56,** 162–168 (1999).

19. Heston, L. L. Psychiatric Disorders in Foster Home Reared Children of Schizophrenic Mothers. *Br. J. Psychiatry* **112,** 819–825 (1966).

20. Ross, C. a, Margolis, R. L., Reading, S. a J., Pletnikov, M. & Coyle, J. T. Neurobiology of schizophrenia. *Neuron* **52,** 139–53 (2006).

21. Ripke, S. *et al.* Genome-wide association analysis identifies 13 new risk loci for schizophrenia. *Nat. Genet.* **45,** 1150–9 (2013).

22. The Schizophrenia Psychiatric Genome-Wide Association Study (GWAS) Consortium. Genome-wide association study identifies five new schizophrenia loci. *Nat. Genet.* **43,** 969–976 (2011).

23. Stefansson, H. *et al.* Common variants conferring risk of schizophrenia. *Nature* **460,** 744–7 (2009).

24. Purcell, S. M. *et al.* A polygenic burden of rare disruptive mutations in schizophrenia. *Nature* **506,** 185–190 (2014).

25. Purcell, S. M. *et al.* Common polygenic variation contributes to risk of schizophrenia and bipolar disorder. *Nature* **460,** 748–52 (2009).

26. Corvin, A. & Morris, D. W. Genome-wide association studies: findings at the major histocompatibility complex locus in psychosis. *Biol. Psychiatry* **75,** 276–83 (2014).

27. Schizophrenia Working Group of the Psychiatric Genomics Consortium. Biological insights from 108 schizophrenia-associated genetic loci. *Nature* **511,** 421–427 (2014).

28. Bassett, A. S., Scherer, S. W. & Brzustowicz, L. M. Copy Number Variations in Schizophrenia: Critical Review and New Perspectives on Concepts of Genetics and Disease. *Am. J. Psychiatry* **167,** 899–914 (2010).

29. St Clair, D. Copy Number Variation and Schizophrenia. *Schizophr. Bull.* **35,** 9–12 (2009).

30. Roth, T. L., Lubin, F. D., Sodhi, M. & Kleinman, J. E. Epigenetic mechanisms in schizophrenia. *Biochim. Biophys. Acta - Gen. Subj.* **1790,** 869–877 (2009).

31. Knable, M. B., Torrey, E. F., Webster, M. J. & Bartko, J. J. Multivariate analysis of prefrontal cortical data from the Stanley Foundation Neuropathology Consortium. *Brain Res. Bull.* **55,** 651–9 (2001).

32. Knable, M. B., Barci, B. M., Webster, M. J., Meador-Woodruff, J. & Torrey, E. F. Molecular abnormalities of the hippocampus in severe psychiatric illness: postmortem findings from the Stanley Neuropathology Consortium. *Mol. Psychiatry* **9,** 609–20, 544 (2004).

33. Knable, M. B., Barci, B. M., Bartko, J. J., Webster, M. J. & Torrey, E. F. Molecular abnormalities in the major psychiatric illnesses : Classification and Regression Tree (CRT) analysis of post-mortem prefrontal markers. *Mol. Psychiatry* **7,** 392–404 (2002).

34. Garey, L. When cortical development goes wrong: schizophrenia as a neurodevelopmental disease of microcircuits. *J. Anat.* **217,** 324–333 (2010).

35. Meltzer, H. Y., Li, Z., Kaneda, Y. & Ichikawa, J. Serotonin receptors: their key role in drugs to treat schizophrenia. *Prog. Neuropsychopharmacol. Biol. Psychiatry* **27,** 1159–72 (2003).

36. Moghaddam, B. & Javitt, D. From revolution to evolution: the glutamate hypothesis of schizophrenia and its implication for treatment. *Neuropsychopharmacol. Rev.* **37,** 4–15 (2012).

37. Howes, O. D. & Kapur, S. The dopamine hypothesis of schizophrenia: version III--the final common pathway. *Schizophr. Bull.* **35,** 549–62 (2009).

38. da Silva Alves, F., Figee, M., van Amelsvoort, T., Veltman, D. & de Haan, L. The revised dopamine hypothesis of schizophrenia: evidence from pharmacological MRI studies with atypical antipsychotic medication. *Psychopharmacol. Bull.* **41,** 121–32 (2008).

39. Meador-Woodruff, J. H. & Healy, D. J. Glutamate receptor expression in schizophrenic brain. *Brain Res. Brain Res. Rev.* **31,** 288–94 (2000).

40. Tsai, G. & Coyle, J. T. Glutamatergic mechanisms in schizophrenia. *Annu. Rev. Pharmacol. Toxicol.* **42,** 165–179 (2002).

41. Stan, A. & Lewis, D. A. Altered Cortical GABA Neurotransmission in Schizophrenia: Insights into Novel Therapeutic Strategies. *Curr Pharm Biotechnol* **13,** 1557–1562 (2012).

42. Nakazawa, K. *et al.* GABAergic interneuron origin of schizophrenia

pathophysiology. *Neuropharmacology* **62,** 1574–1583 (2012).

43. Eggers, A. E. A serotonin hypothesis of schizophrenia. *Med. Hypotheses* **80,** 791–794 (2013).

44. Aghajanian, G. K. & Marek, G. J. Serotonin model of schizophrenia: emerging role of glutamate mechanisms. *Brain Res. Rev.* **31,** 302–312 (2000).

45. Lisman, J. E. *et al.* Circuit-based framework for understanding neurotransmitter and risk gene interactions in schizophrenia. *Trends Neurosci.* **31,** 234–42 (2008).

46. de Leon, J. Smoking and vulnerability for schizophrenia. *Schizophr. Bull.* **22,** 405–9 (1996).

47. Kumari, V. & Postma, P. Nicotine use in schizophrenia: The self medication hypotheses. *Neurosci. Biobehav. Rev.* **29,** 1021–1034 (2005).

48. Barr, R. S. *et al.* The Effects of Transdermal Nicotine on Cognition in Nonsmokers with Schizophrenia and Nonpsychiatric Controls. *Neuropsychopharmacology* **33,** 480–490 (2008).

49. O'Callaghan, E., Sham, P., Takei, N., Murray, R. . & Glover, G. Schizophrenia after prenatal exposure to 1957 A2 influenza epidemic. *Lancet* **337,** 1248–1250 (1991).

50. Sham, P. C. *et al.* Schizophrenia following pre-natal exposure to influenza epidemics between 1939 and 1960. *Br. J. Psychiatry* **160,** 461–466 (1992).

51. Susser, E. S. Schizophrenia After Prenatal Exposure to the Dutch Hunger Winter of 1944-1945. *Arch. Gen. Psychiatry* **49,** 983 (1992).

52. St Clair, D. *et al.* Rates of adult schizophrenia following prenatal exposure to the Chinese famine of 1959-1961. *JAMA* **294,** 557–62 (2005).

53. Selemon, L. D. & Zecevic, N. Schizophrenia: a tale of two critical periods for prefrontal cortical development. *Transl. Psychiatry* **5,** 1–11 (2015).

54. Insel, T. R. Rethinking schizophrenia. *Nature* **468,** 187–93 (2010).

55. Pérez-Iglesias, R. *et al.* White matter defects in first episode psychosis patients: a voxelwise analysis of diffusion tensor imaging. *Neuroimage* **49,** 199–204 (2010).

56. Steen, R. G., Mull, C., McClure, R., Hamer, R. M. & Lieberman, J. A. Brain volume in first-episode schizophrenia: Systematic review and meta-analysis of magnetic resonance imaging studies. *Br. J. Psychiatry* **188,** 510–518 (2006).

57. Witthaus, H. *et al.* Gray matter abnormalities in subjects at ultra-high risk for schizophrenia and first-episode schizophrenic patients compared to healthy controls. *Psychiatry Res.* **173,** 163–9 (2009).

58. Castle, D., Sham, P. & Murray, R. Differences in distribution of ages of onset in males and females with schizophrenia. *Schizophr. Res.* **33,** 179–83 (1998).

59. Faraone, S. V., Chen, W. J., Goldstein, J. M. & Tsuang, M. T. Gender differences in age at onset of schizophrenia. *Br. J. Psychiatry* **164,** 625–629 (1994).

60. Bayer, T. A., Falkai, P. & Maier, W. Genetic and non-genetic vulnerability factors in schizophrenia: The basis of the 'two hit hypothesis.' *J. Psychiatr. Res.* **33,** 543–548 (1999).

61. Daskalakis, N. P., Bagot, R. C., Parker, K. J., Vinkers, C. H. & de Kloet, E. R. The three-hit concept of vulnerability and resilience: toward understanding adaptation to early-life adversity outcome. *Psychoneuroendocrinology* **38,** 1858–73 (2013).

62. Ellman, L. M. *et al.* Structural brain alterations in schizophrenia following fetal exposure to the inflammatory cytokine interleukin-8. *Schizophr. Res.* **121,** 46–54 (2010).

63. Brown, A. S. *et al.* Elevated maternal interleukin-8 levels and risk of schizophrenia in adult offspring. *Am. J. Psychiatry* **161,** 889–95 (2004).

64. Buka, S. L. *et al.* Maternal cytokine levels during pregnancy and adult

psychosis. *Brain. Behav. Immun.* **15,** 411–20 (2001).

65. Clarke, M. C., Harley, M. & Cannon, M. The role of obstetric events in schizophrenia. *Schizophr. Bull.* **32,** 3–8 (2006).

66. Gardner, R. M., Dalman, C., Wicks, S., Lee, B. K. & Karlsson, H. Neonatal levels of acute phase proteins and later risk of non-affective psychosis. *Transl. Psychiatry* **3,** 1–7 (2013).

67. Patten, S. B., Svenson, L. W. & Metz, L. M. Psychotic disorders in MS: population-based evidence of an association. *Neurology* **65,** 1123–5 (2005).

68. Jones, A. L., Mowry, B. J., Pender, M. P. & Greer, J. M. Immune dysregulation and self-reactivity in schizophrenia: do some cases of schizophrenia have an autoimmune basis? *Immunol. Cell Biol.* **83,** 9–17 (2005).

69. Ludvigsson, J. F., Osby, U., Ekbom, A. & Montgomery, S. M. Coeliac disease and risk of schizophrenia and other psychosis: a general population cohort study. *Scand. J. Gastroenterol.* **42,** 179–85 (2007).

70. Hayes, L. N. *et al.* Inflammatory molecular signature associated with infectious agents in psychosis. *Schizophr. Bull.* **40,** 963–72 (2014).

71. Kim, Y. K. *et al.* Th1, Th2 and Th3 cytokine alteration in schizophrenia. *Prog. Neuro-Psychopharmacology Biol. Psychiatry* **28,** 1129–1134 (2004).

72. Watanabe, Y., Someya, T. & Nawa, H. Cytokine hypothesis of schizophrenia pathogenesis: Evidence from human studies and animal models. *Psychiatry Clin. Neurosci.* **64,** 217–230 (2010).

73. Hanson, D. R. & Gottesman, I. I. Theories of schizophrenia: a genetic-inflammatory-vascular synthesis. *BMC Med. Genet.* **6,** 7 (2005).

74. Meyer, U., Feldon, J. & Yee, B. K. A review of the fetal brain cytokine imbalance hypothesis of schizophrenia. *Schizophr. Bull.* **35,** 959–972 (2009).

75. Bechter, K. [Schizophrenia--a mild encephalitis?]. *Fortschr. Neurol. Psychiatr.* **81,** 250–9 (2013).

76. Andreassen, O. A. *et al.* Genetic pleiotropy between multiple sclerosis and schizophrenia but not bipolar disorder: differential involvement of immune-related gene loci. *Mol. Psychiatry* **20,** 207–214 (2015).

77. Steiner, J. *et al.* Increased Prevalence of Diverse N -Methyl-D-Aspartate Glutamate Receptor Antibodies in Patients With an Initial Diagnosis of Schizophrenia. *JAMA Psychiatry* **70,** 271 (2013).

78. S. Kayser, M. & Dalmau, J. Anti-NMDA Receptor Encephalitis in Psychiatry. *Curr. Psychiatry Rev.* **7,** 189–193 (2011).

79. Nielsen, P. R. *et al.* Autoimmune Diseases and Severe Infections as Risk Factors for Schizophenia: A 30-Year Population-Based Register Study. *Am. J. Psychiatry* **168,** 1303–1310 (2011).

80. Yolken, R. H., Dickerson, F. B. & Fuller Torrey, E. Toxoplasma and schizophrenia. *Parasite Immunol.* **31,** 706–15 (2009).

81. Torrey, E. F., Bartko, J. J., Lun, Z.-R. & Yolken, R. H. Antibodies to Toxoplasma gondii in Patients With Schizophrenia: A Meta-Analysis. *Schizophr. Bull.* **33,** 729–736 (2007).

82. Jones-Brando, L., Torrey, E. F. & Yolken, R. Drugs used in the treatment of schizophrenia and bipolar disorder inhibit the replication of Toxoplasma gondii. *Schizophr. Res.* **62,** 237–244 (2003).

83. Landreau, F. *et al.* Effects of two commonly found strains of influenza A virus on developing dopaminergic neurons, in relation to the pathophysiology of schizophrenia. *PLoS One* **7,** e51068 (2012).

84. Khandaker, G. M., Zimbron, J., Dalman, C., Lewis, G. & Jones, P. B. Childhood infection and adult schizophrenia: a meta-analysis of population-based studies. *Schizophr. Res.* **139,** 161–8 (2012).

85. Dickerson, F. *et al.* Antibodies to retroviruses in recent onset psychosis and multi-episode schizophrenia. *Schizophr. Res.* **138,** 198–205 (2012).

86. Severance, E. G. *et al.* Coronavirus Immunoreactivity in Individuals With a Recent Onset of Psychotic Symptoms. *Schizophr. Bull.* **37,** 101–107 (2011).

87. Yao, Y. *et al.* Elevated levels of human endogenous retrovirus-W transcripts in blood cells from patients with first episode schizophrenia. *Genes. Brain. Behav.* **7,** 103–12 (2008).

88. Hobbs, J. A. Detection of adeno-associated virus 2 and parvovirus B19 in the human dorsolateral prefrontal cortex. *J. Neurovirol.* **12,** 190–9 (2006).

89. Karlsson, H. *et al.* Retroviral RNA identified in the cerebrospinal fluids and brains of individuals with schizophrenia. *Proc. Natl. Acad. Sci. U. S. A.* **98,** 4634–9 (2001).

90. Siegel, B. I., Sengupta, E. J., Edelson, J. R., Lewis, D. a. & Volk, D. W. Elevated Viral Restriction Factor Levels in Cortical Blood Vessels in Schizophrenia. *Biol. Psychiatry* **76,** 160–167 (2014).

91. Herberth, M. *et al.* Differential effects on T-cell function following exposure to serum from schizophrenia smokers. *Mol. Psychiatry* **15,** 364–71 (2010).

92. Miller, B. J., Gassama, B., Sebastian, D., Buckley, P. & Mellor, A. Meta-Analysis of Lymphocytes in Schizophrenia: Clinical Status and Antipsychotic Effects. *Biol. Psychiatry* **73,** 993–999 (2013).

93. Drexhage, R. C. *et al.* Inflammatory gene expression in monocytes of patients with schizophrenia: overlap and difference with bipolar disorder. A study in naturalistically treated patients. *Int. J. Neuropsychopharmacol.* **13,** 1369–81 (2010).

94. Gardiner, E. J. *et al.* Gene expression analysis reveals schizophrenia-associated dysregulation of immune pathways in peripheral blood mononuclear cells. *J. Psychiatr. Res.* **47,** 425–37 (2013).

95. Drexhage, R. C. *et al.* An activated set point of T-cell and monocyte inflammatory networks in recent-onset schizophrenia patients involves both pro- and anti-inflammatory forces. *Int. J. Neuropsychopharmacol.* **14,** 746–55 (2011).

96. Steiner, J. *et al.* Acute schizophrenia is accompanied by reduced T cell and increased B cell immunity. *Eur. Arch. Psychiatry Clin. Neurosci.* **260,** 509–18 (2010).

97. Maino, K. *et al.* T- and B-lymphocytes in patients with schizophrenia in acute psychotic episode and the course of the treatment. *Psychiatry Res.* **152,** 173–80 (2007).

98. Müller, N., Riedel, M., Ackenheil, M. & Schwarz, M. J. Cellular and Humoral Immune System in Schizophrenia: A Conceptual Re-Evaluation. *world J. Biol. psychiatry* **1,** 173–179 (2000).

99. Ezeoke, A., Mellor, A., Buckley, P. & Miller, B. A systematic, quantitative review of blood autoantibodies in schizophrenia. *Schizophr. Res.* **150,** 245–251 (2013).

100. Potvin, S. *et al.* Inflammatory cytokine alterations in schizophrenia: a systematic quantitative review. *Biol. Psychiatry* **63,** 801–8 (2008).

101. Miller, B. J., Buckley, P., Seabolt, W., Mellor, A. & Kirkpatrick, B. Meta-analysis of cytokine alterations in schizophrenia: clinical status and antipsychotic effects. *Biol. Psychiatry* **70,** 663–71 (2011).

102. de Witte, L. *et al.* Cytokine alterations in first-episode schizophrenia patients before and after antipsychotic treatment. *Schizophr. Res.* **154,** 23–9 (2014).

103. Herberth, M. *et al.* Identification of a molecular profile associated with immune status in first-onset schizophrenia patients. *Clin. Schizophr. Relat. Psychoses* **7,** 207–15 (2014).

104. Herberth, M. *et al.* Identification of a molecular profile associated with immune status in first onset

schizophrenia patients. *Clin. Schizophr. Relat. Psychoses* **7,** 207–215 (2013).

105. Schwarz, E. *et al.* Identification of Subgroups of Schizophrenia Patients With Changes in Either Immune or Growth Factor and Hormonal Pathways. *Schizophr. Bull.* **40,** 787–795 (2013).

106. Chan, M. K. *et al.* Development of a blood-based molecular biomarker test for identification of schizophrenia before disease onset. *Transl. Psychiatry* **5,** 1–10 (2015).

107. Schwieler, L. *et al.* Increased levels of IL-6 in the cerebrospinal fluid of patients with chronic schizophrenia - significance for activation of the kynurenine pathway. *J. Psychiatry Neurosci.* **39,** 140126 (2014).

108. Bechter, K. *et al.* Cerebrospinal fluid analysis in affective and schizophrenic spectrum disorders: identification of subgroups with immune responses and blood-CSF barrier dysfunction. *J. Psychiatr. Res.* **44,** 321–30 (2010).

109. Felger, J. C. & Lotrich, F. E. Inflammatory cytokines in depression: neurobiological mechanisms and therapeutic implications. *Neuroscience* **246,** 199–229 (2013).

110. Patel, J. P., Frey, B. N., Patel, J. P. & Frey, B. N. Disruption in the Blood-Brain Barrier: The Missing Link between Brain and Body Inflammation in Bipolar Disorder? *Neural Plast.* **2015,** 1–12 (2015).

111. Lass, P. *et al.* Cerebral blood flow in Sjögren's syndrome using 99Tcm-HMPAO brain SPET. *Nucl. Med. Commun.* **21,** 31–5 (2000).

112. Volpato, A. M., Zugno, A. I. & Quevedo, J. Recent evidence and potential mechanisms underlying weight gain and insulin resistance due to atypical antipsychotics. *Rev. Bras. Psiquiatr.* **35,** 295–304 (2013).

113. Fernø, J. *et al.* Olanzapine-induced hyperphagia and weight gain associate with orexigenic hypothalamic neuropeptide signaling without concomitant AMPK phosphorylation. *PLoS One* **6,** e20571 (2011).

114. Tschoner, A. *et al.* Metabolic side effects of antipsychotic medication. *Int. J. Clin. Pract.* **61,** 1356–70 (2007).

115. Schwarz, E., Steiner, J., Guest, P. C., Bogerts, B. & Bahn, S. Investigation of molecular serum profiles associated with predisposition to antipsychotic-induced weight gain. *world J. Biol. psychiatry* **16,** 22–30 (2015).

116. Shelton, R. C. & Miller, A. H. Eating ourselves to death (and despair): the contribution of adiposity and inflammation to depression. *Prog. Neurobiol.* **91,** 275–299 (2010).

117. Nathan, C. Epidemic Inflammation: Pondering Obesity. *Mol. Med.* **14,** 485–492 (2008).

118. Krishnamurthy, D. *et al.* Metabolic, hormonal and stress-related molecular changes in post-mortem pituitary glands from schizophrenia subjects. *World J. Biol. Psychiatry* **14,** 478–89 (2013).

119. Guest, P. C. *et al.* in *International Review of Neurobiology* **101,** 95–144 (2011).

120. Sommer, I. E. *et al.* Efficacy of Anti-inflammatory Agents to Improve Symptoms in Patients With Schizophrenia: An Update. *Schizophr. Bull.* **40,** 181–91 (2014).

121. Tourjman, V. *et al.* Antipsychotics' effects on blood levels of cytokines in schizophrenia: A meta-analysis. *Schizophr. Res.* **151,** 43–7 (2013).

122. Khandaker, G. M. & Dantzer, R. Is there a role for immune-to-brain communication in schizophrenia? *Psychopharmacology (Berl).* **233,** 1559–73 (2015).

123. Haroon, E., Raison, C. L. & Miller, A. H. Psychoneuroimmunology meets neuropsychopharmacology: translational implications of the impact of inflammation on behavior. *Neuropsychopharmacology* **37,** 137–62 (2012).

124. Harrison, N. A. *et al.* Inflammation Causes Mood Changes Through Alterations

in Subgenual Cingulate Activity and Mesolimbic Connectivity. *Biol. Psychiatry* **66,** 407–414 (2009).

125. Najjar, S., Pearlman, D. M., Alper, K., Najjar, A. & Devinsky, O. Neuroinflammation and psychiatric illness. *J. Neuroinflammation* **10,** 43 (2013).

126. Xanthos, D. N. & Sandkühler, J. Neurogenic neuroinflammation: inflammatory CNS reactions in response to neuronal activity. *Nat. Rev. Neurosci.* **15,** 43–53 (2013).

127. Medzhitov, R. Origin and physiological roles of inflammation. *Nature* **454,** 428–35 (2008).

128. Maier, S. F., Goehler, L. E., Fleshner, M. & Watkins, L. R. The role of the vagus nerve in cytokine-to-brain communication. *Ann. N. Y. Acad. Sci.* **840,** 289–300 (1998).

129. Ransohoff, R. M. & Cardona, A. E. The myeloid cells of the central nervous system parenchyma. *Nature* **468,** 253–62 (2010).

130. Kettenmann, H., Hanisch, U., Noda, M. & Verkhratsky, A. Physiology of Microglia. *Physiol. Rev.* **91,** 461–553 (2011).

131. Skaper, S. D., Giusti, P. & Facci, L. Microglia and mast cells: two tracks on the road to neuroinflammation. *FASEB J.* **26,** 3103–17 (2012).

132. Schwartz, E. S., Lee, I., Chung, K. & Chung, J. M. Oxidative stress in the spinal cord is an important contributor in capsaicin-induced mechanical secondary hyperalgesia in mice. *Pain* **138,** 514–24 (2008).

133. Salvemini, D., Little, J. W., Doyle, T. & Neumann, W. L. Roles of reactive oxygen and nitrogen species in pain. *Free Radic. Biol. Med.* **51,** 951–66 (2011).

134. London, A., Cohen, M. & Schwartz, M. Microglia and monocyte-derived macrophages: functionally distinct populations that act in concert in CNS plasticity and repair. *Front. Cell. Neurosci.* **7,** 1–10 (2013).

135. Bal-Price, a & Brown, G. C. Inflammatory neurodegeneration mediated by nitric oxide from activated glia-inhibiting neuronal respiration, causing glutamate release and excitotoxicity. *J. Neurosci.* **21,** 6480–91 (2001).

136. Monji, A. *et al.* Neuroinflammation in schizophrenia especially focused on the role of microglia. *Prog. Neuropsychopharmacol. Biol. Psychiatry* **42,** 115–21 (2011).

137. Muller, N. & Schwarz, M. Schizophrenia as an inflammation-mediated dysbalance of glutamatergic neurotransmission. *Neurotox. Res.* **10,** 131–48 (2006).

138. Drexhage, R. C. *et al.* Immune and neuroimmune alterations in mood disorders and schizophrenia. *Int. Rev. Neurobiol.* **101,** 169–201 (2011).

139. Schwarz, E. *et al.* Identification of a blood-based biological signature in subjects with psychiatric disorders prior to clinical manifestation. *World J. Biol. Psychiatry* **13,** 627–32 (2012).

140. Pinto, R. a, Arredondo, S. M., Bono, M. R., Gaggero, A. a & Díaz, P. V. T helper 1/T helper 2 cytokine imbalance in respiratory syncytial virus infection is associated with increased endogenous plasma cortisol. *Pediatrics* **117,** e878-86 (2006).

141. Müller, N. *et al.* COX-2 inhibition as a treatment approach in schizophrenia: immunological considerations and clinical effects of celecoxib add-on therapy. *Eur. Arch. Psychiatry Clin. Neurosci.* **254,** 14–22 (2004).

142. Leavy, O. Macrophages: Microglial cell origins. *Nat. Rev. Immunol.* **10,** 808–809 (2010).

143. Hagberg, H., Gressens, P. & Mallard, C. Inflammation during fetal and neonatal life: implications for neurologic and neuropsychiatric disease in children and adults. *Ann. Neurol.* **71,** 444–57 (2012).

144. Hu, X. *et al.* Microglial and macrophage polarization—new prospects for brain repair. *Nat. Rev. Neurol.* **11,** 56–64 (2015).

145. Cherry, J. J. D., Olschowka, J. J. A. & O'Banion, M. Neuroinflammation and M2 microglia: the good, the bad, and the inflamed. *J. Neuroinflammation* **11,** 1–15

(2014).

146. Nakagawa, Y. & Chiba, K. Role of microglial m1/m2 polarization in relapse and remission of psychiatric disorders and diseases. *Pharmaceuticals* **7,** 1028–48 (2014).

147. David, S. & Kroner, A. Repertoire of microglial and macrophage responses after spinal cord injury. *Nat. Rev. Neurosci.* **12,** 388–399 (2011).

148. Ransohoff, R. M. & Perry, V. H. Microglial physiology: unique stimuli, specialized responses. *Annu. Rev. Immunol.* **27,** 119–145 (2009).

149. Mosser, D. M. & Edwards, J. P. Exploring the full spectrum of macrophage activation. *Nat. Rev. Immunol.* **8,** 958–969 (2008).

150. Bisht, K. *et al.* Dark microglia: A new phenotype predominantly associated with pathological states. *Glia* **64,** 826–839 (2016).

151. Chhor, V. *et al.* Characterization of phenotype markers and neuronotoxic potential of polarised primary microglia in vitro. *Brain Behav. Immun.* **32,** 70–85 (2013).

152. Ransohoff, R. M. A polarizing question: do M1 and M2 microglia exist? *Nat. Neurosci.* **19,** 987–991 (2016).

153. Trépanier, M. O., Hopperton, K. E., Mizrahi, R., Mechawar, N. & Bazinet, R. P. Postmortem evidence of cerebral inflammation in schizophrenia: a systematic review. *Mol. Psychiatry* **21,** 1009–1026 (2016).

154. Mistry, M., Gillis, J. & Pavlidis, P. Meta-analysis of gene coexpression networks in the post-mortem prefrontal cortex of patients with schizophrenia and unaffected controls. *BMC Neurosci.* **14,** 105 (2013).

155. McCullumsmith, R. E., Hammond, J. H., Shan, D. & Meador-Woodruff, J. H. Postmortem brain: an underutilized substrate for studying severe mental illness. *Neuropsychopharmacology* **39,** 65–87 (2014).

156. Bloomfield, P. S. *et al.* Microglial Activity in People at Ultra High Risk of Psychosis and in Schizophrenia: An [11 C]PBR28 PET Brain Imaging Study. *Am. J. Psychiatry* **173,** 44–52 (2015).

157. Collste, K. *et al.* Lower levels of the glial cell marker TSPO in drug-naive first-episode psychosis patients as measured using PET and [11C]PBR28. *Mol. Psychiatry* **22,** 850–856 (2017).

158. Di Biase, M. A. *et al.* PET imaging of putative microglial activation in individuals at ultra-high risk for psychosis, recently diagnosed and chronically ill with schizophrenia. *Transl. Psychiatry* **7,** 1–8 (2017).

159. Bilbo, S. D. & Schwarz, J. M. Early-life programming of later-life brain and behavior: a critical role for the immune system. *Front. Behav. Neurosci.* **3,** 1–14 (2009).

160. Monji, A., Kato, T. & Kanba, S. Cytokines and schizophrenia: Microglia hypothesis of schizophrenia. *Psychiatry Clin. Neurosci.* **63,** 257–265 (2009).

161. Sekar, A. *et al.* Schizophrenia risk from complex variation of complement component 4. *Nature* **530,** 177–183 (2016).

162. Mayilyan, K. R., Weinberger, D. R. & Sim, R. B. The complement system in schizophrenia. *Drug News Perspect.* **21,** 200–210 (2008).

163. Mayilyan, K. R., Arnold, J. N., Presanis, J. S., Soghoyan, A. F. & Sim, R. B. Increased complement classical and mannan-binding lectin pathway activities in schizophrenia. *Neurosci. Lett.* **404,** 336–341 (2006).

164. Stephan, A. H., Barres, B. a. & Stevens, B. The Complement System: An Unexpected Role in Synaptic Pruning During Development and Disease. *Annu. Rev. Neurosci.* **35,** 369–389 (2012).

165. Ibi, D., Nagai, T., Nabeshima, T. & Yamada, K. PolyI:C-induced neurodevelopmental animal model for schizophrenia. *Nihon Shinkei Seishin Yakurigaku Zasshi* **31,** 201–7 (2011).

166. Juckel, G. *et al.* Microglial activation in a neuroinflammational animal model of schizophrenia--a pilot study. *Schizophr. Res.* **131,** 96–100 (2011).

167. Manitz, M. P. *et al.* Flow cytometric

characterization of microglia in the offspring of PolyI:C treated mice. *Brain Res.* **1636,** 172–82 (2016).

168. Severance, E. G. *et al.* IgG dynamics of dietary antigens point to cerebrospinal fluid barrier or flow dysfunction in first-episode schizophrenia. *Brain. Behav. Immun.* **44,** 148–158 (2015).

169. Mukhin, A. G., Papadopoulos, V., Costa, E. & Krueger, K. E. Mitochondrial benzodiazepine receptors regulate steroid biosynthesis. *Proc. Natl. Acad. Sci. U. S. A.* **86,** 9813–6 (1989).

170. Papadopoulos, V. *et al.* Translocator protein (18kDa): new nomenclature for the peripheral-type benzodiazepine receptor based on its structure and molecular function. *Trends Pharmacol. Sci.* **27,** 402–409 (2006).

171. Banati, R. B. Visualising microglial activation in vivo. *Glia* **40,** 206–217 (2002).

172. Chen, M.-K. & Guilarte, T. R. Translocator protein 18 kDa (TSPO): Molecular sensor of brain injury and repair. *Pharmacol. Ther.* **118,** 1–17 (2008).

173. Messmer, K. & Reynolds, G. P. Increased peripheral benzodiazepine binding sites in the brain of patients with Huntington's disease. *Neurosci. Lett.* **241,** 53–56 (1998).

174. Turner, M. . *et al.* Evidence of widespread cerebral microglial activation in amyotrophic lateral sclerosis: an [11C](R)-PK11195 positron emission tomography study. *Neurobiol. Dis.* **15,** 601–609 (2004).

175. Chauveau, F., Boutin, H., Van Camp, N., Dollé, F. & Tavitian, B. Nuclear imaging of neuroinflammation: a comprehensive review of [11C]PK11195 challengers. *Eur. J. Nucl. Med. Mol. Imaging* **35,** 2304–2319 (2008).

176. Tronel, C. *et al.* Molecular targets for PET imaging of activated microglia: The current situation and future expectations. *Int. J. Mol. Sci.* **18,** 1–22 (2017).

177. Dollé, F., Luus, C., Reynolds, A. & Kassiou, M. Radiolabelled molecules for imaging the translocator protein (18 kDa) using positron emission tomography. *Curr. Med. Chem.* **16,** 2899–923 (2009).

178. Scarf, A. M., Ittner, L. M. & Kassiou, M. The Translocator Protein (18 kDa): Central Nervous System Disease and Drug Design. *J. Med. Chem.* **52,** 581–592 (2009).

179. Howes, O. D. & McCutcheon, R. Inflammation and the neural diathesis-stress hypothesis of schizophrenia: a reconceptualization. *Transl. Psychiatry* **7,** 1–11 (2017).

180. van Berckel, B. N. *et al.* Microglia activation in recent-onset schizophrenia: a quantitative (R)-[11C]PK11195 positron emission tomography study. *Biol. Psychiatry* **64,** 820–2 (2008).

181. Doorduin, J. *et al.* Neuroinflammation in schizophrenia-related psychosis: a PET study. *J. Nucl. Med.* **50,** 1801–7 (2009).

182. Takano, A. *et al.* Peripheral benzodiazepine receptors in patients with chronic schizophrenia: a PET study with [11C]DAA1106. *Int. J. Neuropsychopharmacol.* **13,** 943–950 (2010).

183. Kenk, M. *et al.* Imaging Neuroinflammation in Gray and White Matter in Schizophrenia: An In-Vivo PET Study With [18F]-FEPPA. *Schizophr. Bull.* **41,** 85–93 (2015).

184. Coughlin, J. M. *et al.* In vivo markers of inflammatory response in recent-onset schizophrenia: a combined study using [(11)C]DPA-713 PET and analysis of CSF and plasma. *Transl. Psychiatry* **6,** e777 (2016).

185. van der Doef, T. F. *et al.* In vivo (R)-[11C]PK11195 PET imaging of 18kDa translocator protein in recent onset psychosis. *npj Schizophr.* **2,** 1–5 (2016).

186. Holmes, S. E. *et al.* In vivo imaging of brain microglial activity in antipsychotic-free and medicated schizophrenia: a [11C](R)-PK11195 positron emission tomography study. *Mol. Psychiatry* **21,** 1672–1679 (2016).

187. Hafizi, S. *et al.* Imaging

microglial activation in untreated first-episode psychosis: A PET study with [18F]FEPPA. *Am. J. Psychiatry* **174,** 118–124 (2017).

188. Notter, T. *et al.* Translational evaluation of translocator protein as a marker of neuroinflammation in schizophrenia. *Mol. Psychiatry* **0,** 1–12 (2017).

189. Hafizi, S. *et al.* Imaging Microglial Activation in Individuals at Clinical High Risk for Psychosis: An In-Vivo PET Study with [18F]FEPPA. *Neuropsychopharmacology* **0,** 1–8 (2017).

190. Bromet, E. J. *et al.* Diagnostic shifts during the decade following first admission for psychosis. *Am. J. Psychiatry* **168,** 1186–94 (2011).

191. Dequardo, J. R. Pharmacologic Treatment of First-Episode Schizophrenia: Early Intervention Is Key to Outcome. *J Clin PsychiatryJ Clin Psychiatry* **59,** 9–17 (1998).

192. Guest, J. F. & Cookson, R. F. Cost of Schizophrenia to UK Society. *Pharmacoeconomics* **15,** 597–610 (1999).

193. Mangalore, R. & Knapp, M. Cost of Schizophrenia in England. *J. Ment. Heal. Policy Econ. J Ment Heal. Policy Econ* **109,** 23–41 (2007).

194. Delay, J., Deniker, P. & Harl, J. Therapeutic method derived from hiberno-therapy in excitation and agitation states. *Ann. Med. Psychol. (Paris).* **110,** 267–73 (1952).

195. Mailman, R. B. & Murthy, V. Third generation antipsychotic drugs: partial agonism or receptor functional selectivity? *Curr. Pharm. Des.* **16,** 488–501 (2010).

196. Lieberman, J. A. Dopamine partial agonists: a new class of antipsychotic. *CNS Drugs* **18,** 251–67 (2004).

197. Shapiro, D. A. *et al.* Aripiprazole, A Novel Atypical Antipsychotic Drug with a Unique and Robust Pharmacology. *Neuropsychopharmacology* **28,** 1400–1411 (2003).

198. Casey, D. E., Sands, E. E., Heisterberg, J. & Yang, H.-M. Efficacy and safety of bifeprunox in patients with an acute exacerbation of schizophrenia: results from a randomized, double-blind, placebo-controlled, multicenter, dose-finding study. *Psychopharmacology (Berl).* **200,** 317–331 (2008).

199. Bifeprunox - Atypical Antipsychotic Drug. *Drugdevelopment-technology.com* (2009).

200. Heinrich, J. *et al.* Aplindore (DAB-452), a high affinity selective dopamine D2 receptor partial agonist. *Eur J Pharmacol* **15,** 36–45 (2006).

201. Huhn, M. *et al.* Efficacy of Pharmacotherapy and Psychotherapy for Adult Psychiatric Disorders. *JAMA Psychiatry* **71,** 706–715 (2014).

202. Lally, J. & MacCabe, J. H. Antipsychotic medication in schizophrenia: a review. *Br. Med. Bull.* **114,** 169–179 (2015).

203. Müller, N., Weidinger, E., Leitner, B. & Schwarz, M. J. The role of inflammation in schizophrenia. *Frontiers in Neuroscience* **9,** (2015).

204. Leboyer, M., Oliveira, J., Tamouza, R. & Groc, L. Is it time for immunopsychiatry in psychotic disorders? *Psychopharmacology* **233,** 1651–60 (2016).

205. Miyaoka, T. *et al.* Possible antipsychotic effects of minocycline in patients with schizophrenia. *Prog. Neuropsychopharmacol. Biol. Psychiatry* **31,** 304–7 (2007).

206. Oya, K., Kishi, T. & Iwata, N. Efficacy and tolerability of minocycline augmentation therapy in schizophrenia: a systematic review and meta-analysis of randomized controlled trials. *Hum. Psychopharmacol.* **29,** 483–491 (2014).

207. Giovanoli, S. *et al.* Preventive effects of minocycline in a neurodevelopmental two-hit model with relevance to schizophrenia. *Transl. Psychiatry* **6,** 1–9 (2016).

208. Kobayashi, K. *et al.* Minocycline selectively inhibits M1 polarization of microglia. *Cell Death Dis.* **4,** 1–9 (2013).

209. Seki, Y. *et al.* Pretreatment of aripiprazole and minocycline, but not haloperidol, suppresses oligodendrocyte damage

from interferon-γ-stimulated microglia in co-culture model. *Schizophr. Res.* **151,** 20–28 (2013).

210. Müller, N. *et al.* Celecoxib treatment in an early stage of schizophrenia: results of a randomized, double-blind, placebo-controlled trial of celecoxib augmentation of amisulpride treatment. *Schizophr. Res.* **121,** 118–24 (2010).

211. Pettit, L. K., Varsanyi, C., Tadros, J. & Vassiliou, E. Modulating the inflammatory properties of activated microglia with Docosahexaenoic acid and Aspirin. *Lipids Health Dis.* **12,** 16 (2013).

212. Nitta, M. *et al.* Adjunctive use of nonsteroidal anti-inflammatory drugs for schizophrenia: a meta-analytic investigation of randomized controlled trials. *Schizophr. Bull.* **39,** 1230–41 (2013).

213. Abbott, N. J., Rönnbäck, L. & Hansson, E. Astrocyte–endothelial interactions at the blood–brain barrier. *Nat. Rev. Neurosci.* **7,** 41–53 (2006).

214. Pardridge, W. M. The blood-brain barrier: bottleneck in brain drug development. *J. Am. Soc. Exp. Neurother.* **2,** 3–14 (2005).

215. Yu, Y. J. *et al.* Therapeutic bispecific antibodies cross the blood-brain barrier in nonhuman primates. *Sci. Transl. Med.* **6,** 1–11 (2014).

216. Gaillard, P. J. *et al.* Enhanced brain delivery of liposomal methylprednisolone improved therapeutic efficacy in a model of neuroinflammation. *J. Control. Release* **164,** 364–369 (2012).

217. Fillman, S. G. *et al.* Elevated peripheral cytokines characterize a subgroup of people with schizophrenia displaying poor verbal fluency and reduced Broca's area volume. *Mol. Psychiatry* **21,** 1090–1098 (2016).

218. Dean, B. Understanding the role of inflammatory-related pathways in the pathophysiology and treatment of psychiatric disorders: evidence from human peripheral studies and CNS studies. *Int. J. Neuropsychopharmacol.* **14,** 997–1012 (2011).

219. Humphrey, S. J., James, D. E. & Mann, M. Protein Phosphorylation: A Major Switch Mechanism for Metabolic Regulation. *Trends Endocrinol. Metab.* **26,** 676–687 (2015).

220. Tang, Z. *et al.* Real-time investigation of nucleic acids phosphorylation process using molecular beacons. *Nucleic Acids Res.* **33,** e97 (2005).

221. Ripke, S. *et al.* Biological insights from 108 schizophrenia-associated genetic loci. *Nature* **511,** 421–427 (2014).

222. Boja, E. S. & Rodriguez, H. The Path to Clinical Proteomics Research: Integration of Proteomics, Genomics, Clinical Laboratory and Regulatory Science. *Korean J. Lab. Med.* **31,** 61 (2011).

223. Herberth, M. *et al.* Peripheral profiling analysis for bipolar disorder reveals markers associated with reduced cell survival. *Proteomics* **11,** 94–105 (2011).

224. Gomez-Nicola, D. & Perry, V. H. Microglial Dynamics and Role in the Healthy and Diseased Brain. *Neurosci.* **21,** 169–184 (2015).

225. Jaroszeski, M. J. & Radcliff, G. Fundamentals of flow cytometry. *Mol. Biotechnol.* **11,** 37–53 (1999).

226. Rahman, M. *Introduction to Flow Cytometry*. *AbD Serotec* (2014).

227. Coppin, E. *et al.* Flow cytometric analysis of intracellular phosphoproteins in human monocytes. *Cytometry B. Clin. Cytom.* **0,** 5–8 (2015).

228. Goldeck, D. *et al.* Multi-parametric phospho-flow cytometry: A crucial tool for T lymphocyte signaling studies. *Cytom. Part A* **83A,** 265–272 (2013).

229. Wu, S., Jin, L., Vence, L. & Radvanyi, L. G. Development and application of 'phosphoflow' as a tool for immunomonitoring. *Expert Rev. Vaccines* **9,** 631–43 (2010).

230. Krutzik, P. O., Clutter, M. R., Trejo, A. & Nolan, G. P.

in *Current protocols in cytometry* **55,** 6.31.1-6.31.15 (2011).

231. Edwards, B. S., Oprea, T., Prossnitz, E. R. & Sklar, L. A. Flow cytometry for high-throughput, high-content screening. *Curr. Opin. Chem. Biol.* **8,** 392–398 (2004).

232. Black, C. B., Duensing, T. D., Trinkle, L. S. & Dunlay, R. T. Cell-based screening using high-throughput flow cytometry. *Assay Drug Dev. Technol.* **9,** 13–20 (2011).

233. Yufeng Shen *et al.* High-Efficiency Nanoscale Liquid Chromatography Coupled On-Line with Mass Spectrometry Using Nanoelectrospray Ionization for Proteomics. *Anal. Chem.* **74,** 4235–4249 (2002).

234. Yates, J. R. *et al.* Direct analysis of protein complexes using mass spectrometry. *Nat. Biotechnol.* **17,** 676–682 (1999).

235. Loo, J. A., DeJohn, D. E., Du, P., Stevenson, T. I. & Ogorzalek Loo, R. R. Application of mass spectrometry for target identification and characterization. *Med. Res. Rev.* **19,** 307–19 (1999).

236. Nilsen, T. W. & Graveley, B. R. Expansion of the eukaryotic proteome by alternative splicing. *Nature* **463,** 457–463 (2010).

237. Huang, J. T. J. *et al.* CSF biomarker discovery using label-free nano-LC-MS based proteomic profiling: technical aspects. *J. Sep. Sci.* **30,** 214–25 (2007).

238. Picotti, P. & Aebersold, R. Selected reaction monitoring–based proteomics: workflows, potential, pitfalls and future directions. *Nat. Methods* **9,** 555–566 (2012).

239. Gerszten, R. E., Carr, S. A. & Sabatine, M. Integration of Proteomic-Based Tools for Improved Biomarkers of Myocardial Injury. *Clin. Chem.* **56,** 194–201 (2010).

240. Kiyonami, R. *et al.* Increased Selectivity, Analytical Precision, and Throughput in Targeted Proteomics. *Mol. Cell. Proteomics* **10,** 1–11 (2011).

241. McLuckey, S. A. Principles of collisional activation in analytical mass spectrometry. *J. Am. Soc. Mass Spectrom.* **3,** 599–614 (1992).

242. Lange, V., Picotti, P., Domon, B. & Aebersold, R. Selected reaction monitoring for quantitative proteomics: a tutorial. *Mol. Syst. Biol.* **4,** 222 (2008).

243. Gevaert, K. *et al.* Stable isotopic labeling in proteomics. *Proteomics* **8,** 4873–4885 (2008).

244. World Medical Association. World Medical Association Declaration of Helsinki: ethical principles for medical research involving human subjects. *JAMA* **310,** 2191–4 (2013).

245. Kleiner, G., Marcuzzi, A., Zanin, V., Monasta, L. & Zauli, G. Cytokine levels in the serum of healthy subjects. *Mediators Inflamm.* **2013,** 1–6 (2013).

246. Pisa, P., Stenke, L., Bernell, P., Hansson, M. & Hast, R. Tumor necrosis factor-alpha and interferon-gamma in serum of multiple myeloma patients. *Anticancer Res.* **10,** 817–20 (1990).

247. Brandt, C. T. *et al.* Evaluation of the cytokines IL-10 and IL-13 as mediators in the progression of Symmers fibrosis in patients with hepatosplenic schistosomiasis mansoni. *Rev. Col. Bras. Cir.* **37,** 333–337 (2010).

248. Berktas, M. *et al.* Change in serum concentrations of interleukin-2 and interferon-γ during treatment of tuberculosis. *J. Int. Med. Res.* **32,** 324–330 (2004).

249. Krutzik, P. O. & Nolan, G. P. Fluorescent cell barcoding in flow cytometry allows high-throughput drug screening and signaling profiling. *Nat. Methods* **3,** 361–368 (2006).

250. Lago, S. G. *et al.* Drug discovery in neuropsychiatric disorders using high-content single-cell screening of signaling network responses ex vivo. *submitted*

251. Krutzik, P. O., Crane, J. M., Clutter, M. R. & Nolan, G. P. High-content single-cell drug screening with phosphospecific flow cytometry. *Nat. Chem. Biol.* **4,** 132–142 (2008).

252. Knöchel, C. *et al.* Altered apolipoprotein C expression in association with

cognition impairments and hippocampus volume in schizophrenia and bipolar disorder. *Eur. Arch. Psychiatry Clin. Neurosci.* **267,** 199–212 (2017).

253. Ozcan, S. *et al.* Towards reproducible MRM based biomarker discovery using dried blood spots. *Sci. Rep.* **7,** 1–10 (2017).

254. Kiyonami, R. & Domon, B. in *LC-MS/MS in Proteomics* 155–166 (2010). doi:10.1007/978-1-60761-780-8_9

255. Bauer, D. F. Constructing Confidence Sets Using Rank Statistics. *J. Am. Stat. Assoc.* **67,** 687–690 (1972).

256. Fisher, R. A. On the interpretation of χ^2 from contingency tables, and the calculation of P. *J. R. Stat. Soc.* **85,** 87–94 (1922).

257. Zhang, J.-H., Chung, T. D. Y. & Oldenburg, K. R. A Simple Statistical Parameter for Use in Evaluation and Validation of High Throughput Screening Assays. *J. Biomol. Screen.* **4,** 67–73 (1999).

258. Hothorn, T. *et al.* Implementing a class of permutation tests: The coin package. *J. Stat. Softw.* **28,** 1–23 (2008).

259. MacLean, B. *et al.* Skyline: an open source document editor for creating and analyzing targeted proteomics experiments. *Bioinformatics* **26,** 966–8 (2010).

260. Savitzky, A. & Golay, M. J. E. Smoothing and Differentiation of Data by Simplified Least Squares Procedures. *Anal. Chem.* **36,** 1627–1639 (1964).

261. Sachs, K., Perez, O., Pe'er, D., Lauffenburger, D. A. & Nolan, G. P. Causal protein-signaling networks derived from multiparameter single-cell data. *Science* **308,** 523–9 (2005).

262. Lawrence, T. & Natoli, G. Transcriptional regulation of macrophage polarization: enabling diversity with identity. *Nat. Rev. Immunol.* **11,** 750–761 (2011).

263. van Rees, G. F. *et al.* Evidence of microglial activation following exposure to serum from first-onset drug-naïve schizophrenia patients. *Brain Behav. Immun.* **67,** 364–373 (2018).

264. Bodenmiller, B. *et al.* Multiplexed mass cytometry profiling of cellular states perturbed by small-molecule regulators. *Nat. Biotechnol.* **30,** 858–867 (2012).

265. Martinez, F. O. & Gordon, S. The M1 and M2 paradigm of macrophage activation: time for reassessment. *F1000Prime Rep.* **6,** 1–13 (2014).

266. Lv, M. *et al.* Roles of inflammation response in microglia cell through Toll-like receptors 2/interleukin-23/interleukin-17 pathway in cerebral ischemia/reperfusion injury. *Neuroscience* **176,** 162–172 (2011).

267. Iwakura, Y. The IL-23/IL-17 axis in inflammation. *J. Clin. Invest.* **116,** 1218–1222 (2006).

268. Kim, S. H., Smith, C. J. & Van Eldik, L. J. Importance of MAPK pathways for microglial pro-inflammatory cytokine IL-1 beta production. *Neurobiol. Aging* **25,** 431–9 (2004).

269. Zhou, X., Spittau, B. & Krieglstein, K. TGFβ signalling plays an important role in IL4-induced alternative activation of microglia. *J. Neuroinflammation* **9,** 706 (2012).

270. Veremeyko, T. *et al.* IL-4/IL-13-Dependent and Independent Expression of miR-124 and Its Contribution to M2 Phenotype of Monocytic Cells in Normal Conditions and during Allergic Inflammation. *PLoS One* **8,** e81774 (2013).

271. Mia, S., Warnecke, A., Zhang, X.-M., Malmström, V. & Harris, R. A. An optimized protocol for human M2 macrophages using M-CSF and IL-4/IL-10/TGF-β yields a dominant immunosuppressive phenotype. *Scand. J. Immunol.* **79,** 305–14 (2014).

272. Rocher, C. *et al.* SMAD-PI3K-Akt-mTOR Pathway Mediates BMP-7 Polarization of Monocytes into M2 Macrophages. *PLoS One* **8,** e84009 (2013).

273. Gadani, S. P., Cronk, J. C., Norris, G. T. & Kipnis, J. IL-4 in the Brain: A Cytokine To Remember. *J. Immunol.* **189,** (2012).

274. Gosselin, D. *et al.* An environment-dependent transcriptional network specifies human microglia identity. *Science* **356,** 1–11 (2017).

275. Rosenstiel, P., Lucius, R., Deuschl, G., Sievers, J. & Wilms, H. From theory to therapy: Implications from an in vitro model of ramified microglia. *Microsc. Res. Tech.* **54,** 18–25 (2001).

276. Aloisi, F. Immune function of microglia. *Glia* **36,** 165–79 (2001).

277. Ponomarev, E. D., Novikova, M., Maresz, K., Shriver, L. P. & Dittel, B. N. Development of a culture system that supports adult microglial cell proliferation and maintenance in the resting state. *J. Immunol. Methods* **300,** 32–46 (2005).

278. Boucsein, C. *et al.* Purinergic receptors on microglial cells: functional expression in acute brain slices and modulation of microglial activation in vitro. *Eur. J. Neurosci.* **17,** 2267–76 (2003).

279. Davalos, D. *et al.* ATP mediates rapid microglial response to local brain injury in vivo. *Nat. Neurosci.* **8,** 752–758 (2005).

280. Nimmerjahn, A., Kirchhoff, F. & Helmchen, F. Resting microglial cells are highly dynamic surveillants of brain parenchyma in vivo. *Science* **308,** 1314–1318 (2005).

281. Raivich, G. Like cops on the beat: the active role of resting microglia. *Trends Neurosci.* **28,** 571–573 (2005).

282. Butovsky, O. *et al.* Identification of a unique TGF- b – dependent molecular and functional signature in microglia. *Nat. Neurosci.* **17,** 131–143 (2014).

283. Hickman, S. E. *et al.* The microglial sensome revealed by direct RNA sequencing. *Nat. Neurosci.* **16,** 1896–905 (2013).

284. Miller, J. A., Horvath, S. & Geschwind, D. H. Divergence of human and mouse brain transcriptome highlights Alzheimer disease pathways. *Proc. Natl. Acad. Sci. U. S. A.* **107,** 12698–703 (2010).

285. Aaronson, D. S. & Horvath, C. M. A Road Map for Those Who Don't Know JAK-STAT. *Science* **296,** 1653–1655 (2002).

286. Kato, T. a *et al.* Aripiprazole inhibits superoxide generation from phorbol-myristate-acetate (PMA)-stimulated microglia in vitro: implication for antioxidative psychotropic actions via microglia. *Schizophr. Res.* **129,** 172–82 (2011).

287. Bian, Q. *et al.* The effect of atypical antipsychotics, perospirone, ziprasidone and quetiapine on microglial activation induced by interferon-gamma. *Prog. Neuropsychopharmacol. Biol. Psychiatry* **32,** 42–8 (2008).

288. Nathan, C. F., Murray, H. W., Wiebe, M. E. & Rubin, B. Y. Identification of interferon-gamma as the lymphokine that activates human macrophage oxidative metabolism and antimicrobial activity. *J. Exp. Med.* **158,** 670–89 (1983).

289. Darnell, J., Kerr, I. & Stark, G. Jak-STAT pathways and transcriptional activation in response. *Science* **264,** 1415–1421 (1994).

290. Hoffmann, J. A. The immune response of Drosophila. *Nature* **426,** 33–38 (2003).

291. Kawanokuchi, J. *et al.* Production of interferon-gamma by microglia. *Mult. Scler.* **12,** 558–64 (2006).

292. Perry, V. H. & Teeling, J. Microglia and macrophages of the central nervous system: the contribution of microglia priming and systemic inflammation to chronic neurodegeneration. *Semin. Immunopathol.* **35,** 601–12 (2013).

293. Watford, W. T. *et al.* Signaling by IL-12 and IL-23 and the immunoregulatory roles of STAT4. *Immunol. Rev.* **202,** 139–156 (2004).

294. Stein, M., Keshav, S., Harris, N. & Gordon, S. Interleukin 4 potently enhances murine macrophage mannose receptor activity: a marker of alternative immunologic macrophage activation. *J. Exp. Med.* **176,** 287–92 (1992).

295. Doherty, T. M., Kastelein, R., Menon, S., Andrade, S. & Coffman, R. L.

Modulation of murine macrophage function by IL-13. *J. Immunol.* **151,** 7151–60 (1993).

296. Doyle, A. G. *et al.* Interleukin-13 alters the activation state of murine macrophagesin vitro: Comparison with interleukin-4 and interferon-γ. *Eur. J. Immunol.* **24,** 1441–1445 (1994).

297. Van Dyken, S. J. & Locksley, R. M. Interleukin-4- and interleukin-13-mediated alternatively activated macrophages: roles in homeostasis and disease. *Annu. Rev. Immunol.* **31,** 317–43 (2013).

298. Murray, P. J. The JAK-STAT Signaling Pathway: Input and Output Integration. *J. Immunol.* **178,** 2623–2629 (2007).

299. Attisano, L. & Wrana, J. L. Signal Transduction by the TGF-β Superfamily. *Science* **296,** 1646–1647 (2002).

300. Zhang, Y. E. Non-Smad pathways in TGF-beta signaling. *Cell Res.* **19,** 128–39 (2009).

301. Chen, G., Deng, C. & Li, Y.-P. TGF-β and BMP Signaling in Osteoblast Differentiation and Bone Formation. *Int. J. Biol. Sci.* **8,** 272–288 (2012).

302. Paglinawan, R. *et al.* TGFbeta directs gene expression of activated microglia to an anti-inflammatory phenotype strongly focusing on chemokine genes and cell migratory genes. *Glia* **44,** 219–231 (2003).

303. Rocher, C., Singla, R., Singal, P. K., Parthasarathy, S. & Singla, D. K. Bone morphogenetic protein 7 polarizes THP-1 cells into M2 macrophages. *Can. J. Physiol. Pharmacol.* **90,** 947–951 (2012).

304. Dudvarski Stankovic, N., Teodorczyk, M., Ploen, R., Zipp, F. & Schmidt, M. H. H. Microglia-blood vessel interactions: a double-edged sword in brain pathologies. *Acta Neuropathol.* **131,** 347–363 (2016).

305. Najjar, S. *et al.* Neurovascular Unit Dysfunction and Blood–Brain Barrier Hyperpermeability Contribute to Schizophrenia Neurobiology: A Theoretical Integration of Clinical and Experimental Evidence. *Front. Psychiatry* **8,** 1–11 (2017).

306. Qin, H. *et al.* Signal transducer and activator of transcription- axis in myeloid cells regulates neuroinflammation. *PNAS* **109,** 5004–5009 (2012).

307. Li, D. *et al.* mTORC1 pathway disruption ameliorates brain inflammation following stroke via a shift in microglia phenotype from M1 type to M2 type. *FASEB J.* **30,** 3388–3399 (2016).

308. Dello Russo, C., Lisi, L., Tringali, G. & Navarra, P. Involvement of mTOR kinase in cytokine-dependent microglial activation and cell proliferation. *Biochem. Pharmacol.* **78,** 1242–51 (2009).

309. Yeh, F. L., Wang, Y., Tom, I., Gonzalez, L. C. & Sheng, M. TREM2 Binds to Apolipoproteins, Including APOE and CLU/APOJ, and Thereby Facilitates Uptake of Amyloid-Beta by Microglia. *Neuron* **91,** 328–40 (2016).

310. Borda, J. T. *et al.* CD163, a marker of perivascular macrophages, is up-regulated by microglia in simian immunodeficiency virus encephalitis after haptoglobin-hemoglobin complex stimulation and is suggestive of breakdown of the blood-brain barrier. *Am J Pathol* **172,** 725–737 (2008).

311. You, W. *et al.* Inhibition of mammalian target of rapamycin attenuates early brain injury through modulating microglial polarization after experimental subarachnoid hemorrhage in rats. *J. Neurol. Sci.* **367,** 224–231 (2016).

312. Fillman, S. G. *et al.* Increased inflammatory markers identified in the dorsolateral prefrontal cortex of individuals with schizophrenia. *Mol. Psychiatry* **18,** 206–14 (2013).

313. Tomasik, J., Rahmoune, H., Guest, P. C. & Bahn, S. Neuroimmune biomarkers in schizophrenia. *Schizophr. Res.* **176,** 3–13 (2016).

314. Saetre, P. *et al.* Inflammation-related genes up-regulated in schizophrenia brains. *BMC Psychiatry* **7,** 1–10 (2007).

315. Montesinos-Rongen, M. *et al.* Gene expression

profiling suggests primary central nervous system lymphomas to be derived from a late germinal center B cell. *Leukemia* **22,** 400–405 (2008).

316. Law, R. H. P. *et al.* An overview of the serpin superfamily. *Genome Biol.* **7,** 1–11 (2006).

317. Carrizo, E. *et al.* Coagulation and inflammation markers during atypical or typical antipsychotic treatment in schizophrenia patients and drug-free first-degree relatives. *Schizophr. Res.* **103,** 83–93 (2008).

318. Levin, Y. *et al.* Global proteomic profiling reveals altered proteomic signature in schizophrenia serum. *Mol. Psychiatry* **15,** 1088–100 (2010).

319. Yang, Y. *et al.* Altered Levels of Acute Phase Proteins in the Plasma of Patients with Schizophrenia. *Anal. Chem.* **78,** 3571–3576 (2006).

320. Jiang, L. *et al.* Proteomic analysis of the cerebrospinal fluid of patients with schizophrenia. *Amino Acids* **25,** 49–57 (2003).

321. Cudaback, E. *et al.* Apolipoprotein C-I is an APOE genotype-dependent suppressor of glial activation. *J. Neuroinflammation* **9,** 1–13 (2012).

322. Jaros, J. A. J. *et al.* Protein phosphorylation patterns in serum from schizophrenia patients and healthy controls. *J. Proteomics* **76,** 43–55 (2012).

323. Rudduck, C., Franzén, G., Fröhlander, N. & Lindström, L. Haptoglobin and transferrin types in schizophrenia. *Hum. Hered.* **35,** 65–8 (1985).

324. Yee, J. Y. *et al.* Peripheral blood gene expression of acute phase proteins in people with first episode psychosis. *Brain. Behav. Immun.* **65,** 337–341 (2017).

325. Zhao, X. *et al.* Neuroprotective role of haptoglobin after intracerebral hemorrhage. *J. Neurosci.* **29,** 15819–27 (2009).

326. Skurkovich, S. V. *et al.* Improvement in Negative Symptoms of Schizophrenia With Antibodies to Tumor Necrosis Factor-alpha and to Interferon-gamma. *J. Clin. Psychiatry* **64,** 734–735 (2003).

327. Kato, T., Monji, A., Hashioka, S. & Kanba, S. Risperidone significantly inhibits interferon-gamma-induced microglial activation in vitro. *Schizophr. Res.* **92,** 108–15 (2007).

328. Li, Y. *et al.* Label-free quantitative proteomic analysis reveals dysfunction of complement pathway in peripheral blood of schizophrenia patients: evidence for the immune hypothesis of schizophrenia. *Mol. Biosyst.* **8,** 2664–2671 (2012).

329. Athanas, K. M., Mauney, S. L. & Woo, T.-U. W. Increased extracellular clusterin in the prefrontal cortex in schizophrenia. *Schizophr. Res.* **169,** 381–385 (2015).

330. Chen, X. *et al.* Expression and localization of Inter-alpha Inhibitors in rodent brain. *Neuroscience* **324,** 69–81 (2016).

331. Weis, N., Weigert, A., von Knethen, A. & Brune, B. Heme Oxygenase-1 Contributes to an Alternative Macrophage Activation Profile Induced by Apoptotic Cell Supernatants. *Mol. Biol. Cell* **20,** 1280–1288 (2009).

332. Sanson, M., Distel, E., Fisher, E. A., Drechsler, M. & Papac-Milicevic, N. HDL Induces the Expression of the M2 Macrophage Markers Arginase 1 and Fizz-1 in a STAT6-Dependent Process. *PLoS One* **8,** e74676 (2013).

333. Miklossy, G., Hilliard, T. S. & Turkson, J. Therapeutic modulators of STAT signalling for human diseases. *Nat. Rev. Drug Discov.* **12,** 611–629 (2013).

334. Wakahara, R. *et al.* Phospho-Ser727 of STAT3 regulates STAT3 activity by enhancing dephosphorylation of phospho-Tyr705 largely through TC45. *Genes Cells* **17,** 132–45 (2012).

335. Krebs, D. L. & Hilton, D. J. SOCS Proteins: Negative Regulators of Cytokine Signaling. *Stem Cells* **19,** 378–387 (2001).

336. Carow, B. & Rottenberg, M. E. SOCS3, a Major Regulator of Infection

and Inflammation. *Front. Immunol.* **5,** 1–13 (2014).

337. Pedranzini, L., Leitch, A. & Bromberg, J. Stat3 is required for the development of skin cancer. *J. Clin. Invest.* **114,** 619–22 (2004).

338. Müller-Newen, G. The Cytokine Receptor gp130: Faithfully Promiscuous. *Sci. Signal.* **2003,** 1–3 (2003).

339. Upthegrove, R., Manzanares-Teson, N. & Barnes, N. M. Cytokine function in medication-naive first episode psychosis: A systematic review and meta-analysis. *Schizophr. Res.* **155,** 101–108 (2014).

340. Yang, J. *et al.* Unphosphorylated STAT3 accumulates in response to IL-6 and activates transcription by binding to NFkappaB. *Genes Dev.* **21,** 1396–408 (2007).

341. Dibble, C. C. & Cantley, L. C. Regulation of mTORC1 by PI3K signaling. *Trends Cell Biol.* **25,** 545–555 (2015).

342. Yang, H. *et al.* mTOR kinase structure, mechanism and regulation. *Nature* **497,** 217–223 (2013).

343. Costa-Mattioli, M. & Monteggia, L. M. mTOR complexes in neurodevelopmental and neuropsychiatric disorders. *Nat. Neurosci.* **16,** 1537–1543 (2013).

344. Laplante, M. & Sabatini, D. M. mTOR signaling at a glance. *J. Cell Sci.* **122,** 3589–94 (2009).

345. Pearce, L. R., Komander, D. & Alessi, D. R. The nuts and bolts of AGC protein kinases. *Nat. Rev. Mol. Cell Biol.* **11,** 9–22 (2010).

346. Gururajan, A. & van den Buuse, M. Is the mTOR-signalling cascade disrupted in Schizophrenia? *J. Neurochem.* **129,** 377–387 (2014).

347. Kim, J. Y. *et al.* DISC1 Regulates New Neuron Development in the Adult Brain via Modulation of AKT-mTOR Signaling through KIAA1212. *Neuron* **63,** 761–773 (2009).

348. Zhou, M. *et al.* mTOR Inhibition Ameliorates Cognitive and Affective Deficits Caused by Disc1 Knockdown in Adult-Born Dentate Granule Neurons. *Neuron* **77,** 647–654 (2013).

349. Song, Q., Xie, D., Pan, S. & Xu, W. Rapamycin protects neurons from brain contusion-induced inflammatory reaction via modulation of microglial activation. *Mol. Med. Rep.* **12,** 7203–7210 (2015).

350. Srivastava, I. N., Shperdheja, J., Baybis, M., Ferguson, T. & Crino, P. B. mTOR pathway inhibition prevents neuroinflammation and neuronal death in a mouse model of cerebral palsy. *Neurobiol. Dis.* **85,** 144–154 (2016).

351. Xie, L. *et al.* mTOR signaling inhibition modulates macrophage/microglia-mediated neuroinflammation and secondary injury via regulatory T cells after focal ischemia. *J. Immunol.* **192,** 6009–19 (2014).

352. Nikolaeva, I., Crowell, B., Valenziano, J., Meaney, D. & D'Arcangelo, G. Beneficial Effects of Early mTORC1 Inhibition after Traumatic Brain Injury. *J. Neurotrauma* **33,** 183–193 (2016).

353. Harris, H. & Rubinsztein, D. C. Control of autophagy as a therapy for neurodegenerative disease. *Nat. Rev. Neurol.* **8,** 108–117 (2011).

354. Merenlender-Wagner, A. *et al.* Autophagy has a key role in the pathophysiology of schizophrenia. *Mol. Psychiatry* **20,** 126–132 (2015).

355. Kim, H. *et al.* Deficient autophagy in microglia impairs synaptic pruning and causes social behavioral defects. *Mol. Psychiatry* **0,** 1–9 (2016).

356. Gassen, N. C., Hartmann, J., Schmidt, M. V & Rein, T. FKBP5/FKBP51 enhances autophagy to synergize with antidepressant action. *Autophagy* **11,** 578–80 (2015).

357. Gassen, N. C. *et al.* Association of FKBP51 with Priming of Autophagy Pathways and Mediation of Antidepressant Treatment Response: Evidence in Cells, Mice, and Humans. *PLoS Med.* **11,** 1–20 (2014).

358. Motoi, Y., Shimada, K., Ishiguro, K. & Hattori, N. Lithium and autophagy. *ACS Chem. Neurosci.* **5,** 434–42

(2014).

359. Perl, A. mTOR activation is a biomarker and a central pathway to autoimmune disorders, cancer, obesity, and aging. *Ann. N. Y. Acad. Sci.* **1346,** 33–44 (2015).

360. Fernandez, D., Bonilla, E., Mirza, N., Niland, B. & Perl, A. Rapamycin reduces disease activity and normalizes T cell activation–induced calcium fluxing in patients with systemic lupus erythematosus. *Arthritis Rheum.* **54,** 2983–2988 (2006).

361. Calne, R. Y. *et al.* Rapamycin for immunosuppression in organ allografting. *Lancet* **334,** 227 (1989).

362. Verheijden, S. *et al.* Identification of a chronic non-neurodegenerative microglia activation state in a mouse model of peroxisomal β-oxidation deficiency. *Glia* **63,** 1606–1620 (2015).

363. Wen, Z., Zhong, Z. & Darnell, J. E. Maximal activation of transcription by Stat1 and Stat3 requires both tyrosine and serine phosphorylation. *Cell* **82,** 241–50 (1995).

364. Yokogami, K., Wakisaka, S., Avruch, J. & Reeves, S. A. Serine phosphorylation and maximal activation of STAT3 during CNTF signaling is mediated by the rapamycin target mTOR. *Curr. Biol.* **10,** 47–50 (2000).

365. Yu, C.-R. *et al.* Suppressor of Cytokine Signaling 3 Regulates Proliferation and Activation of T-helper Cells. *J. Biol. Chem.* **278,** 29752–29759 (2003).

366. Yamamoto, K., Yamaguchi, M., Miyasaka, N. & Miura, O. SOCS-3 inhibits IL-12-induced STAT4 activation by binding through its SH2 domain to the STAT4 docking site in the IL-12 receptor β2 subunit. *Biochem. Biophys. Res. Commun.* **310,** 1188–1193 (2003).

367. Powell, J. D., Lerner, C. G. & Schwartz, R. H. Inhibition of cell cycle progression by rapamycin induces T cell clonal anergy even in the presence of costimulation. *J. Immunol.* **162,** 2775–84 (1999).

368. Weir, M. R. *et al.* mTOR inhibition: the learning curve in kidney transplantation. *Transpl. Int.* **23,** 447–460 (2010).

369. McMahon, G., Weir, M. R., Li, X. C. & Mandelbrot, D. A. The Evolving Role of mTOR Inhibition in Transplantation Tolerance. *J. Am. Soc. Nephrol.* **22,** 408–415 (2011).

370. Weichhart, T. *et al.* The TSC-mTOR signaling pathway regulates the innate inflammatory response. *Immunity* **29,** 565–77 (2008).

371. Ohtani, M. *et al.* Mammalian target of rapamycin and glycogen synthase kinase 3 differentially regulate lipopolysaccharide-induced interleukin-12 production in dendritic cells. *Blood* **112,** 635–43 (2008).

372. Powell, J. D., Pollizzi, K. N., Heikamp, E. B. & Horton, M. R. Regulation of immune responses by mTOR. *Annu. Rev. Immunol.* **30,** 39–68 (2012).

373. Gordon, S. & Martinez, F. O. Alternative Activation of Macrophages: Mechanism and Functions. *Immunity* **32,** 593–604 (2010).

374. Matsushita, M. Ficolins in complement activation. *Mol. Immunol.* **55,** 22–26 (2013).

375. Hakobyan, S., Boyajyan, A. & Sim, R. B. Classical pathway complement activity in schizophrenia. *Neurosci. Lett.* **374,** 35–37 (2005).

376. Veerhuis, R., Nielsen, H. M. & Tenner, A. J. Complement in the brain. *Mol. Immunol.* **48,** 1592–1603 (2011).

377. Schafer, D. P. *et al.* Microglia Sculpt Postnatal Neural Circuits in an Activity and Complement-Dependent Manner. *Neuron* **74,** 691–705 (2012).

378. Stevens, B. *et al.* The Classical Complement Cascade Mediates CNS Synapse Elimination. *Cell* **131,** 1164–1178 (2007).

379. Jacob, A. & Alexander, J. J. Complement and blood-brain barrier integrity. *Mol. Immunol.* **61,** 149–152 (2014).

380. Flierl, M. A. *et al.* Inhibition of complement C5a prevents breakdown of the blood-brain barrier and pituitary dysfunction in experimental sepsis. *Crit.*

Care **13,** R12 (2009).

381. Kettenmann, H., Kirchhoff, F. & Verkhratsky, A. Microglia: New Roles for the Synaptic Stripper. *Neuron* **77,** 10–18 (2013).

382. Paolicelli, R. C. *et al.* Synaptic Pruning by Microglia Is Necessary for Normal Brain Development. *Science* **333,** 1456–1458 (2011).

383. Cunningham, C. L., Martinez-Cerdeno, V. & Noctor, S. C. Microglia Regulate the Number of Neural Precursor Cells in the Developing Cerebral Cortex. *J. Neurosci.* **33,** 4216–4233 (2013).

384. Hong, S. *et al.* Complement and microglia mediate early synapse loss in Alzheimer mouse models. *Science* (2016).

385. Ballanti, E. *et al.* Role of the complement system in rheumatoid arthritis and psoriatic arthritis: Relationship with anti-TNF inhibitors. *Autoimmun. Rev.* **10,** 617–623 (2011).

386. Okroj, M., Heinegård, D., Holmdahl, R. & Blom, A. M. Rheumatoid arthritis and the complement system. *Ann. Med.* **39,** 517–530 (2007).

387. Walport, M. J. Complement and systemic lupus erythematosus. *Arthritis Res.* **4,** S279–S293 (2002).

388. Yang, Y. *et al.* Gene Copy-Number Variation and Associated Polymorphisms of Complement Component C4 in Human Systemic Lupus Erythematosus (SLE): Low Copy Number Is a Risk Factor for and High Copy Number Is a Protective Factor against SLE Susceptibility in European America. *Am. J. Hum. Genet.* **80,** 1037–1054 (2007).

389. Hoirisch-Clapauch, S., Amaral, O. B., Mezzasalma, M. A. U., Panizzutti, R. & Nardi, A. E. Dysfunction in the coagulation system and schizophrenia. *Transl. Psychiatry* **6,** 1–8 (2016).

390. Fan, Z., Wu, Y., Shen, J., Ji, T. & Zhan, R. Schizophrenia and the risk of cardiovascular diseases: A meta-analysis of thirteen cohort studies. *J. Psychiatr. Res.* **47,** 1549–1556 (2013).

391. Hennekens, C. H., Hennekens, A. R., Hollar, D. & Casey, D. E. Schizophrenia and increased risks of cardiovascular disease. *Am. Heart J.* **150,** 1115–1121 (2005).

392. Chow, V. *et al.* Global hypercoagulability in patients with schizophrenia receiving long-term antipsychotic therapy. *Schizophr. Res.* **162,** 175–182 (2015).

393. Hoirisch-Clapauch, S. & Nardi, A. E. Psychiatric remission with warfarin: Should psychosis be addressed as plasminogen activator imbalance? *Med. Hypotheses* **80,** 137–141 (2013).

394. Jiang, T. *et al.* TREM2 modifies microglial phenotype and provides neuroprotection in P301S tau transgenic mice. *Neuropharmacology* **105,** 196–206 (2016).

395. Ulrich, J. D., Ulland, T. K., Colonna, M. & Holtzman, D. M. Elucidating the Role of TREM2 in Alzheimer's Disease. *Neuron* **94,** 237–248 (2017).

396. Srinivasan, K. *et al.* Untangling the brain's neuroinflammatory and neurodegenerative transcriptional responses. *Nat. Commun.* **7,** 11295 (2016).

397. Zhang, Y. *et al.* An RNA-Sequencing Transcriptome and Splicing Database of Glia, Neurons, and Vascular Cells of the Cerebral Cortex. *J. Neurosci.* **34,** 11929–11947 (2014).

398. Banati, R. B., Myers, R. & Kreutzberg, G. W. PK ('peripheral benzodiazepine')--binding sites in the CNS indicate early and discrete brain lesions: microautoradiographic detection of [3H]PK11195 binding to activated microglia. *J. Neurocytol.* **26,** 77–82 (1997).

399. Cagnin, A., Kassiou, M., Meikle, S. R. & Banati, R. B. Positron emission tomography imaging of neuroinflammation. *Neurotherapeutics* **4,** 443–452 (2007).

400. van Kesteren, C. F. M. G. *et al.* Immune involvement in the pathogenesis of schizophrenia: a meta-analysis on postmortem brain studies. *Transl. Psychiatry* **7,** 1–11 (2017).

401. Lavisse, S. *et al.* Reactive Astrocytes Overexpress TSPO and Are

Detected by TSPO Positron Emission Tomography Imaging. *J. Neurosci.* **32,** 10809–10818 (2012).

402. Cosenza-Nashat, M. *et al.* Expression of the translocator protein of 18kDa by microglia, macrophages and astrocytes based on immunohistochemical localization in abnormal human brain. *Neuropathol. Appl. Neurobiol.* **35,** 306–328 (2009).

403. Sandiego, C. M. *et al.* Imaging robust microglial activation after lipopolysaccharide administration in humans with PET. *Proc. Natl. Acad. Sci.* **112,** 12468–12473 (2015).

404. Leucht, S. *et al.* What does the PANSS mean? *Schizophr. Res.* **79,** 231–8 (2005).

405. Batarseh, A. & Papadopoulos, V. Regulation of translocator protein 18kDa (TSPO) expression in health and disease states. *Mol. Cell. Endocrinol.* **327,** 1–12 (2010).

406. Bloomfield, P. S. *et al.* Microglial activity in people at ultra high risk of psychosis and in schizophrenia: An [11C]PBR28 PET brain imaging study. *Am. J. Psychiatry* **173,** (2016).

407. Lawrie, S. *et al.* Reduced frontotemporal functional connectivity in schizophrenia associated with auditory hallucinations. *Biol. Psychiatry* **51,** 1008–1011 (2002).

408. Shergill, S. S. *et al.* Functional Magnetic Resonance Imaging of Impaired Sensory Prediction in Schizophrenia. *JAMA Psychiatry* **71,** 28 (2014).

409. Sanfilipo, M. *et al.* Volumetric Measure of the Frontal and Temporal Lobe Regions in Schizophrenia. *Arch. Gen. Psychiatry* **57,** 471 (2000).

410. Mathew, I. *et al.* Medial Temporal Lobe Structures and Hippocampal Subfields in Psychotic Disorders. *JAMA Psychiatry* **71,** 769–777 (2014).

411. Keshavan, M. S., Tandon, R., Boutros, N. N. & Nasrallah, H. a. Schizophrenia, 'just the facts': What we know in 2008Part 3: Neurobiology. *Schizophr. Res.* **106,** 89–107 (2008).

412. Strasser, H. C. *et al.* Hippocampal and ventricular volumes in psychotic and nonpsychotic bipolar patients compared with schizophrenia patients and community control subjects: A pilot study. *Biol. Psychiatry* **57,** 633–639 (2005).

413. Seidman, L. J. *et al.* A review and new report of medial temporal lobe dysfunction as a vulnerability indicator for schizophrenia: a magnetic resonance imaging morphometric family study of the parahippocampal gyrus. *Schizophr. Bull.* **29,** 803–30 (2003).

414. Narr, K. L. *et al.* Regional specificity of hippocampal volume reductions in first-episode schizophrenia. *Neuroimage* **21,** 1563–1575 (2004).

415. Szeszko, P. R. *et al.* Smaller Anterior Hippocampal Formation Volume in Antipsychotic-Naive Patients With First-Episode Schizophrenia. *Am. J. Psychiatry* **160,** 2190–2197 (2003).

416. Velakoulis, D. *et al.* Hippocampal and Amygdala Volumes According to Psychosis Stage and Diagnosis. *Arch. Gen. Psychiatry* **63,** 139 (2006).

417. Chaves, C. *et al.* Effects of minocycline add-on treatment on brain morphometry and cerebral perfusion in recent-onset schizophrenia. *Schizophr. Res.* **161,** 439–445 (2015).

418. Lang, R. Tuning of macrophage responses by Stat3-inducing cytokines: molecular mechanisms and consequences in infection. *Immunobiology* **210,** 63–76 (2005).

419. Koscsó, B. *et al.* Adenosine augments IL-10-induced STAT3 signaling in M2c macrophages. *J. Leukoc. Biol.* **94,** 1309–1315 (2013).

420. Kwon, S.-H. *et al.* Dysfunction of Microglial STAT3 Alleviates Depressive Behavior via Neuron-Microglia Interactions. *Neuropsychopharmacology* **42,** 2072–2086 (2017).

421. Hill, M. J. *et al.* Transcriptional consequences of schizophrenia candidate miR-137 manipulation in human neural progenitor cells. *Schizophr. Res.* **153,** 225–30 (2014).

422. Luo, X. *et al.* Systematic prioritization and integrative analysis of copy number variations in schizophrenia reveal key schizophrenia susceptibility genes. *Schizophr. Bull.* **40,** 1285–99 (2014).

423. Li, Y. *et al.* Biomarker identification and effect estimation on schizophrenia – a high dimensional data analysis. *Front. public Heal.* **3,** 1–8 (2015).

424. Stefan, N. *et al.* Alpha2-Heremans-Schmid glycoprotein/fetuin-A is associated with insulin resistance and fat accumulation in the liver in humans. *Diabetes Care* **29,** 853–7 (2006).

425. Notter, T. & Meyer, U. Microglia and schizophrenia: where next? *Mol. Psychiatry* **22,** 788–789 (2017).

426. Hou, Y. *et al.* Effects of clozapine, olanzapine and haloperidol on nitric oxide production by lipopolysaccharide-activated N9 cells. *Prog. Neuropsychopharmacol. Biol. Psychiatry* **30,** 1523–8 (2006).

427. Schwarz, E. *et al.* Biomarker Insights Validation of a Blood-Based Laboratory Test to Aid in the Confirmation of a Diagnosis of Schizophrenia. *Biomark Insights* **12,** 39–47 (2010).

428. Hercher, C., Chopra, V. & Beasley, C. L. Evidence for morphological alterations in prefrontal white matter glia in schizophrenia and bipolar disorder. *J. Psychiatry Neurosci.* **39,** 130277 (2014).

429. Leweke, F. M. *et al.* Antibodies to infectious agents in individuals with recent onset schizophrenia. *Eur. Arch. Psychiatry Clin. Neurosci.* **254,** 4–8 (2004).

430. Casamayor, A., Morrice, N. A. & Alessi, D. R. Phosphorylation of Ser-241 is essential for the activity of 3-phosphoinositide-dependent protein kinase-1: identification of five sites of phosphorylation in vivo. *Biochem. J.* **342,** 287–92 (1999).

431. Beaulieu, J.-M., Gainetdinov, R. R. & Caron, M. G. Akt/GSK3 signaling in the action of psychotropic drugs. *Annu. Rev. Pharmacol. Toxicol.* **49,** 327–47 (2009).

432. Lovestone, S., Killick, R., Di Forti, M. & Murray, R. Schizophrenia as a GSK-3 dysregulation disorder. *Trends Neurosci.* **30,** 142–149 (2007).

433. Jaaro-Peled, H. *et al.* Neurodevelopmental mechanisms of schizophrenia: understanding disturbed postnatal brain maturation through neuregulin-1–ErbB4 and DISC1. *Trends Neurosci.* **32,** 485–495 (2009).

434. Hashimoto, R. *et al.* Impact of the DISC1 Ser704Cys polymorphism on risk for major depression, brain morphology and ERK signaling. *Hum. Mol. Genet.* **15,** 3024–33 (2006).

435. Kanakry, C. G., Li, Z., Nakai, Y., Sei, Y. & Weinberger, D. R. Neuregulin-1 Regulates Cell Adhesion via an ErbB2/Phosphoinositide-3 Kinase/Akt-Dependent Pathway: Potential Implications for Schizophrenia and Cancer. *PLoS One* **2,** e1369 (2007).

436. Kumarasinghe, N. *et al.* Gene expression profiling in treatment-naive schizophrenia patients identifies abnormalities in biological pathways involving AKT1 that are corrected by antipsychotic medication. *Int. J. Neuropsychopharmacol.* **16,** 1483–1503 (2013).

437. Willock, C. & Franke, T. Akt signaling in fear memory processing and depression-like behaviors. *FASEB J.* **29,** 931.5 (2015).

438. Leibrock, C. *et al.* Akt2 Deficiency is Associated with Anxiety and Depressive Behavior in Mice. *Cell. Physiol. Biochem.* **32,** 766–777 (2013).

439. Alimohamad, H., Rajakumar, N., Seah, Y.-H. & Rushlow, W. Antipsychotics alter the protein expression levels of β-catenin and GSK-3 in the rat medial prefrontal cortex and striatum. *Biol. Psychiatry* **57,** 533–542 (2005).

440. Kang, U. G. *et al.* The effects of clozapine on the GSK-3-mediated signaling pathway. *FEBS Lett.* **560,** 115–119 (2004).

441. Beaulieu, J.-M. Not only lithium: regulation of glycogen synthase kinase-3 by antipsychotics and serotonergic drugs. *Int. J. Neuropsychopharmacol.* **10,** 3 (2007).

442. Beurel, E., Grieco, S. F. & Jope, R. S. Glycogen synthase kinase-3 (GSK3): regulation, actions, and diseases. *Pharmacol. Ther.* **148,** 114–31 (2015).

443. Jope, R. S. & Roh, M.-S. Glycogen synthase kinase-3 (GSK3) in psychiatric diseases and therapeutic interventions. *Curr. Drug Targets* **7,** 1421–34 (2006).

444. Emamian, E. S. AKT/GSK3 signaling pathway and schizophrenia. *Front. Mol. Neurosci.* **5,** 33 (2012).

445. Emamian, E. S., Hall, D., Birnbaum, M. J., Karayiorgou, M. & Gogos, J. a. Convergent evidence for impaired AKT1-GSK3beta signaling in schizophrenia. *Nat. Genet.* **36,** 131–7 (2004).

446. Eikelenboom, P. *et al.* Innate immunity and the etiology of late-onset Alzheimer's disease. *Neurodegener. Dis.* **10,** 271–273 (2012).

447. Elliott, D. A., Weickert, C. S. & Garner, B. Apolipoproteins in the brain: implications for neurological and psychiatric disorders. *Clin. Lipidol.* **51,** 555–573 (2010).

448. Snipes, G. J. & Suter, U. Cholesterol and myelin. *Subcell. Biochem* **28,** 173–204 (1997).

449. Jordan, B. D. Genetic influences on outcome following traumatic brain injury. *Neurochem. Res.* **32,** 905–915 (2007).

450. Pitas, R. E., Boyles, J. K., Lee, S. H., Hui, D. & Weisgraber, K. H. Lipoproteins and their receptors in the central nervous system. Characterization of the lipoproteins in cerebrospinal fluid and identification of apolipoprotein B,E(LDL) receptors in the brain. *J. Biol. Chem.* **262,** 14352–60 (1987).

451. Sehayek, E. & Eisenberg, S. Mechanisms of inhibition by apolipoprotein C of apolipoprotein E-dependent cellular metabolism of human triglyceride-rich lipoproteins through the low density lipoprotein receptor pathway. *J. Biol. Chem.* **266,** 18259–67 (1991).

452. Weisgraber, K. H. *et al.* Apolipoprotein C-I modulates the interaction of apolipoprotein E with beta-migrating very low density lipoproteins (beta-VLDL) and inhibits binding of beta-VLDL to low density lipoprotein receptor-related protein. *J. Biol. Chem.* **265,** 22453–9 (1990).

453. Kowal, R. C. *et al.* Opposing effects of apolipoproteins E and C on lipoprotein binding to low density lipoprotein receptor-related protein. *J. Biol. Chem.* **265,** 10771–9 (1990).

454. Petit-Turcotte, C. *et al.* Apolipoprotein C-I expression in the brain in Alzheimer's disease. *Neurobiol. Dis.* **8,** 953–63 (2001).

455. Berbée, J. F. P. *et al.* Apolipoprotein CI knock-out mice display impaired memory functions. *J. Alzheimers. Dis.* **23,** 737–47 (2011).

456. Abildayeva, K. *et al.* Human apolipoprotein C-I expression in mice impairs learning and memory functions. *J. Lipid Res.* **49,** 856–869 (2008).

457. Song, F. *et al.* Plasma Apolipoprotein Levels Are Associated with Cognitive Status and Decline in a Community Cohort of Older Individuals. *PLoS One* **7,** e34078 (2012).

458. Serra-Grabulosa, J. *et al.* Apolipoproteins E and C1 and brain morphology in memory impaired elders. *Neurogenetics* **4,** (2003).

459. Dantzer, R., O'Connor, J. C., Freund, G. G., Johnson, R. W. & Kelley, K. W. From inflammation to sickness and depression: when the immune system subjugates the brain. *Nat. Rev. Neurosci.* **9,** 46–56 (2008).

460. Perry, V. H., Cunningham, C. & Holmes, C. Systemic infections and inflammation affect chronic neurodegeneration. *Nat. Rev. Immunol.* **7,** 161–167 (2007).

461. Perry, V. H., Nicoll, J. A. R. & Holmes, C. Microglia in neurodegenerative disease. *Nat. Rev. Neurol.* **6,** 193–201 (2010).

462. Lago, S. G. *et al.* Exploring the neuropsychiatric spectrum using high-content functional analysis of single-cell signaling networks ex vivo. *submitted*

463. Bauer, S., Kerr, B. J. & Patterson, P. H. The

neuropoietic cytokine family in development, plasticity, disease and injury. *Nat. Rev. Neurosci.* **8,** 221–232 (2007).

464. Nomura, I., Kishi, T., Ikuta, T. & Iwata, N. Statin add-on therapy in the antipsychotic treatment of schizophrenia: A meta-analysis. *Psychiatry Res.* **260,** 41–47 (2018).

465. Jay, T. R., von Saucken, V. E. & Landreth, G. E. TREM2 in Neurodegenerative Diseases. *Mol. Neurodegener.* **12,** 1–33 (2017).

466. Kleinberger, G. *et al.* The FTD-like syndrome causing TREM2 T66M mutation impairs microglia function, brain perfusion, and glucose metabolism. *EMBO J.* **36,** 1837–1853 (2017).

467. Mazaheri, F. *et al.* TREM2 deficiency impairs chemotaxis and microglial responses to neuronal injury. *EMBO Rep.* **18,** 1186–1198 (2017).

468. Ulland, T. K. *et al.* TREM2 Maintains Microglial Metabolic Fitness in Alzheimer's Disease. *Cell* **170,** 649–663 (2017).

469. Hong, S. & Stevens, B. TREM2: Keeping Microglia Fit during Good Times and Bad. *Cell Metab.* **26,** 590–591 (2017).

470. Falk, A. *et al.* Modeling psychiatric disorders: from genomic findings to cellular phenotypes. *Mol. Psychiatry* **21,** 1167–1179 (2016).

471. Sullivan, P. F. Puzzling over schizophrenia: Schizophrenia as a pathway disease. *Nat. Med.* **18,** 210–211 (2012).

472. Zheng, W., Thorne, N. & McKew, J. C. Phenotypic screens as a renewed approach for drug discovery. *Drug Discov. Today* **18,** 1067–73 (2013).

473. Young, J. J., Bruno, D. & Pomara, N. A review of the relationship between proinflammatory cytokines and major depressive disorder. *J. Affect. Disord.* **169,** 15–20 (2014).

474. Dowlati, Y. *et al.* A Meta-Analysis of Cytokines in Major Depression. *Biol. Psychiatry* **67,** 446–457 (2010).

475. Goldsmith, D. R., Rapaport, M. H. & Miller, B. J. A meta-analysis of blood cytokine network alterations in psychiatric patients: comparisons between schizophrenia, bipolar disorder and depression. *Mol. Psychiatry* **21,** 1696–1709 (2016).

476. Lee, E. E., Hong, S., Martin, A. S., Eyler, L. T. & Jeste, D. V. Inflammation in Schizophrenia: Cytokine Levels and Their Relationships to Demographic and Clinical Variables. *Am. J. Geriatr. Psychiatry* **25,** 50–61 (2016).

477. Girotti, M., Donegan, J. J. & Morilak, D. A. Influence of hypothalamic IL-6/gp130 receptor signaling on the HPA axis response to chronic stress. *Psychoneuroendocrinology* **38,** 1158–1169 (2013).

478. Voorhees, J. L. *et al.* Prolonged Restraint Stress Increases IL-6, Reduces IL-10, and Causes Persistent Depressive-Like Behavior That Is Reversed by Recombinant IL-10. *PLoS One* **8,** e58488 (2013).

479. Ohayon, M. M. Epidemiology of depression and its treatment in the general population. *J. Psychiatr. Res.* **41,** 207–213 (2007).

480. Kessler, R. C. *et al.* The Epidemiology of Major Depressive Disorder. *JAMA* **289,** 3095 (2003).

481. Blair-West, G. W., Mellsop, G. W. & Eyeson-Annan, M. L. Down-rating lifetime suicide risk in major depression. *Acta Psychiatr. Scand.* **95,** 259–263 (1997).

482. Mathers, C. D. *et al.* Projections of Global Mortality and Burden of Disease from 2002 to 2030. *PLoS Med.* **3,** 2011–2030 (2006).

483. Buckley, P. F., Miller, B. J., Lehrer, D. S. & Castle, D. J. Psychiatric comorbidities and schizophrenia. *Schizophr. Bull.* **35,** 383–402 (2009).

484. Siris, S. G. & Bench, C. in *Schizophrenia* 142–167 (Blackwell Science Ltd). doi:10.1002/9780470987353.ch9

485. Erhart, S. M., Marder, S. R. & Carpenter, W. T. Treatment of Schizophrenia Negative Symptoms: Future Prospects. *Schizophr. Bull.* **32,** 234–237 (2006).

486. Licinio, J. Translational Psychiatry: leading the

transition from the cesspool of devastation to a place where the grass is really greener. *Transl. Psychiatry* **1,** 1–2 (2011).

487. Agid, Y. *et al.* How can drug discovery for psychiatric disorders be improved? *Nat. Rev. Drug Discov.* **6,** 189–201 (2007).

488. Schooler, N. R. *et al.* Defining therapeutic benefit for people with schizophrenia: focus on negative symptoms. *Schizophr. Res.* **162,** 169–174 (2015).

489. Réus, G. Z. *et al.* The role of inflammation and microglial activation in the pathophysiology of psychiatric disorders. *Neuroscience* **300,** 141–54 (2015).

490. Zhu, F., Liu, Y., Zhao, J. & Zheng, Y. Minocycline alleviates behavioral deficits and inhibits microglial activation induced by intrahippocampal administration of Granulocyte-Macrophage Colony-Stimulating Factor in adult rats. *Neuroscience* **266,** 275–81 (2014).

491. Zhang, L. & Zhao, J. Profile of minocycline and its potential in the treatment of schizophrenia. *Neuropsychiatr. Dis. Treat.* **10,** 1103–1111 (2014).

492. Curatolo, P., Moavero, R. & de Vries, P. J. Neurological and neuropsychiatric aspects of tuberous sclerosis complex. *Lancet. Neurol.* **14,** 733–45 (2015).

493. Chaudhry, I. B. *et al.* Minocycline benefits negative symptoms in early schizophrenia: a randomised double-blind placebo-controlled clinical trial in patients on standard treatment. *J. Psychopharmacol.* **26,** 1185–93 (2012).

494. Millan, M. J., Fone, K., Steckler, T. & Horan, W. P. Negative Symptoms of Schizophrenia: Clinical Characteristics, Pathophysiological Substrates, Experimental Models and Prospects for Improved Treatment. *Eur. Neuropsychopharmacol.* **24,** 645–692 (2014).

495. The negative symptoms of schizophrenia. They are pervasive but sometimes invisible--and especially difficult to treat. *Harv. Ment. Health Lett.* **23,** 1–3 (2006).

496. Eßlinger, M. *et al.* Schizophrenia associated sensory gating deficits develop after adolescent microglia activation. *Brain. Behav. Immun.* **58,** 99–106 (2016).

497. Sellgren, C. M. *et al.* Patient-specific models of microglia-mediated engulfment of synapses and neural progenitors. *Mol. Psychiatry* **22,** 170–177 (2017).

498. Werner, F.-M. & Coveñas, R. Long-term administration of antipsychotic drugs in schizophrenia and influence of substance and drug abuse on the disease outcome. *Curr. Drug Abuse Rev.* (2017). doi:10.2174/1874473710666171020104524

499. Agarwal, S. & Rao, A. V. Tomato lycopene and low density lipoprotein oxidation: a human dietary intervention study. *Lipids* **33,** 981–984 (1998).

500. Lockhart, A. *et al.* The peripheral benzodiazepine receptor ligand PK11195 binds with high affinity to the acute phase reactant α1-acid glycoprotein: Implications for the use of the ligand as a CNS inflammatory marker. *Nucl. Med. Biol.* **30,** 199–206 (2003).

501. Palin, K., Cunningham, C., Forse, P., Perry, V. H. & Platt, N. Systemic inflammation switches the inflammatory cytokine profile in CNS Wallerian degeneration. *Neurobiol. Dis.* **30,** 19–29 (2008).

502. Cunningham, C. *et al.* Systemic Inflammation Induces Acute Behavioral and Cognitive Changes and Accelerates Neurodegenerative Disease. *Biol. Psychiatry* **65,** 304–312 (2009).

503. Pott Godoy, M. C., Tarelli, R., Ferrari, C. C., Sarchi, M. I. & Pitossi, F. J. Central and systemic IL-1 exacerbates neurodegeneration and motor symptoms in a model of Parkinson's disease. *Brain* **131,** 1880–94 (2008).

504. Nguyen, M. D., D'Aigle, T., Gowing, G., Julien, J.-P. & Rivest, S. Exacerbation

of motor neuron disease by chronic stimulation of innate immunity in a mouse model of amyotrophic lateral sclerosis. *J. Neurosci.* **24,** 1340–9 (2004).

505. Holmes, C. *et al.* Systemic inflammation and disease progression in Alzheimer disease. *Neurology* **73,** 768–74 (2009).

506. Huang, J. T.-J. *et al.* Disease biomarkers in cerebrospinal fluid of patients with first-onset psychosis. *PLoS Med.* **3,** 2145–58 (2006).

507. Harris, L. W. *et al.* Comparison of peripheral and central schizophrenia biomarker profiles. *PLoS One* **7,** 1–9 (2012).

508. Chapple, M. R., Johnson, G. D. & Davidson, R. S. Fluorescence quenching; a practical problem in flow cytometry. *J. Microsc.* **159,** 245–53 (1990).

509. Brown, C. M. Fluorescence microscopy--avoiding the pitfalls. *J. Cell Sci.* **120,** 1703–5 (2007).

510. Illien, F. *et al.* Quantitative fluorescence spectroscopy and flow cytometry analyses of cell-penetrating peptides internalization pathways: optimization, pitfalls, comparison with mass spectrometry quantification. *Sci. Rep.* **6,** 1–13 (2016).

511. Man, S. M. *et al.* Inflammasome activation causes dual recruitment of NLRC4 and NLRP3 to the same macromolecular complex. *Proc. Natl. Acad. Sci. U. S. A.* **111,** 7403–8 (2014).